THE JOURNAL OF PHYSICAL CHEMISTRY

THE ION-PAIR CONCEPT: ITS EVOLUTION AND SOME APPLICATIONS

By CHARLES A. KRAUS

Metcalf Research Laboratory, Providence, R. I.

Received August 17, 1955

After a brief introduction, the following topics are discussed: (1) *Bjerrum's Theory.* Some implications of this theory are pointed out; (2) *Ion-pairs at Dielectric Constants just Below the Critical.* The association process is followed as the dielectric constant passes through values where ion association sets in; (3) *Solutions in Benzene.* Values of Bjerrum's parameter *a*, as derived from dissociation constants, are compared with the distance between ions as derived for dipole moments; (4) *Ion Pairs in Solvents of Higher Dielectric Constant.* The dependence of *K* on dielectric constant and various constitutional and structural factors is discussed. Systems are also considered where other than Coulombic forces are involved; (5) *Electrolytes Derived from Less Electropositive Metals.* Derivatives of third and fourth group elements are considered, including aluminum halides and triarylmethyl compounds. The effect of complexing bases is discussed; (6) *Localized Ion Pairs: Micellar Electrolytes.* The effect of ion size on the properties of micellar electrolytes is discussed; (7) *Dependence of K on Temperature.* The effect of temperature on the ion pair equilibria is examined for solutions in solvents of low and high dielectric constant in the light of Bjerrum's theory; (8) *Reversal of the Association Process in Highly Concentrated Solutions.* This is illustrated by means of solutions of bromine in fused trimethylammonium bromide at 25°.

I. Introduction

The problem of electrolyte solutions centers around the interactions of ions with one another and with solvent molecules. We have some fairly satisfactory theories of dilute solutions but these are not only limiting theories, they are also approximations in that terms of higher order are usually omitted in order to make the equations conveniently handable. The experimenter has no means of knowing whether observed deviations are due to the absence of neglected terms or to the fact that he has exceeded the concentration at which the theory is applicable. The problem confronting us today is to bring some order into the confusion presently existing in the intermediate and higher concentration ranges. These solutions bridge the gap between dilute solutions, on the one hand, and fused salts on the other.

In the development of the electrolyte field, it was not possible to interpret existing data until the ion concept had been developed and we had some knowledge of atomic dimension and the structure of matter. In early days, it was difficult to understand how, under the action of Coulomb forces, ions could exist free in solution. Clausius, in the 1850's, suggested that electrolytes might be dissociated into free ions to a small extent. The investigations of Hittorf and of Kohlrausch indicated that a slight dissociation into free ions was not sufficient to account for observed results.

Arrhenius, in the 80's, made the bold assumption that electrolytes are completely dissociated into their ions in the limit of infinite dilution and he ascribed the decrease of equivalent conductance with increasing concentration to association of the ions to neutral molecules. He also assumed that the interaction of the ions with one another and with the neutral molecules conformed to the law of mass action. He further assumed that the degree of dissociation of the electrolyte to free ions at any given concentration was equal to the ratio of the observed conductance, Λ, to the limiting conductance, Λ_0, at infinite dilutions.

The Arrhenius theory was found to apply fairly well to solutions of weak acids and bases in water but it failed completely in the case of strong electrolytes such as ordinary salts and strong acids and bases. When the degree of dissociation, γ, of the electrolyte, as computed from conductance data, was substituted in the mass action equation, the expression $C\gamma^2/(1 - \gamma)$ did not remain constant with changing concentration. At low concentrations, it had very small values which increased continuously and largely with increasing concentration.

It was not until 1923 that the solution of the electrolyte problem was supplied by Debye and Hückel.[1] Their theory accounted admirably for the thermodynamic properties of electrolyte solutions. Onsager's extension of this theory shortly thereafter[2] accounted satisfactorily for the conductance of electrolyte solutions. Debye and Hückel, as also Onsager later, assumed that strong electrolytes are completely dissociated into their ions in aqueous solution. Not a few physical chemists at that time jumped to the conclusion that strong electrolytes are completely dissociated

(1) P. Debye and E. Hückel, *Physik. Z.*, **25**, 305 (1923).
(2) L. Onsager, *ibid.*, **28**, 27 (1927).
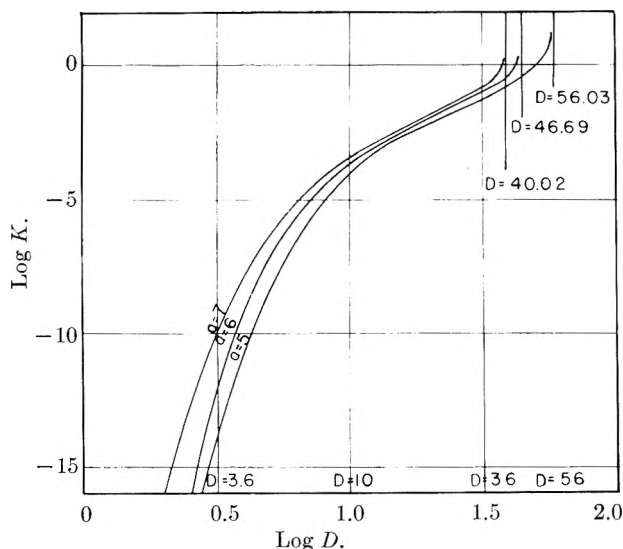
Fig. 1.—Plots of Bjerrum's equation.

in all solvents; but not so, Bjerrum.[3] He developed a theory that took into account the interaction of ions at short range. He introduced the ion-pair concept and showed how the mass action constant of the equilibrium between ions and ion-pairs is dependent on the dielectric constant of the solvent as well as on temperature and the size of the ions.

The correctness of the assumption of Debye and Hückel that strong electrolytes are completely dissociated in aqueous solution rested on the fact that the resultant theories accounted satisfactorily for experimental observations. Some twenty years ago, Fuoss and Kraus[4] supplied independent evidence of its validity. From conductance data, they evaluated the dissociation constant K of the ion-pair equilibrium for i-Am$_4$NNO$_3$ in dioxane–water mixtures and showed that the values of the constant conformed to Bjerrum's equation relating K to the dielectric constant, D. On the basis of their data and Bjerrum's theory, they found that for values of D greater than about 44, the ions of this salt are unassociated in dioxane–water mixtures.

II. Bjerrum's Theory

While this theory does not reproduce the experimental data in a strictly quantitative manner, it nevertheless approximates them and is invaluable in interpreting experimental results as a function of dielectric constant and temperature. The theory relates the dissociation constant, K, of the ion-ion pair equilibrium with the dielectric constant, D, and the absolute temperature, T, by means of the equation[3]

$$\frac{1}{K} = \frac{4\pi N}{1000} \frac{\epsilon^2}{DkT} Q(b) \qquad (1)$$

where

$$b = \epsilon^2/aDkT \qquad (2)$$

Here, N is Avogadro's number, ϵ is the unit of charge and a is an empirical parameter. Values of $Q(b)$ have been computed by Bjerrum (1) for values of b from 1 to 15 and by Fuoss and Kraus[4] for values from 15 to 80. The parameter a may be interpreted as the distance between centers of charge of the ions in the ion-pairs when the ions are in contact. Thus K is related to D and T through the parameter a.

The dependence of K on DT and a cannot well be visualized from an inspection of equation 1. Accordingly, in

Fig. 1, plots are shown of log K vs. log D for $t = 25°$ and for a having the values 5, 6 and 7 Å., respectively.

On inspection of the figure, it will be seen that K reaches very small values at $D = 3$, the values range from 2×10^{-15} for $a = 5$ Å. to 2.8×10^{-11} for $a = 7$ Å. For $D = 10$, they range from 0.9×10^{-4} to 3.7×10^{-4}; at $D = 36$, they range from 0.9×10^{-1} to 2.7×10^{-1}.

At higher values of D, the plots cross the axis and become positively infinite. This occurs at $D = 40.0$, 46.7 and 56.0 for $a = 7$, 6 and 5 Å., respectively. For values of the dielectric constant above the critical, D_c, electrolytes having a values of 7, 6 and 5 Å., respectively, are unassociated. The larger the value of a, the lower the dielectric constant above which ion association does not occur.

In the range of D from 10 to 36, values of K may be determined fairly readily by means of conductance measurements. In this range, the values of K are not very sensitive to the magnitude of a values as they increase only slowly as D increases.

It will be noted that, for a given value of a at a given temperature, the value of K is dependent only on the dielectric constant of the solvent medium. If the value of a for a given electrolyte does not change greatly in going from one solvent to another, then we can, if we know the value of K in any one solvent, approximate its value in any other solvent. So, also, if the value of a for different salts does not differ too greatly, we can approximate the value of K for a given salt in any solvent if we know the value of its dielectric constant.

Equation 1 also supplies useful information concerning the dependence of K on temperature. The value of K depends on the value of the product DT. In solvents of higher dielectric constant, the value of D decreases markedly with increasing temperature and the value of DT decreases as T increases. In such solvents, the dissociation constant, K, decreases with increasing temperature; in other words, ion association increases with increasing values of T. While we have few quantitative data on the association of ions at higher temperatures, there are abundant qualitative data that establish this fact conclusively. In solvents of low dielectric constant, DT increases with temperature, since D changes only little. Accordingly, in such solvents, the value of K increases with T; i.e., association decreases as T increases

As stated above, a may be interpreted as the distance between the centers of charge in the ion-pairs when the ions are in contact. On this basis, we should expect that a would be large for electrolytes having large ions and, conversely, small for those having small ions. Accordingly, we shall examine the available data in order to determine how K depends on ion dimensions and, in turn, how these correlate with values of a.

III. Ion-Pairs at D Values Just Below the Critical Dielectric Constant

With the exception of one mixture of $D = 38$, the measurements of Fuoss and Kraus with Am$_4$NNO$_3$ in dioxane–water mixtures cover the range of D from 2.38 to 11.9. Values of K conform rather well with Bjerrum's equation for a mean a value of 6.4 Å. The one mixture at $D = 38$ does not enable one to determine how closely Bjerrum's equation applies for dielectric constants approaching the critical value of D. Martel and Kraus[5] working with dioxane–water mixtures, have shown that Am$_4$NNO$_3$, Bu$_4$NI and NaBrO$_3$ are not associated for dielectric constants above about 50. However, except for NaBrO$_3$, the number of different mixtures measured with these salts was too small to permit of finding how well Bjerrum's theory accounts for the observed K values. The bromate was measured in four different mixtures and it was

(3) N. Bjerrum, Kgl. Danske Selskab, 7, No. 9 (1926).

(4) R. M. Fuoss and C. A. Kraus, J. Am. Chem. Soc., 55, 1019 (1933).

(5) R. W. Martel and C. A. Kraus, Proc. Nat. Acad. Sci., 41, 9 (1955).

found that the value of a increased as D decreased. In going from $D = 48.9$ to $D = 31.5$, the value of a increased from 5.02 to 5.83 Å.

Recently, Mercier[6] has measured solutions of Bu$_4$NBr and Me$_4$NPi in dioxane–water mixtures down to a dielectric constant of 19.07. In evaluating K from conductance data by means of the Fuoss procedure,[7] Mercier employed the method devised by Martel and Kraus.

In Table I, column 2, are shown values of K as computed from conductance data. Values of D appear in column 1, and values of a as computed from K values by means of Bjerrum's equation appear in column 3. In column 4 are shown values of the critical dielectric constant, D_c, as calculated by means of Bjerrum's equation from the corresponding values of K.

TABLE I

CONSTANTS OF SALTS IN DIOXANE–WATER MIXTURES AT 25°

D	K	a (Å.)	D_c	D	K	a (Å.)	D_c
A.	Tetrabutylammonium bromide			B.	Tetramethylammonium picrate		
48.91	0.77	5.09	55.0	27.21	0.33	10.1	27.7
44.54	.46	5.34	52.5	25.15	.27	11.0	25.5
40.20	.28	5.74	48.8	23.14	.098	11.2	25.0
35.85	.18	6.18	45.3	21.12	.049	11.4	24.6
31.53	.10	6.68	41.9	19.07	.038	12.7	22.1
27.21	.049	6.96	40.3				
23.14	.023	7.15	39.2				
19.07	.0086	6.77	41.4				

While it is difficult to evaluate the error attached to the various computed K values, it certainly is not great enough to account for the regular increase in the value of a as D decreases. We must conclude that, in the region investigated, the parameter a of Bjerrum's equation varies as the dielectric constant changes. The lower value of a for Bu$_4$NBr at $D = 19.07$ may be in error or it may be real.

Values of D_c computed from the a values at higher dielectric constant are probably not greatly in error. However, values calculated from a values at lower dielectric constants are definitely in error. For example, for Bu$_4$NBr at $D = 23.14$, $D_c = 39.2$; conductance measurements show conclusively that for this salt, D_c lies between 50 and 55. So, also, for Me$_4$NPi, at $D = 19.07$, $D_c = 22.1$; conductance measurements place D_c between 27.2 and 31.5. The change in the value of a with decreasing dielectric constant cannot be accounted for on the basis of experimental error. The solution of this problem will be found in further investigations, to lower dielectric constants and with a greater variety of electrolytes.

It is of some interest to follow the association process as it proceeds from the unassociated electrolyte in solvents of high dielectric constant to increasing degrees of association for $D < D_c$ as the dielectric constant decreases. In Fig. 2 is shown the degree of association, $1 - \gamma$, in per cent., for Bu$_4$NBr and Me$_4$NPi at $C = 3 \times 10^{-4}$.

It will be noted that ion association sets in at the critical dielectric constant about 55 for Bu$_4$NBr

(6) P. L. Mercier, Thesis, Brown University, June, 1955.
(7) R. M. Fuoss, J. Am. Chem. Soc., **57**, 488 (1935).
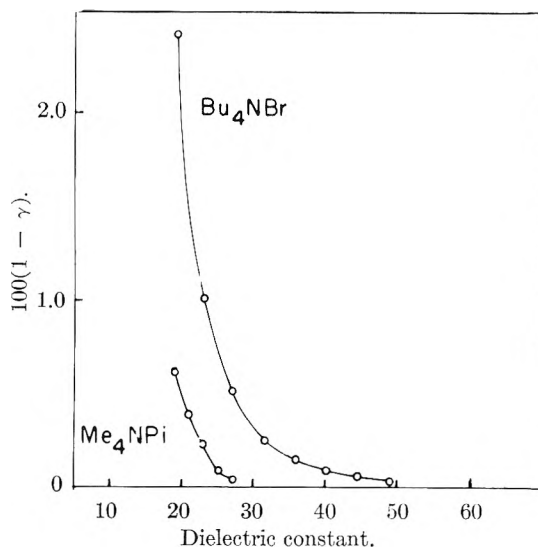
Fig. 2.—Per cent. of association vs. D.

and 28 for Me$_4$NPi. At first the degree of association increases slowly as D decreases but then it increases more rapidly, somewhat in an exponential fashion. The degree of association in the solvents of lowest D is only about 2.5% for Bu$_4$NBr and 0.75% for Me$_4$NPi. The $1 - \gamma$ vs. D plot rises more steeply for Me$_4$NPi than for Bu$_4$NBr. This corresponds to the fact that a increases less rapidly for the picrate than for the bromide as D decreases. It will be noted that the value of a for the picrate is much larger than that for the bromide. This corresponds to the greater distance between centers of charge in the ion-pairs of the picrate. This phase of the subject will be considered at greater length in other sections.

IV. Solutions in Benzene

The only solutions in solvents of low dielectric constant concerning which we have considerable knowledge are those in benzene. In certain respects, solutions in benzene yield more useful information than do solutions in solvents of higher dielectric constant. For one thing, in benzene we are able to measure the polar moment of the ion-pairs and thus find the distance between centers of charge of the ions in the ion-pairs. Furthermore, since the concentration of ions is exceedingly low, the determination of K values by means of conductance measurements is not complicated by ion atmosphere effects.

1. **Dipole Moments.**—We have reliable values for the dipole moments for some 13 electrolytes in benzene.[8] In Table II are shown values of molecular polarization, P_v, dipole moment, μ, and the distance d between the centers of charge in the dipoles. The last is simply obtained by dividing the dipole moment by the unit charge, 4.77×10^{-16} e.s.u.

Bearing in mind the fact that the distribution of charge in the free ions is not known and that this distribution may be affected by the force of the counter charges in the ion-pairs, the values of d accord reasonably well with atomic dimensions. The first electrolyte in the list has much the largest ions and the value of $d = 4.13$ Å. For Am$_4$NPi and Bu$_4$NPi, these values are both large and differ by 0.1 Å. For tributylammonium iodide, bromide and chloride, the

(8) (a) J. A. Geddes and C. A. Kraus, Trans. Faraday Soc., **32**, 585 (1936); (b) G. S. Hooper and C. A. Kraus, J. Am. Chem. Soc., **56**, 2265 (1934).

TABLE II

CONSTANTS OF ELECTROLYTES IN BENZENE

Electrolytes	P_0	$\mu \times 10^{18}$	$d \times 10^8$
Tetra-n-butylammonium hydroxytriphenylboron	8270	19.7	4.13
Tetra-isoamylammonium picrate	7090	18.3	3.82
Tetra-n-butylammonium picrate	6740	17.8	3.72
Tetra-isoamylammonium thiocyanate	5050	15.4	3.23
Tetra-n-butylammonium perchlorate	4250	14.1	2.96
Tri-isoamylammonium picrate	3830	13.3	2.79
Tri-n-butylammonium picrate	3670	13.1	2.74
Tetra-n-butylammonium bromide	2900	11.6	2.43
Tetra-n-butylammonium acetate	2690	11.2	2.35
Tri-n-butylammonium iodide	1440	8.09	1.69
Tri-n-butylammonium bromide	1280	7.61	1.59
Tri-n-butylammonium chloride	1140	7.17	1.50
Silver perchlorate	2400	10.7	2.25

d values are, respectively, 1.69, 1.59 and 1.50 Å., differing by about 0.1 Å. These differences seem reasonable. For AgClO$_4$, $d = 2.25$ Å. This is 0.41 Å. less than that of Bu$_4$NClO$_4$. The silver ion is markedly smaller than the tetrabutylammonium ion as was to be expected. The perchlorate crystallizes with two molecules of benzene. It would seem that dipole moments provide us with reliable values for the distance between centers of charge in the ion-pairs. We can now compare these with values of a as derived for the same salts from their dissociation constants by means of Bjerrum's theory.

2. **Dissociation Constants.**—To determine the dissociation constant of electrolytes in benzene, it is necessary to carry out the measurements at concentrations below about 5×10^{-6} N. Above this concentration the ions interact with ion-pairs to form triple ions. The concentration of free ions in the 1–5×10^{-6} N range is of the order of 1×10^{-11}, since the degree of dissociation of the ion-pairs is little greater than 1×10^{-6}. A single conductance measurement yields the value of K by means of Ostwald's dilution law. There is some uncertainty in the value of K so determined since, for a given salt, it is assumed that $\Lambda_0\eta$ has the same value for solutions in different solvents. The uncertainty so introduced will not measurably affect any conclusion that we may draw.

Values of K for a number of salts are given in column 2 of Table III. In the computations, values of Λ_0 are based on values of $\Lambda_0\eta$ for the same salts in ethylene chloride or, in a few cases, in other non-aqueous solvents. In Table III are also shown values of the parameter a in column 3, of the dipole moment in column 4 and of the distance, d, between centers of charge in column 5.

TABLE III

CONSTANTS OF SALTS IN BENZENE AT 25°

Salt	$K \times 10^{18}$	$a \times 10^8$	$\mu \times 10^{18}$	$d \times 10^8$
Am$_4$NPi	21.8[9]	5.95	18.3	3.82
Am$_4$NI	21.3[9]	5.94	..	..
Am$_4$NSCN	19.3[9]	5.92	15.4	3.23
Bu$_4$NBr	14.2[10]	5.88	11.6	2.43
Bu$_4$NClO$_4$	13.0[11]	5.87	..	..
Bu$_4$NAc	0.9[11]	5.49	11.2	2.35
AgClO$_4$	0.04[11]	5.03	10.7	2.25
Am$_3$NHPi	0.004[12]	4.87	13.3	2.79

The order of the a values is, of course, the same as that of the D_c values. The value of a seems not unreasonable for the salts of largest K value but seems much too large for salts of small K value. In going from $K = 4 \times 10^{-21}$ to K

(9) R. M. Fuoss and C. A. Kraus, *J. Am Chem Soc.*, **55**, 3614 (1933).

(10) L. E. Strong and C. A. Kraus, *ibid.*, **72**, 166 (1950).

(11) W. F. Luder, P. B. Kraus, C. A. Kraus and R. M. Fuoss, *ibid.*, **58**, 255 (1936).

(12) C. A. Kraus and R. M. Fuoss, *ibid.*, **55**, 21 (1933).

$= 21.8 \times 10^{-18}$, a increases from 4.87 to 5.95 Å. The actual distance between centers of charge, d, ranges from 2.79 to 3.82 Å.; the dipole moments range from 13.3 to 18.3 $\times 10^{-18}$. Bjerrum's theory does not approximate the size of the dipoles very closely; the discrepancies are greatest with salts of smaller dipole moment.

The dissociation constants follow the order of the dipole moments with one exception. The dipole moment of Am$_3$NHPi is 13.3×10^{-18}. We should expect the value of K to fall somewhat below that of Am$_4$NSCN and above that of Bu$_4$NBr, that is, somewhere in the neighborhood of 16×10^{-18}. Actually, the value for this salt is 4×10^{-21}. The reason for this is that hydrogen bonding takes place between the ions. We shall return to this matter again in our discussion of solutions in nitrobenzene.

3. **Polyionic Structures of Higher Order.**—As we proceed from low to high concentrations, ion-pairs or ion dipoles, represent the first stage in the formation of polyionic structures due to interaction between the charges. The present discussion is limited to ion-pairs in accordance with the subject matter of this symposium. However, the effect of dimensional and constitutional factors on interactions comes to light so much more clearly in the interactions between ion-pairs than it does in those between ions that we shall digress briefly to discuss this phase of the problem of interactions due to Coulomb forces.

In benzene, the first interaction of higher order is that between ions and ion-pairs with the formation of triple ions[12] at about 1×10^{-5} N. The formation of triple ions is evidenced by the appearance of a minimum in the Λ vs. C plots. Such a minimum appears, not only in benzene, but in all solvents of dielectric constant less than about 15 or 20. However, as the dielectric constant increases, the concentration at which the minimum appears moves to higher values.

Depending on the dipole moment of the ion pairs and the size of the ions, the dipoles interact to form quadripoles in varying degree. In some cases, the formation of quadripoles may be detected at concentrations as low as 5×10^{-5} N by means of dielectric measurements.

If the dipole moment is large and the ions are large, the association to quadripoles is marked; if the ions are large and the dipole moment is small, association to quadripoles is small; if the dipole moment is large and one ion is small, association is very great and soon proceeds far beyond the quadripole stage.

Tetraisoamylammonium picrate has two large ions and a large dipole moment (18.3×10^{-18}). At 4×10^{-3} N, its association number, n (formula weights per mole) is[13] 1.40. In other words, it is associated to quadripoles to the extent of 40%. Triisoamylammonium picrate has two large ions and a dipole moment of 13.3×10^{-18}. At 3.8×10^{-3} N, n is 1.033; it is associated to the extent of only 3.3%. The difference in the association of these salts to quadripoles can only be due to the difference in the magnitude of their dipole moments. Tetraisoamylammonium thiocyanate[14] has a dipole moment of 15.4×10^{-18}. At 3.8×10^{-3} N, it has an association number of 5.47; association has proceeded far beyond the quadripole stage. Silver perchlorate[13] has a dipole moment of 10.7×10^{-18}. At 4.7×10^{-3} N, its association number is 1.50, much the same as that of Am$_4$NPi and much greater than that of Am$_3$NHPi. Clearly, the high degree of association of the thiocyanate is due to the fact that one of the ions, SCN$^-$, is small. The ion dipoles of all salts having one large and one small ion are all highly associated.

The degree of association of all salts increases with increasing concentration for concentrations below 0.1 m (molal). For salts having one small and one large ion, the association number reaches very high values. For i-Am$_4$NSCN, it reaches a value of 25.8 at $m = 0.123$. Beyond this concentration, the degree of association decreases rapidly, reaching a value of 11.5 at $m = 0.425$. This phenomenon of a maximum degree of association is quite general and the maximum lies between about 0.1 and 0.3 m. It is clear that for all electrolytes there is a certain concentration, C_m, above which the law of mass action suffers a reversal; the degree of association decreases with increasing concentration. This appears to hold very generally for all electrolytes and for all solvents in which ion association occurs.

(13) F. M. Batson and C. A. Kraus, *ibid.*, **56**, 2017 (1934).

(14) D. T. Copenhafer and C. A. Kraus, *ibid.*, **73**, 4557 (1951).

TABLE IV

DISSOCIATION CONSTANTS AND a VALUES OF Bu$_4$NPi IN DIFFERENT SOLVENTS AT 25°

Solvent	C$_6$H$_4$Cl$_2$[15]	CH$_3$-CHCl$_2$[16]	CH$_2$ClCH$_2$Cl[17]	C$_6$H$_6$N[18]	(CH$_3$)$_2$CO[19]
D	9.927	10.00	10.23	12.01	20.47
K	1.71×10^{-5}	4.54×10^{-5}	2.26×10^{-4}	12.8×10^{-4}	22.3×10^{-3}
$a \times 10^8$	4.09	4.32	5.77	7.91	9.1

V. Ion-pairs in Solvents of Higher Dielectric Constant

1. Dependence of K on Dielectric Constant.—

Aside from benzene, we have little information as to the dissociation constant of electrolytes in solutions of dielectric constant lower than about 10. In the range of D between 10 and 35 we have fairly extensive data. However, for dielectric constants greater than 25 or 30, where the dissociation constants become high, values of K become uncertain because of lack of knowledge of how ion conductances vary as a function of concentration. In general, Onsager's equation does not apply, since in water and in dioxane–water mixtures, the deviations from this equation are often marked and they may be either positive or negative, depending on the salt. For this reason, there is little point in considering solutions in methanol ($D = 32.6$) or nitrobenzene ($D = 34.8$), even though there are reliable conductance data for solutions of various salts in these solvents.

In Table IV are given values of K for Bu$_4$NPi in o-dichlorobenzene, ethylidene chloride, ethylene chloride, pyridine and acetone. The value of D is given in the second line, that of K in the third line and that of Bjerrum's parameter, a, in the last line.

It will be noted that the values of K increase regularly as we proceed from the solvent of lowest to that of highest dielectric constant. However, it should be noted that, while the dielectric constant for the first three solvents is the same within about 2%, the value of K differs markedly. This difference cannot be accounted for on the basis of Bjerrum's theory. Thus, in going from o-dichlorobenzene to ethylene chloride, the constant increases 13-fold, while the dielectric constant increases only 2.3%. In going from ethylene chloride to pyridine, K increases 6-fold while D increases 18%.

The value of a increases in quite regular fashion from 4.09 Å. for o-dichlorobenzene to 9.1 Å. for acetone. This increase in a with increasing dielectric constant indicates that the salt is relatively more highly associated in the solvents of lower dielectric constant. The manner in which a varies with D for these solvents is similar to that found for salts in dioxane–water mixtures. Bjerrum's theory is clearly an approximation although a very useful one.

2. Dependence of K on Dimensional Factors. a. Positive Ions.—

In salts of quaternary ammonium and other similar ions, the effect of ion dimensions on the values of K is clearly brought to light. In Table V are shown values of K for different quaternary ammonium picrates in ethylene chloride, pyridine and acetone. The corresponding values of a are shown alongside those of K.

With one exception, the value of K increases as the number of carbon atoms in the substituent chains increases. For Am$_4$NPi in pyridine, K is slightly smaller than it is for Bu$_4$NPi. This is doubtless due to experimental error. The magnitude of the increase, in going from the salt of one ion to that of a larger ion, depends on the solvent. Thus, the ratio of K values for Me$_4$NPi and Bu$_4$NPi is 7, 1.9 and 2 in ethylene chloride, pyridine and acetone, respectively. In ethylene chloride the K value of the methyl salt is relatively

much smaller than it is for other solvents, but all salts show a greater change of K with ion size in ethylene chloride than in the other two solvents.

TABLE V

VALUES OF K AND a FOR QUATERNARY AMMONIUM PICRATES IN DIFFERENT SOLVENTS

Salt	C$_2$H$_4$Cl$_2$[17] $D = 10.23$ $K \times 10^4$	$a \times 10^8$	C$_6$H$_6$N[18,20] $D = 12.01$ $K \times 10^4$	$a \times 10^8$	(CH$_3$)$_2$CO[19,20b,21] $D = 20.47$ $K \times 10^4$	$a \times 10^8$
Me$_4$NPi	0.32	4.20	6.7	5.94	112	6.67
Et$_4$NPi	1.59	5.34	10.4	7.07	175	8.66
Pr$_4$NPi	1.94	5.59	11.7	7.39	..	..
Bu$_4$NPi	2.26	5.77	12.8	7.91	223	9.71
Am$_4$NPi	2.38	6.20	11.3	7.43	..	..

The a values parallel the K values but they are markedly greater for pyridine than for ethylene chloride and those for acetone are markedly greater than those for pyridine. The a values appear to be greater in the solvents of higher dielectric constant.

Altogether, the a values do not differ too greatly for a given salt in different solvents, nor do they differ too greatly from those in benzene, on the one hand, and dioxane–water mixtures, on the other.

b. Negative Ions.—

Negative ions of greatly different size are not as readily available as are positive ions. It is only in liquid ammonia that we are able to obtain stable negative ions with a variety of organic substituents. Before proceeding to a discussion of salts of these ions, we shall compare the dissociation constants of salts of the halide ions.

In Table VI are shown values of K and a for tetrabutylammonium chloride,[21] bromide and iodide[19] in acetone at 25° and for potassium salts of the same ions in liquid ammonia[22] at −33.3°. Values are also shown for NaBr in ammonia.

TABLE VI

K AND a VALUES OF HALIDE SALTS IN ACETONE AND AMMONIA

Salt	$K \times 10^4$	$a \times 10^8$	Salt	$K \times 10^4$	$a \times 10^8$
A. Acetone, $D = 20.5$			B. Liquid NH$_3$, $D = 22.4$		
Bu$_4$NCl	22.8	3.07	KCl	8.71	3.04
Bu$_4$NBr	32.9	3.51	KBr	18.9	3.77
Bu$_4$NI	64.8	4.71	KI	40.7	5.15
			NaBr	29.0	4.32

As may be seen from the table, the values of K and a increase markedly in both acetone and ammonia in going from chloride to iodide. The a values are not exceptionally large and are much the same for the salts of the different halides in the two solvents. Sodium bromide is a markedly stronger electrolyte than potassium bromide.

In Table VII are shown values of K and a for sodium and potassium salts in liquid ammonia[23] at −33.3°. The negative ions of these salts differ in size and constitution. It will be noted that the values of K for sodium and

(15) F. Accascina, E. L. Swarts, P. L. Mercier and C. A. Kraus, Proc. Nat. Acad. Sci., **39**, 1917 (1953).

(16) F. H. Healey and A. E. Martell, J. Am. Chem. Soc., **73**, 3296 (1951).

(17) L. M. Tucker and C. A. Kraus, ibid., **69**, 454 (1947).

(18) W. F. Luder and C. A. Kraus, ibid., **69**, 248 (1947).

(19) M. B. Reynolds and C. A. Kraus, ibid., **70**, 1709 (1948).

(20) (a) D. S. Burgess and C. A. Kraus, ibid., **70**, 706 (1948); (b) H. L. Pickering and C. A. Kraus, ibid., **71**, 3288 (1949).

(21) M. J. McDowell and C. A. Kraus, ibid., **73**, 3293 (1951).

(22) V. F. Hnizda and C. A. Kraus, ibid., **71**, 1565 (1949).

(23) (a) Nitrogen compounds: C. A. Kraus and W. W. Hawes, ibid., **55**, 2776 (1933); W. W. Hawes, ibid., **55**, 4422 (1933); (b) Oxygen compounds: C. A. Kraus and E. G. Johnson, ibid., **55**, 3542 (1933); (c) Tin compounds: C. A. Kraus and H. W. Kahler, ibid., **55**, 3537 (1933).

potassium amides are exceptionally small as are also the values of a. One suspects interactions other than Coulombic. We shall return to this point again.

TABLE VII

CONSTANTS OF ELECTROLYTES IN LIQUID NH₃

$D = 22.34, t = -33.3°$

Salt	$K \times 10^4$	$a \times 10^4$	Salt	$K \times 10^4$	$a \times 10^8$
NaNH₂	0.27	1.97	KNH₂BPh₃	130	10.4
NaNHPh	8.2	3.1	NaOPh	3.82	2.68
NaNPh₂	58	6.7	Naα–Naph	6.50	2.91
NaNH₂BPh₃	150	10.9	Naβ–Naph	8.08	2.99
NaSnPh₃	130	10.4	NaSEt	22.5	3.94
KNH₂	0.73	2.16	NaSPh	36.0	4.95
KNPh₂	50.5	6.0			

On substituting one phenyl group onto the amide ion, the dissociation constant of the Na salt is increased some 30-fold, on substituting a second phenyl group, the constant is again increased about 8-fold. Clearly the dissociation constant of these amide salts depends very definitely on the size of the negative ions. When the amide ion is complexed on triphenylboron, the value of K increases to 150×10^{-4}, more than 500 times that of sodium amide. In accord with the large size of the triphenylstannide ion, the dissociation constant of the sodium salt is 130×10^{-4}. The a values for the sodium salts seem reasonable. For NaNH₂BPh₃, a reaches the large value of 10.9 Å.

The K and a values for the potassium salts parallel those of the sodium salts but are a little smaller, as was noted above for the bromides.

When we consider the salts of phenolic compounds, we find the dissociation constants exceptionally low for these oxygenated compounds. For NaOPh, $K = 3.82 \times 10^{-4}$, while it is 8.2×10^{-4} for NaNHPh. The constants for the two naphthalates are markedly higher than that of the phenolate with that of the β compound much the larger.

The low value of K for the phenolates is due to the oxygen atom. If we replace oxygen by sulfur in the thiophenolate, the value of K is raised to 36×10^{-4}, nearly 10 times that of the corresponding oxygen compound. Even sodium ethyl sulfide has a constant nearly three times that of sodium phenolate. On the basis of the size of the oxygen and sulfur atoms, we would not expect so great a difference in the dissociation constants of the salts of the two phenolic types of ions.

It is of interest to compare the K and a values of quaternary ammonium salts with those of onium salts of elements other than nitrogen. In Table VIII are given values of K and a for salts of this type derived from phosphorus, arsenic, sulfur and iodine.[24]

TABLE VIII

CONSTANTS OF ONIUM SALTS IN ETHYLENE CHLORIDE

Salt	$K \times 10^4$	$a \times 10^3$
Bu₄NPi	2.26	5.77
Bu₄PPi	1.60	5.32
Bu₄AsPi	1.42	5.22
Bu₃SPi	0.449	4.38
Ph₂IPi	0.0233	3.43

It will be noted that K decreases as we go from nitrogen to arsenic. Obviously, it is not the size of the central atom of the onium ion that determines the effective size of the onium ion in the ion-pairs. As was to be expected, the constant for sulfonium picrate is markedly less than that of the corresponding compounds of the fifth group elements. Due to the size and shape of the iodonium ion, its picrate has a very small K value.

The a values for the quaternary onium salts do not differ greatly and seem of reasonable magnitude. The a value for iodonium picrates is rather small and indicates that the positive change is largely localized on the iodine atom.

3. Dependence of K on Constitutional Factors.

—The results already presented in the preceding section show clearly that constitutional factors have a significant effect on the dissociation

constant of electrolytes. In this section we shall examine how the introduction of negative atoms or groups into the ions affects the value of K.

When negative atoms or groups are introduced into the structures of organic acids, the dissociation constants of the acids are greatly increased. This is exemplified in such acids as picric and trichloroacetic acids. We have little information as to how the dissociation constants of salts of such acids are affected by the introduction of negative atoms.

We have meager data for solutions of acetates and monochloroacetates in ethylene chloride and in pyridine. In the former solvent, the constants for the acetate and the chloroacetate of octd·Me₃N⁺ are, respectively, 0.062 and 0.123 $\times 10^{-4}$. In pyridine, the constants for the acetate and the chloroacetate of octd·Bu₃N⁺, are, respectively, 3.88 and 3.90×10^{-4}. In ethylene chloride, the value of K is slightly greater for the chloroacetate; in pyridine, the presence of the chlorine atom has no effect.

We shall now consider salts in which negative atoms, or groups, are introduced into one of the alkyl groups of quaternary ammonium ions. In Table IX are shown K and a values for a number of salts whose cations contain negative atoms or groups.

TABLE IX

CONSTANTS FOR ONIUM SALTS WHOSE IONS CONTAIN NEGATIVE ATOMS

Salt	$K \times 10^5$	$a \times 10^8$	Salt	$K \times 10^5$	$a \times 10^8$
A. Ethylene chloride[25]					
C₂H₅(CH₃)₃NPi	4.6	4.38	BrC₂H₄(CH₃)₃NPi	1.32	3.90
HOC₂H₄(CH₃)₃NPi	0.66	3.56	BrCH₂(CH₃)₃NPi	0.78	3.65
CH₃OCH₂(CH₃)₃NPi	2.55	4.09	ICH₂(CH₃)₃NPi	1.10	3.74
ClC₂H₄(CH₃)₃NPi	1.25	3.78	(CH₃)₄NPi	3.2	4.20
B. Pyridine[26]					
C₂H₅(CH₃)₃NPi	8.2	6.22	BrCH₂(CH₃)₃NPi	4.8	5.39
HOC₂H₄(CH₃)₃NPi	1.5	4.12	(CH₃)₄NPi	6.7	5.94
BrC₂H₄(CH₃)₃NPi	5.8	5.62			

The effect of negative atoms in the substituent groups of ethyltrimethyl- and tetramethylammonium picrates is to decrease the value of K significantly. The introduction of OH into the ethyl group of the ethyltrimethylammonium ion decreases the constant from 4.6 to 0.66×10^{-5} in ethylene chloride. The methoxy methyl derivative, which is isomeric with the hydroxy derivative, has a K value of 2.55×10^{-5}. Thus, it is the hydroxyl group rather than the oxygen atom that is responsible for the decrease in K. The effect of chlorine is slightly greater than that of bromine when substituted in the ethyl group. The effect of bromine is greater than that of iodine when substituted in the methyl group.

These effects are small but they are consistent in both ethylene chloride and pyridine. In what manner the negative atoms affect the interactions between the ions is not obvious. They may lead to a redistribution of charge in the positive ion or they may introduce a dipole into the ion which interacts with the charge on the negative ion.

4. Systems in which Interactions Occur in Addition to those Due to Coulomb Forces.

—There are many systems in which interaction occurs between the ions of ion pairs which are not due to Coulomb forces. In such cases, the stability of the ion-pair is greater than it otherwise would be and the dissociation constant of the ion pair equilibrium is exceptionally small as is also the value of the Bjerrum parameter a. In other cases, reactions occur which involve non-ionic species. There may be systems in which covalent forces are involved.

(24) E. R. Kline and C. A. Kraus, J. Am. Chem. Soc., **69**, 814 (1947).

(25) D. J. Mead, R. B. Ramsey, D. A. Rothrock and C. A. Kraus, ibid., **69**, 528 (1947).

(26) D. S. Burgess and C. A. Kraus, ibid., **70**, 706 (1948).

a. **Hydrogen Bonding.**—In discussing solutions in benzene, we saw that the dissociation constant of Am_3NHPi is only 4×10^{-21} while its dipole moment is 13.3×10^{-18}. Quaternary ammonium salts having about the same dipole moment have a constant of about 15×10^{-18}. The low value of K for the picrate of the tertiary amine is doubtless due to hydrogen bonding.

In ethylene chloride, Bu_3NHPi[27] has a K value of 2.1×10^{-8} and an a value of 2.4 Å. These low values are undoubtedly the result of hydrogen bonding.

In Table X are shown values of K and a for a series of picrates from ammonium to tetrabutylammonium ions[28] in nitrobenzene.

TABLE X

K AND a VALUES FOR PICRATES OF PARTIALLY SUBSTITUTED AMMONIUM IONS IN NITROBENZENE

Ion	$K \times 10^4$	$a \times 10^8$	Ion	$\frac{K}{\times 10^4}$	$\frac{a}{\times 10^8}$
Bu_4N^+	>2000	>6.29	$BuNH_3^+$	1.49	0.992
Bu_3NH^+	1.90	1.02	NH_4^+	1.46	.990
$Bu_2NH_2^+$	1.56	0.997	$HO(CH_3)_3N^+$	0.17	.845

The precise value of K for Bu_4NPi is uncertain and the salt may even be unassociated. On replacing one butyl group by hydrogen, the value of K falls to 1.90×10^{-4}. On further substitution, the value of K decreases only slightly. The values of a are much too small considering the dipole moments of salts of this kind. If a hydrogen of the positive ion is coupled to nitrogen through oxygen as in the case of trimethylhydroxyammonium picrate, the constant falls to the low value of 0.17×10^{-4}. Clearly, the stability of ion-pairs of the incompletely substituted ammonium picrates is largely due to hydrogen bonding.

b. **Acid–Base Dissociation.**—When dissolved in a non-basic solvent and the acid and base of an electrolyte are sufficiently weak, the ion-pairs are in equilibrium with free ions on the one hand and with free acid and base on the other. The concentration of free acid and base will be proportional to the concentration of free ions. It has been suggested that the electrolyte exists in two forms, one of which is ionic and the other non-ionic, and that it is this last form which dissociates into free acid and base.[29] As we shall see presently, a non-ionic form is not present to an appreciable extent in solutions of pyridonium picrate in nitrobenzene. The presence or absence of a non-ionic form in solutions of sufficiently weak acids and bases might be demonstrated by means of dielectric measurements of solutions in a non-polar solvent such as benzene.

When the conductance data for pyridonium picrate in nitrobenzene are analyzed by the method of Fuoss, a linear plot is obtained, which extrapolates to a Λ_0 value of 22.5; this is obviously too low. On adding 0.001 N acid or base to the solvent, the acid–base dissociation is completely repressed and values of Λ_c and K may be obtained for the ion-pairs.

Knowing the value of Λ_0 and of K for the ion-pair equilibrium, the value of k for the acid–base equilibrium may readily be found. In Table XI are shown values of K and k along with the true values of Λ_0 as well as the false values of Λ_0 found on extrapolating the Fuoss plots for solutions in pure nitrobenzene.[28]

TABLE XI

ION-PAIR AND ACID–BASE DISSOCIATION CONSTANTS FOR SEVERAL SALTS IN NITROBENZENE

Salt	Apparent Λ_0	True Λ_0	$K \times 10^8$	$k \times 10^4$
$C_6H_5NH_3Pi$	2	52	2.0	80
$C_6H_5(CH_3)_2NHPi$	9.6	52	4.1	2.5
C_5H_5NHPi	22.5	54.8	5.54	0.163

Λ_0 values for the first two salts were approximated by means of Walden's rule. While values of K differ little for the three electrolytes, values of k increase greatly as the strength of the base decreases. For bases having dissocia-

tion constants of the order of 1×10^{-5} or greater, acid–base dissociation is negligible. Maryott[30] could find no evidence of the formation of a non-ionic form of tribenzylammonium picrate in benzene by means of dielectric measurements.

5. Alkali Metal Picrates.—Salts of the alkali metals are generally insoluble in most organic solvents other than alcohols and amines. However, the picrates of these metals are sufficiently soluble in nitrobenzene, acetone and pyridine to permit of determination of their dissociation constants.

In Table XII are given K and a values for lithium, sodium and potassium picrates in nitrobenzene,[28] acetone[19] and pyridine.[20a]

TABLE XII

CONSTANTS OF ALKALI METAL PICRATES IN SEVERAL SOLVENTS

	Nitrobenzene		Acetone		Pyridine	
Salt	$\frac{K}{\times 10^4}$	$\frac{a}{\times 10^8}$	$\frac{K}{\times 10^4}$	$\frac{a}{\times 10^8}$	$\frac{K}{\times 10^4}$	$\frac{a}{\times 10^8}$
LiPi	0.0004	0.61	10.3	2.50	0.83	3.61
NaPi	0.28	0.88	13.5	2.71	0.43	3.45
KPi	6.86	1.15	34.3	3.30	1.00	3.84

As may be seen from the table, the three picrates have very small dissociation constants in nitrobenzene. Lithium picrate, in particular, is an exceptionally weak electrolyte with a K value of only 4×10^{-8}. This contrasts with the constant of this salt in pyridine where $K = 0.83 \times 10^{-4}$. The constant in pyridine ($D = 12.01$) is 200 times that in nitrobenzene ($D = 34.8$). For nitrobenzene and acetone, K increases in the order K > Na > Li. In pyridine, however, K is larger for lithium than for sodium.

Actually, these picrates are weaker electrolytes than we might expect in all these solvents. The value of a is much lower than we should expect on the basis of Bjerrum's theory and ion dimensions. In general, this theory leads to a values that are larger than the distance between the ions in the ion-pairs as determined from dipole moments. For acetone, the a values are also lower than expected on the basis of ion dimensions and the same is true of solutions in pyridine, although the effect is less marked than in the other solvents.

The low values of K must be due to forces other than Coulombic. For lack of a better term, we may call these covalent forces. In nitrobenzene the ions must be unsolvated. This is indicated by the increase of K as we go from lithium to potassium. The ions may be solvated in acetone and they certainly are in pyridine. Presumably, in this solvent, Li^+ is more highly solvated than Na^+. That the ions are solvated in pyridine is shown by the fact that on addition of ammonia to solutions of their picrates, the conductance of Li^+ and Na^+ ions may be increased as much as 50%.[31]

As may be seen from Table VII, the K and a values for sodium and potassium amide in liquid ammonia are exceptionally small. The values of a are, respectively, 1.97 and 2.16×10^{-8}. Considering that the values of a for normal electrolytes are usually much larger than the distance between ions as obtained from dipole moments, it seems necessary to conclude that with these amides in liquid ammonia, as with the alkali metal picrates in nitrobenzene, the energy of the ion-pairs cannot be accounted for on the basis of Coulomb forces alone. In this connection, it might be pointed out that the salts of phenolic compounds, quite generally, have smaller a values than might be expected on the basis of ion size.

VI. Electrolytes Derived from the Less Electropositive Metals

Thus far we have been discussing salts of strongly electropositive ions with ions of varying degrees of electronegativity. We shall now consider elec-

(27) D. J. Mead, R. M. Fuoss and C. A. Kraus, *J. Am. Chem. Soc.*, **61**, 3257 (1939).

(28) C. R. Witschonke and C. A. Kraus, *ibid.*, **69**, 2472 (1947).

(29) M. A. Elliott and R. M. Fuoss, *ibid.*, **61**, 294 (1939).

(30) A. A. Maryott, *J. Research Natl. Bur. Standards*, **41**, No. 1, 7 (1948).

(31) C. J. Carignan and C. A. Kraus, *J. Am. Chem. Soc.*, **71**, 2983 (1949).

trolytes in which the negative ions are strongly electronegative while the positive ions vary in the degree of their electropositiveness. In the first case, with strongly electropositive ions, the dissociation constant of the ion-pairs, as we have seen, depends only on the size of the ions and the dielectric constant and temperature of the medium. In the second case, the dissociation constant is also dependent on the stability of the valence bonds of the compound and on the nature of the solvent medium. In the pure state or dissolved in non-basic solvents, these substances are weak electrolytes; when dissolved in suitable basic solvents, they may be strong electrolytes. The acids are typical examples of this class of substances.

We shall not discuss the acids but shall consider compounds of the less electropositive metals with strongly electronegative elements, such as the halogens. Practically all the metallic elements, with the exception of the alkali metals, the metals of the alkaline earths, the rare earth metals and the terminal elements of the 5th, 6th and 7th groups, belong to this class of substances. The number of different compounds that belong to this class is very large and our knowledge of them is very limited.

Furthermore, the terminal elements of groups 2, 3 and 4, form compounds in which one or more valences may be satisfied by alkyl or aryl groups. These compounds, also, exhibit electrolytic properties in suitable solvents. The organic derivatives of the 4th group elements are of particular importance; they are characterized by their stability toward oxygen. Compounds of the type R_3AX are of greatest interest. Here R is an organic group, A is the central metallic element and X is a halogen atom or negative group. The triarylmethyl derivatives of carbon are typical examples of this class. While only the aryl derivatives of carbon exhibit electrolytic properties, the trialkyl as well as the triaryl derivatives of the other 4th group elements exhibit electrolytic properties in suitable solvents.

1. Derivatives of Terminal Elements of Groups 2 and 3. a. AlX_3 in Pure Solvents.—Except for salts of some of the more electropositive elements of this class, such as magnesium and zinc in aqueous solutions and salts of less electropositive elements in a lower state of valence, such as thallous salts, we have more knowledge of aluminum halides than we have of any other derivatives of this class. In Table XIII are shown values of the molecular conductance, Λ_m, for aluminum bromide in pyridine, nitrobenzene and methyl bromide.[32]

TABLE XIII

CONDUCTANCE OF $AlBr_3$ IN DIFFERENT SOLVENTS

A. Pyridine, $D = 12.9$

$C \times 10^3$	0.713	0.296	0.129	0.0372	0.0107
Λ_m	29.0	42.0	59.4	97.4	150.0

B. Nitrobenzene, $D = 34.8$

$C \times 10^3$	38.16	16.33	6.42	1.143	0.338
Λ_m	3.36	3.28	3.14	3.57	6.94

C. Methyl bromide, $D = 10.6$

C	0.902	0.49	0.327	0.361
$\Lambda_m \times 10^2$	4.29	2.62	2.46	2.41

(32) W. J. Jacober and C. A. Kraus, J. Am. Chem. Soc., 71, 2405 (1949).

It will be noted that, in pyridine, $AlBr_3$ behaves like a strong 3-1 electrolyte. At $C = 1 \times 10^{-5}$ molar, $\Lambda_m = 150$; Λ_0 for 1-1 electrolytes in this solvent is of the order of 90. At $C = 1.07 \times 10^{-5}$, $AlBr_3$ in pyridine is dissociated to the extent of 55%; at $C = 3 \times 10^{-4}$, the dissociation is 15.5%. On the other hand, at $C = 3.4 \times 10^{-4}$ in nitrobenzene, $AlBr_3$ is dissociated to the extent of only 6.9%; the value of Λ_0 for a 1-1 electrolyte in nitrobenzene is approximately 33. Thus the dissociation of $AlBr_3$ in nitrobenzene of dielectric constant 34.8 is only about one-half that in pyridine of dielectric constant 12.0. The reason for this is, of course, that $AlBr_3$ complexes with more than one pyridine molecule, while it complexes with only one molecule of nitrobenzene.[33]

In Table XIII, are shown values of Λ_m for $AlBr_3$ in methyl bromide. Although this solvent is much more fluid than nitrobenzene, the conductance of $AlBr_3$ is about $1/200$ that in nitrobenzene. Obviously, the bromide is only slightly dissociated in CH_3Br, although the dielectric constant is 10.6 at 0°, not greatly different from that of pyridine. It is evident that when solvation does not occur, the dissociation process is very sensitive to the dielectric constant of the solvent.

Actually, the dissociation of $AlBr_3$ in nitrobenzene is much greater than is indicated above. Doubtless only one of the three bromine atoms dissociates from the aluminum atom to form ions. If only one of the three bromine atoms is involved, $AlBr_3$ is dissociated to the extent of about 20% at 3.4×10^{-4} molar in nitrobenzene.

b. Effect of Complexing Agents.—The effect of various complexing agents on the conductance of aluminum and gallium halides in different solvents has been investigated by Jacober[34] and by Van Dyke.[35]

In Fig. 3 are shown plots of the specific conductance of $AlBr_3$ in nitrobenzene at a concentration of about 0.1 m on addition of ammonia, trimethylamine and dimethyl ether. On addition of ammonia, the conductance passes through a flat maximum and then decreases to a minimum a little lower than that of the pure salt. On addition of trimethylamine, the conductance decreases continuously and almost linearly to a minimum value about one-half that of the pure salt. On addition of dimethyl ether, the conductance decreases to a value one-tenth that of the pure $AlBr_3$. The weaker the base, the greater is the conductance decrease on addition of base; and, in all cases, the minimum is reached on addition of one mole of base per mole of salt.

When the added base exceeds one mole per mole of salt, the conductance rises sharply. Obviously, a new process is setting in at that point. For additions of base less than mole/mole, the base complexes the aluminum atom by completing the electron octet. This tends to stabilize the bromine–aluminum bonds. Above a mole ratio of 1/1, the base complexes with the aluminum ions already present. Thus a new and larger positive ion is formed and the degree of dissociation increases as indicated by increased conductance.

The equilibrium of dimethyl ether with $AlBr_3$ is readily followed by the vapor pressure of the ether over the solution; the vapor pressure of nitrobenzene at 25° is only 0.45 mm. Up to one mole of added ether per mole of solute, all the ether combines with $AlBr_3$ and there is none in the vapor phase or in solution. For greater additions, there is an equilibrium in accordance with the reaction equation

$$Me_2OAlBr_3 + Me_2O \rightleftarrows (Me_2O)_2AlBr_2{}^+ \cdot Br^- \rightleftarrows$$
$$\text{I} \qquad\qquad \text{II} \qquad\qquad\qquad \text{III}$$
$$(Me_2O)_2AlBr_2{}^+ + Br^- \quad (1)$$
$$\text{IV}$$
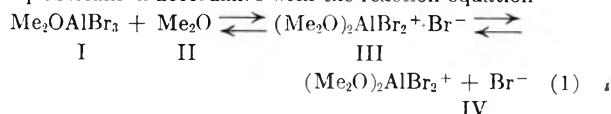
Assuming C_{IV} negligible in comparison with C_{III}, the constant of this equilibrium is in the neighborhood of 0.6 and varies somewhat with the concentration of $AlBr_3$. The amounts of the substances I, II and III + IV are readily found from the known vapor pressure of ether over the solution. Thus, the state of $AlBr_3$ in solution may be determined.

We may consider an example: a 0.301 m solution of $AlBr_3$ in nitrobenzene had a specific conductance of 12.46

(33) W. Nespital, Z. physik. Chem., B16, 153 (1932).

(34) W. J. Jacober and C. A. Kraus, J. Am. Chem. Soc., 71, 2049 (1949).

(35) (a) R. E. Van Dyke and C. A. Kraus, ibid., 71, 2694 (1949); (b) R. E. Van Dyke, ibid., 72, 2624, 3619 (1950); (c) R. E. Van Dyke and T. S. Harrison, ibid., 73, 575 (1951); (d) R. E. Van Dyke and H. E. Crawford, ibid., 73, 2022 (1951).
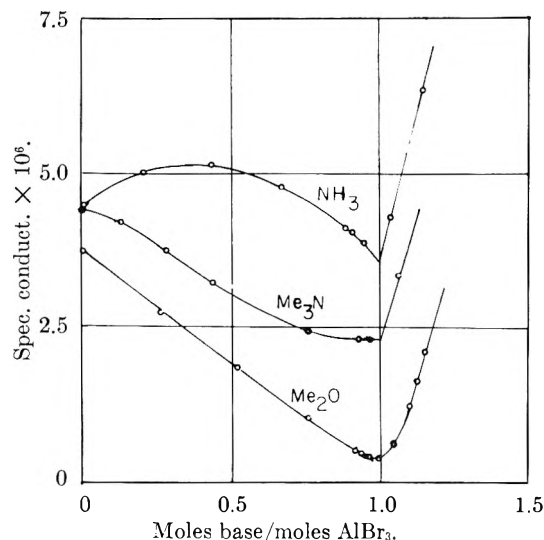
Fig. 3.—Conductance of AlBr₃ in nitrobenzene on addition of base.

Fig. 4.—Conductance of aluminum halides in MeBr on addition of Me₂O.

$\times$ 10^{-4} and a molecular conductance of 4.15. The mono-etherate in this solution had a specific conductance of 0.930 $\times$ 10^{-4} and Λ_m = 0.309. On complexing the mono-etherate with 0.163 mole of ether, the concentration of the dietherate (III + IV) was 0.049 m and the specific conductance of the solution was 4.18 $\times$ 10^{-4}. Allowing for the conductance of the monoetherate, the specific conductance of the dietherate was 3.4 $\times$ 10^{-4} and the molecular conductance of the dietherate was then 7.0.

Tetrabutylammonium bromide, a typical electrolyte, has a Λ_0 value of 33.5; at C = 5.5 $\times$ 10^{-3} N, Λ = 25.2. It seems certain that at a concentration of 0.05 N, Λ would be of the order of about 12 to 14. This is not taking account of the fact that a 0.3 m solution of AlBr₃ must have a much higher viscosity than the pure solvent. With a Λ value of 7 at a concentration of 0.049 m, it follows that the dietherate is dissociated into the free ions (Me₂O)₂AlBr₂$^+$ and Br$^-$ to the extent of 50% or more; the ionic complex is largely, if not completely, dissociated into its ions.

Jacober[34] has investigated the conductance of AlBr₃, MeAlBr₂ and Me₂AlBr in methyl bromide at 0° on addition of dimethyl ether. Typical results are shown in Fig. 4, where specific conductances are plotted against moles of added ether per mole of solute. The solutions had a concentration of approximately 0.3 m. For the solutions of AlBr₃ shown in the figure, the conductance rose from a value of 2.80 $\times$ 10^{-6} at the minimum to 137 $\times$ 10^{-6} on the addition of 2.66 moles of ether per mole of bromide. The minimum appeared on the addition of 0.95 instead of 1.0 mole. This was due to the presence of a small amount of basic impurity. The same effect was observed with nitrobenzene that had not been recrystallized.

For MeAlBr₂ and Me₂AlBr, the conductance rises sharply on addition of ether to maxima of 6.97 and 5.28 $\times$ 10^{-6} from values of 2.63 $\times$ 10^{-6} and 1.75 $\times$ 10^{-6}, respectively, in the pure solvents. In both cases, the maximum appears at about 0.7 mole of ether per mole of solute. The maximum is doubtless due to the fact that the solutes exist in bimolecular form and the dissociation of this form, on complexing with ether, is greater than that of the monomolecular form.

The striking fact about the methylated aluminum bromides is their behavior on adding ether beyond the 1:1 ratio. While the conductance of AlBr₃ rises sharply at this point, the conductance of the methylated bromides remains practically constant. The methylated compounds are weak electrolytes but they are definitely dissociated into ions. It seems that, when the aluminum atom is coupled with a methyl group, the ion which results on dissociation is incapable of coupling with an ether molecule. For this reason, the dissociation of the solute does not increase on adding ether beyond the 1:1 ratio. Here we have a case of dissociation in which ion-pairs are not involved even though a complexing agent is present.

2. **Electrolytes from Terminal Elements of Group 4.—** We shall discuss only compounds of the type R₃AX where R
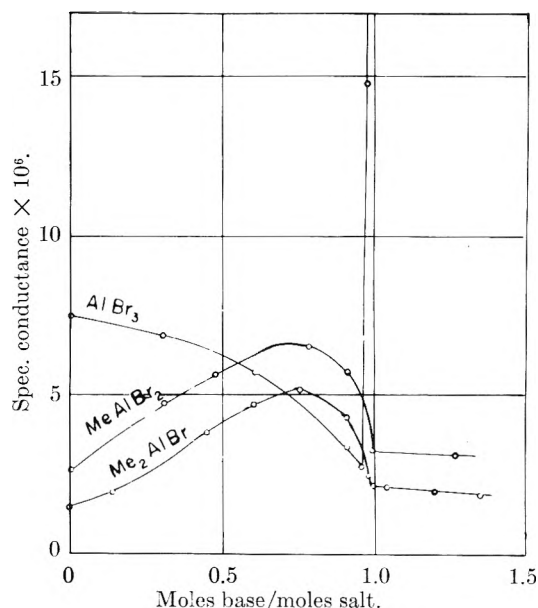
is an alkyl or aryl group. A is a tetravalent element and X is a negative atom. Groups of the type R₃A are amphoteric, they may exist in the free state or as loosely coupled dimers. With strongly electropositive elements, such as the alkali metals, they form strong electrolytes whose ions associate to ion-pairs in solvents of lower dielectric constant; their behavior is in every way normal.

The compounds of these groups with electronegative elements or groups, with a few exceptions, are non-ionic in the pure state. Dissolved in non-basic solvents, they are weak electrolytes; dissolved in basic solvents, they are electrolytes, the strength of which depends on the strength of the solvent base, the dielectric constant of the solvent and the nature of the substituent alkyl or aryl groups. With the exception of carbon, the compounds of the type R₃AX exhibit electrolytic properties under suitable conditions, irrespective of whether the substituents are alkyl or aryl groups. In the case of carbon, however, only the aryl derivatives exhibit electrolytic properties.

Witschonke and Kraus[28] have measured the conductance of Ph₃CBr in nitrobenzene from 6.5 $\times$ 10^{-2} to 6 $\times$ 10^{-4} N. At the lowest concentration, the equivalent conductance is 0.130, corresponding to a dissociation of about 0.4%. A plot of log Λ $vs.$ log C is linear but the slope is 0.55 instead of 0.5 which would be expected if Ostwald's dilution law held. The value of K computed on the basis of the dilution law is 1 $\times$ 10^{-8} for the most dilute point and 0.5 $\times$ 10^{-8} for the most concentrated. There are reasons for suspecting the presence of basic impurities in the solvent. Although the specific conductance of the solvent as prepared by fractional distillation was 1 $\times$ 10^{-10}, Van Dyke[35a] found that the conductance of AlBr₃ in this solvent was much greater than it was in one that had previously been treated with AlCl₃. Van Dyke found that even this solvent was not completely free from basic impurities which could be eliminated only by recrystallizing the nitrobenzene. It is, therefore, uncertain whether or not the triphenylmethyl halides are somewhat dissociated in non-basic solvents.

Triphenylmethyltetrafluoroboron is a strong electrolyte in nitrobenzene with a dissociation constant at least as large as 0.01. In this respect, it resembles the corresponding perchlorate.

The conductance of numerous different triarylmethyl compounds has been measured in a variety of solvents. With a few exceptions, the concentrations have been too high and the precision too low to permit of interpretation. However, Lichtin and Bartlett[36a] and Lichtin and Glazer[36b] have measured the conductance of a considerable number of different compounds in SO₂ under conditions that enabled them to evaluate dissociation constants satisfactorily.

(36) (a) N. N. Lichtin and P. D. Bartlett, J. Am. Chem. Soc., **73**, 5530 (1951); (b) N. N. Lichtin and H. Glazer, ibid., **73**, 5537 (1951).
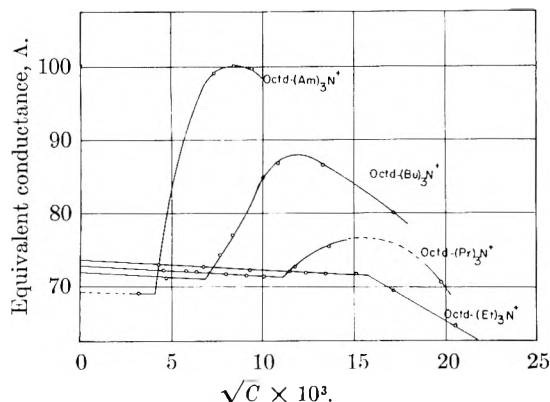
Fig. 5.—Conductance of micellar electrolytes in H_2O.

On the basis of conductance values of compounds of different structures in SO_2, Ziegler and Wollschitt[37] concluded that these compounds exist in solution in two forms, one ionic, the other covalent. The ionic form is in equilibrium with the free ions. For perchlorates, where a covalent bond cannot be formed with the carbon atom, structural factors were found to have little effect other than on ion mobility.

Lichtin and Bartlett measured a series of compounds all the way from triphenylmethyl chloride to tri-p-t-butylphenylchloromethane. The dissociation constants of the two extreme members of the series were found to be, respectively, 4.03×10^{-5} and 800×10^{-5}. These K values correspond to a values of 2.79 and 13.8 Å., respectively. There can be little doubt that the triphenylmethyl compound exists partly in a non-ionic form while the t-butylphenyl derivative exists largely in the ionic form whose dissociation constant is large. Some idea can be gained of the degree to which the phenyl derivative exists in the non-ionic form by assuming that the dissociation constant of the ionic form is much the same as that of the t-butylphenyl derivative.

Some writers are inclined to the view that the triarylmethyl perchlorates are completely dissociated into their ions in SO_2 at $0°$. This seems doubtful. While the measurements of Ziegler and Wollschitt[37] are not sufficiently precise to answer this question definitely, they do show that the conductance values are lower than predicted by Onsager's equation. In any case, the triarylmethyl compounds are much stronger electrolytes than we might expect on the basis of a dielectric constant of 15.6. Unfortunately, there are no adequate data for ordinary salts.

Conductance data for triarylmethyl compounds in basic solvents other than sulfur dioxide would be of interest. So also would be measurements with these compounds in non-basic solvents such as nitrobenzene. It would be of interest to investigate the equilibrium of the triphenylmethyl compounds with basic molecules in a non-basic solvent.

While all the elements of the carbon group form compounds of the type R_3AX, we have conductance measurements at lower concentrations for only trimethyltin chloride in ethanol[38] at $25°$. This chloride is a non-ionic compound melting at $37°$. It complexes with two molecules of ammonia, one of which is bound only weakly. It also complexes with other basic molecules. The mono-ammonia complex is quite stable and is insoluble in non-polar organic solvents; it vaporizes at higher temperature without melting.

The dissociation constant of Me_3SnCl in ethanol is 2.22×10^{-5} and the corresponding a value is 1.24 Å. It is apparent that Me_3SnCl is a weak electrolyte in ethanol and it may be concluded that here, as with the corresponding triphenylmethyl derivative, a non-ionic or covalent form is present.

The specific conductances of Me_3SnCl in nitrobenzene, acetone, pyridine and 95% alcohol are, respectively, 1.9×10^{-3}, 3.9×10^{-2}, 0.295 and 4.35 at $0.1\ N$.

VII.   Localized Ion-pairs: Micellar Electrolytes

In certain systems we meet with aggregates of ions all of which have the same charge which may

be either positive or negative. Examples of these are micellar or colloidal electrolytes, polyelectrolytes and ion-exchange resins. We shall limit ourselves to a brief discussion of micellar electrolytes.

Ions having long hydrocarbon chains, such as the soaps, form aggregates (called micelles) in aqueous solution or in water-rich solvent mixtures. Such electrolytes behave normally at low concentrations but with increasing concentration a point is reached where the properties begin to change in a different manner as concentration is increased. Thus, the conductances of such solutions decrease with increasing concentration in accordance with Onsager's theory. At a certain concentration, called the critical, the equivalent conductance suddenly follows a new course, either decreasing or increasing as concentration increases.

At low concentration, the electrolyte exists as simple ions; at the critical concentration, the long chain ions begin to form micelles. These micelles consist of a very large number of unit ions and the transference number of these micellar ions is much larger than that of the simple ions because per unit ion the resistance to motion is smaller for multiply charged ions than it is for simple ions. We should, therefore, expect that the equivalent conductance would begin to increase at the critical concentration. For most micellar electrolytes, it decreases. The reason for this is that the ions of the micellar structure interact with the counter ions to form ion-pairs on the micelle, thus reducing its effective charge.

The counter ions are under the action of the over-all charge on the micelles, but as an ion approaches a given unit charge on the micelle, it also interacts with that charge. The force between the counter ions and the single ion of the micelle is insufficient to produce a stable ion-pair. But when this force is supplemented by that due to all the charges of the micelle, ion-pairs are formed.

The stability of these ion-pairs depends on the size of the individual micellar ion as well as upon that of the counter ion. We should, therefore, expect that, with a given counter ion, the proportion of ion-pairs formed would be the smaller, the larger the individual micellar ion. If both ions are large, then we might expect that when the critical concentration is reached, the conductance would increase rather than decrease. For, if no ion pairs were formed on the micelle, the conductance would necessarily increase.

The effect of increasing the size of the substituent alkyl groups of a series of octadecyltrialkylammonium ions[39] is shown in Fig. 5. The bromate served as counter ion in all cases. With the tetraethyl derivative, ion-pairs are formed to such an extent that the conductance decreases at the critical point. With the propyl derivative, however, a smaller proportion of the counter ions forms ion-pairs, and the conductance increases. This increase becomes still larger with the butyl derivative and very large with the amyl derivative.

At solute concentrations not too far above the critical, the concentration of simple long chain ions remains substantially constant; any added electrolyte goes to form micelles. It is then possible to calculate the equivalent conductance of the micellar ions.[40]

At a concentration of $1.039 \times 10^{-5}\ N$, just below the critical, where there are no micelles, the conductance of octadecyltriamylammonium bromate is 68.97 which differs negligibly from Λ_0. At a concentration of 1.926×10^{-5}, the conductance is 73.21. The critical concentration is 1.625×10^{-5} and the conductance differs negligibly from that at $1.039 \times 10^{-5}\ N$. If we now compute the equivalent conductance of the micellar electrolyte, we obtain 114.32, an increase of approximately 65% in going from just below to just above the critical concentration.

VIII.   Dependence of K on Temperature

In a previous section, it was noted that the dissociation constant, K, is related to the product of dielectric constant times temperature, DT, by Bjerrum's equation. From this equation, it follows that in solvents of low dielectric constant, K

(37) K. Ziegler and H. Wollschitt, *Ann.*, **479**, 108 (1930).

(38) C. A. Kraus and C. C. Callis, *J. Am. Chem. Soc.*, **45**, 2624 (1923)

(39) M. J. McDowell and C. A. Kraus, *ibid.*, **73**, 2173 (1951).

(40) C. A. Kraus, *Proc. Nat. Acad. Sci.*, **39**, 1213 (1953).

will increase with temperature while in solvents of high dielectric constant, it will decrease. For, in the former solvents, D changes but little with temperature and DT increases, while, in the latter, D decreases greatly with increasing temperature and DT decreases. We have little in the way of quantitative data but it can be shown that Bjerrum's equation accounts for observations in a qualitative fashion.

In Table XIV are shown values of K and a for Am_4NI in benzene at $25°$[9] and $60°$.[11]

Table XIV

Constants of Am_4NI in Benzene at 25 and 60°

$t°$	25	60
$K \times 10^{18}$	21.8	126
$a \times 10^8$	5.94	5.82

In a temperature interval of 35°, K increases approximately 6 times. The value of a computed from the K values decreases markedly, indicating that, if K for 60° were calculated from the value of a at 25°, it would be larger than the observed. The value so calculated is 890 $\times 10^{-18}$, approximately 6 times the observed.

We have data for Am_4NNO_3 and Am_4NPi in anisole[11] ($D =$ 4.34) for the temperature range -33 to 95°. Assuming that the constants for the two triple ion equilibria have the same value,[42] dissociation constants for the ion-pair equilibria were evaluated at the different temperatures. For Am_4NNO_3, the K values increased from 2.1×10^{-11} at $-33°$ to 23×10^{-11} at 95°. The parameter a of Bjerrum's equation had a value of 4.91×10^{-8} and was constant within 1% over this entire temperature range. Similar results were obtained for this picrate.

There is some question as to the validity of the underlying assumption that the constants of the two triple ion equilibria have the same value. This assumption does not hold for electrolytes in benzene where K values may be derived from conductance measurements by means of Ostwald's dilution law at very low concentration. As of now, the results in anisole remain uncertain. The question could be resolved readily by means of conductance measurements in anisole at concentrations sufficiently low so that effects due to triple ions would be negligible and K could be evaluated by means of the dilution law.

In any case, the dissociation constant of salts in anisole increases with temperature, although much less than in benzene.

For solvents of higher dielectric constant, quantitative data relating to the dependence of K on temperature are very limited. Stern and Martell[43] have recently measured the dissociation constants of several salts in ethylene chloride over short temperature intervals. Their results for Bu_4NPi are shown in Table XV.

Table XV

K Values for Bu_4NPi in Ethylene Chloride at Different Temperatures

t, °C.	D	$K \times 10^4$ Obsd.	$K \times 10^4$ Calcd.
5.69	11.35	3.01	3.76
25	10.23	2.26	(2.26)
35	9.85	2.01	1.84

Observed values of K are shown in column 3. In column 4 are shown values of K calculated by means of Bjerrum's equation for 5.69 and 35°, based on $K = 2.26 \times 10^{-4}$ at 25°. It will be noted that the calculated, like the observed values of K, decrease with increasing temperature but the spread for the observed values is only 50% while that for the calculated values is 100%. Bjerrum's equation gives a qualitative but not a quantitative account of observed data.

(41) G. S. Bien, R. M. Fuoss and C. A. Kraus, *J. Am. Chem. Soc.*, **56**, 1860 (1934).

(42) R. M. Fuoss and C. A. Kraus, *ibid.*, **55**, 2387 (1933).

(43) K. E. Stern and A. E. Martell, *ibid.*, **77**, 1983 (1955).

While quantitative data relating to K as a function of temperature in solvents of higher dielectric constant are limited, there is no doubt that in such solvents K decreases with increasing temperature. This is clearly shown by conductance measurements; for solutions in solvents of dielectric constant greater than about 10 and in the concentration range between 0.1 and 0.01 N, it has been found that at low temperatures, the conductance increases with increasing temperature due to decreasing viscosity. But, as the temperature increases, the conductance increase decreases; the conductance passes through a maximum and, thereafter, continues to decrease until the critical temperature is reached. The lower the dielectric constant, the lower the temperature of the maximum at any given concentration. Thus for KI in methylamine ($D_{25°} = 9.4$), ammonia[44] ($D_{-33.3°} = 22.4$) and methanol[45] ($D_{25°} = 32.8$), the conductance maximum appears at -15, 25 and 150°, respectively.

At lower temperatures, the conductance increases because of the decreasing viscosity of the solution. As the temperature rises, ion association increases until the decrease due to association just offsets the increase due to increasing fluidity at the temperature of maximum conductance. Thereafter, association increases more and more with increasing temperature and the conductance continues to decrease. Since the concentration of the solution changes little with temperature in these conductance measurements, the conductance, either specific or equivalent, provides us with a rough measure of the increasing degree of association with increasing temperature. The true degree of association is greater than indicated by conductance because the fluidity of the solution increases with temperature and the observed conductance is greater than it otherwise would be.

In the dielectric constant range from 36 to 10, the change in K with decreasing dielectric constant is relatively small as may be seen from Fig. 1. When D falls below 10, the value of K decreases greatly as D decreases. It is for this reason that the conductance maximum lies at much higher temperatures for solvents of higher dielectric constant.

In Fig. 6, are shown plots of the conductance of KI in methanol through the critical region at a concentration of approximately 0.05 N. Plots are shown for three different phases, the liquid, the vapor and the gas phase above the critical point.

To illustrate the behavior of the systems in the immediate neighborhood of the critical point, the same data are plotted for this region on an expanded scale in the same figure. The conductance values (specific) are adjusted for change in the volume of the liquid phase.

As already noted, the conductance passes through a maximum at 150°. The curve is everywhere concave toward the axis of temperature but it is very nearly linear as it approaches the critical point which is about 242°. Beginning at about 235°, the conductance of the vapor phase becomes

(44) E. C. Franklin and C. A. Kraus, *Am. Chem. J.*, **24**, 83 (1900).

(45) C. A. Kraus, *Phys. Rev.*, **18**, 4089 (1904).
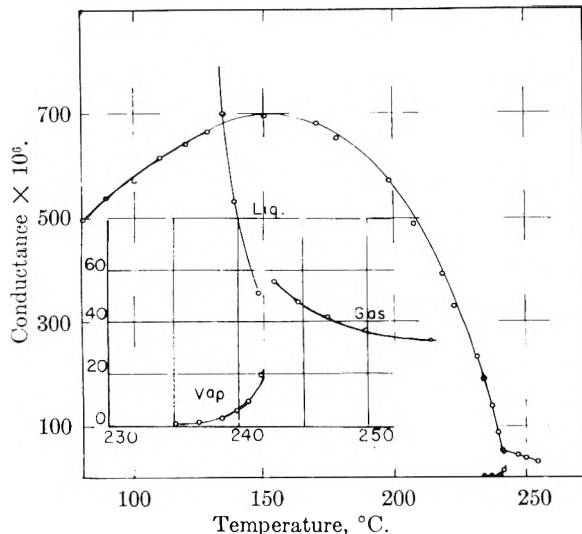
Fig. 6.—Conductance of KT in MeOH at high temperature.

appreciable and increases rapidly as the critical temperature is approached. Once the critical point has been reached, the conductance decreases slowly with increasing temperature.

The specific conductance of the solution at the maximum is 14.2×10^{-4}; at 240°, just below the critical, it is 1.66×10^{-4}; just above the critical (243.1°), it is 0.535×10^{-4}. At the temperature where the meniscus disappeared, the liquid volume was 0.31 the volume of the containing tube; above the critical point, the solution was contained in a volume 3.23 times that of the liquid at 241°.

If we make allowance for this expansion of the liquid phase, the conductance at 241° would be 0.514×10^{-4}. We should expect this value to be lower than that above the critical for, at 241°, a portion of the electrolyte was dissolved in the vapor phase whose volume was 2.2 times that of the liquid phase.

The conductance of KI just above the critical is 3.8% that of the same solution at 88°. The degree of association of the electrolyte in the critical region is very large but it is not complete.

IX. Reversal of the Association Process in Highly Concentrated Solutions

Taking into account the effect of the ion atmosphere, the law of mass action appears to apply satisfactorily to dilute electrolyte solutions. Even at higher concentrations, the ion-ion pair equilibrium conforms qualitatively to the law of mass action in that the degree of association of the ions increases with increasing concentration. It is obvious, however, that this association process cannot continue indefinitely, for, in the end, the fused salt is reached and in this we know the ions to be unassociated.

For every typical salt in any solvent of dielectric constant such that association occurs in less concentrated solutions, there is a concentration, C_m, at which the degree of association is a maximum. Toward lower concentrations, the degree of association decreases with *descending* concentration, toward higher concentration, it decreases with *increasing* concentration.

To exemplify this phenomenon, we shall consider some recent measurements with solutions of trimethylammonium bromide in bromine[6] at 25°. The bromide ion of this salt complexes with 1, 2 and 3 molecules of bromine forming compounds which melt, respectively, at 34, 5 and 1.5°. The first of these compounds is quite stable and may readily be handled at 25° in the supercooled state.

In Fig. 7 are shown plots of the equivalent conductance, Λ, and of the conductance–viscosity product, $\Lambda\eta$, as a function of the mole fraction, x, of the salt, $(CH_3)_3NH_2Br \cdot Br_2$. It will be noted that the conductance increases from a small value at the lowest concentration (4.23 at $x = 0.0142$) to a maximum of 37 at $x = 0.153$. Thereupon, the conductance decreases to a value of 7.4 at $x = 1$. The conductance decrease is due to the increasing viscosity of the solution; at the maximum ($x = 0.153$), the viscosity is 3 3 times that of bromine and, at $x = 1$, it is 27 times that of bromine.
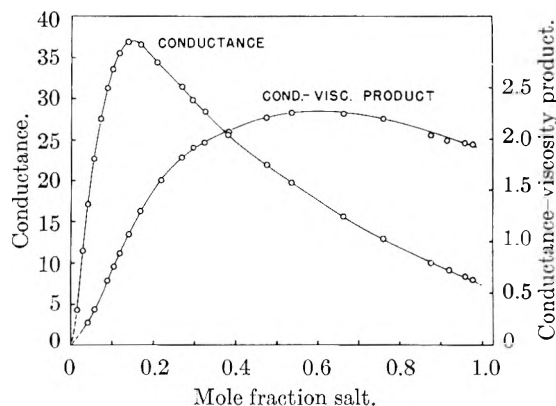
Fig. 7.—Λ and $\Lambda\eta$ product of Me_3NHBr in bromine.

If the degree of dissociation of the electrolyte and the mobility of its ions does not change, then, according to Walden's rule, the product $\Lambda\eta$ remains approximately constant. If $(\Lambda\eta)_0$ is the value of the product for the fused salt, then $\Lambda\eta/(\Lambda\eta)_0$ gives us an approximate measure of the degree of dissociation, γ, and the degree of association, $1 - \gamma$ of the ion-pairs.

At lower concentrations, the increase in $\Lambda\eta$ is due to the increasing dissociation of ion-pairs with increasing concentration. At $x = 0.33$, $\Lambda\eta$ reaches a value of 2, thereupon, it increases slowly to 2.27 at $x = 0.6$ and then decreases to 1.9 at $x = 1$. In the concentration range from $x = 0.33$ to $x = 1$, we are dealing with fused salt mixtures; for $x = 1$, it is $Me_3NH_2Br \cdot Br_2$; at lower salt concentrations we are dealing, also, with $Me_3NH_2Br \cdot 2Br_2$ and $Me_3NH_2Br \cdot 3Br_2$. That these solutions contain little free bromine is indicated by the low vapor pressure of these solutions. At $x = 0.33$, the vapor pressure is 20% that of bromine and at $x = 1$, it is 1%.

In Fig. 8 is shown a plot of the relative vapor pressure lowering, $\Delta p/p_0$. The broken line indicates the pressure lowering if Raoult's law applied. It will be noted that at low concentrations, the lowering is much smaller than required by Raoult's law. Since as many as 2 or more molecules of bromine are complexed with the bromide ion, the line should be drawn toward $x = 0.5$ rather than $x = 1.0$. In that case, the deviation from Raoult's law at low concentrations would be even greater. The very small vapor pressure lowerings at low concentration are doubtless due to association of the ion-pairs to quadripoles or more complex polyionic structures, much as in the case of solutions of electrolytes in benzene.

We can follow the association process by means of the values of $\Lambda\eta/(\Lambda\eta)_0$. In these calculations, we have assumed a mean value of 2.1 (at $x = 0.4$) for $(\Lambda\eta)_0$. We, of course, cannot calculate the value of $(1 - \gamma)$ very accurately when the degree of association is small but, for larger values of $(1 - \gamma)$, the approximation is not too greatly in error.

In Fig. 8, lower curve, is shown a plot of $1 - \gamma$ vs. x. It will be noted that at about $x = 0.4$, $(1 - \gamma)$ begins to increase greatly as x decreases. For $x = 0.27$, $(1 - \gamma) = 0.13$; for $x = 0.02$, $(1 - \gamma) = 0.96$. In other words, in diluting the solutions, roughly, in the ratio of 1 to 14, the degree of association increases from 13 to 96%.

In the range $x = 0.4$ to $x = 1.0$, we are dealing with a mixture of fused salts. There is little free bromine in the solution; the vapor pressure at $x = 0.4$ is about $1/10$ that of pure bromine. Altogether, there are 2.5 bromine molecules over and above that of the compound $Me_3NH_2Br \cdot Br_2$. Since compounds exist containing as many as two additional molecules of bromine, there is probably less than one molecule of free bromine present per molecule of salt at $x = 0.4$. Ion association sets in rapidly as free bromine appears in the fused mixture.

To speak of the dielectric constant of a concentrated solution has little or no meaning. Yet, it should be noted that the association process on adding a solvent to a fused salt depends on the dielectric constant of the solvent. When water is added to a fused salt, ion association does not occur. On adding butanol to fused Bu_4NPi, association sets in immediately[46] and continues until the solution becomes about 0.08 N, at which point about 80% of the salt is associated. At lower concentrations, the ion-pairs dissociate with decreasing concentration. So also in benzene, the degree of association increases with increasing concentration to a maximum in the neighborhood of 0.2 m. Thereafter, the degree of association decreases with increasing concentration.

X. Conclusion

The equation of Bjerrum is not an exact one. The parameter a does not yield the true distance between centers of charge of the ions in the ion-pairs; its value is dependent on the dielectric constant, the temperature and the nature of the sol-

(46) R. P. Seward, *J. Am. Chem. Soc.*, **73**, 515 (1951).
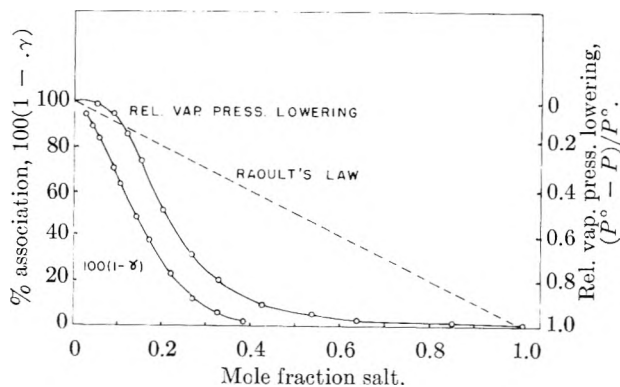
Fig. 8.—Vapor pressure lowering and % association of Me_3-NHBr in bromine.

vent medium. Nevertheless, the equation is a sufficiently close approximation to render it extremely useful in interpreting the properties of solution of typical electrolytes in a great variety of different solvents under rather widely varying conditions.

As for highly concentrated solutions, where the law of mass action suffers a reversal, no theory appears to be in sight at this time.

DIARYLIODONIUM SALTS. IV. ION-PAIRS AND COPPER CATALYSIS IN THE REACTIONS OF DIPHENYLIODONIUM IONS WITH HALIDE IONS AND HYDROXYLIC SOLVENTS[1,2]

By F. Marshall Beringer, Emil J. Geering, Irving Kuntz and Marvin Mausner

Contribution from the Department of Chemistry of the Polytechnic Institute of Brooklyn, Brooklyn, N. Y.

Diphenyliodonium chloride decomposed to chlorobenzene and iodobenzene by first-order kinetics rapidly in dimethylformamide and more slowly in diethylene glycol and by second-order kinetics very slowly in water. In diethylene glycol the competitive solvolysis was repressed by potassium chloride and removed by catalytic amounts of cuprous chloride, which greatly accelerated the formation of chlorobenzene (E_a dropped from 31 to 19 kcal./mole). The formation of chlorobenzene in the absence of catalyst is viewed as proceeding through the reversible formation and irreversible decomposition of diphenyliodonium chloride ion-pairs, while the solvolysis is viewed as proceeding through free diphenyliodonium cations. The catalyzed reaction may proceed through a complex between the diphenyliodonium cation and a copper(I) species, such as the dichlorocuprate(I) anion.

Introduction

About ten years after the discovery[3] of iodonium

(1) This paper is taken from the dissertations of Emil J. Geering, Irving Kuntz and Marvin Mausner, submitted in partial fulfillment of the requirements for the degree of Doctor of Philosophy in 1954, 1955 and 1956, respectively. The work has been reported in part at meetings of the American Chemical Society, in New York in September, 1954 (Abstracts of Papers, p. 97-O) and in Minneapolis in September, 1955 (Abstracts of Papers, p. 37-R).

(2) Previous papers: (a) F. M. Beringer, M. Drexler, E. M. Gindler and C. C. Lumpkin, *J. Am. Chem. Soc.*, **75**, 2705 (1953); (b) F. M. Beringer, A. Brierley, M. Drexler, E. M. Gindler and C. C. Lumpkin, *ibid.*, **75**, 2708 (1953); (c) F. M. Beringer and E. M. Gindler, *ibid.*, **77**, 3200, 3203 (1955).

(3) C. Hartman and V. Meyer, *Ber.*, **27**, 502, 1594 (1894).

salts, Büchner reported a preliminary study[4,5] of the decomposition of diphenyliodonium chloride and iodide to halogenobenzenes with light and heat. The decomposition of the chloride in aqueous solu-

$$C_6H_5\overset{+}{I}C_6H_5 - Cl \longrightarrow C_6H_5Cl + C_6H_5I \quad (A)$$

(4) E. H. Büchner, *Koninkliike Akad. v. Wettenschappen te Amsterdam, Proc. Sec. of Sciences*, **5**, 646 (1903) (in English).

(5) Büchner, ref. 4. "Very small quantities of acid retard the reaction to a remarkable extent or bring it to a standstill; the presence of traces of iodine causes a regular fall in the reaction coefficient; a little of the free base (diphenyliodonium hydroxide) accelerates, on the other hand, the decomposition in a strong degree. The halogenobenzenes formed during the reaction appeared however to be inert." See also footnote 23.

tion at 99.1° was reported to be of second order and to be strongly influenced by trace impurities.[5]

Fletcher and Hinshelwood[6] in 1935 found in a kinetic study of the decomposition of solid diphenyliodonium iodide to iodobenzene that most of the decomposition occurred in the liquid product phase, in which the energy of activation for the reaction was about 26 kcal./mole. In the next year Lucas, Kennedy and Wilmot[7] showed that 2,2'-dimethyldiphenyliodonium iodide on thermal decomposition yielded only 2-iodotoluene and concluded that the reaction was ionic rather than radical. Sandin, Kulka and McCready[8] later found that in the thermal decomposition of 4-methoxydiphenyliodonium halides at least 87% of the reaction proceeded with attachment of the halide to the unsubstituted ring. Further, Beringer and co-workers reported[2b] that while the decomposition of diphenyliodonium bromide in refluxing aqueous solution was about 90% complete in three weeks, comparable reactions of 2- and 3-nitrodiphenyliodonium bromide (to give 2- and 3-nitrobromobenzene and iodobenzene) were complete within two days. The evidence of these workers[2b] strongly indicated that many of the reactions of diphenyliodonium salts with bases occurred by nucleophilic attack of a base at a 1-carbon of a diphenyliodonium ion to give iodobenzene and a phenyl derivative of the base.

Reactions closely related to those considered above are the decompositions of sulfonium[9-14] and ammonium[9,15,16] salts. In a classical study in 1909, von Halban[9] investigated the decomposition of triethylsulfonium bromide to ethyl bromide and diethyl sulfide in hydroxylic and non-hydroxylic solvents. The rates were of first order over-all and

$$(CH_3CH_2)_3\overset{+}{S}\overset{-}{Br} \longrightarrow CH_3CH_2Br + (CH_3CH_2)_2S \quad (B)$$

generally less than one hundredth as fast in the hydroxylic solvents (paralleling an increase in the energy of activation). Taylor and Lewis[10a] and Corran[10c] reinvestigated this same reaction in a search for evidence for the radiation hypothesis of thermal chemical reactions.[17] Corran extended the range of von Halban's studies to mixed solvents and subjected the data to more critical analysis by correcting for the reverse reaction. Gleave,

Hughes and Ingold[11] have reported the first-order decomposition of trimethylsulfonium chloride and bromide in ethanol. Von Halban[9] and other workers[15] showed that quaternary ammonium halides decomposed in non-polar solvents to alkyl halides and tertiary amines in a manner similar to that of sulfonium salts.

Hughes, Ingold and co-workers have reported that with stronger bases (hydroxide, ethoxide and phenoxide ions) both trialkylsulfonium[11,12] and quaternary ammonium[16] salts reacted by second-order kinetics; for example

$$(CH_3)_3\overset{+}{S} + C_6H_5\overset{-}{O} \xrightarrow{C_2H_5OH} CH_3OC_6H_5 + CH_3SCH_3 \quad (C)$$
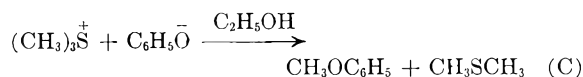
With alkyl groups larger than methyl the displacement (S_N2) reaction was in competition with the elimination (E2) reaction.[12]

These workers also found that t-butyldimethylsulfonium[13] iodide in water or ethanol and diisopropylmethylsulfonium[11] iodide or hydroxide in water solvolyzed at a rate proportional to cation concentration and independent of anion concentration. A typical reaction[13] was thus

$$\begin{array}{c} CH_3 \quad CH_3 \\ \diagdown \overset{+}{S}\!\!-\!\!\overset{|}{C}\!\!-\!\!CH_3 + 2H_2O \longrightarrow \\ CH_3 \quad CH_3 \end{array}$$

$$CH_3SCH_3 + (CH_3)_3COH + H_3O^+ \quad (D)$$
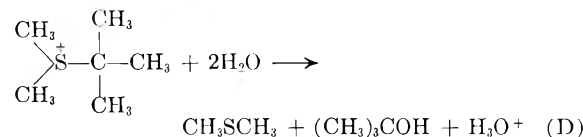
In the present work it was found that the diphenyliodonium halides reacted analogously to the previously studied sulfonium and ammonium halides.

Ion-pairs as Intermediates.[18] Symbols.[2c]— Quite recently Beringer and Gindler[2c] have proposed that the reactions between oppositely charged ions be considered as proceeding by the reversible formation of ion-pairs and their irreversible decomposition to products. The reaction of diphenyliodonium ions with phenoxide ions to give diphenyl ether and iodobenzene was examined in water–dioxane mixtures and found to be slow and of second order in water-rich mixtures and fast and of first order in dioxane-rich mixtures.

Let us tentatively assume a similar mechanism for the decomposition of the diphenyliodonium halides, and for the reaction scheme

$$R\overset{+}{I}R + \overset{-}{X} \underset{}{\overset{K}{\rightleftarrows}} R\overset{+}{I}R\,\overset{-}{X} \xrightarrow{k} RX + RI \quad (E)$$
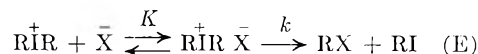
where R = phenyl and X = halogen, let the symbols be as follows.[2c] (For convenience some symbols not used until later are also defined here.)

A = concn. of free $R\overset{+}{I}R$

a = $A + C$; a_0 = initial concn. of iodonium cation

B = concn. of free $\overset{-}{X}$

b = $B + C$; b_0 = initial concn. of halide ion

C = concn. of ion pairs, $R\overset{+}{I}R\,\overset{-}{X}$

H = concn. of acid

k = first-order rate constant for the irreversible decomp. of $R_2\overset{+}{I}\,\overset{-}{X}$ ion pairs to products (see reaction E)

k_{cat} = first-order rate constant for decomp. of diphenyliodonium dichlorocuprate(I) ion-pairs or complexes to products (see reaction L)

(6) C. J. M. Fletcher and C. N. Hinshelwood, J. Chem. Soc., 596 (1935).

(7) H. J. Lucas, E. R. Kennedy and C. A. Wilmot, J. Am. Chem. Soc., 58, 157 (1936).

(8) R. B. Sandin, M. Kulka and R. McCready, ibid., 59, 2014 (1937).

(9) H. von Halban, Z. physik. Chem., 67, 129 (1909).

(10) (a) H. A. Taylor and W. C. McC. Lewis, J. Chem. Soc., Trans., 121, 665 (1922); (b) H. Essex and O. Gelormini, J. Am. Chem. Soc., 48, 882 (1926); (c) R. F. Corran, Trans. Faraday Soc., 23, 605 (1927).

(11) J. L. Gleave, E. D. Hughes and C. K. Ingold, J. Chem. Soc., 236 (1935).

(12) E. D. Hughes, C. K. Ingold and G. A. Maw, ibid., 2072 (1948); E. D. Hughes, C. K. Ingold and L. I. Woolf, ibid., 2084 (1948).

(13) E. D. Hughes and C. K. Ingold, ibid., 1571 (1933).

(14) Triphenylsulfonium bromide was recovered unchanged from attempts, in this Laboratory, to cleave it by prolonged heating with concentrated aqueous potassium hydroxide. Pyrolysis of the salt at 280° gave bromobenzene and diphenyl sulfide. Milton Scheiman, B.S. Thesis, Polytechnic Institute of Brooklyn, June, 1952.

(15) (a) E. Wedekind, O. Wedekind and J. Paschke, Ber., 41, 1029 (1908); (b) W. C. Davies and R. G. Cox, J. Chem. Soc., 614 (1937).

(16) E. D. Hughes, C. K. Ingold and C. S. Patel, ibid., 526 (1933).

(17) W. C. McC. Lewis, J. Chem. Soc., Trans., 109, 796 (1916).

(18) The first paper of footnote 2c gives leading references on ion-pair equilibria and ion-pairs as reaction intermediates.

k_m = exptl. rate constant for the over-all reaction between $R\overset{+}{I}R$ and $\overset{-}{X}$ of empirical m-th order in stoichiometric X^-

k_s = exptl. first-order rate constant for the solvolysis of the diphenyliodonium ion (see reactions F and G)

$K = C/AB$ = equil. constant for ion-pair association between $R_2\overset{+}{I}$ and X^- (see reactions E and I)

K_{cat} = equil. constant for ion-pair association (or complex formation) between $R_2\overset{+}{I}$ and $CuCl_2^-$ ions (see reaction K)

m = kinetic order in stoichiometric $\overset{-}{X}$
n = kinetic order in cuprous chloride as monomer

If as assumed[2c]

$$-da = -db = kC\, dt \qquad (1)$$

and $a = b$, then

$$d(1/B) - K\, d\ln C = kK\, dt \qquad (2)$$

On the basis of this mechanism it may be predicted that for diphenyliodonium halides in polar media where K is small, the rate of decomposition will be low because of the low concentration of ion pairs. Also, the kinetics will approach second order (eq. 3).[19]

$$d(1/b) = kK\, dt \qquad (3)$$

On the other hand, in less polar media where K for ion-pair formation by diphenyliodonium halides is relatively large, it may be predicted that the rate of decomposition will be greater, and the kinetics will approach first order (eq. 4).[19]

$$-d\ln b = k\, dt \qquad (4)$$

The experimental results presently reported are in accord with these predictions.

Decompositions in Dimethylformamide.—The decompositions of diphenyliodonium chloride, bromide and iodide in dimethylformamide were of first order in stoichiometric chloride ion (and over-all) to about 90% reaction. Table I summarizes the rate constant at various temperatures and gives the derived Arrhenius[20] (eq. 5) and Eyring (eq. 6) parameters.

TABLE I

DECOMPOSITION OF DIPHENYLIODONIUM HALIDES IN DIMETHYLFORMAMIDE[a]

Halide	k_1, hour^{-1} 60.0°	80.0°	100.0°	119.6°	log PZ,[b] sec.$^{-1}$	E_a,[c] kcal. mole^{-1}	$\Delta H\ddagger$,[c]	$\Delta S\ddagger$,[d] e.u.
Chloride	0.0047	0.076	0.91	8.1	15.4	32.4	31.7	8.6
Bromide	.0054	.100	1.04	8.6	15.4	32.3	31.6	9.6
Iodide	.0179	.233	2.12		13.9	29.3	28.6	2.9

[a] Initial concentrations were 0.04–0.08 mole/kg.; k_1 has been shown to be independent of initial concentration in the range 0.04–0.20 mole/kg. Duplicate runs at the three lower temperatures generally agreed within 2%. Because of the rapid decomposition of the salts at 119.6°, these rate constants were determined less accurately and were not used to calculate the activation parameters. [b] Calculated for 80.0°; estimated error ±0.2. [c] Estimated error ±0.3. [d] Estimated error ±2.

$$\ln k_1 = \ln PZ - E_a/RT \qquad (5)$$
$$\ln (k_1/T) = \ln R/Nh + \Delta S\ddagger/R - \Delta H\ddagger/RT \qquad (6)$$

As discussed in the preceding section, the first-order kinetics obtained here suggest that in this solvent diphenyliodonium chloride existed largely as ion-pairs. The rates at which these ion-pairs collapsed to give products increased with the nucleophilicity[21] of the halide ions, showing that the anions participated in the rate-determining step.[2b,22] The decompositions in a non-polar solvent of diphenyliodonium halides are thus similar kinetically[19] to those of sulfonium[9–11] and ammonium[9,15] halides.

In Table II are collected rate constants from runs in the presence of added compounds. First, it may be noted that rates were depressed 20–30% by added polar materials (water, hydrogen chloride, lithium chloride, lithium nitrate) present in about 1.5–3.5 times the initial concentration of the diphenyliodonium salt. These results are in accord with the results of von Halban[9] and of Corran[10c] on the effect of solvent polarity on the decomposition of triethylsulfonium bromide and with the concept that these polar materials solvate and stabilize the ion-pairs more than the transition states in their decomposition.

Earlier work on the decomposition of diphenyliodonium chloride in water (to be discussed in the next section) had disclosed the extreme catalytic efficiency of copper salts. In dimethylformamide cuprous and cupric chloride did accelerate the decomposition of diphenyliodonium chloride when present in ten down to 0.275 mole % of the initial concentration of iodonium salt. That copper salts are not as effective catalysts in dimethylformamide as in diethylene glycol (Table VII) or in water (Table IV) is an interesting observation. In diethylene glycol cuprous chloride decreases the energy of activation of the decomposition of diphenyliodonium chloride about 12 kcal./mole. Apparently, copper salts decrease the energy of activation in dimethylformamide also as the catalytic efficiency of these salts decreases with increasing temperature.

Decomposition in Water.—The decompositions of diphenyliodonium chloride and bromide in water, the first solvent studied, were very slow at 98.3°, the half-life of a 0.1 N solution being of the order of weeks.[23] Under these conditions there were found to be a number of complicating factors which in the present work precluded a rigorous kinetic analysis.

While the main reaction of the diphenyliodonium ions was with halide ions, hydrolysis was a competitive reaction. In a typical decomposition of one-tenth molar solution of

$$ROH + R\overset{+}{I} + H_3O^+ \underset{H_2O}{\overset{k_s}{\longleftarrow}} R\overset{+}{I}R + \overset{-}{X} \underset{}{\overset{K}{\rightleftharpoons}}$$

$$R\overset{+}{I}R\ \overset{-}{X} \overset{k}{\longrightarrow} RX + RI \qquad (F)$$
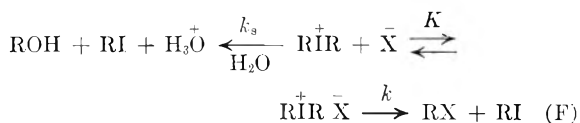
diphenyliodonium chloride in refluxing aqueous solution, about 90% of the diphenyliodonium ions reacted with chloride ions to give chlorobenzene and iodobenzene, while 10% reacted with water to give phenol, oxonium ion and iodobenzene. The main reaction was probably of second order: plots of reciprocal concentration with time were linear to 35–75% reaction and thus gave k_2, the empirical second-order rate constant. That the hydrolysis was of first order in diphenyliodonium ion is highly probable but not definitely proved.

(19) The first order decompositions of trialkylsulfonium halides (ref. 9, 10 and 11) and of quaternary ammonium salts (ref. 9 and 15) in organic solvents are rationalized by the concept that these salts exist there largely as ion pairs (or higher aggregates), the decomposition of which is unimolecular. In polar solvents such as water or glycerol the decomposition of these salts has not been studied successfully because the position of equilibrium is too close to the starting salts. However, with stronger bases, hydroxide, phenoxide and ethoxide ions, which give irreversible reactions, both the sulfonium salts (ref. 11 and 12) and the ammonium salts (ref. 16) react by second order kinetics, indicating that the reaction ions are mostly not paired. Compare the reaction of diphenyliodonium and phenoxide ions (ref. 2c).

(20) The pre-exponential factor is represented here by PZ, although this is not strictly appropriate, because the symbols A and B have been assigned to other quantities; see preceding section.

(21) C. G. Swain and C. B. Scott, J. Am. Chem. Soc., **75**, 246 (1953).

(22) That the anions are similarly involved in the decomposition of quaternary ammonium salts is shown by the fact that the relative rates of racemization in chloroform of optically active methylpropylphenylbenzylammonium chloride, bromide and iodide were approximately 1:5:25 (ref. 15a).

(23) As the work by Büchner (ref. 4) was found only at the end of the work here reported, all his claims were not directly checked. Thus in the present work there has been no evaluation of the effect of light, base or iodine on the rate of reaction between diphenyliodonium and chloride ions in water. Büchner reported no solvolytic reaction, while one was found in the present work. The acid formed in the solvolytic reaction did not appear to inhibit the main reaction, as acid (in higher concentration) was reported to do by Büchner. The main reaction was found in the present work to be much slower than reported by Büchner. Finally, while Büchner reported the product halogenobenzenes inert, the present workers found that they accelerated the decomposition of diphenyliodonium chloride, especially in the runs catalyzed by cupric chloride.

Table II

DECOMPOSITION OF DIPHENYLIODONIUM CHLORIDE IN DIMETHYLFORMAMIDE: EFFECT OF ADDED COMPOUNDS

Temp., °C.	a_0, moles/kg.	Added compd.	Concn.,[a] moles/kg.	k_1, hour⁻¹
60.0	0.05	...	...	0.0047
	.036	H_2O	0.054	.0048
	.039	DEG[b]	.028	.0049
	.04	LiCl	.145	.0038
	.04	CuCl	.00017	.0105
	.04	$CuCl_2$	.00011	.0084
80.0	0.08	...	...	0.079
	.04	CuCl	0.00016	.10
98.3	0.08	...	...	0.80
	.08	$LiNO_3$	0.164	.62
	.08	LiCl	.153	.56
	.08	HCl	.155	.61
	.08	$CuCl_2$	.00013	.87

[a] Concentration of added compound. [b] Diethylene glycol, $O(CH_2CH_2OH)_2$.

Relevant kinetic equations for the decomposition of diphenyliodonium halides in water follow, for the case where $a = b$. It has been shown that within experimental error diphenyliodonium chloride in water is completely dissociated.[24]

$$-db = kKab \ dt = k_2ab \ dt \tag{7}$$
$$dH = k_s a \ dt \tag{8}$$

Combining (7) and (8) gives (9).

$$\frac{-dH}{d \ln b} = \frac{k_s}{k_2} \tag{9}$$

Plots according to (9), such as those of Fig. 1, were indeed linear and gave the ratios of the rate constants, k_s/k_2. With
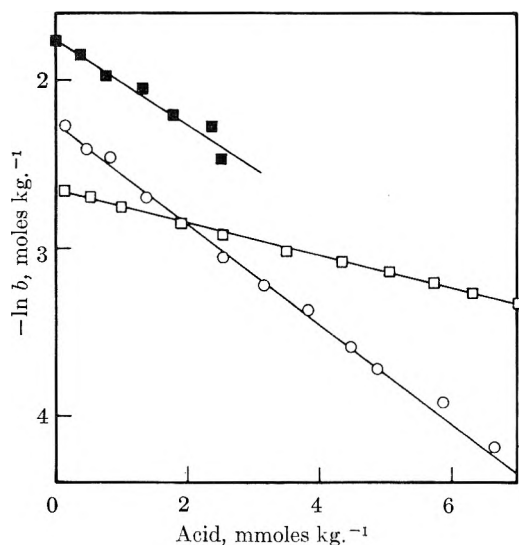
Fig. 1.—Determination of k_s/k_2 for the decomposition of diphenyliodonium chloride in water at 98.3°; see eq. 9. After each symbol are given: a_0 in mmoles/kg., $CuCl_2$ in µmoles/kg. and other added materials if present: ■, 172, —; ○, 107, 158; □, 70, 155, 523 mmoles/kg. of potassium p-toluenesulfonate and 5 ml. per kg. each of chlorobenzene and iodobenzene.

k_2 and k_s/k_2 both known, k_s was calculated. Tables III and IV give values for these constants as determined in water under different conditions.

(24) Conductimetric and cryoscopic measurements to be published later have shown that in water diphenyliodonium chloride is as dissociated as sodium or potassium chloride. See also E. C. Sullivan, *Z. physik. Chem.*, **28**, 523 (1899).

Table III

UNCATALYZED DECOMPOSITION OF DIPHENYLIODONIUM HALIDES IN WATER

X	Temp., °C.	a_0, mole/kg.	$10^3 k_2$, kg./mole hr.	$10^2 (k_s/k_2)$, mole/kg.	$10^5 k_s$, hour⁻¹
Cl	98.3	0.20	12	3.6	4.5
Cl	98.3	.17	38	3.7	14
Cl[a,b]	98.3	.07	3.4	15	5
Cl[a,c]	98.3	.08	9.9	..	..
Cl	80.1	.17	7.4	6.3	4.6
Cl	80.1	.17	4.1	2.1	0.9
Br	98.3	.06	39	3.0	11
Br	98.3	.06	14	5.1	7.2
Br	80.1	.04	11	6.4	7.3

[a] Iodobenzene and chlorobenzene, 5 ml./kg. each, added at the start of each run. [b] Potassium p-toluenesulfonate present, 0.582 mole/kg. [c] Sodium chloride present, 0.166 mole/kg.

A second complication lay in the lack of reproducibility of supposedly identical runs initiated at different times or with different batches of salt. Careful purification of the water and of the diphenyliodonium chloride caused lower rates of reaction, but not reproducible ones; the variation in rate constants was about three-fold. Indeed, it was this observation which led to the screening of metal salts for catalytic activity and brought to light the very strong catalysis by copper metal and copper salts. Thus the rate constants for the uncatalyzed decomposition of diphenyliodonium chloride and bromide in water are probably known only within a factor of perhaps three to five. Table III summarizes representative uncatalyzed runs. It is possible to say that the chloride and the bromide decomposed at approximately the same rate.[25] No reliable information is available regarding the effect of temperature on rates.

A final complicating factor in the decompositions in water was the accelerating effect of the second product phase of chlorobenzene and iodobenzene in copper-catalyzed runs.[26] The acceleration may have resulted from the distribution of the diphenyliodonium salt between the two phases, with a more rapid decomposition occurring in the organic phase. To hold this factor constant, 0.5 vol. % each of chlorobenzene and iodobenzene was added to some of the later runs; second-order kinetics were more closely followed.

Table IV summarizes the effect of micromolar amounts of cupric chloride on the decomposition of diphenyliodonium chloride in water, while Fig. 2 shows second-order plots of some typical runs. The second-order rate constant, k_2, is seen to increase with the concentration of cupric chloride, but not as fast as would be predicted by a simple proportionality. More striking is the constancy of the k_s/k_2 ratio while k_2 is increasing several hundred-fold.

Table IV

DECOMPOSITION OF DIPHENYLIODONIUM CHLORIDE IN WATER CONTAINING CUPRIC CHLORIDE AT 98.3°

a_0, moles/kg.	$CuCl_2$, moles/kg.	% linear[d]	k_2, kg./mole hr.	$10^3 (k_s/k_2)$, mole/kg.	$(10^3 k_s)$, hr.⁻¹
0.196	...	27	0.012	3.6	0.045
.078	3[a]	45	0.44	3.5	1.54
.104	96	68	3.0	3.5	10.2
.075	97[a]	62	3.7	3.5	12.8
.080	95[b]	80	1.8	2.7	4.9
.075	159[a]	59	4.8	4.0	18.9
.070	155[a,c]	51	3.0	11.2	33.8

[a] Iodobenzene and chlorobenzene, 5 ml./kg. each, added at the start of each run. [b] Sodium chloride 0.126 mole/kg. [c] Potassium p-toluenesulfonate present, 0.523 mole/kg. [d] Per cent. reaction to which second-order plot was linear from time zero.

(25) Diphenyliodonium iodide was not studied because of its low solubility in water.

(26) A similar acceleration was observed in the reaction between diphenyliodonium and phenoxide ions in water (ref. 2c).
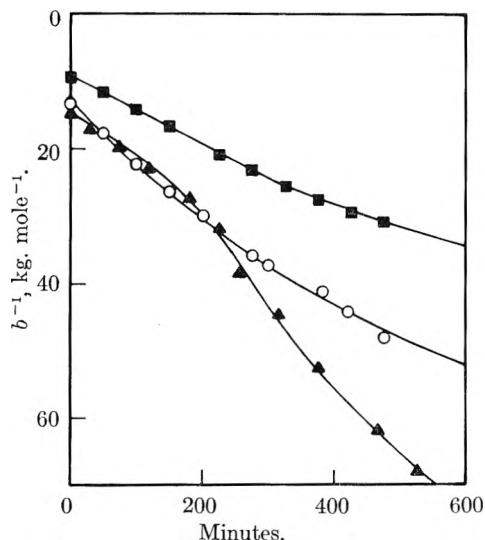
Fig. 2.—Second-order plots for the decomposition of diphenyliodonium chloride in water at 98.3° with cupric chloride. After each symbol are given: a_0 in mmoles/kg., $CuCl_2$ in μmoles/kg. and other added materials if present: ■, 104, 96.1; ▲, 69.5, 154; ○, 75.4, 159, 5 ml. per kg. each of chlorobenzene and iodobenzene.

These results permit, along with many others, the following tentative reaction scheme for the copper-catalyzed reactions. The diphenyliodonium cation complexes with a copper-containing species,[27] possibly to form an ion-pair. This complex now decomposes to products, either directly or on attack by halide ion. It is hoped that studies now in progress will give a further insight into the mechanism of catalysis by cupric chloride.

Decompositions in Diethylene Glycol.—As a solvent in which the decomposition of diphenyliodonium chloride might be conveniently studied, diethylene glycol had several advantages. First, starting materials, products and salts had conveniently high solubilities (thus avoiding the problem of a second phase). Next, there was a small solvolytic reaction of the diphenyliodonium ions competing with the predominant reaction with chloride ions (thus permitting a study of the relative effect of conditions on these two reactions). Finally, copper salts were found to be effective catalysts in this solvent.

Diphenyliodonium chloride[28] was found to decompose in diethylene glycol somewhat more slowly than in dimethylformamide.[29] In the decomposition of a 0.32 molar solution of this salt, a small amount of acid, corresponding to a six-tenths per cent. yield of hydrogen chloride, was formed, presumably according to the equation

$$\overset{+}{R}IR + (HOCH_2CH_2)_2O + \bar{C}l \longrightarrow$$

(R = phenyl)

$$RI + \underset{H}{\overset{+}{R}OCH_2CH_2OCH_2CH_2OH} + \bar{C}l \quad (G)$$

$$\Big\downarrow\Big\uparrow$$

$$ROCH_2CH_2OCH_2CH_2OH + HCl$$
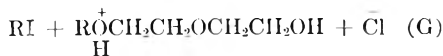
As it appeared that the hydrogen chloride formed in the solvolytic reaction catalyzed the decomposition of diphenyliodonium chloride to chlorobenzene and iodobenzene, attention was focused on the reaction at zero time, when $a_0 = b_0$. Table V collects the initial first-order rate constants obtained by extrapolating plots of algebraic first-order rate constants *versus* time to zero time. Since the data col-

(27) This is not known to be a copper(II) species because of the possibility of reduction in solution. For an example of such a reduction, see the later discussion of the catalyzed reaction in diethylene glycol.

(28) No other diphenyliodonium halides were studied in diethylene glycol.

(29) Von Halban (ref. 9) reported that triethylsulfonium bromide decomposed more slowly in hydroxylic than in non-hydroxylic solvents.
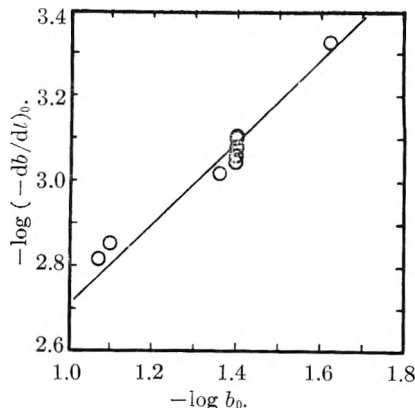
Fig. 3.—Determination of the kinetic order (*m*) in stoichiometric chloride ion for the uncatalyzed decomposition of diphenyliodonium chloride in diethylene glycol at 98.3°; see eq. 10.

lected in Table V do not demonstrate the kinetic order of the reactions, this was determined by plotting the data of Table V according to the empirical equation 10 as shown in

$$\log(-db/dt)_0 = m \log b_0 + \log(k_m)_0 \quad (10)$$

Fig. 3. From this graph *m* was determined to be 0.96; *i.e.*, the decomposition of diphenyliodonium chloride in diethylene glycol was indeed of the first order.

TABLE V

INITIAL FIRST-ORDER RATE CONSTANTS FOR THE DECOMPOSITION OF DIPHENYLIODONIUM CHLORIDE IN DIETHYLENE GLYCOL AT 98.3°

a_0, mole/kg.	$(k_1)_0$, hr.$^{-1}$	a_0, mole/kg.	$(k_1)_0$, hr.$^{-1}$
0.0240	0.0196	0.0400	0.0218
.0400	.0197	.0400	.0224
.0400	.0199	.0437	.0219
.0400	.0209	.0793	.0177
.0400	.0210	.0848	.0180

Av. $(k_1)_0$ 0.0203 ± 0.0013

Tentative mechanisms for the reactions of diphenyliodonium chloride in diethylene glycol might now be proposed.

$$\overset{+}{R}IR + \bar{C}l \underset{}{\overset{K}{\rightleftharpoons}} \overset{+}{R}IR\ \bar{C}l \overset{k}{\longrightarrow} RCl + RI \quad (E)$$

$$k_s\Big\downarrow O(CH_2CH_2OH)_2$$

$$RI + \underset{H}{\overset{+}{R}OCH_2CH_2OCH_2CH_2OH} + \bar{C}l$$

$$\Big\downarrow\Big\uparrow$$

$$ROCH_2CH_2OCH_2CH_2OH + HCl \quad (G)$$
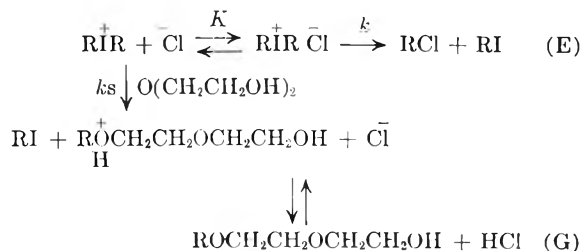
As in dimethylformamide the first-order kinetics are believed to arise from the existence of most diphenyliodonium and chloride ions in ion-pairs. Further, the magnitude of the solvolytic reaction reflects the amount of free diphenyliodonium cation in solution.

One way of *decreasing* the concentration of free diphenyliodonium ion would be the addition of a common ion salt which would shift the point of equilibrium toward the ion-pair by the mass effect.[30] The experiments with added potassium chloride reported in Table VI indicate that while a small amount of this salt was ineffective in influencing the magnitude of the solvolytic reaction, probably because potassium chloride is a weaker electrolyte in diethylene glycol at 98.3° than is diphenyliodonium chloride, a larger amount of potassium chloride did appreciably decrease the amount of acid formed. The experiments reported in Table VI were performed with the same batches of reagents

(30) C. K. Ingold, "Structure and Mechanism in Organic Chemistry," Cornell University Press, Ithaca, N. Y., 1953, p. 360 ff.

TABLE VI

THE DECOMPOSITION OF DIPHENYLIODONIUM CHLORIDE IN DIETHYLENE GLYCOL AT 98.3° IN THE PRESENCE OF ADDED SALTS

a_0	Moles/kg. KCl	KOTs[a]	$(100H/a_0)$[b]	$(k_1)_0$, hr.$^{-1}$
0.044	...	...	4.8	0.022
.038	0.008	...	4.5	.023
.038	.043	...	2.6	.022
.053	...	0.023	10.7	.020
.042	...	.045	16.5	.018
.040	...	.103	20.5	.012
.037	.038	.045	3.7	.022

[a] Potassium p-toluenesulfonate. [b] Per cent. of initial diphenyliodonium chloride which had produced acid after 24 hours.

and are strictly comparable. The fourth column of the table reports the acid formed after 24 hours as the percentage of the initial concentration of iodonium salt and serves as a
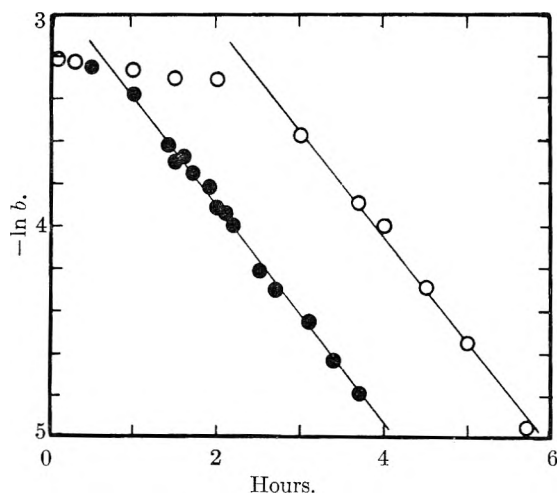
Fig. 4.—First-order plots of the decomposition of diphenyliodonium chloride in diethylene glycol at 98.3° catalyzed by copper salts (39 μmoles/kg.) ○, CuCl$_2$; ●, CuCl.
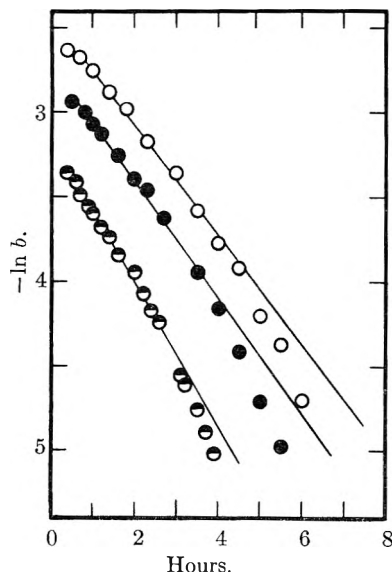
Fig. 5.—First-order plots of the decomposition of diphenyliodonium chloride in diethylene glycol at 98.3° catalyzed by cuprous chloride (37 μmoles/kg.); symbol, a_0: ◓, 40; ●, 60; ○, 80 mmoles/kg.
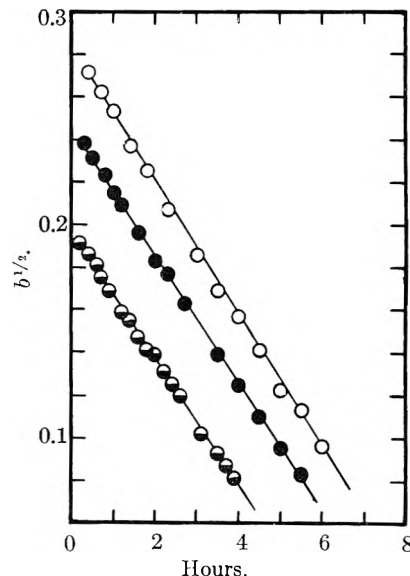
Fig. 6.—Half-order plots of the same runs as in Fig. 5.

convenient measure of the magnitude of the solvolytic reaction.

Other experiments were concerned with a method of increasing the concentration of free diphenyliodonium cation by enhancing the ionizing power of the solvent by the addition of an "inert" salt. In one experiment added potassium p-toluenesulfonate increased the solvolysis several-fold. Note, too, that while added potassium chloride did not affect the initial rate constant which measures the collapse of ion pairs to yield chlorobenzene, the rate constants obtained in the presence of added potassium tosylate were regularly smaller. These results suggest that in the presence of added tosylate ions the concentration of diphenyliodonium chloride ion-pairs was lowered. The result of the experiment with both potassium chloride and potassium tosylate present is interesting in that it suggests the "mass effect" is able to outweigh the influence of the tosylate salt and to reduce slightly the magnitude of the solvolytic reaction while leaving the rate constant for the collapse of ion-pairs unaffected.

Copper-catalyzed Decompositions in Diethylene Glycol.—Cupric chloride was found to be highly effective as a catalyst for the decomposition of diphenyliodonium chloride in diethylene glycol, as it had been found earlier to be in water. Product analyses showed the complete absence of acid, from the solvolytic reaction, with chlorobenzene and iodobenzene as the only isolated products. The absence of benzene and biphenyl in the products suggests that copper catalysis did not proceed by a mechanism involving free phenyl radicals.

TABLE VII

EFFECT OF COPPER SALTS ON THE DECOMPOSITION OF DIPHENYLIODONIUM CHLORIDE IN DIETHYLENE GLYCOL AT 98.3°

a_0, moles/kg.	CuCl$_2$ μmoles/kg.	CuCl	k_1,[a] hr.$^{-1}$
0.040	..	..	0.021[b]
.040	3.8	..	.049
.037	20	..	.19
.040	39	..	.49
.040	79	..	1.06
.040	..	20	0.20
.040	..	39	0.52

[a] For the runs containing cupric chloride these are the graphical limiting rate constants as shown in Fig. 4. [b] Average of six runs; see Table V.

Table VII represents some results from experiments with micromolar amounts of copper salts, while graphs such as those from which the data were obtained are given in Figs. 4, 5, 6; one graph indicates quite clearly that the early points in experiments with cupric chloride do not conform

to a first-order treatment. The rate constants for the cupric chloride experiments reported in Table VII were determined from the limiting slopes defined by the later points.

This behavior suggested that an induction period was operative in catalysis by cupric chloride. As the reaction proceeded the first-order rate constant increased over the initial few hours and then appeared to reach a limiting value. This behavior would be predicted if cupric chloride were not itself catalytically active but yielded a product which was the true catalytic species. These speculations led to experiments with cuprous chloride.

Experiments with cuprous chloride are shown in Figs. 4 and 5. These graphs indicate that the induction period was eliminated when cuprous chloride was used as catalyst. The agreement between the limiting rate constants for runs with cupric chloride and those with cuprous chloride was good; see Table VII. These results support the view that cuprous chloride was much more active than cupric chloride in catalyzing the decomposition of diphenyliodonium chloride in diethylene glycol and that the induction period observed was a reflection of the reduction of Cu(II) to Cu(I). Diethylene glycol containing cupric chloride was heated overnight and then used directly as solvent for the decomposition of diphenyliodonium chloride. A first-order graph of this run showed no induction period and was linear to about 80% reaction. The reduction of cupric to cuprous chloride may have been accomplished by the carbinol groups,[31] as in (H), or possibly by the peroxides rapidly

$$O(CH_2CH_2OH)_2 + 2CuCl_2 \longrightarrow$$
$$HOCH_2CH_2OCH_2CHO + Cu_2Cl_2 + 2HCl \quad (H)$$
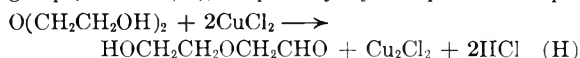
formed in trace amounts in the diethylene glycol.

To complete the study of catalysis by copper in its various valence states, an experiment was performed with copper powder. This experiment showed a long induction period during which the first-order rate constant gradually increased. After about five hours the curve steepened sharply, indicating a rapid disappearance of chloride ion. Thus copper metal itself could act as the source of the catalytic species.

Experiments were now designed for the determination of the kinetic order of the catalyzed reactions, i.e., the determination of m and n in equation 11, and are reported in Table VIII.

$$-db/dt = k_m b^m [CuCl]^n \quad (11)$$

TABLE VIII

CATALYZED DECOMPOSITIONS OF DIPHENYLIODONIUM CHLORIDE IN DIETHYLENE GLYCOL AT 98.3°

a_0, moles/kg.	CuCl$_2$ μmoles/kg.	CuCl	k_1,^{a} hour.$^{-1}$	$k_{1/2}$^{b}
0.040	39	..	0.49	0.057
.078	39	..	.32	.060
.040	..	37	.45	.057
.060	..	37	.35	.060
.080	..	37	.30	.063

^{a} First-order rate constants. For runs with cupric chloride these are the limiting rate constants. ^{b} Half-order rate constants for which units are mole$^{1/2}$ kg.$^{-1/2}$ hour^{-1}.

The experiments catalyzed by cuprous chloride indicated that the empirical first-order rate constant decreased about 33% on doubling the initial concentration of iodonium salt. This unexpected observation led to a re-examination of the kinetic order of the catalyzed reaction in stoichiometric chloride ion.

Equation 11 and the last three runs of Table VIII were used to determine the order of the reaction in chloride ion in a fashion similar to that used earlier for the uncatalyzed reaction. With this equation the apparent first-order rate constants were used merely as empirical constants to determine the initial rate of disappearance of stoichiometric chloride ion. From the graph based on equation 11, a value for the slope of 0.56 was obtained. This result suggested that the order of the reaction in stoichiometric chloride was one-half; i.e., $m = 0.5$ in equation 11.

(31) Compare the reported photochemically activated reduction of cupric to cuprous chloride by ethanol: F. P. Venable, J. Am. Chem. Soc., 21, 220 (1899).

With this result at hand, the first-order plots previously used for the determination of the rate constants for the catalyzed decomposition were re-examined. Such plots were satisfactorily linear to about 70% reaction. Beyond this range there was a downward drift of the experimentally observed points, indicating that the reaction was proceeding faster than expected for a first-order process. This drift in a first-order plot is in accord with a process of order less than unity. Figure 5 shows this behavior for the last three experiments described in Table VIII. Figure 6 plots these same experiments in a half-order fashion, the square-root of the stoichiometric chloride ion concentration versus time. There can be no question that this function better describes the data, the plots being linear to more than 90% reaction. The half-order rate constants which were obtained by doubling the slope of such plots are reported in Table VIII. Although the value for $k_{1/2}$ increased slightly as the initial concentration of iodonium salt was increased, this was probably a reflection of experimental variation. From the last three experiments of Table VIII at a concentration of cuprous chloride of 37×10^{-6} moles/kg., the half order rate constant was 0.060 ± 0.003 mole$^{1/2}$ kg.$^{-1/2}$ hour^{-1}. Re-examination of all the experimental results dealing with catalysis led to results similar to those just demonstrated in that the data were described more adequately by a half-order than by a first-order treatment. The balance of the half-order rate constants are collected in Table IX.

TABLE IX

HALF-ORDER RATE CONSTANTS FOR THE COPPER-CATALYZED DECOMPOSITION OF DIPHENYLIODONIUM CHLORIDE IN DIETHYLENE GLYCOL AT 98.3°

a_0, mole/kg.	CuCl$_2$ μmoles/kg.	CuCl	$k_{1/2}$^{a}
0.040	3.8	..	0.0073
.037	20	..	.029
.040	79	..	.11
.040	..	20	.029
.040	..	39	.065
.040	39^b	..	.063

^{a} Units are mole$^{1/2}$ kg.$^{-1/2}$ hour^{-1}. In experiments with cupric chloride, these are the limiting rate constants defined by the later points. ^{b} The cupric chloride had been heated in the solvent overnight before the introduction of the diphenyliodonium chloride.

After the conclusion that the catalyzed reaction was one-half order in stoichiometric chloride ion, the next question considered was the order of the reaction in cuprous chloride, that is the evaluation of n in equation 11. Figure 7 shows a plot of the half-order rate constant versus the concentration of copper halide in experiments with the same initial concentration of diphenyliodonium chloride. The linear nature of the graph indicates that over the range of catalyst concentrations employed the reaction is first-order in cuprous chloride, and n of equation 11 is unity.

Both unknowns of equation 11 have thus been determined, and the experimental rate expression can be written as 12 or 13; [CuCl]$_s$ represents stoichiometric cuprous chloride.

$$-db/dt = k_{1/2} b^{1/2} [CuCl]_s \quad (12)$$

$$-db^{1/2}/dt = \frac{k_{1/2}}{2} [CuCl]_s \quad (13)$$

It was of interest to attempt to devise a mechanism for the catalyzed decomposition of diphenyliodonium chloride in diethylene glycol which would yield a kinetic expression of the form observed.

$$R_2\overset{+}{I} + \overset{-}{Cl} \underset{}{\overset{K}{\rightleftarrows}} R_2\overset{+}{I} \overset{-}{Cl} \quad (I)$$

$$CuCl + \overset{-}{Cl} \longrightarrow CuCl_2^- \quad (J)$$

$$R_2\overset{+}{I} + CuCl_2^- \underset{}{\overset{K_{cat}}{\rightleftarrows}} R_2ICuCl_2 \quad (K)$$

$$R_2ICuCl_2 \overset{k_{cat}}{\longrightarrow} RCl + RI + CuCl \quad (L)$$
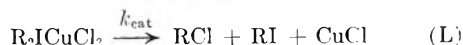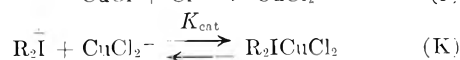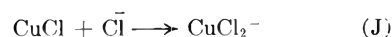
The sequence outlined involves the formation and decomposition to products of a diphenyliodonium cuprochloride
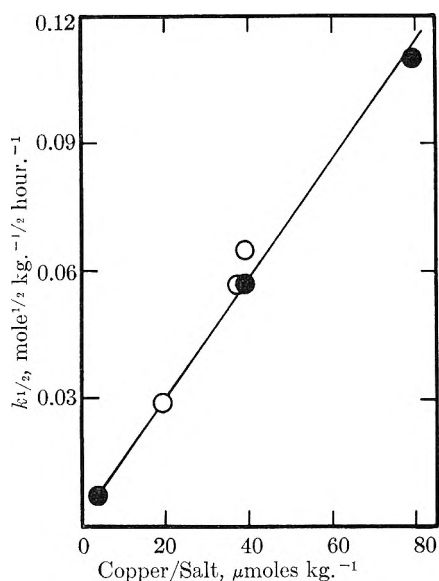
Fig. 7.—Determination of the kinetic order (n) in stoichiometric copper for the decomposition of diphenyliodonium chloride in diethylene glycol at 98.3° catalyzed by cuprous chloride, open circles, or cupric chloride, filled circles; see eq. 11. For runs with cupric chloride limiting rate constants are used; see Fig. 4 and Table VIII.

complex, which may simply be an ion-pair. The dichlorocuprate(I) ($CuCl_2^-$) ion has recently been described[32] as the catalytic species for the Sandmeyer reaction in water.

Since (L) is the only reaction which consumes chloride ions, a simple rate expression may be written, as equation 14.

$$-db/dt = k_{cat}[R_2ICuCl_2] \qquad (14)$$

Making use of the mass action relationship defined by (K), one may obtain an expression (15) which involves the concentration of free diphenyliodonium cation. Several simplifications are possible for this equation 15.

$$-db/dt = k_{cat}K_{cat}[R_2\overset{+}{I}][CuCl_2^-] = k_{cat}K_{cat}A[CuCl_2^-] \qquad (15)$$

It seems quite likely that throughout the reaction the stoichiometric concentration of cuprous chloride is present as the $CuCl_2^-$ species. For most of the experiments the concentration of diphenyliodonium chloride even at 99% reaction is a hundredfold greater than the concentration of catalyst. We can formalize this assumption as shown in equation 16. (The subscript s indicates stoichiometric cuprous chloride.) As

$$[CuCl]_s = [CuCl_2^-] \qquad (16)$$

mentioned previously, if diphenyliodonium chloride is a very weak electrolyte in diethylene glycol at 98.3°, then the stoichiometric chloride ion concentration is a good approximation of the concentration of ion pairs. Since the catalyzed reaction is free of the solvolytic mode of decomposition, the concentration of free diphenyliodonium ion is equal to the concentration of free chloride ion and is given by (17).

$$C \cong b = KAB = KA^2; \quad A = K^{-1/2}b^{1/2} \qquad (17)$$

The substitution of (16) and (17) into (15) gives (18)

$$-db/dt = k_{cat}K_{cat}K^{-1/2}b^{1/2}[CuCl]_s \qquad (18)$$

This expression is equivalent to empirical equation (12) if

$$k_{1/2} = k_{cat}K_{cat}K^{-1/2} \qquad (19)$$

Decompositions in Diethylene Glycol–Water.—The decomposition of diphenyliodonium chloride in various diethylene glycol–water mixtures was studied. The reaction mixtures were homogeneous throughout. The results shown in Table X indicate that adding water to diethylene glycol influenced the reaction in two ways. The initial first-order rate constant for the reaction which consumes chloride ion decreased as water was added to the reaction

(32) W. A. Cowdrey and D. S. Davies, *J. Chem. Soc.*, Supplement, 548 (1949); *Quart. Rev.*, **6**, 358 (1952).

Table X

DECOMPOSITION OF DIPHENYLIODONIUM CHLORIDE IN DIETHYLENE GLYCOL–WATER MIXTURES AT 98.3°

$a_0 = 0.040$ mole/kg.

% Water[a]	$(100H/a_0)$[b]	$(k_1)_0,$[c] hr.[-1]
0.0	3.75	0.021
0.1	11.0	.017
0.9	15.0	.014
9.1	52.5	.004
0.9[d]	0.00	.061[e]

[a] Weight % water. [b] The % of diphenyliodonium chloride which had produced acid after 24 hours. [c] Initial first-order rate constants. [d] CuCl present, 37 × 10^{-8} mole/kg. [e] Half-order rate constant, units mole$^{1/2}$ kg.$^{-1/2}$ hour^{-1}.

mixture.[33] When the solvent contained 9% by weight of water the rate constant was about one-fifth of that observed in the dry solvent. The other effect was the increase in acid formed as the solvent became more aqueous. In the solvent with 9.1% water, the acid produced after 24 hours corresponded to about 50% of the initial diphenyliodonium chloride. The data do not indicate whether in the wet diethylene glycol the solvolytic reaction involved water to yield phenol or diethylene glycol to yield 2-(2′-phenoxyethoxy)-ethanol; see reactions F and G.

The experiments with wet diethylene glycol are consistent with the mechanisms previously outlined which suggested the decomposition of diphenyliodonium chloride ion-pairs to give chlorobenzene and the solvolysis of free diphenyliodonium cations to give acid. The experimental results indicate that added water is effective in increasing the concentration of free cations at the expense of ion-pairs.

The result of the experiment with wet diethylene glycol (0.9% water) containing cuprous chloride was especially interesting. The half-order rate constant $(k_{1/2})$ was approximately that observed in the dry solvent. Even after 48 hours no acid had been produced, despite the extreme sensitivity of the solvolytic reaction to added water, as shown by the other data of Table X.

Activation Parameters.—From the temperature dependence of the uncatalyzed and catalyzed decompositions of diphenyliodonium chloride in diethylene glycol, the usual activation parameters have been calculated and are collected in Table XI. For the uncatalyzed reaction the rate constants are the initial first-order rate constants obtained by extrapolation of plots of k_1 versus time to zero time. At the various temperatures the data for the catalyzed reactions were excellently described by half-order graphs. The rate constants reported in the table have been corrected for the concentration of catalyst.

Table XI

ACTIVATION PARAMETERS FOR THE DECOMPOSITION OF DIPHENYLIODONIUM CHLORIDE IN DIETHYLENE GLYCOL

$a_0 = 0.040$ mole/kg.

79.4°	Rate constants 98.3°	119.3°	$\Delta H\ddagger$, kcal./mole	log PZ[a]	$\Delta S\ddagger$
0.01195[b,d]	0.0203[b,d]	0.193[b,d]	31	13	−1
408[c]	1550[c]	7350[c]	19	11	−9

[a] Units of PZ are the same as k, with time in seconds. [b] Initial first-order rate constants, units, hour^{-1}. [c] Cuprous chloride present, 37 × 10^{-6} mole/kg. The rate constant is that defined by equation 12 and was obtained from the empirical $k_{1/2}$ by dividing by $[CuCl]_s$. Units are kg.$^{1/2}$ mole$^{-1/2}$ hour^{-1}. [d] When 50% of the initial chloride ion had reacted, the mole % of the initial diphenyliodonium cation which had reacted by solvolysis at 79.4° was 23%, at 98.3° was 5%, and at 119.3° was 4%.

The energy of activation for the uncatalyzed decomposition of diphenyliodonium chloride in diethylene glycol was 31 kcal./mole, within experimental error the value found for the corresponding reaction in dimethylformamide. The decrease in the energy of activation when cuprous chloride is present is large, about 12 kcal./mole. It should be noted

(33) The decomposition of triethylsulfonium bromide in acetone was likewise slowed by the addition of water (ref. 9).

that according to equation 19 the temperature dependence of the catalyzed reaction is governed by the temperature dependence of a number of equilibrium and rate constants.

Conclusions and Discussion

(1) **Reactions with Anions.**—The present work substantiates the picture[2c] of reactions between ions of opposite charge proceeding by the reversible formation and irreversible decomposition of ion-pairs. With ion-pairs from 'onium salts the decomposition proceeds by nucleophilic displacement by the anion on the α-carbon of the 'onium cation. As the polarity of the solvent decreases, the kinetic order of such reactions between oppositely charged ions decreases from second to first order with an accompanying increase in the rate of the reaction.[2c] Even in solvents in which the decomposition is of the first order, rates of decomposition generally increase with decreasing solvent polarity[9] and concentration of salts.

Progress in the evaluation and prediction of K, the equilibrium constant for ion-pair formation, awaits a better understanding of electrolyte–solvent interactions.[34]

(2) **Solvolysis.**—From the work here presented it appears that the free, solvated diphenyliodonium ion is an intermediate in the reaction with water or diethylene glycol (solvolysis). There are only a few other examples of which the present authors are aware in which a similar difference in reactivity of free ions and ion pairs has been noted. Mitchell[35] showed that in reaction of sodium guiacoxide with ethyl iodide in ethanol only the free guiacoxide

(M)
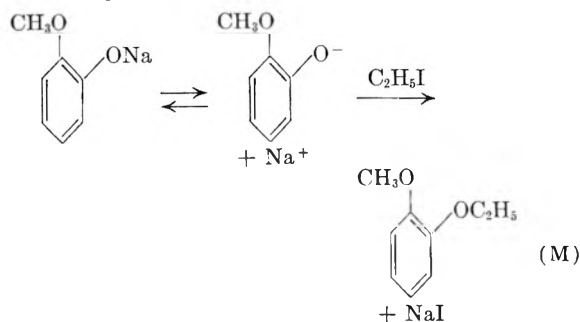
ions are effective. Similarly le Roux and Swart,[36] using radioactive lithium bromide to study isotopic exchange with alkyl bromides in acetone, distinguished between bromide ion in ion-pairs and free bromide ion as only the latter participates in displacement reactions. On the other hand Davies

$$\overset{*}{\text{Li}}\text{Br} \rightleftharpoons \overset{+}{\text{Li}} + \overset{*}{\text{Br}}^- \xrightarrow{\text{RBr}} \text{R}\overset{*}{\text{Br}} + \bar{\text{Br}} \quad \text{(N)}$$

and Wyatt[37] showed that barium thiosulfate ion-pairs are more reactive than free thiosulfate ions in the displacement of bromine from bromoacetate ions
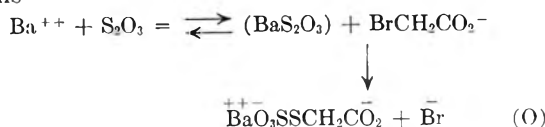
$$\text{Ba}^{++} + \text{S}_2\text{O}_3 = \rightleftharpoons (\text{BaS}_2\text{O}_3) + \text{BrCH}_2\text{CO}_2^-$$

$$\downarrow$$

$$\overset{++-}{\text{BaO}_3\text{SSCH}_2\text{CO}_2} + \bar{\text{Br}} \quad \text{(O)}$$

In the present case, then, it seems that the reaction of the diphenyliodonium cation with one of the water or glycol molecules of its solvent cage is inhibited by a paired chloride ion, which is probably located close to the iodine atom. This nearby chloride ion may inhibit the solvolysis by lowering the energy of the diphenyliodonium cation more than it does the energy of transition state for solvolysis (in which the positive charge is more widely distributed).

Hydroxylic solvents differ both in their ionizing power and in their nucleophilicity.[38] Thus while the concentration of free diphenyliodonium cations increases as the solvent is changed from diethylene glycol through water–diethylene glycol to water, the rate of solvolysis is intermediate in diethylene glycol, greatest in water–diethylene glycol and least in water; see Table X. It seems clear that diphenyliodonium cations solvated by diethylene glycol or by water and diethylene glycol solvolyze faster than diphenyliodonium cations solvated by water. Since in this solvolysis a positive charge is dispersed in going from the ground state to the transition state, the more polar solvent, water, would stabilize the ground state more than the transition state and thus slow the reaction of the solvated ions.

(3) **Catalysis by Copper Salts.**—On the work here presented four important questions may be posed concerning copper catalysis. First, in diethylene glycol why is the effective copper(I) species, presumably CuCl_2^-, a more effective nucleophilic agent than chloride ion? Second, in water and in dimethylformamide is there catalysis by a copper(I) species, a copper(II) species or by both? Thirdly, why is the effectiveness of copper catalysis (measured as the ratio of the rate constant of the catalyzed reaction at unit catalyst concentration to that of the uncatalyzed reaction) least in dimethylformamide, the solvent in which the uncatalyzed reaction was fastest and greatest in water, in which the uncatalyzed reaction was slowest? Finally, by what mechanism does some copper species accelerate the solvolysis of the diphenyliodonium cation in water while cuprous chloride inhibits its solvolysis in diethylene glycol?

It is only the first question to which possible answers may now be suggested. Edwards[39] has shown that nucleophilicity is related to oxidation-reduction potential. As the dichlorocuprate(I) ion is oxidized to cupric chloride at a lower potential than chloride ions are oxidized to chlorine, Edwards' scheme might suggest that the dichlorocuprate(I) ion should also be more nucleophilic than the chloride ion.[40]

It is also possible that the copper of the CuCl_2^- ion is bonded to the iodine atom (by d-orbitals presumably) while the chlorine makes its nucleophilic attack on carbon.

Work in progress is designed to answer some of the questions posed above.

(34) H. Sadek and R. M. Fuoss, *J. Am. Chem. Soc.*, **76**, 5897 (1954), and earlier papers of this series.

(35) J. A. Mitchell, *J. Chem. Soc.*, 1792 (1937).

(36) J. L. le Roux and E. R. Swart, *ibid.*, 1475 (1955).

(37) C. W. Davies and P. A. H. Wyatt, *Trans. Faraday Soc.*, **45**, 770 (1949); P. A. H. Wyatt and C. W. Davies, *ibid.*, **45**, 774 (1949).

(38) For a consideration of the ionizing power and nucleophilicity of hydroxylic solvents see S. Winstein and E. Grunwald, *J. Am. Chem. Soc.*, 828 and 846 (1948), and S. Winstein, E. Grunwald and H. W. Jones, *ibid.*, **73**, 2700 (1951).

(39) J. O. Edwards, *ibid.*, **76**, 1540 (1954).

(40) This suggestion omits, for lack of data, a consideration of Edward's second factor, involving the pK_a's of the conjugate acids of chloride and dichlorocuprate(I) ions.

Experimental[41]

Starting Materials. Diphenyliodonium Chloride.—A suspension of potassium iodate (200 g., 0.93 mole) in acetic anhydride (200 ml.) and benzene (180 ml., 2.0 moles) was prepared by rapid stirring and cooled to 0–5°. Separately, a solution of concentrated sulfuric acid (140 ml., 2.6 moles) in acetic anhydride (200 ml.) had been prepared by adding the acid with stirring to a cooled solution of the anhydride; during the addition the temperature did not exceed 20°. The cooled acetic anhydride–sulfuric acid solution was slowly added[42] to the vigorously stirred benzene–iodate mixture at 0–5°. The addition required 2.5 hours. Stirring was continued while the reaction mixture warmed to room temperature and thereafter for 48 hours.

The reaction mixture was then cooled to 5°, and 400 ml. of twice-distilled water was added at such a rate that the temperature of the suspension did not exceed 10°. Ether (150 ml.) was added to the reaction mixture, which was stirred for five minutes and then filtered to remove potassium salts. Two further extractions with ether and one with petroleum ether followed. A solution of 100 g. of ammonium chloride in 300 ml. of twice-distilled water was added, and the precipitated diphenyliodonium chloride was collected by suction filtration. Addition of ammonium chloride to the filtrate gave a second crop of crystals. A further yield of diphenyliodonium bromide or diphenyliodonium iodide could be obtained from the mother liquor by addition of aqueous sodium bromide or iodide.

The combined crude diphenyliodonium chloride was crystallized from approximately one liter of redistilled methanol, using activated carbon. A first crop (157 g.) and a second crop (28 g.) were obtained (63% yield) of m.p. 228–229° (cor., dec., into bath at 210°).

Diphenyliodonium bromide and iodide were prepared as above except that the precipitations were by sodium bromide or potassium iodide rather than by ammonium chloride. After recrystallization from methanol, these salts had melting points of 231–232° (cor., dec.) and 182–183° (cor., dec.), respectively.

All iodonium salts were recrystallized three times from methanol before use in kinetic runs. Samples were stored in brown bottles at 0–5°. After a year of storage, diphenyliodonium chloride showed no change in its rate of decomposition in dimethylformamide.

Water for kinetic runs was obtained by redistilling ordinary distilled water through all-glass apparatus. Dimethylformamide obtained from Matheson, Coleman and Bell was redistilled, b.p. 152–153°. Diethylene glycol from the same source was redistilled under nitrogen with only the middle fraction, b.p. 108° (2.5 mm.), n^{25}_D 1.4464 used.

Copper Salts.—Fisher Certified Reagent cupric chloride and Eimer and Amend Tested Purity Reagent cuprous chloride were used. For some runs in diethylene glycol dilute stock solutions of the copper salts in that solvent were prepared.

Potassium p-toluenesulfonate prepared from p-toluenesulfonic acid and potassium hydroxide was crystallized from methanol. An aqueous solution of this salt was neutral and free of halide ions.

Kinetic Runs.—Runs were made in 200–300 ml. round-bottomed flasks with long necks fitted with standard taper joints. The flasks were used with short condensers and pipets which reached through the condensers almost to the bottom of the flasks. For decompositions run in water the condensers were topped by small mercury-filled U-tubes. Some of the later experiments were performed in flasks with built-in pipets and a small paddle stirrer.

Analyses. Determination of Acid.—Aliquots of the kinetic solutions were removed, added to 125-ml. erlenmeyer flasks cooled in an ice-bath, weighed and titrated with 0.01 N sodium hydroxide using a mixed indicator[43] of brom cresol green and methyl red which undergoes its color change at pH 5.1. When the titer was small, a 5-ml. buret calibrated

to 0.01 ml. was used. **Determination of Halide Ion.**—Aliquots of runs in diethylene glycol or dimethylformamide were diluted with redistilled methanol before titration. Aqueous mercuric nitrate (0.02 N) stabilized with nitric acid and standardized against the three times recrystallized corresponding diphenyliodonium halide was used for titration, with one drop of 10% aqueous sodium nitroprusside per five ml. of final solution added as indicator.[44]

Large-Scale Decompositions. Diphenyliodonium Chloride in Diethylene Glycol Containing Cuprous Chloride.—A solution of diphenyliodonium chloride was prepared from 0.2 mole of the salt in 500 ml. of diethylene glycol containing cuprous chloride (21 μmoles/kg.). After being heated at 90–100° for four days, the reaction mixture was distilled. All material boiling up to 225° was collected, the heavy oil in the distillate was separated, and the upper layer was diluted with 100 ml. of saturated sodium chloride solution and extracted three times with 15-ml. portions of ether. The ether extracts were combined with the original heavy oil.

The residue in the still-pot was diluted with one liter of water and directly steam distilled. The heavy oil so obtained was combined with the previous yield. After the ether had been removed, the residue was fractionated to give chlorobenzene (20.95 g., 93% yield) of b.p. 132–135°, n^{25}_D 1.523, and iodobenzene (37.2 g., 91% yield) of b.p. 53–59° (8 mm.), n^{25}_D 1.615.

Diphenyliodonium Chloride in Diethylene Glycol.—A solution identical to that used in the previous experiment was prepared except that no catalyst was employed. The solution was heated at 90–100° for eleven days, after which time the titration of an aliquot indicated a concentration of acid 2.2×10^{-3} mole/kg., corresponding to a 0.6% yield of acid. The reaction mixture was worked up as described in the previous experiment. Chlorobenzene (19.1 g., 85% yield) was collected at atmospheric pressure and iodobenzene (33.7 g., 83% yield) at 10 mm.

Diphenyliodonium Chloride in Dimethylformamide.—Fifty grams of diphenyliodonium chloride (0.16 mole) dissolved in 400 g. of dimethylformamide was held at 100° for one day, when analysis for chloride ion indicated 99.5% reaction. To the reaction mixture was added 1.5 liters of water saturated with ammonium chloride, with separation of a second phase. The aqueous layer was extracted five times with 50 ml. of petroleum ether of b.p. 33–37°. The combined organic layers were dried and distilled to give 14.5 g. of chlorobenzene, b.p. 129–131°, n^{25}_D 1.516–1.519 (compared to 1.523 for pure chlorobenzene) and 26.0 g. of iodobenzene, b.p. 188.5–189° (corr.), n^{25}_D 1.616–1.617 (compared to 1.618 for pure iodobenzene).

Since 43.7 g. of the reaction mixture had been withdrawn for analyses, the theoretical yields of chlorobenzene and iodobenzene were 15.9 and 28.9 g., respectively. Isolation of chlorobenzene and iodobenzene from a synthetic mixture in dimethylformamide as above gave a 92.4% combined recovery.

Decompositions of Diphenyliodonium Chloride in Water.—Fifty grams (0.158 mole) of diphenyliodonium chloride in 1500 ml. of water was decomposed by heating at reflux according to three different procedures: (A) no catalyst; insolubles were collected as formed in a Dean-Stark trap; (B) no catalyst; reaction under simple reflux; (C) 18 μ moles of cupric chloride present; reaction under simple reflux. At the termination of the reaction, acid and chloride ion were determined. The results are summarized in Table XII.

Table XII

Decomposition of 158 Mmoles of Diphenyliodonium Chloride in 1500 Ml. of Water at Reflux

	Procedure		
	A	B	C
Final chloride ion	26.4[a]	14.5[a]	42[a]
Final acid	22.2[a]	15[a]	7.9[a]
Iodonium reacted	153.8[a]	158[a]	116[a]
% Chloride reaction	85.5	90.5	93.6
% Water reaction	14.5	9.5	6.4

[a] Millimoles.

As a check on the analytical procedure reaction C was worked up in a standard way to give 109 mmoles of chlorobenzene, 114 mmoles of iodobenzene and 6.2 mmoles of phenol (as 2,4,6-tribromophenol, m.p. 93–94°).

(41) Boiling points and melting points are uncorrected unless otherwise noted.

(42) It was found that temperature control was critical and that the addition of the acid mixture should be halted immediately if the temperature exceeded 10°. Other workers have experienced highly exothermic reactions when the sulfuric acid–anhydride mixture was added too quickly or when stirring was not efficient.

(43) I. M. Kolthoff and E. B. Sandell, "Textbook of Quantitative Inorganic Analysis," Third Ed., The Macmillan Co., New York, N. Y., 1952, p. 432.

(44) I. M. Kolthoff and E. B. Sandell, ref. 43, p. 547.

THE IONIZATION CONSTANT OF ACETIC ACID IN WATER–METHANOL MIXTURES AT 25° FROM CONDUCTANCE MEASUREMENTS

By Theodore Shedlovsky and Robert L. Kay

Contribution from the Laboratories of the Rockefeller Institute for Medical Research, New York, N. Y.

Received August 17, 1955

Data are reported on the conductances of dilute solutions of hydrochloric acid and of acetic acid in water–methanol solvent mixtures from 10 to 100% methanol at 25°. From these and supplementary data on the difference between the conductances of sodium chloride and sodium acetate solutions at the same concentration and the same solvent composition, values for Λ_0 and the ionization constants K are computed for both acids. Hydrochloric acid shows evidence of some association in the methanol-rich solvents, reaching a value of $K = 0.059$ in methanol. Acetic acid decreases in strength from a value of $K = 1.753 \times 10^{-5}$ in water to $K = 2.37 \times 10^{-10}$ in methanol. Unlike salts, which exhibit relatively flat minima in Λ_0 near the middle of the water–methanol composition region, which is not inconsistent with the changes in the viscosity of the solvents, the corresponding curves for the acids fall to a minimum at about 90% methanol by weight, beyond which the curves rise sharply.

Studies on the electrochemical behavior of glass membranes in buffered water–methanol mixtures over the entire range of solvent composition require for their interpretation a knowledge of the ionization constants of the weak acid components in the buffer systems employed. Such constants also can serve the practical purpose of establishing pH scales in the mixed solvents.

In this paper we shall report values for the ionization constants of acetic acid at 25°, derived from electrical conductance measurements covering the complete range of water–methanol composition.

Ionization constants for acetic acid in water–methanol mixtures, derived from electromotive force measurements have been reported by other workers,[1-3] but since the solvent composition range was too narrow[1,3] for our purposes, or the glass electrode itself was used,[2] and since an independent method, based on different theoretical considerations and assumptions, is desirable in any case, we chose the conductivity method.

From the data presented, which include measurements on dilute solutions of acetic acid and of hydrochloric acid, the limiting equivalent conductances, as well as the ionization constants, are obtained.

Theoretical

The extrapolation of conductance data on weak electrolytes for determining the limiting equivalent conductance, Λ_0, and the ionization constant K can be achieved by means of equations derived by combining the mass action law, the Debye–Hückel activity equation, and an expression for the degree of ionization, obtained either from a synthesized hypothetical conductance function for the ionized part of the weak electrolyte[4] or from the measured conductance on the weak electrolyte itself.[5]

In this paper we shall, in a sense, combine both of these methods, by obtaining values of Λ_0 for acetic acid synthetically from the Λ_0 conductances on

(1) H. S. Harned and N. D. Embree, *J. Am. Chem. Soc.*, **57**, 1669 (1935).
(2) A. L. Bacarella, E. Grunwald and H. P. Marshall, *J. Org. Chem.*, **20**, 747 (1955).
(3) L. J. Minnick and M. Kilpatrick, This Journal, **43**, 259 (1939).
(4) D. A. MacInnes and T. Shedlovsky, *J. Am. Chem. Soc.*, **54**, 1430 (1932).
(5) R. M. Fuoss, *ibid.*, **57**, 488 (1935); T. Shedlovsky, *J. Franklin Inst.*, **225**, 739 (1938); R. M. Fuoss and T. Shedlovsky, *J. Am. Chem. Soc.*, **71**, 1496 (1949).

hydrochloric acid, sodium acetate and sodium chloride and using the Fuoss–Shedlovsky weak electrolyte type of conductance equations,[5] with the Λ_0 already thus determined, for obtaining the ionization constants K. The reason for this procedure is that for electrolytes as weak as acetic acid is in water–methanol mixtures the extrapolated values for Λ_0 by the Fuoss–Shedlovsky equations, which are linear with a slope of $1/K\Lambda_0^2$, cannot be obtained with sufficient accuracy to yield values of K within the degree of precision we desire.

The degree of ionization x is obtained by solving the conductance equation, quadratic in $x^{1/2}$

$$\frac{x}{\Lambda} = \frac{1}{\Lambda_0} + \frac{\alpha\Lambda_0 + \beta}{\Lambda_0^2}\sqrt{cx} \qquad (1)$$

in which c is the concentration and $\alpha = 8.203 \times 10^5/(DT)^{3/2}$; $\beta = 82.43/\eta(DT)^{1/2}$ are the Onsager coefficients which involve the dielectric constant (D), the viscosity (η) and the absolute temperature (T). The solution for equation 1 is

$$x = \frac{\Lambda S}{\Lambda_0} \qquad (1')$$

where

$$S \equiv (Z/2 + \sqrt{1 - (Z/2)^2})^2 \text{ and } Z = \frac{\alpha\Lambda_0 + \beta}{\Lambda_0^{3/2}}\sqrt{c\Lambda}$$

For the measurements reported in this paper $S = 1 + Z$ is a sufficient approximation.

The mass action equation we require is

$$K = \frac{cx^2f^2}{1 - x} \qquad (2)$$

where the activity coefficient (f) is given by the Debye–Hückel equation

$$-\log f^2 = a\sqrt{cx} \qquad (3)$$

in which

$$a = \frac{3.649 \times 10^6}{(DT)^{3/2}}$$

By combining (1') with (2) there is obtained the weak electrolyte conductance equation[5]

$$\frac{1}{\Lambda S} = \frac{1}{\Lambda_0} + \frac{c\Lambda Sf^2}{K\Lambda_0^2} \qquad (4)$$

for which f^2 is computed from equations 1' and 3. However, as we have mentioned above, a plot of $1/\Lambda S$ vs. $C\Lambda Sf^2$ involves, in effect, too long an extrapolation for obtaining Λ_0 and, therefore, K with sufficient accuracy unless Λ_0 can be more accurately determined from other data.

One of the most serious difficulties in conductance work with weak acids is the matter of the appropriate solvent conductance correction. Unlike the case of unhydrolyzed salts, in which the measured solvent conductance is simply subtracted from the corresponding conductance measurements on the solutions, the acids present a special problem in this respect. If the solvent conductance is all due to a weak acid (such as CO_2 or the solvent itself) which is so much weaker than the one to be measured that its ionization can be neglected in the stronger acid medium, no solvent correction need be applied. If, on the other hand, the solvent conductance is due almost entirely to neutral salt, then this solvent conductance should be subtracted. An alkaline impurity would add to this complication still further, of course.

In the present research we have taken care to work with solvents as reasonably free from impurities as was practicable and to exclude atmospheric CO_2 with hydrogen. The solvent correction, if any, was then determined in the following manner rather than from the measured solvent conductance which was, of course, also obtained.

By combining the square root of mass action equation 2 and equation 1′, and substituting the definition for the equivalent conductance, Λ

$$\Lambda = \frac{L - L_0}{c} \quad (5) \qquad \text{and} \qquad \Lambda^* = L/C \quad (5')$$

in which L and L_0 are one thousand times the measured specific conductance and solvent conductance, respectively, we obtain

$$L - L_0 = \frac{\Lambda_0 K^{1/2} c^{1/2}}{Sf} \left[1 - \frac{\Lambda^* S}{\Lambda_0} \left(1 - \frac{L_0}{L} \right) \right]^{1/2} \quad (6)$$

Since the factor in brackets on the right, the degree of *association*, was never too far from unity in most cases, we have used, as a first approximation

$$L - L_0 = \frac{\Lambda_0 K^{1/2} c^{1/2}}{Sf} \left[1 - \frac{\Lambda^* S}{\Lambda_0} \right]^{1/2} \quad (6')$$

From plots of equation 6′ and 6, which were linear, L_0, the solvent correction $\times 10^3$ was obtained. Also, from the slopes of the graphs, K could be computed once we knew Λ_0.

For this purpose, we made use of our measurements on dilute solutions of HCl, using plots of $\Lambda_0' \equiv [\Lambda + \beta\sqrt{c}]/[1 - \alpha\sqrt{c}]$ *vs.* c for purposes of extrapolation[6] for $\Lambda_0(\text{HCl})$. No solvent correction was required for an acid as strong as HCl. However, in solvent mixtures relatively rich in alcohol, HCl, itself, showed signs of association and in these cases the data were plotted with the use of equation 4 from which both $\Lambda_0(\text{HCl})$ and $K(\text{HCl})$ were found. Finally, by combining these $\Lambda_0(\text{HCl})$ values with $\Lambda_0(\text{NaAc})$ and $\Lambda_0(\text{NaCl})$

$$\Lambda_0(\text{HAc}) = \Lambda_0(\text{HCl}) - [\Lambda_0(\text{NaCl}) - \Lambda_0(\text{NaAc})] \quad (7)$$

the limiting conductances, Λ_0, for acetic acid were computed. To do this, we made use of graphs of the terms on the right-hand of equation 7 plotted against the composition of the solvent. The values for NaCl were computed from the data of Longsworth and MacInnes[7] and our own deter-

(6) T. Shedlovsky, *J. Am. Chem. Soc.*, **54**, 1405 (1932).

(7) L. G. Longsworth and D. A. MacInnes, THIS JOURNAL, **43**, 239 (1939).

minations for NaAc, both at $c = 0.05$. We obtained $[\Lambda_0(\text{NaCl}) - \Lambda_0(\text{NaAc})]$ from $[\Lambda(\text{NaCl}) - \Lambda(\text{NaAc})]_{c=0.05}$ by multiplying the latter value by $(1 + \alpha\sqrt{c} = 0.05)$. This procedure is based on the modified Onsager equation for strong electrolytes

$$\Lambda_0 = \Lambda + (\alpha\Lambda + \beta)\sqrt{c} \quad (8)$$

When applied to $\Lambda(\text{NaCl})$ minus $\Lambda(\text{NaAc})$ at the same concentration, the electrophoretic terms, $\beta\sqrt{c}$, cancel and deviations from equation 8, which would appear as higher terms for the two salts, will tend to do so likewise.

Experimental

The conductance measurements were made with an alternating current bridge[8] using a cathode ray tube instead of telephones as a detector.[9] The cell, which was of the quartz flask type (cell constant 0.7422), and the techniques were substantially the same as formerly described.[10] However, since it was found that the cell resistances showed some drifts on repeated fillings with the water–methanol solutions, hydrogen gas was substituted for nitrogen, which then effectively eliminated this difficulty.

All measurements were made at $25 \pm 0.002°$, and all the stock solutions, as well as the mixed solvents, were prepared by weight, using a quartz buret for the acid stock solutions.

Conductivity water was prepared by de-ionizing distilled water through a column of mixed bed ion-exchange resin (Amberlite MB-2*). It had a specific conductance of approximately 2×10^{-7} ohm. The methyl alcohol was a good grade of material which was further purified by passage through a similar resin column and subsequent distillation in an efficient fractionating Pyrex glass still. The specific conductance of the purified material was approximately 2×10^{-8} ohm.

Synthetic acetic acid was purified by distillation from 2% $KMnO_4$, redistillation with a fractionating column and finally by fractional freezing. A small quantity of water in some of the glacial acetic acid samples used for making up solutions was determined from the lowering of the freezing point, taking $16.60°$ as the value of the 100% acid and using a cryoscopic constant of 3.90.

Constant boiling hydrochloric acid was prepared from Reagent Grade acid and the concentration of the product was computed from the data of Foulk and Hollingsworth.[11] This was used in preparing the stock solutions of HCl in the water–methanol mixtures, except in the case of methanol itself. Here, the stock solution was prepared with dry HCl gas, generated from NaCl in concentrated HCl by the addition of pure H_2SO_4. The concentration was determined by careful titration with carbonate-free NaOH solution standardized against Bureau of Standards potassium acid phthalate.

For the sodium acetate solutions, the Reagent Grade of trihydrate was used to which was added about 1% of acetic acid to suppress hydrolysis.

In preparing all the solutions, which were always on a vacuum corrected weight basis, we used the density data of Carr and Riddick[12] and of Longsworth and MacInnes,[7] for the water–methanol solvents. Although the HCl solutions were sufficiently dilute for assuming the density to be that of the solvent, in the case of the acetic acid and of the sodium acetate solutions, which rose to higher concentration values, corrections were made on the basis of I. C. T. density data for these substances in H_2O and in CH_3OH.

Results and Discussion

The Onsager conductance constants, α and β for equation 1, the Debye-Hückel activity coefficient constants for equation 3 and the dielectric

(8) T. Shedlovsky, *J. Am. Chem. Soc.*, **52**, 1793 (1930).

(9) H. Eisenberg and R. M. Fuoss, *ibid.*, **75**, 2914 (1953).

(10) T. Shedlovsky, *ibid.*, **54**, 1411 (1932).

(11) C. W. Foulk and M. Hollingsworth, *ibid.*, **45**, 1220 (1923).

(12) C. Carr and J. A. Riddick, *Ind. Eng. Chem.*, **43**, 692 (1951).

TABLE I
THEORETICAL CONSTANTS FOR METHANOL–WATER MIXTURES AT 25°

Wt. % CH₃OH	D	η, millipoise	α	β	a
0	78.49	8.949	0.2291	60.21	1.0192
10	74.21	11.58	.2492	47.85	1.1085
20	70.01	14.00	.2720	40.75	1.2098
40	60.92	15.93	.3351	38.39	1.4904
60	51.71	14.03	.4285	47.31	1.9059
80	42.60	10.06	.5730	72.70	2.5489
90	37.88	7.67	.6834	101.12	3.0398
95	35.37	6.51	.7574	123.37	3.3691
100	32.64	5.41	.8543	154.33	3.8005

constants[13] and viscosities[7] are listed in Table I for the range of methanol–water solvent composition.

The data on the conductance of dilute solutions of HCl from 10 to 100% methanol are reported in Table II as $\Lambda_0' \equiv [\Lambda + \beta\sqrt{c}]/[1 - \alpha\sqrt{c}]$ for compactness and to show the trends in deviation from the Onsager conductance equation. They were interpolated for the round concentrations given from plots of Λ_0' vs. c which also served for extrap-
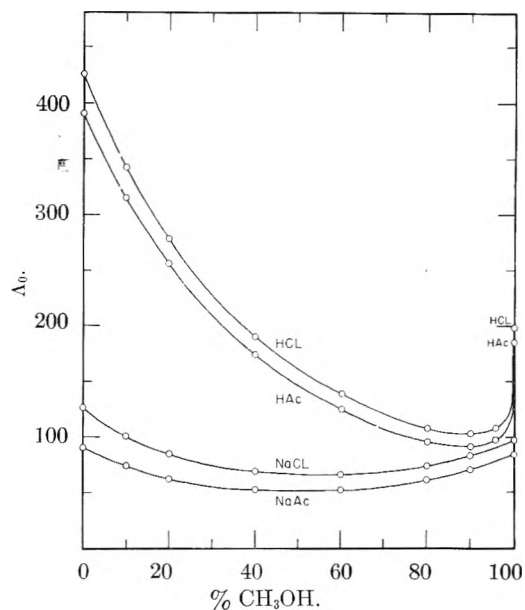
Fig. 2.—Variation in Λ_0 for hydrochloric acid, acetic acid, sodium chloride and sodium acetate with solvent composition.

TABLE II
Λ_0' CONDUCTANCES OF HCl IN METHANOL–WATER MIXTURES AT 25°

Wt., % CH₃OH → C × 10⁴	10	20	40	60	80	90	95.79	100
0	(343.2)	(278.3)	(190.1)	(138.7)	(108.0)	(103.4)	(108.5)	(199.7)
5	343.3	278.4	190.2		108.0	103.3	108.2	198.4
10	343.3	278.4	190.2	138.8			108.1	197.4
15	343.4	278.5	190.3	138.8	108.2	103.3	108.1	196.8
25	343.5	278.6	190.4	138.9	108.4	103.4	108.4	196.0
40			190.6	139.1	108.7	103.7	108.6	195.4
50				139.3	108.9	103.9	108.8	
75						104.5	109.5	

olating to Λ_0 for solvents up to 40% CH₃OH. For solvents richer in alcohol, HCl appeared to show signs of incomplete ionization and in these cases equation 4 was used and the plots are shown in Fig. 1. The Λ_0 values listed in Table III are on these bases, except for Λ_0 in pure water which is taken

from earlier work in this Laboratory. The corresponding values for the ionization constant K for
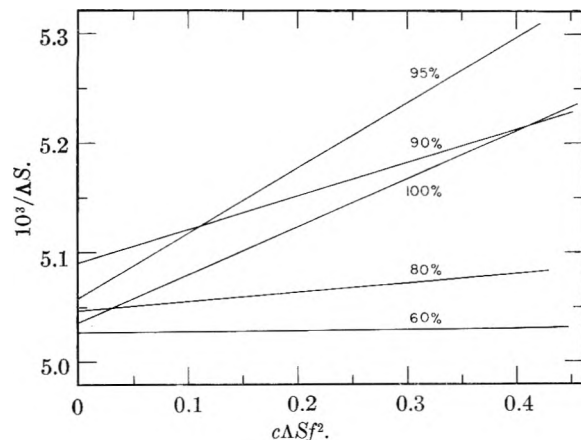
Fig. 1.—Plot of equation 4 for HCl from 60 to 100% methanol. For 60, 80, 90, 95.79% methanol 2.2, 4.2, 4.6 and 4.2, respectively, must be added to the ordinates as shown on the plot.
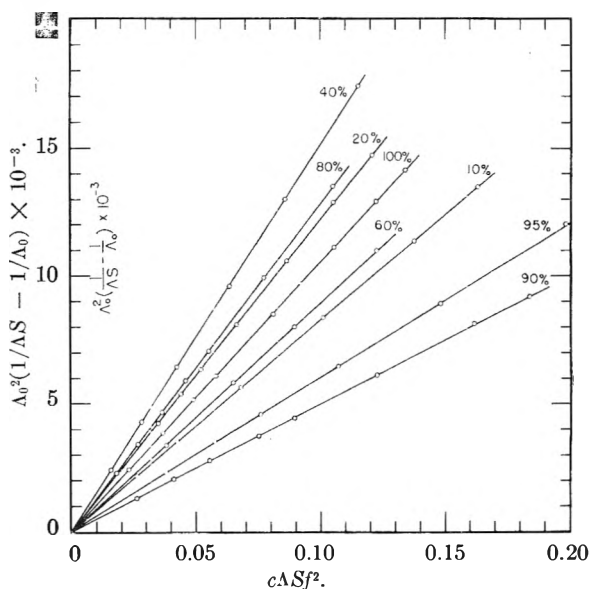
Fig. 3.—Plot of equation 4 for acetic acid at various solvent compositions. For 10, 20, 40, 60, 80, 90, 95 and 100% methanol the abscissas must be multiplied by 1, 0.5, 0.5, 0.1, 0.05, 0.02, 0.01 and 0.005 and the ordinates by 1, 0.5, 1, 1, 2, 10, 20 and 200, respectively.

(13) L. J. Gosting and P. S. Albright, *J. Am. Chem. Soc.*, **68**, 1061 (1946); T. T. Jones and R. M. Davies, *Phil. Mag.*, **28**, 307 (1939).
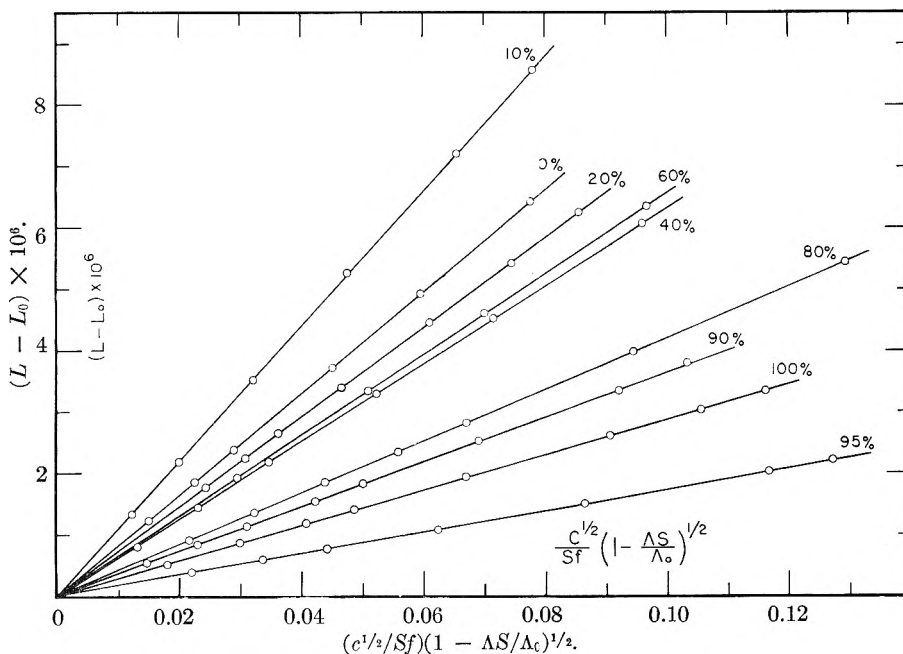
Fig. 4.—Plot of equation 6 for acetic acid at various solvent compositions. For 0, 10, 20, 40, 60, 80, 90, 95 and 100% methanol the abscissas must be multiplied by 1, 2, 1, 2, 1, 1, 2, 2 and 2 and the ordinates by 20, 20, 10, 10, 2, 1, 1, 1 and 0.2, respectively.

HCl are 4.0, 1.2, 0.29, 0.14 and 0.059 for 60, 80, 90, 95.8 and 100% methanol, respectively. In this table are also listed the differences $[\Lambda(NaCl) - \Lambda(NaAc)]$ at $c = 0.05$ and $[\Lambda_0(NaCl) - \Lambda_0(NaAc)]$ which yield the $\Lambda_0(HAc)$ values on subtraction from the corresponding $\Lambda_0(HCl)$.

TABLE III

Wt. % CH₃OH	$\Lambda_0(HCl)$	$\Lambda(NaCl) -$ $\Lambda(NaAc)$	$\Lambda_0(NaCl) -$ $\Lambda_0(NaAc)$	$\Lambda_0(HAc)$
0	426.1			390.7
10	343.2	25.8	27.2	316.0
20	278.3	20.7	22.0	256.3
40	190.1	14.9	16.0	174.1
60	138.7	12.8	14.0	124.7
80	108.0	11.0	12.4	95.6
90	103.2	10.4	12.0	91.2
95.79	108.1	9.0	10.6	97.5
100	198.5	10.9	13.0	185.5

In Fig. 2 the curves of Λ_0 for hydrochloric acid, acetic acid, sodium chloride and sodium acetate are plotted against the composition of the solvent. It is interesting to note that while the salt curves show flat minima which are not too inconsistent with the solvent viscosity changes, the acid curves fail to pass through a minimum until a composition of over 90% methanol has been reached, and rise sharply thereafter. Looking at these acid curves from the alcohol end of the graph, the sharp drop can be explained in the following manner. On the addition of traces of water, protons bound to H_2O molecules will not tend to jump to CH_3OH molecules of lower dipole moment. Thus, a corresponding decrease in conductance will take place. When sufficient water has been added, however, proton jumps from H_2O to H_2O become progressively more probable and the conductance will begin to rise again.

The data on the conductances of acetic acid solutions are listed in Table IV in which L is the meas-

TABLE IV

CONDUCTANCES OF ACETIC ACID IN METHANOL–WATER MIXTURES AT 25°

10.01% CH₃OH

$C \times 10^4$	$L \times 10^3$	S	
6.774	27.08	1.0037	0.9883
16.857	43.82	1.0047	9850
42.20	70.61	1.0060	.9810
92.32	105.57	1.0073	.9769
170.22	144.29	1.0086	.9733
239.70	171.72	1.0093	.9705

$\Lambda_0 = 316.0$ $K = 1.212 \times 10^{-5}$ $L_0 = 0.21 \times 10^{-3}$

20.01% CH₃OH

6.502	17.82	1.0036	0.9884
10.187	22.57	1.0040	.9870
13.949	26.58	1.0044	.9859
22.51	34.10	1.0050	.9840
38.10	44.74	1.0057	.9817
55.93	54.50	1.0063	.9798
73.44	62.65	1.0067	.9784

$\Lambda_0 = 256.3$ $K = 8.16 \times 10^{-6}$ $L_0 = 0.03 \times 10^{-3}$

20.04% CH₃OH

12.469	25.09	1.0043	0.9863
17.167	29.63	1.0046	.9851
24.83	35.85	1.0051	.9836
44.97	48.67	1.0059	.9809
63.30	58.01	1.0065	.9792
78.79	64.89	1.0069	.9778

$\Lambda_0 = 256.2$ $K = 8.13 \times 10^{-6}$ $L_0 = 0.10 \times 10^{-3}$

40.02% CH₃OH

7.020	8.242	1.0038	0.9884
21.54	14.653	1.0051	.9844
48.23	22.110	1.0063	.9808
107.29	33.183	1.0077	.9765
199.83	45.467	1.0089	.9725
356.28	60.922	1.0104	.9683

$\Lambda_0 = 174.1$ $K = 3.30 \times 10^{-6}$ $L_0 = 0.14 \times 10^{-3}$

TABLE IV (*Continued*)

60.05% CH$_3$OH

$C \times 10^4$	$L \times 10^3$	S	f
8.814	3.897	1.0045	0.9877
25.86	6.722	1.0059	.9840
48.70	9.254	1.0069	.9812
91.73	12.744	1.0082	.9780

$\Lambda_0 = 124.6$ $K = 1.12 \times 10^{-6}$ $L_0 = 0.030 \times 10^{-3}$

80.03% CH$_3$OH

4.743	0.937	1.0042	0.9908
10.406	1.385	1.0050	.9889
19.25	1.880	1.0060	.9870
30.81	2.373	1.0067	.9854
44.56	2.855	1.0073	.9840
87.86	4.015	1.0087	.9811
163.81	5.479	1.0102	.9779

$\Lambda_0 = 95.6$ $K = 1.95 \times 10^{-7}$ $L_0 = 0.021 \times 10^{-3}$

90.02% CH$_3$OH

8.458	0.549	1.0044	0.9914
20.88	0.852	1.0055	.9893
38.37	1.150	1.0064	.9876
70.01	1.561	1.0074	.9856
98.81	1.852	1.0081	.9843
187.54	2.539	1.0095	.9816
332.10	3.379	1.0109	.9788
425.67	3.822	1.0116	.9774

$\Lambda_0 = 91.2$ $K = 4.01 \times 10^{-8}$ $L_0 = 0.018 \times 10^{-3}$

95.02% CH$_3$OH

19.31	0.406	1.0042	0.992
44.65	0.604	1.0051	.990
77.08	0.795	1.0059	.989
153.36	1.114	1.0070	.987
294.19	1.538	1.0082	.985
534.27	2.055	1.0095	.982
635.39	2.238	1.0097	.981

$\Lambda_0 = 96.4$ $K = 8.1 \times 10^{-9}$ $L_0 = 0.017 \times 10^{-3}$

99.99% CH$_3$OH

16.61	0.148	1.0015	0.996
41.62	.217	1.0018	.995
74.42	.280	1.0021	.995
104.45	.328	1.0022	.994
196.56	.436	1.0026	.993
345.98	.567	1.0029	.992
464.53	.650	1.0032	.992
561.81	.712	1.0033	.992

$\Lambda_0 = 185.5$ $K = 2.37 \times 10^{-10}$ $L_0 = 0.033 \times 10^{-3}$

ured specific conductance times 10^3, S is the function in equation 1′ and f the mean ionic activity coefficient. The values for Λ_0, the solvent correction, L_0, and the dissociation constant K were obtained from the data in the manner described earlier in this paper.

The plots of equations 4 and 6 for the data in Table IV after the solvent conductance correction had been made are shown in Figs. 3 and 4, respectively.

Finally, it is of interest to compare our values of K for acetic acid with that of earlier workers who used a method based on e.m.f. measurements. Harned and Embree[1] reported $K = 1.247 \times 10^{-5}$ and $K = 8.34 \times 10^{-6}$ for 10 and 20 weight % methanol, respectively. Our values are 1.212×10^{-5} and 8.16×10^{-6} for these solvents. The disagreement is probably not beyond the degree of precision of the two different methods.

TABLE V

IONIZATION CONSTANTS FOR ACETIC ACID AT ROUND VOLUME % METHANOL COMPOSITION

Vol. % CH$_3$OH	K (S & K)	K (B, G, & M)
0	(1.753×10^{-5})	1.753×10^{-5}
10	1.31×10^{-5}	
20	9.59×10^{-6}	9.75×10^{-6}
40	4.52×10^{-6}	4.63×10^{-6}
60	1.82×10^{-6}	1.56×10^{-6}
80	3.96×10^{-7}	3.16×10^{-7}
90	9.71×10^{-8}	
95	2.07×10^{-8}	1.39×10^{-8}
100	2.37×10^{-10}	$(1.91 \times 10^{-10})^a$

^{a} Reference 3.

In column 2 of Table V are listed our values for K at round volume % methanol composition. The corresponding values, taken from the work of Bacarella, Grunwald and Marshall[2] are listed in column 3. The agreement is good up to 40% methanol but hardly so beyond this solvent composition.

We wish to acknowledge the able technical assistance of Joan Berdick and Regina Curtin during the progress of this research.

BOLAFORM ELECTROLYTES.   V.   CONDUCTANCE OF SOME BISQUATERNARY SALTS IN METHANOL AND IN ETHANOL

By Ormond V. Brody[1] and Raymond M. Fuoss

Contribution No. 1327 from the Sterling Chemistry Laboratory of Yale University, New Haven, Conn.

Received August 17, 1955

Conductance data at 25° in methanol are given for the following salts over the approximate range $3 \times 10^{-5} \leqslant c \leqslant 1 \times 10^{-3}$ equiv./l.: diethyl sulfide bis-β,β'-trimethylammonium diiodide, diethyl sulfide bis-β,β'-diethylmethylammonium diiodide, diethyl ether bis-β,β'-(N-methylpiperidinium) diiodide, diethyl ether bis-β,β'-(N-methylmorpholinium) diiodide, diethyl ether β-(N-methylmorpholinium), β'-trimethylammonium diiodide, N,N'-bis-(β-dimethylaminoethyl)-malonamide bis-methiodide and N,N'-bis-(β-dimethylaminoethyl)-glutaramide bis-methiodide. Conductances in ethanol and in methanol at 25° are given for 1,6-bis-(trimethylammonium)-hexamethylene dibromide (VIII) 1,10-bis-(trimethylammonium)-decamethylene diiodide (X) and d-tubocurarine dichloride (IX). All the salts show association of one anion to the doubly charged cation in methanol, with k_2 of the order of 10^{-3}; good correlation between limiting conductance and structure and between association constants and structure is found. Compound IX has $k_2 = 8.0 \times 10^{-3}$; the much larger value is ascribed to steric hindrance of anion approach by the bulk of the cation. In ethanol, first association constants are about one twentieth of the values found in methanol; for compounds VIII and X, clear evidence was found for association of the second anion above $c = 3 \times 10^{-4}$. The Walden products in ethanol are about 15% larger than in methanol.

Introduction

By connecting two quaternary ammonium groups by a chain of uncharged atoms, and then measuring the conductance of the bis-quaternary salt in a smenogenic[2] solvent, it is possible to estimate the distance between the charged sites of the cation in solution. It has been found that this distance does not always agree with that measured on molecular models; for example, in the series $Me_3N^+CH_2CH_2$-$NHCO(CH_2)_nCONHCH_2CH_2N^+Me_3$, the distance between charged nitrogens was found[3] to be substantially independent of n. In this case, it was concluded that hydrogen bonding between the two amide groups in the chain caused the connecting methylene chain to coil behind the plane of the cyclized amide structure. Comparison[4] of R_3N^+-$(CH_2)_mN^+R_3$ salts with those in which one of the methylenes is replaced by an oxygen atom shows that the latter case corresponds to a shorter charge–charge distance. Conductance of bisquaternary salts thus appears to be a useful tool for studying the configuration of certain charged molecules in solution.

The purpose of this paper is to present conductance data for ten more bisquaternary salts in methanol at 25° and to compare the results with those found previously for salts of related structures. They include two members of the amide series ($n = 1$ and 3), three of the series in which quaternary salts are obtained by β,β'-substitution of quaternary groups in diethyl ether, two thio-analogs of the latter salts, two of the polymethylene ($m = 6, 10$) series and finally d-tubocurarine chloride. The three last named salts were also measured in ethanol at 25°; due to the lower dielectric constant of the latter, ion association is greater than in methanol, and the reliability of the association constants is correspondingly increased.[5]

(1) Du Pont Postdoctoral Research Fellow, 1954–1955.

(2) A smenogenic solvent is a solvent whose dielectric constant is low enough to make the electrostatic potential of oppositely charged ions larger than kT and thereby cause association of ions to pairs, triples, etc., the extent of association depending on dielectric constant of solvent and concentration of electrolyte. *Cf.* R. M. Fuoss, *J. Chem. Education*, **32**, 527 (1955).

(3) H. Eisenberg and R. M. Fuoss, *J. Am. Chem. Soc.*, **75**, 2914 (1953).

(4) J. C. Nichol and R. M. Fuoss, *ibid.*, **77**, 198 (1955).

(5) R. M. Fuoss and T. Shedlovsky, *ibid.*, **71**, 1496 (1949).

The structures of the salts are given in Table I, together with code numbers for later reference. We take this opportunity to thank Dr. J. Fakstorp of Pharmacia Laboratories (Copenhagen) for research samples of compounds I-V and Drs. R. Baltzly and A. P. Phillips of the Wellcome Research Laboratories for compounds VI-IX.

Table I

Structures of Electrolytes

No.	Anion	Cation
I	I'	$Me_3N^+CH_2CH_2SCH_2CH_2N^+Me_3$
II	I'	$Et_2MeN^+CH_2CH_2SCH_2CH_2N^+MeEt_2$
III[a]	I'	$C_5H_{10}N^+MeCH_2CH_2OCH_2CH_2MeN^+C_5H_{10}$
IV[b]	I'	$C_4H_8ON^+MeCH_2CH_2OCH_2CH_2MeN^+C_4H_8O$
V	I'	$C_4H_8ON^+MeCH_2CH_2OCH_2CH_2N^+Me_3$
VI	I'	$Me_3N^+(CH_2)_2NHCOCH_2CONH(CH_2)_2N^+Me_3$
VII	I'	$Me_3N^+(CH_2)_2NHCO(CH_2)_3CONH(CH_2)_2N^+Me_3$
VIII	Br'	$Me_3N^+(CH_2)_6N^+Me_3$
IX[c]	Cl'	$Me_2N^+C_{34}H_{32}O_6N^+Me_2$
X	I'	$Me_3N^+(CH_2)_{10}N^+Me_3$

^{a} $C_5H_{10}N^+Me$ = N-methylpiperidinium. ^{b} $C_4H_8ON^+Me$ = N-methylmorpholinium. ^{c} d-Tubocurarinium cation.[6-8]

Experimental

Materials.—The compounds provided by Dr. Fakstorp[9] consisted of diethyl sulfide bis-β,β'-trimethylammonium diiodide (I), diethyl sulfide bis-β,β'-diethylmethylammonium diiodide (II), diethyl ether bis-β,β'-(N-methylpiperidinium) diiodide (III), diethyl ether bis-β,β'-(N-methylmorpholinium) diiodide (IV) and diethyl ether β-(N-methylmorpholinium), β'-trimethylammonium diiodide (V). The compounds[10] received from the Wellcome Laboratories were N,N'-bis-(β-dimethylaminoethyl)-malonamide bis-methiodide (VI), N,N'-bis-(β-dimethylaminoethyl)-glutaramide bis-methiodide (VII), 1,6-bis-(trimethylammonium)-hexamethylene dibromide ("hexamethonium" dibromide, VIII) and d-tubocurarine chloride (IX). 1,10-Bis-(trimethylammonium) diiodide ("decamethonium" diiodide, X) was purchased from L. Light and Co., Ltd. (Colnbrook, Bucks., England). Compounds I-V were measured as received and again after recrystallization. The other compounds were only measured as received, because their melting points were quite sharp and the halogen analyses agreed closely with the theoretical.

Methanol was purified by redistilling absolute C.P. methanol (Matheson) from aluminum amalgam after refluxing overnight. A mixture of 25 g. of aluminum powder and 5 g. of mercury bichloride was placed in a dry still and about

(6) J. D. Dutcher, *Ann. N. Y. Acad. Sci.*, **54**, 326 (1951).

(7) H. King, *J. Chem. Soc.*, 1381 (1935).

(8) O. Wintersteiner and J. D. Dutcher, *Science*, **97**, 467 (1943).

(9) J. Fakstorp and J. Christiansen, *Acta Chem. Scand.*, **8**, 346, 350 (1954).

(10) A. P. Phillips, *J. Am. Chem. Soc.*, **73**, 5822 (1951).

4 l. of methanol was added. One amalgam charge served to treat 4–5 batches of methanol. The conductance κ_0 of the distillate varied between 1.0 and 5.0 × 10^{-8} (average 2.7 × 10^{-8}); the maximum solvent correction tolerated was 1%. A small conductance cell ($k \approx 0.1$) sealed to the delivery end of the condenser and connected to the receiver by a siphon provided a very convenient means of continuously monitoring the quality of the solvent. Ethanol was also purified by amalgam treatment, but we later found that ethanol of excellent conductance ($\kappa_0 < 10^{-8}$) could be obtained by distilling absolute U. S. P. ethanol (U. S. Industrial Chemical Co.) from magnesium filings (Grignard quality) in a gentle stream of dry nitrogen, after previously refluxing about 12 hr. over magnesium under nitrogen. Maintenance of the nitrogen flow is imperative if ethanol of high resistance is to be obtained; if the flow is interrupted, the next test cell collected will show about half the resistance of the previous one.

Both dilution and concentration methods were used. In the former, solvent was added to solution in the conductance cell; the amount added was determined by reweighing the cell, so evaporation errors were eliminated. For the concentration method, a weight buret involving no stopcock was used. A solution (approximately 0.005 N) was made up by weighing salt (microbalance) into the buret and then adding solvent. A portion of solution for adding to the conductance cell could be pregaged by tipping some solution into the intermediate reservoir of the buret; a ridge blown in the neck on the side toward the reservoir facilitated this step.

Conductance cells of the Nichol-Fuoss design[11] were used. Several improvements in the original design have been made. These include extending the platinum tube about 5 mm. above the top of the Teflon cap and providing a Teflon plug for it to prevent liquids from accidentally getting into the tube and shunting the cell. A better finger grip for the Teflon cap was provided by starting with oversize Teflon rod and turning it down to standard taper for about 0.8 of its length; the projecting disc above the taper made it much easier to remove the electrode assembly from the cell. Finally, the cell compartment was made about 3 cm. longer; the bottom is now flat rather than hemispherical. A Teflon-enclosed iron stirrer is dropped into the cell before adding solvent, and during measurement, the cell is placed above a magnetic drive in the thermostat. The stirrer completely eliminated the drifts which had previously[4] been observed, and gave faster results because it is no longer necessary to remove the cell from the bath to mix its contents after adding solution from the weight buret. A constriction in the wall of the electrode compartment below the cylindrical electrodes ensures that the stirrer will not strike the electrode assembly. The cell used in this work had a constant of 0.04624 cm.$^{-1}$ as determined by direct comparison with a cell whose constant was 2.4445; the latter was determined over the range 0.001–0.05 N, using Shedlovsky's results for aqueous potassium chloride.[12] The cell constant was rechecked by stepwise comparison using intermediate cells of constants 0.31030 and 1.4873. Electrical equipment and other details have already been described.[3,4] All measurements were made at 25.00 ± 0.01°.

Results and Discussion

The conductance data for the methanol solutions are summarized in Table II and for ethanol in Table III. Concentrations c are given in equivalents per liter; they were calculated from the observed weight concentrations assuming equality of solution and solvent densities. The equivalent conductance Λ equals 1000 κ/c, where κ is observed specific conductance minus solvent conductance. The various salts are identified by the code numbers of Table I; the average values of 10^8 κ_0 are given in parentheses after the code numbers; at least one concentration and one dilution run was made for each salt.

(11) J. C. Nichol and R. M. Fuoss, This Journal, **58**, 696 (1954).

(12) T. Shedlovsky, A. S. Brown and D. A. MacInnes, *Trans. Electrochem. Soc.*, **66**, 165 (1934).

TABLE II
Conductances in Methanol at 25°

10⁴c	Λ	10⁴c	Λ
I (2.3)		VI (2.9)	
0.4877	121.77	0.7152	117.51
0.6535	119.79	1.1405	115.39
1.1140	115.71	1.3369	114.63
1.5920	112.62	3.086	108.63
2.886	105.51	11.159	94.34
3.482	102.79		
II (3.7)		VII (3.9)	
0.2677	125.02	0.5471	115.15
0.6095	121.37	0.6610	114.59
0.7772	119.84	1.4330	110.94
1.5590	113.96	2.193	108.14
2.620	108.06	2.954	105.68
3.776	103.07	6.870	97.03
III (1.8)		VIII (3.3)	
0.4651	126.74	0.3235	127.57
1.0125	122.67	0.6916	124.96
1.6798	118.38	1.3620	121.01
2.808	113.12	1.5012	120.51
4.591	106.73	3.219	113.89
		5.850	107.07
IV (3.5)		IX (1.5)	
0.4571	123.33	0.7170	93.08
0.9000	119.85	1.1656	91.73
1.2770	116.81	2.020	90.00
2.347	110.58	2.719	88.77
3.642	105.22	7.088	83.32
V (2.3)		X (2.2)	
0.5779	127.27	0.4129	125.03
1.1335	123.17	0.5372	124.11
2.176	117.18	1.3867	120.62
3.194	112.66	4.986	111.49
		12.949	99.93

TABLE III
Conductances in Ethanol at 25°

10⁴c	Λ	10⁴c	Λ
VIII (3.1)		X (3.9)	
0.6155	42.70	0.5826	48.98
0.9849	39.32	0.9370	46.43
1.3361	37.04	1.3612	44.12
1.6525	35.44	1.5636	43.20
2.748	31.75	2.497	39.96
3.622	29.83	3.323	37.89
7.811	25.19	9.523	30.58
15.550	21.63	14.044	28.03
16.300	21.43	17.247	26.83
31.50	18.62	32.87	23.23
87.27	14.87		
IX (4.0)			
1.0745	36.36		
1.5418	34.95		
2.640	32.57		
4.192	30.27		

The phoreograms ($\Lambda - c^{1/2}$ curves) for the methanol solutions approximate linearity in our working range of concentration; the slope is considerably higher than that of the limiting tangent for a 2-1 salt, due to association of one of the anions to the bisquaternary cations in this concentration range.

Analysis of the conductance data[13] gives linear extrapolation plots from which Λ_0 and k_2 can be determined. Here k_2 describes the association
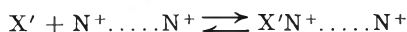
$$X' + N^+ \ldots N^+ \rightleftharpoons X'N^+ \ldots N^+$$

where

$$k_2 = [X'][N^+ \ldots N^+]/[X'N^+ \ldots N^+]$$

and the bracketed quantities refer to activities of the corresponding molecular species. Table IV summarizes the derived properties.

Table IV
Properties in Alcohols at 25°

Cpd.	Λ_0	λ^0_2	$10^3 k_2$	$10^8 R$
		Methanol		
I	(129.6)	(66.9)	(0.68)	. .
II	130.4	67.6	0.73	5.7
III	133.7	71.0	1.01	6.5
IV	130.7	68.0	0.82	6.0
V	135.1	72.4	0.99	6.4
VI	123.8	61.1	1.89	8.4
VII	120.9	58.1	1.69	8.0
VIII	132.0	75.4	1.58	7.3
IX	97.0	44.6	8.04	(23.3)
X	129.5	66.8	2.73	10.2
		Ethanol		
VIII	57.2	31.4	0.075	6.6
IX	42.6	18.3	0.402	(41.0)
X	56.9	29.0	0.210	. .

The thio compounds present a puzzling case: compound II, which is obtained from I by replacing four of the terminal methyl groups by four ethyls appears to have a somewhat higher cation mobility than I. Nichol[4] found, as expected, a *decrease* of 6.2 units for the corresponding change in the otherwise identical ether derivatives. If we compare sulfur and oxygen compounds with identical terminal groups, $\Delta\Lambda_0$ for those terminated in Me_3N^+ is 12.5 and for those terminated in Et_2MeN^+ is 5.6. These violations of additivity can be rationalized by assuming that at least one of the thio compounds does not have the structure assigned to it. (Nichol's sequence for his compounds IV-V-VI argues that the structures of the ether derivatives are correct.) One might expect some decrease in mobility due to replacing a medial oxygen by a sulfur; if so, 5.6 seems more reasonable than 12.5, because the replacement of a medial CH_2 in a 5-atom chain by oxygen causes an increase[4] of 2.1. The increase was accounted for by assuming attraction between the oxygen and the cationic nitrogens; since this should be about the same for sulfur, the effect of the bulk of the sulfur compared to that of oxygen should be a decrease. If we assume that compound II is correct, then the cation conductance for compound I is $67.6 + 6.2 = 79.4 - 5.6 = 73.8$. The alternative is to assume the results for compound I correct; then λ^0_2 for compound II calculates to 60.7, which seems much too small when compared with other cations of related structure which have been investigated. We shall tentatively assume that compound II is correct and

disregard the numerical results for compound I. This example shows how conductance can be used as a tool in certain problems of structure.

The ethers of Table I (compounds III, IV and V) form a consistent series with previously measured ethers. Replacing terminal Et_2MeN^+ groups (Nichol VI) by terminal methylpiperidinium groups (III) decreases λ^0_2 from 73.2 to 71.0; the piperidine ring can be imagined to be formed by bridging two ethyls by a methylene, and the resulting puckered ring would have a greater viscous drag. Replacing the methylpiperidinium groups by pyridinium groups (Nichol VIII) has the expected effect; λ^0_2 increases to 75.0. If, however, the piperidinium groups are replaced by morpholinium groups (IV), λ^0_2 drops to 68.0. This value suggests that the morpholinium groups are solvated by methanol hydrogen-bonded to the ring oxygens. For the ether terminated by Me_3N^+ groups, Nichol found $\lambda^0_2 = 79.4$ for his compound IV; replacement of one of these by a methylmorpholinium group (V) decreases λ^0_2 to 72.4; and as we have just seen, replacement of the second one decreases λ^0_2 still further to 68.0. Our present model is unable to account for the fact that replacement of the second terminal Me_3N^+ by methylmorpholinium has a smaller effect on λ^0_2 than replacement of the first. Another unexplained feature is the value of k_2 for compound IV: compound V and Nichol's compound IV have identical values of k_2 which argues that the first anion goes preferentially to the Me_3N^+ end of the chain. But k_2 for our compound IV is smaller than that for V, which argues that attraction is greater toward the methylmorpholinium end.

The two amide derivatives VI and VII are especially interesting when compared with those measured by Eisenberg. The malonamide derivative VI cannot form a hydrogen bonded ring as was postulated for the oxalamide and the succinamide and accordingly gives a smaller k_2 than either. While the glutaramide with three methylenes between amide groups can bend around to a ring, the ring is not planar; the still smaller k_2 argues that it does not cyclize. The values of cation mobilities (see Fig. 1) also show a tendency to alternation, superimposed on a steady decrease with increasing bulk of the methylene chain.

The two polymethylene derivatives VIII and X with, respectively, 6 and 10 methylenes round out Chu's series.[13] Evidently Chu's values of λ^0_2 for the ethylene derivative is a little low, as seen in Fig. 2. The decrease of mobility with increasing chain length is less rapid for chains terminated by pyridinium groups than for those terminated by trimethylammonium groups, which is equivalent to saying that the chains contribute relatively less to the total friction for the pyridinium derivatives. Values of charge–charge distances[14] for the two series lie approximately on the same curve (Fig. 1). The values of R, however, are based on a structure in which an anion has associated with one end of the cation while the mobilities refer to the unassociated ions; one would expect the charge–charge distance to be less in the former case, and to be much less dependent on the bulk of the terminal groups than

(13) R. M. Fuoss and V. F. H. Chu, *J. Am. Chem. Soc.*, **73**, 949 (1951).

(14) Ref. 3, eq. 6.
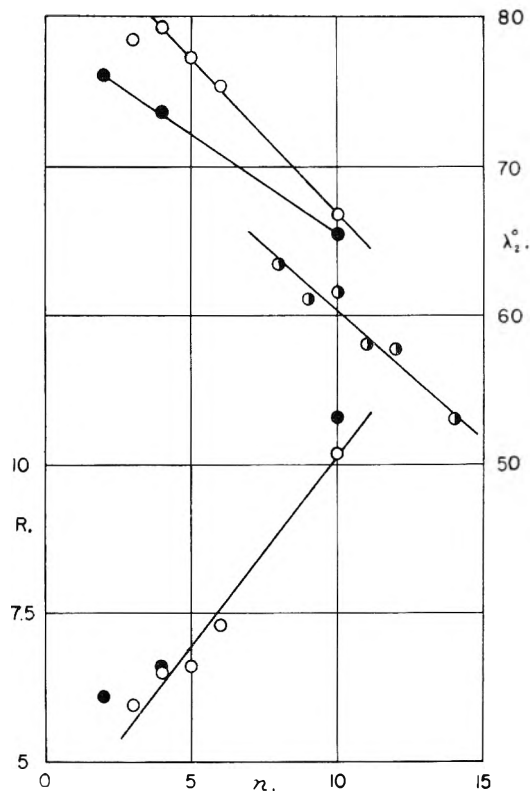
Fig. 1.—Dependence of single ion conductances (ordinates upper right) and intercharge distances (ordinates lower left) on number n of chain atoms: open circles, terminal Me_3N^+; solid circles, terminal Py^+ in polymethylene series; half-shaded circles, amide series.

Fig. 2.—Hexamethonium bromide in ethanol: open circles, $\Lambda - c^{1/2}$, abscissa scale below; solid circles, $\Lambda' - x$, abscissa scale above.

the mobility. Coincidence of the two R-series in Fig. 1 supports this argument.

Tubocurare, with its massive cation (molecular weight = 624) has, as expected, a quite small value of cation conductance. The charged sites are Me_2N^+ groups which are parts of six-membered rings; one might be tempted to guess that the value of k_2 would therefore be not much different from that of the other salts in Table I, since the energy of electrostatic binding between an anion and a quaternary nitrogen should not vary much with substituents if at least two small groups are present. Actually, tubocurarine chloride has the largest value of k_2 so far observed for a bisquaternary salt. More detailed consideration immediately makes it clear, of course, why association occurs less with this salt than with the chain-like ones. The constant k_2^{-1} is a measure of the probability of formation of an ion pair on one cationic site of the bisquaternary salt. It is proportional to two factors: the Boltzmann exponential involving the electrostatic potential and a steric factor which measures the probability of favorable approach of an anion. For the chain electrolytes, the latter is approximately the same for all and has been set equal to unity in our previous calculations. But in the curare ion, the bulk of the various ring structures sterically shields the quaternary nitrogens from approach by an anion for a large fraction of the angular space surrounding them, and hence the steric factor here is less than unity. To illustrate the importance of the steric factor for bulky cat-

ionic sites, we computed[15] R for compound IX, using the same formula as for the others: we obtained 23.3 Å. According to a molecular model of the compound, the two nitrogens of curare cannot be farther than about 13 Å. apart and could approach as near as 8 Å. The value of 23.3 obviously has no physical significance, and illustrates the need for caution in applying theoretical formulas. We can, however, perform the inverse operation in order to estimate the steric factor: for a bisquaternary salt with $R = 10$ Å. in methanol, k_2 would be 2.6×10^{-3}; the ratio of this to the observed 8.0×10^{-3} gives 0.33 for the steric factor. In other words, the bulk of the curare molecule reduces the probability of ion association to about one third that of a bisquaternary ion in which the two cationic sites are connected by a simple chain.

In ethanol, the equivalent conductances are naturally lower than in methanol because the viscosity is higher, but Walden's rule is not followed. The $\Lambda_0\eta$ products[16] have the following values in methanol and ethanol, respectively: compound VIII, 0.719 and 0.617; compound X, 0.705 and 0.613; compound IX, 0.528 and 0.459. In each instance, the conductance is relatively lower in ethanol than in methanol. This result parallels Sadek's[17] observation for tetrabutylammonium bromide in these two solvents and again argues for solvation: solvation by the bulkier ethanol molecules would give a relatively slower ion than sol-

(15) The computation is based on the value of $K = 0.0336$ for Me_4NCl in methanol, which was calculated from data published by T. L. Mead, O. L. Hughes and H. Hartley, J. Chem. Soc., 1207 (1933).

(16) Viscosities $\eta(MeOH) = 0.05445$, W. N. Maclay and R. M. Fuoss, J. Polymer Sci., 6, 511 (1951); $\eta(EtOH) = 0.01078$, O. L. Hughes and H. Hartley, Phil. Mag., 15, 610 (1933).

(17) H. Sadek and R. M. Fuoss, J. Am. Chem. Soc., 76, 5902 (1954).

vation by methanol. The relative effect on compounds VIII-X-IX is the same: the ratios of the $\Lambda_0\eta$ products in methanol and in ethanol are 1.165, 1.150 and 1.150. For Bu₄NBr, it is 1.100.

As expected, the three salts show a higher degree of association in ethanol than in methanol; the values of k_z decrease to about one twentieth of the methanol values. Again tubocurarine chloride is the least associated and the effect of steric screening here is immediately apparent. Its phoreogram is concave down over the working range of concentration, while the curves for decamethonium iodide and hexamethonium bromide are concave-up.

The effect of the low dielectric constant is strikingly visible in the case of hexamethonium bromide (VIII). In Fig. 2, in addition to the $\Lambda - c^{1/2}$ curve, the $\Lambda' - x$ curve[13] is shown. Unlike the linear $\Lambda' - x$ curves in methanol, the ethanol curve becomes concave-down and then at $x = 0.087$ reverses its direction with increasing concentration and eventually gives negative x-values. This re-

versal is clear evidence for the association of the second anion to the chain,[18] to give a structure of the type $(-) (+ \ldots \ldots +) (-)$. The value of k_2 in Table IV is therefore temporary; correction for the second association will be made later when data for other (more highly associated) salts in ethanol are presented. The single ion conductances used in the above calculation are based on the value of 0.71 for the transport number of hydrogen ion in ethanol.[19] The decamethonium salt is considerably less associated than VIII, corresponding to the greater separation of cationic sites. But it also shows evidence of association of the second anion: the first seven data of Table III (X) give $\Lambda' - x$ points which lie on a straight line, while the last two give points which drop sharply, indicating the onset of the second association.

(18) F. M. Sacks and R. M. Fuoss, J. Electrochem. Soc., **99**, 483 (1952).

(19) J. W. Woolcock, H. Hartley and O. L. Hughes, Phil. Mag., **11**, 222 (1931); M. Barak and H. Hartley, Z. physik. Chem., **165**, 290 (1933).

IONIZATION AND DISSOCIATION EQUILIBRIA IN LIQUID SULFUR DIOXIDE. III. THE DISSOCIATION OF SPHERICAL IONS[1]

By Norman N. Lichtin and Harry P. Leftin

Contribution from the Department of Chemistry, Boston University, Boston, Mass.

The conductivity behavior in liquid sulfur dioxide of KCl, KBr, KI and (CH₃)₄NBr has been investigated at 0.12 and −8.93°. Shedlovsky's procedure has been applied to equivalent conductance data over the dilution range 2000 to 80,000 liters per mole to yield ion-pair dissociation constants and limiting conductances. Distances of closest approach calculated from the equilibrium data by means of Bjerrum's equation for spherical ions differ little (0.0–0.3 Å.) from corresponding sums of ionic radii. Limiting conductance values calculated for KCl, KBr and KI by means of Stokes' law are slightly greater than the observed quantities, while for (CH₃)₄NBr the calculated values are considerably smaller than the observed. The sequence of the solutes with respect to $\Delta F°_{exp}$ appears to be determined by the $\Delta S°_{exp}$ term in agreement with theory.

Introduction

Preceding papers[2] in this series have dealt with solutes of the triarylchloromethane variety. These molecules are not ionized in the crystal and their electrolytic equilibria have accordingly been interpreted in terms of two processes: ionization of the carbon to chlorine bond and dissociation of the resulting ion-pair. In order to provide a foundation for the quantitative correlation of these complex equilibria with structure it appeared necessary to have information concerning electrolytes that may reasonably be assumed to be wholly ionic in solution. Alkali halides and tetraalkyl ammonium halides are of this class and offer the further advantage that their ions are essentially spherical and therefore appropriate to the statistical theories[3] of Bjerrum and of Fuoss and Kraus. The measurements reported here were undertaken because very few relevant data have been reported heretofore.[4]

(1) Based on a dissertation submitted by H. P. Leftin in partial fulfillment of the requirements for the Ph.D., May, 1955.

(2) (a) N. N. Lichtin and P. D. Bartlett, J. Am. Chem. Soc., **73**, 5530 (1951); (b) N. N. Lichtin and H. Glazer, ibid., **73**, 5537 (1951).

(3) (a) N. Bjerrum, Kgl. Danske Videnskab. Selskab., **7**, No. 9 (1926); (b) R. M. Fuoss and C. A. Kraus, J. Am. Chem. Soc., **55**, 1019 (1933).

(4) E. C. Franklin, This Journal, **15**, 675 (1911).

Experimental

The conductivity cell, thermostat and bridge assembly have been described previously.[2b] The temperatures of measurement were 0.12 ± 0.02° and −8.93 ± 0.03°. The indicated uncertainty represents extremes of variation in temperature. The vacuum line was similar to that employed in earlier work[2b] but lower pumping pressures (10⁻⁵–10⁻³ mm.) were used routinely and MgClO₄ was substituted for CaCl₂ and "Drierite" in the gas-drying columns. Procedures were like those previously reported. With potassium chloride it proved more convenient to introduce aliquots (2 ml.) of a dilute standard aqueous solution and to pump off the water since solubility considerations reduced the sample size to about 1 mg. Solutions prepared in this way gave results identical with those for solutions prepared from samples of pure solute weighed with a micro balance.

Sulfur dioxide was Virginia Smelting Co. "Extra Dry Es-O-TOO" (refrigeration grade). Solvent conductivity determined at the end of each run was almost always in the range 1.0 × 10⁻⁷ to 2.2 × 10⁻⁷ mhos cm.⁻¹. For about half of the runs the solvent was degassed by pumping for 1 to 2 hours prior to distillation from the helix-packed bulb into the cell. This treatment had no significant effect on either solvent conductivity or the behavior of solutions.[5]

Potassium chloride was J. T. Baker C.P., recrystallized from distilled water, pulverized and oven-dried at 120° for four hours. Potassium bromide was Merck Reagent Grade twice recrystallized from distilled water and dried by washing, first with 95% ethanol then with diethyl ether, heating

(5) This is in contrast with the behavior of solutions of hexaphenylethane which we have reported elsewhere: J. Am. Chem. Soc., **76**, 2593 (1954).

at 115° for one hour and finally heating the pulverized material in a vacuum oven at 130° for four hours. Two batches of potassium iodide were prepared. Lot I was J. T. Baker C.P., twice recrystallized from distilled water, washed with diethyl ether, and oven-dried at 115° after being pulverized. Lot II was prepared similarly from Merck Reagent Grade material. In order to minimize opportunity for oxidation of iodide, hot water which had been boiled immediately before use was employed, aqueous solutions were handled under streaming nitrogen, ether wash was replaced by acetone followed by petroleum ether and the crystals were not ground. The two samples gave concordant results. Tetramethylammonium bromide was Eastman Kodak Co. "White Label" recrystallized twice from 95% ethanol. The crystals were washed with ethanol followed by petroleum ether, oven-dried at 110° for two hours and then powdered and heated at 125° under vacuum for four hours. All solutes were stored in desiccators in the dark.

Solutions of KI in SO_2 were greenish-yellow. The other solutes yielded colorless solutions.

Data[6]

Equivalent conductance data from single runs

TABLE I
CONDUCTANCE DATA
0.12°

V^a × 10³	Λ^b	V^a × 10³	Λ^b
KCl		**KI**	
2.972	99.1	0.3584	88.1
6.821	129	0.8197	112
15.64	160.5	1.875	139
35.86	189.5	4.298	167
82.23	213	9.851	193
		22.55	211
		51.68	224
KBr		**(CH₃)₄NBr**	
0.2289	54.2	0.3614	134
0.5256	73.1	0.8323	157
1.208	96.8	1.915	180
2.777	125	4.403	199.5
6.393	156	10.13	214
14.72	186.5	23.31	222
33.90	209	53.80	227
78.07	225		

−8.93°

V^a × 10³	Λ^b	V^a × 10³	Λ^b
KCl		**KI**	
2.742	101	0.1906	70.9
6.309	130	0.4363	92.0
14.49	159	0.9987	116
33.43	185	2.286	143
76.89	204	5.235	168
		12.01	188
		27.55	201
		63.17	209
KBr		**(CH₃)₄NBr**	
0.2256	56.9	0.3580	126
0.5186	75.8	0.8245	149
1.187	99.0	1.897	169
2.729	126.5	4.361	186
6.309	154	10.03	197
14.50	180	23.08	204
33.41	198	53.27	209
76.86	210		

a Liters/mole. *b* Mhos cm.²/mole; corrected for solvent conductivity.

(6) The symbols employed in this article have the meaning assigned by H. S. Harned and B. B. Owen, "The Physical Chemistry of Electrolytic Solutions," Reinhold Publ. Corp., New York, N. Y., 1950, pp. XIII–XXVII.

for each solute are assembled in Table I. At least two runs were carried out for each solute at each temperature. The average scatter of the data about a smooth curve for a set of corresponding runs was found to be less than ±1%.

Although Jander[7] has reported "solvolysis" of KBr and KI in liquid SO_2, apparently at a rate inversely proportional to solute concentration, our solutions appeared to be quite stable over the periods required for their measurement, i.e., about 12 hours. Thus, no precipitates formed, resistance values did not change with time, results were reproducible, and although Jander has designated K_2SO_4 as a "solvolysis" product our data conformed quite well to 1:1 electrolyte behavior.[8]

Dissociation constants (K_{exp}) and Λ^0 values calculated from the data in the range 2000–80,000 liters per mole by means of Shedlovsky's procedure[9] are summarized in Table II. Individual data points were used directly in this calculation. The slope ($1/K(\Lambda^0)^2$) and intercept ($1/\Lambda^0$) of the resulting straight line were evaluated by the least square procedure with $1/\Lambda S(z)$ as the dependent variable. The upper dilution limit was chosen to assure a maximum solvent correction equal to less than 10% of the total conductivity. The lower limit was chosen somewhat arbitrarily in order to minimize uncertainty arising from the use of the Debye–Hückel limiting law for evaluating mean activity coefficients and from deviations of ionic conductance from Shedlovsky's modification of the Onsager equation. Over this dilution range the scatter of individual points about the least square line is random, i.e., no curvature is apparent. The mean deviation of the dependent variable relative to the least square line averages ±0.5% for all the data.

TABLE II
CONSTANTS FROM SHEDLOVSKY TREATMENT

Solute	Temp., °C.	Λ^0, mhos cm.²/mole	$10^5 K_{exp}$, mole/l.
KCl	0.12	243	7.4 ·
KCl	−8.93	222	10.8
KBr	0.12	249	14.3
KBr	−8.93	228	19.9
KI	0.12	244	30
KI	−8.93	221	43
(CH₃)₄NBr	0.12	236	118
(CH₃)₄NBr	−8.93	215	146

The values of dielectric constant (D) and viscosity (η) employed in the calculations related to this paper differ from those selected previously.[2] The dielectric constant data of Vierk[10] for the temperature range −38.8 to −16.5° were expressed, with a mean deviation of ±0.32%, in the form of eq. 1 where T is in °K. Values at 0.12° (15.35)

$$D = 95.12 \exp(-6.676 \times 10^{-3}T) \qquad (1)$$

and −8.93° (16.30) were then calculated from this

(7) G. Jander, "Die Chemie in Wasserähnlichen Lösungsmitteln," Springer–Verlag, Berlin, 1949, pp. 264–267.

(8) It may be significant in this connection that, with KI as solute, poor reproducibility, resistance drifts and anomalous dependence of conductance on dilution were associated with the presence of a pin-hole in the cell.

(9) T. Shedlovsky, J. Franklin Inst., **225**, 739 (1938).

(10) A. L. Vierk, Z. anorg. Chem., **261**, 279 (1950).

TABLE III

BJERRUM a VALUES CALCULATED FROM DATA FOR VARIOUS SOLVENTS

Solute	Solvent	$10^5 K_{exp}$ at 25° mole/liter	Bjerrum a Å.	r_+ for spherical ions, Å.	r_- Å.
K Picrate	Nitrobenzene	68.6[a]	0.93	1.33[f]	
K Picrate	Acetone	343[b]	3.44	1.33[f]	
KI	Acetone	802[b]	5.32	1.33[f]	2.17[f]
$(n\text{-}C_4H_9)_4NBr$	Acetone	329[b]	3.42	6.0[g]	1.95[f]
$(n\text{-}C_4H_9)_4NBr$	Pyridine	25[c]	4.55	6.0[g]	1.95[f]
$(n\text{-}C_4H_9)_4NI$	Pyridine	41[c]	5.09	6.0[g]	2.17[f]
$(CH_3)_4NF$	Acetone	77[b]	2.45	3.30[h]	1.34[f]
$(n\text{-}C_4H_9)_4N$ Picrate	Pyridine	128[c]	7.83	6.0[f]	
$(n\text{-}C_4H_9)_4N$ Picrate	Ethylene chloride	22.6[d]	4.06	6.0[f]	
$(n\text{-}C_4H_9)_4N$ Picrate	Ethylidene chloride	4.54[d]	4.61	6.0[f]	
$(n\text{-}C_4H_9)_4N$ Picrate	Propylene chloride	2.67[d]	5.08	6.0[f]	
$o\text{-}CH_3OC_6H_5N(CH_3)_3ClO_4$	Ethylene chloride	8.10[e]	4.76		2.36[i]
$o\text{-}CH_3OC_6H_5N(CH_3)_3ClO_4$	Ethylidene chloride	1.12[e]	3.92		2.36[i]

[a] C. R. Witschonke and C. A. Kraus, *J. Am. Chem. Soc.*, **69**, 2472 (1947). [b] M. B. Reynolds and C. A. Kraus, *ibid.*, **70**, 1709 (1948). [c] W. F. Luder and C. A. Kraus, *ibid.*, **69**, 2481 (1947). [d] Ref. 16. [e] Ref. 13. [f] L. Pauling, "Nature of the Chemical Bond," Cornell University Press, Ithaca, N. Y., 1940, p. 358. [g] Estimated from Fisher–Hirschfelder–Taylor models. The indicated radius corresponds to the most compressed conformation. The radius of the most extended conformation is 7.8 Å. [h] Estimated from Fisher–Hirschfelder–Taylor models. [i] K. B. Yatsimirskii, *Izvest. Akad. Nauk. USSR, Otdel. Khi Nauk.*, 398 (1948) [*C. A.* **42**, 8604 (1948)].

expression. The viscosity data of Luchinskii[11] were expressed by eq. 2, where t is in °C., with a mean deviation of ±0.36%, yielding 4.02 and 4.35

$$1000 \, \eta = 4.03 - 0.0363t \quad (2)$$

millipoises at 0.12 and −8.93°, respectively.

Discussion

Recent analyses[12] of the Bjerrum theory[3] of ion pairing have underlined its distinctly limited validity. In brief, it has been observed repeatedly that a, the distance of closest approach for a given pair of ions, calculated from equilibrium data and Bjerrum's equation, is not independent of the solvent. Even in media of essentially identical dielectric constant, a for a given solute is found to vary. It has been suggested[13] that in some cases the macroscopic dielectric constant is not appropriate and that a value of D characteristic of the medium in the vicinity of the ionic field should be employed. Alternatively, it has been postulated[12b] that Bjerrum's equation is applicable only to ions separated by at least a monolayer of solvent molecules and that a tighter association accompanies ejection of solvent. On this basis Sadek and Fuoss have derived eq. 3, where K_s measures the ratio of tight ion pairs to solvent separated pairs.

$$K_{exp} = K_{Bjerrum}/(1 + K_s) \quad (3)$$

Table III summarizes a values calculated directly from the Bjerrum relationship, eq. 4, with typical data in various media. Only values of K_{exp}

$$K^{-1} = \left(\frac{4\pi N}{1000}\right)\left(\frac{\epsilon^2}{DkT}\right)^3 Q(b) \quad (4)$$

smaller than 0.01 were employed in order to avoid the large uncertainties in the determination of K which arise when it exceeds this magnitude. In most cases the resulting a values are significantly smaller than the corresponding sums of ionic radii.

(11) G. P. Luchinskii, *J. Phys. Chem. (USSR)*, **12**, 280 (1938).

(12) (a) C. A. Kraus, THIS JOURNAL, **58**, 673 (1954); (b) H. Sadek and R. M. Fuoss, *J. Am. Chem. Soc.*, **76**, 5905 (1954).

(13) J. T. Denison and J. B. Ramsey, *ibid.*, **77**, 2615 (1955).

This is also true of the value (4.25 Å.) arrived at by Sadek and Fuoss for tetra-n-butylammonium bromide in mixtures of nitrobenzene and carbon tetrachloride by means of eq. 3, a procedure which can lead only to a values equal to or larger than those calculated with eq. 4. Kraus has, furthermore, pointed out[12a] that distances between centers of charge derived from polar moments[14] are considerably shorter than corresponding Bjerrum a values.

There appears to be no basis in fact or theory for identifying Bjerrum a values with sums of ionic radii. Yet the data for spherically symmetrical ions in sulfur dioxide solution (*cf.* Table IV) lead

TABLE IV

BJERRUM a VALUES CALCULATED FROM DATA FOR SULFUR DIOXIDE

Compd.	Temp., °C.	$r_+ + r_-$,[a] Å.	Bjerrum a
KCl	0.12	3.14	2.96
KCl	−8.93	3.14	3.10
KBr	0.12	3.28	3.28
KBr	−8.93	3.28	3.31
KI	0.12	3.50	3.58
KI	−8.93	3.50	3.78
Me₄NBr	0.12	5.25	5.25
Me₄NBr	−8.93	5.25	5.27

[a] Ionic radii are those given by L. Pauling in "Nature of the Chemical Bond," Cornell University Press, Ithaca, N. Y., 1940, p. 358, except for Me₄N⁺ which was estimated from Fisher–Hirschfelder–Taylor models.

to a values that deviate but little from sums of ionic radii.[15] This equivalence appears to be unique. It is conceivable that it may arise coincidentally from a compensation of polarization effects, which tend to diminish a, by tight solvation

(14) J. A. Geddes and C. A. Kraus, *Trans. Faraday Soc.*, **32**, 585 (1936).

(15) The observed correspondence is not a consequence of very low sensitivity of a to K_{exp}. The largest discrepancy (KI at −8.93°) corresponds to a difference of 31% between K_{exp} and $K_{Bjerrum}$ calculated with a taken equal to the sum of crystal radii.

of ions, which eliminates contiguous ion-pairs. Alternatively these observations may signify that the Bjerrum relationship is a limiting form of a more exact expression. However, it is not at present apparent why sulfur dioxide should be a "limiting" solvent. Nevertheless, these results provide a path toward detection of covalent association and a basis for estimating effective radii for non-spherical ions in this medium.

It is worth noting that the simplified treatment of the Bjerrum model by Denison and Ramsey[13] does not yield agreement with experiment when the sum of ionic radii is identified with a in their expression. On substitution of appropriate quantities into eq. 5, values of K_{DR} result which, for the

$$- \ln K_{DR} = \epsilon^2/aDkT \qquad (5)$$

alkali halides, are approximately $1/25$ of the corresponding magnitudes of K_{exp}. For $(CH_3)_4NBr$, K_{DR} is about $1/2$ of K_{exp}.

Thermodynamic quantities at $0.12°$ are assembled in Table V. In calculating $\Delta H°_{exp}$ this quantity was assumed not to vary with temperature. Although constancy of $\Delta H°$ over temperature ranges greater than that described here has been reported for ion-pair equilibria in other media[13,16] this assumption may not be true for sulfur dioxide solutions and the tabulated values must be regarded with caution.[17] Differentiation of Bjerrum's equation[12] provides a theoretical expression for $\Delta H°$ (eq. 6, where $L = - \partial \ln D/\partial T = 6.676 \times 10^{-3}$). Values of $\Delta H°_{Bjerrum}$ obtained from eq. 6 by identifying a with the sum of ionic radii are incorporated in Table V. Denison and Ramsey's simplified treatment[13] has provided an expression for $\Delta H°$ (eq. 7) which, following their

$$\Delta H°_{Bjerrum} = RT(1 - LT) \left(3 + \frac{e^b}{Q(b)b^3}\right) \qquad (6)$$

practice, we have used semi-empirically, i.e., by inserting $\Delta F°_{exp}$ values rather than the quite different values (cf. above) obtained on substituting sums of ionic radii for a in their expression for $\Delta F°$.

$$\Delta H°_{DR} = \Delta F°(1 - LT) \qquad (7)$$

If it is assumed that the tabulated $\Delta H°_{exp}$ values deviate sufficiently little from the correct quantities to permit comparisons to be made, it follows that the order of decreasing $\Delta F°_{exp}$ is determined by the entropy term and is largely contrary to the en-

(16) K. H. Stern and A. E. Martell, J. Am. Chem. Soc., **77**, 1983 (1955).

(17) A plot of $10^3/T$ vs. log K_{exp} based on Franklin's data[4] for KBr at $+10, 0, -10, -20$ and $-33.5°$ deviates only slightly from linearity in the range $+10$ to $-20°$. The corresponding plot for KI approximates linearity from 0 to $-33.5°$ but deviates appreciably at $+10°$.

thalpy term. This agrees with both theoretical treatments.

Comparison of limiting conductance data with theory reveals a useful relationship. The data of Table VI demonstrate that, for the inorganic solutes, insertion of ionic radii into Stokes Law[18] leads to limiting conductances in approximate agreement with observed values. The much larger difference observed with tetramethylammonium bromide suggests that although a tetraalkylammonium ion may possess spherical symmetry, its "frictional" surface area may be smaller than that of the corresponding sphere. These results provide approximate values of ionic limiting conductances in sulfur dioxide, quantities which are otherwise lacking.

TABLE V

Thermodynamic Quantities at $0.12°$[a]

Compd.	$\Delta F°_{exp}$,[b] kcal./ mole	$\Delta H°_{exp}$,[c] kcal./ mole	$\Delta H°_{Bjerrum}$[d] kcal./ mole	$\Delta H°_{DR}$,[e] kcal./ mole	$\Delta S°_{exp}$, cal./mole deg.
KCl	$+5.16$	-5.92	-4.76	-4.25	-40.6
KBr	$+4.81$	-5.26	-4.54	-3.97	-37.0
KI	$+4.40$	-5.60	-4.17	-3.63	-36.7
Me$_4$NBr	$+3.66$	-3.36	-2.49	-3.02	-25.7

[a] Variation in pressure is assumed to have negligible consequences. [b] $\Delta F°_{exp} = -RT \ln K_{exp}$. [c] $\Delta H°_{exp} = R(\ln K_{0.12} - \ln K_{-8.93})/(1/264.23) - (1/273.28)$. [d] Values of $\Delta H°_{Bjerrum}$ at $-8.9°$ are $-4.15, -3.96, -3.60$ and -2.20 kcal./mole for KCl, KBr, KI and Me$_4$NBr, respectively. [e] Substitution into eq. 7 of $\Delta F°$ values from eq. 5 yields $\Delta H°_{DR} = -5.70°, -5.45, -5.10, -3.40$ kcal./mole for solutes in tabulated order.

TABLE VI

Observed and Calculated[a] Values of $\Lambda°$

Compound	Temp., °C.	$\Lambda°_{exp}$	$\Lambda°_{Stokes}$
KCl	0.12	243	264
KCl	-8.93	222	244
KBr	0.12	249	256
KBr	-8.93	228	237
KI	0.12	244	245
KI	-8.93	221	227
Me$_4$NBr	0.12	236	165
Me$_4$NBr	-8.93	215	153

[a] From the relationship: $\Lambda° = (0.8147 \times 10^{-8})/\eta \Sigma 1/a_j$ where $\eta = 4.03$ and 4.35 millipoises at 0.12 and $-8.93°$, respectively, and a is taken as equal to the ionic radius.

(18) H. S. Harned and B. B. Owen, "The Physical Chemistry of Electrolyte Solutions," Reinhold Publ. Corp., New York, N. Y. 1950, p. 183.

IONIZATION AND DISSOCIATION EQUILIBRIA IN SULFUR DIOXIDE. IV. ALKYL AND ARYL DERIVATIVES OF TRIPHENYLCHLOROMETHANE AT 0 AND −8.9°

By Norman N. Lichtin and Harry P. Leftin[1]

Contribution from the Department of Chemistry, Boston University, Boston, Mass.

Received August 17, 1955

Conductivity data in liquid sulfur dioxide solution have been secured for triphenylchloromethane, its mono-, di- and tri-*m*-phenyl, mono-, di- and tri-*p*-phenyl, mono-*m*- and mono-*p*-*t*-butyl derivatives at −8.9° and, where previously lacking, at 0°. Shedlovsky's procedure has been applied to the data in the dilution range 2000 to 80,000 liters per mole to calculate values of K_{exp} and Λ^0. Values of ΔH^0_{exp} have been approximated by assuming constancy of this quantity over the temperature range employed. The relationship between ΔH^0_{exp} and ΔF^0_{exp} values for this series of compounds is quite different from that observed with KCl, KI, KBr and $(CH_3)_4NBr$. This difference is presumed to be associated with the occurrence of covalent association in the present cases. Ion-pair dissociation constants have been calculated on the basis of an assumed model and some of the consequences of this procedure have been explored.

Introduction

There has been described already[2] a considerable amount of evidence that solutions in sulfur dioxide of derivatives of triphenylchloromethane belong to a class of electrolytes the equilibria of which have been investigated relatively little, namely, those in which ions associate covalently as well as electrostatically. Perhaps most pertinent is the observation[2b] that at 0° K_{exp}, the dissociation constant obtained from conductance data, is about five times greater for the mono-*p*-phenyl derivative than for the parent compound, whereas for the mono-*m*-phenyl derivative it is only three-fourths as large as for the parent compound. Since the mono-*m*- and *p*-substituted triphenylcarbonium ions are of similar size and shape this cannot be a consequence of structural influence on electrostatic ionic association which is now known[3] to adhere remarkably closely to Bjerrum's equation in this medium.

Conductance data for most of these solutes were secured in the earlier work at only one temperature, 0°, two compounds having been investigated at −17° as well.[2a] Measurements reported herein have been carried out largely at −8.9° and in part at 0°, so that useful information on the temperature dependence of K_{exp} for eight solutes of this type is now available. The observed relationship between K_{exp} and its temperature dependence is quite different from that found with solutes consisting of spherical ions which associate only electrostatically.

It has been assumed[2] that the equilibria represented by eq. 1 maintain in these systems. Here RCl represents the covalently associated species

$$RCl \underset{K_1}{\overset{K_1}{\rightleftarrows}} R^+Cl^- \underset{K_2}{\overset{K_2}{\rightleftarrows}} R^+ + Cl^- \quad (1)$$
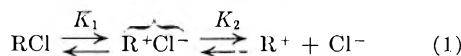
and R^+Cl^- represents the electrostatically associated species (ion pair). K_1 and K_2, the constants for ionization and dissociation, respectively, are related to K_{exp} as shown in eq. 2, where the quantities in parentheses are activities.

$$K_{exp} = (R^+)(Cl^-)/[(RCl) + (R^+Cl^-)] =$$
$$K_2/(1 + 1/K_1) \quad (2)$$

Equation 2 is identical in form with the relationship (their eq. 10) which Sadek and Fuoss[4] have recently presented. It differs, however, in that K_1 measures the equilibrium of ionization of a covalent bond and its dependence on structure is therefore subject to correlation with established group effects.

The observed temperature dependence is consistent with this analysis. An attempt also has been made to apply these equations to the quantitative correlation of the measured equilibria with structure.

Experimental

Apparatus, procedures and solvent were those referred to in the preceding paper.[3] The samples of triphenylchloromethane, its mono-*m*-*t*-butyl, mono-*p*-*t*-butyl, mono-*m*-phenyl and mono-*p*-phenyl derivatives were drawn from batches of these compounds which have been described previously[2a,b] and which, having been stored in desiccators in the dark, gave no evidence of decomposition.

Syntheses.—Solutes were prepared with emphasis on purity and little regard for yield. All-glass equipment was used throughout and moisture and oxygen were excluded[5] wherever necessary. Solvents were of C.P. grade or higher and thoroughly dried before use. Grignard solutions were subjected to acidimetric analysis of aliquots of hydrolysate before use.

The **di- and tri-*m*-phenyl derivatives of triphenylcarbinol** were prepared by the reaction of Eastman Kodak Co. "White Label" ethyl benzoate or ethyl carbonate[6] (dried over anh. $CaSO_4$), respectively, with *m*-biphenylylmagnesium bromide. The Grignard reagent was prepared by treating freshly prepared turnings of Dow Chemical Company "Super Pure" magnesium with one equivalent of *m*-bromobiphenyl in dry ether containing 5–10% dry benzene.[7] The carbinols were obtained after steam distillation and attempted purification by crystallization as impure yellow powders of wide melting range.

Di-*m*-biphenylylphenylchloromethane, previously unreported, was prepared from the impure carbinol (5 g.) by refluxing (4 hr.) with freshly distilled acetyl chloride (15 ml.). Removal of excess acetyl chloride by suction, trituration of the resulting oil and standing for 3 days with petroleum ether followed by washing with this solvent produced a yellow powder. This material was recrystallized three times from 1:1 acetyl chloride–petroleum ether, washed with petroleum ether and dried at room temperature under

(1) Based in part on a dissertation submitted by H. P. Leftin in fulfillment of a requirement for the Ph.D. degree, Boston University, May, 1955.

(2) (a) N. N. Lichtin and P. D. Bartlett, *J. Am. Chem. Soc.*, **73**, 5530 (1951); (b) N. N. Lichtin and H. Glazer, *ibid.*, **73**, 5537 (1951).

(3) N. N. Lichtin and H. P. Leftin, This Journal, **60**, 160 (1956).

(4) H. Sadek and R. M. Fuoss, *J. Am. Chem. Soc.*, **76**, 5905 (1954).

(5) For instance, *cf.* L. F. Fieser, "Experiments in Organic Chemistry," Part II, D. C. Heath and Co., New York, N. Y., 1941, p. 404.

(6) C. S. Marvel, E. Ginsberg and M. B. Mueller, *J. Am. Chem. Soc.*, **61**, 77 (1939).

(7) N. N. Lichtin and H. P. Leftin, *ibid.*, **74**, 4207 (1952).

high vacuum to yield a white powder, m.r. 113.5–114.5°.) *Anal.*[8] Calcd. for $C_{31}H_{23}Cl$: C, 86.4; H, 5.4; Cl, 8.2. Found: C, 86.4; H, 5.5; Cl, 8.3. Another sample was obtained from partially purified carbinol by reaction with acetyl chloride as before. Solid product was obtained from the reaction mixture on standing in the freezing compartment of a refrigerator for ten days and was purified by recrystallizing twice from acetyl chloride, washing with petroleum ether and pumping under high vacuum for eight days to yield white crystals, m.r. 117.6–118.5°. The analysis[8] for Cl was 8.2%. Conductivity data obtained with the two samples at –8.9° were in excellent agreement.

Tri-*m*-biphenylylchloromethane was obtained by refluxing the crude carbinol (5 g.) with freshly distilled acetyl chloride (25 ml.) for 3 hr., adding enough benzene (15 ml.) to bring the product into solution and chilling for 12 hr. The product was recrystallized once from benzene containing a few drops of acetyl chloride and dried by pumping to give minute white needles, m.r. 201–202° (cor.). *Anal.*[8] Calcd. for $C_{37}H_{27}Cl$: C, 87.6; H, 5.4; Cl, 7.0. Found: C, 86.7, 88.2; H, 5.3, 5.2; Cl, 6.7. A portion of this material was recrystallized twice more from dry benzene containing a few drops of acetyl chloride, then once from dry benzene and dried by pumping to yield crystals with m.r. 200–201° (cor.). The analysis[8] for C was 87.1%, H, 5.8%; Cl, 7.1, 7.0%. Conductivity data obtained with the two samples at both 0.1 and –8.9° were in excellent agreement.

Di-*p*-biphenylylphenylcarbinol[9] was prepared by the reaction of phenylmagnesium bromide with di-*p*-biphenylyl ketone.[10] Di-*p*-biphenylyl ketone was synthesized by distilling phosgene (1 mole) into a mixture of biphenyl (0.88 mole), Al_2Cl_6 (0.62 mole) and carbon disulfide (450 ml.) and stirring for 14 hours. After hydrolysis, the crude product was extracted in a Soxhlet apparatus with 1:1 acetone–benzene. The extract deposited crystals which were recrystallized from 1:1 benzene–pyridine and then from toluene to yield small yellow–green crystals, m.r. 235–237° (cor.). Phenyl Grignard (0.22 mole) was prepared in ether solution and the ether replaced by anisole (200 ml.) before adding a solution of the ketone (0.073 mole) in anisole (70 ml.). After completion of the reaction (steam-bath for 4 hours, room temperature for 12 hours), hydrolysis and steam distillation, the product was crystallized from 1:1 benzene–ether (90 ml.) to yield white di-*p*-biphenylylphenylcarbinol (0.043 mole), m.r. 153.5–154.5° (cor.).

Di-*p*-biphenylylphenylchloromethane was prepared from a sample of carbinol (3.0 g.) by refluxing (0.5 hour) with 25 ml. of 1:4 benzene–ether containing acetyl chloride; the solvents were removed on the aspirator and petroleum ether added. The precipitate was recrystallized from 25 ml. of 4:1 petroleum ether–methylene chloride containing a few drops of acetyl chloride and dried at 35° by pumping at 0.1 mm. for 12 hours. The crystals were pale purple, m.r. 136–137° (cor.). The purity, estimated by acidimetric analysis of the hydrolysate, was 100.3 ± 0.3%. The analysis[8] for C was 86.1%, H 5.4%.

Tri-*p*-biphenylylcarbinol[9,11] was prepared by the reaction of *p*-bromobiphenyl with ethyl carbonate and sodium. A solution of 0.32 mole of *p*-bromobiphenyl (Eastman Kodak Co. "White Label" recrystallized twice from 95% ethanol) and 0.10 mole of ethyl carbonate (Eastman Kodak Co. "White Label" freshly distilled, $n^{20}D$ 1.3847) in 100 ml. of dry benzene was added with stirring over a period of 1 hour to 0.83 mole of sodium dispersion (National Distillers Products Corp. 50% dispersion in toluene) in 100 ml. of boiling dry benzene. After the reaction was complete (2 hr. in all), ethanolysis, steam distillation and recrystallization from toluene–ligroin gave 0.042 mole of almost white product, m.r. 205–208° (uncor.).

Tri-*p*-biphenylylchloromethane was prepared from the carbinol (5.0 g.) by refluxing with 5 ml. of freshly distilled acetyl chloride in 60 ml. of 5:1 benzene–petroleum ether for one hour. The resulting crystals were recrystallized from 2:1 methylene chloride–petroleum ether (10 ml.) and pumped at 0.1 mm. for 12 hours to yield pale violet crystals, m.r. 197–198° (cor.). The purity, estimated by acidimetric

analysis of the hydrolysate, was 99.9 ± 0.2%. The analysis[8] for C was 87.5%, H 5.5%.

Data

Conductance data from typical individual runs are recorded in Table I. Values of Λ^0 and K_{exp} were calculated from the data of at least three runs for each compound at each temperature except for the mono-*m*-*t*-butyl and mono-*m*-phenyl derivatives at –8.9°, for which the data of two runs were employed. The average scatter of experimental points about the smoothed plot of Λ *vs.* V was found to be of the order of ±1% (of Λ) or less for each compound in the dilution range employed in the Shedlovsky calculations.

Values of K_{exp} and Λ^0 were calculated by applying Shedlovsky's procedure[12,13] to individual data points in the dilution range 2000–80,000 liters per mole (*cf.* the preceding paper[3] for the basis for choice of this range). Values of the dielectric constant and viscosity were calculated by means of eqs. 1 and 2 of the preceding paper.[3] The least-square procedure was employed to determine the slope $[1/K(\Lambda^0)^2]$ and intercept $(1/\Lambda^0)$ of the Shedlovsky line. New values of K_{exp} and Λ_0 were also calculated in exactly the same way from earlier data[2a,b] so that more accurate comparisons of structural and temperature effects could be made. Table II summarizes these quantities. Data, not reported here, also were collected at –8.9° for the di-*p*-*t*-butyl and tri-*p*-phenyl derivatives of trityl chloride. In these cases the percentage change in the Shedlovsky ordinate $[1/\Lambda S(z)]$ over the range of abscissa $(\Lambda S(z)f_{\pm}^2/V)$ corresponding to the selected dilution limits was too small (relative to the precision of the data) to permit accurate determination of the slope of the Shedlovsky line. Thus, in addition to the fundamental uncertainty[14] involved in application of the Shedlovsky procedure to solutes that are almost completely dissociated, an upper limit to the values of K_{exp} which can be determined with some degree of accuracy is imposed by the precision of the data. This difficulty must also be recognized in the case of the above two compounds at 0° where the data yield an approximately 5% change in Shedlovsky ordinate over the selected range.

Also assembled in Table II are values of ΔF°_{exp} calculated from the relationship $\Delta F^\circ_{exp} = -RT \ln K_{exp}$ and of ΔH°_{exp} calculated by means of eq. 3 on the assumption that ΔH°_{exp} is temperature independent over the range employed. The data for trityl chloride are, however, contrary to this

$$\Delta H^\circ_{exp} = R \ln (K/K')/[(1/T') - (1/T)] \quad (3)$$

assumption. Although the data are too few to permit accurate analysis, it is possible to state ΔH°_{exp} as a function of temperature for trityl chloride by establishing an empirical expression relating $R \ln K$ to temperature and differentiating this expression with respect to T^{-1}. This process yields $\Delta H^\circ = 1.178 \times 10^5 - 3.372 \times 10^7 T^{-1}$. Substitution of appropriate values of T suggests that over the range +0.1 to –17° ΔH° varies linearly with T. It is thus possible to use the rela-

(8) Compounds were analyzed by Dr. Carol H. Fitz.

(9) W. Schlenk, *Ann.*, **368**, 301 (1909).

(10) P. Adam, *Ann. chim. phys.*, [6], **15**, 200 (1888).

(11) W. E. Bachmann and F. Y. Wiselogle, *J. Org. Chem.*, **1**, 371 (1936).

(12) T. Shedlovsky, *J. Frank. Inst.*, **225**, 739 (1938).

(13) H. M. Daggett, *J. Am. Chem. Soc.*, **73**, 4977 (1951).

(14) C. A. Kraus, THIS JOURNAL, **58**, 673 (1954).

Table I

Conductance Data for Typical Single Runs[a,b]

V	Λ	V	Λ
Unsubstituted $-8.93 \pm 0.03°$		Mono-p-t-Butyl $-8.85 \pm 0.07°$	
		260.2	90.8
585.8	40.5	600.2	109
1333	55.5	1385	127
3042	74.9	3194	140
6942	97.8	7370	156
15860	122	17020	164
36200	144	39300	168
83750	161	90928	173
Mono-m-t-butyl $-8.77 \pm 0.02°$		Mono-p-phenyl $-8.93 \pm 0.03°$	
526.9	68.1	631.9	78.6
1223	88.7	1448	99.4
2841	110	3303	120
6600	132	7557	138
15340	148.5	17300	151
35650	157	39600	158
82860	164	90760	161
Mono-m-penyl $-8.93 \pm 0.03°$		Di-p-phenyl $-8.90 \pm 0.01°$	
433.5	27.1		
994.7	38.4	873.7	114
2288	53.5	1991	131
5265	72.5	4543	145
12110	94.7	10363	154
27850	118	23671	160
64070	138	54061	161.5
Di-m-phenyl $-8.93 \pm 0.03°$		Tri-m-phenyl $-8.93 \pm 0.03°$	
194.9	14.9	1032	23.2
444.0	21.2	2355	32.8
1012	30.0	5374	45.7
2298	41.8	12270	62.4
5223	57.1	28000	81.7
11910	76.4	63870	102
27200	98.4	145800	119
62230	119		
141700	141		
Di-p-phenyl $0.10 \pm 0.01°$		Di-m-phenyl $0.12 \pm 0.03°$	
434.2	96.6	309.5	15.2
978.4	118.5	711.2	21.7
2206	138	1631	30.9
4974	153	3742	43.4
11210	164	8588	59.7
25300	171	19680	79.2
57060	176	45110	100
		103300	120
Tri-p-phenyl $0.10 \pm 0.01°$		Tri-m-phenyl $0.12 \pm 0.03°$	
823.3	132.5	690.0	16.3
1871	148	1600	23.7
4254	159	3706	33.9
9668	166	8583	47.7
21980	169	19880	65.2
50013	170	46040	86.1
		106700	106

[a] V is in liters/mole, Λ in mhos cm.²/mole. Temperatures (°C.) and their average mean deviations correspond

to all runs with the indicated solute and temperature. All conductances are corrected for solvent conductivity which fell in the range $0.7 - 2.0 \times 10^{-7}$ mhos cm.$^{-1}$. [b] Solutes are indicated in terms of the substituents introduced into triphenylchloromethane. Thus, di-m-phenyl indicates
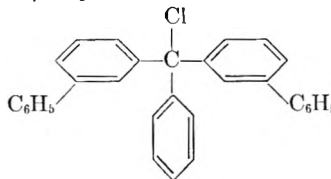
tionship of Douglas and Crockford[15] (eq. 4) to determine the temperature for which the value arrived at by means of eq. 3 is the correct value of $\Delta H°$. For the interval $+0.1$ to $-8.9°$ this is $-5.2°$. If it is assumed that for all compounds of

$$T_0 = \ln(T_2/T_1)/[(1/T_1) - (1/T_2)] \qquad (4)$$

this series $\Delta H°$ varies linearly with temperature over the range $+0.1$ to -8.9, then it follows that the tabulated values all correspond to this temperature and are comparable. Additional data are, of course, needed to test this assumption. Values of $\Delta S°$ have not been tabulated since the values of $\Delta H°$ and $\Delta F°$ correspond to different temperatures.

Discussion

If the significance ascribed to values of $\Delta H°_{exp}$ is justified, these quantities can be compared with the predictions of theory. Denison and Ramsey's semi-empirical[3,16] equation (eq. 5, $L = -\partial \ln D/\partial T = 6.676 \times 10^{-3}$), which yields a trend in $\Delta H°$

$$\Delta H°_{DR} = \Delta F°_{exp}(1 - LT) \qquad (5)$$

similar to that obtained experimentally for equilibria involving electrostatic association of spherical ions in sulfur dioxide obviously fails for the present series of compounds since it cannot accommodate the increase in exothermicity of $\Delta H°_{exp}$ associated with decrease in endothermicity of $\Delta F°_{exp}$ observed for compounds 1 through 6. It is equally clear that there is no relationship between $\Delta H°_{exp}$ and ionic dimensions as would be expected from a Bjerrum type of expression for $\Delta H°$ (eq. 8).

The observed variation of $\Delta H°_{exp}$ with $\Delta F°_{exp}$ is consistent, however, with eq. 2 and the assumptions upon which it is founded. Equation 6 is readily derived from eq. 2. At the limit of large K_1 the second term of eq. 6 vanishes and $\Delta H°_{exp}$ becomes identical with $\Delta H°_2$.

$$\Delta H°_{exp} = \Delta H°_2 + [R/(1 + 1/K_1)][\partial(1/K_1)/\partial(1/T)] \qquad (6)$$

At the limit of small K_1 the second term of eq. 6 becomes equal to $[R/(1/K_1)][\partial(1/K_1)/\partial(1/T)]$ and $\Delta H°_{exp}$ equals $\Delta H°_2 + \Delta H°_1$. Meta- and para-substituents which influence K_1 through electronic effects acting on the ease of ionization of the carbon to chlorine bond would be expected to affect $\Delta H°_1$ and $\Delta F°_1$ similarly.[17] A qualitative parallelism of this sort between $\Delta H°_{exp}$ and $\Delta F°_{exp}$ is apparent in the data of Table II for compounds 1 through 6. This suggests that, for these solutes, K_1 is sufficiently small that $\Delta H°_{exp}$ reflects changes

(15) T. B. Douglas and H. D. Crockford, J. Am. Chem. Soc., 57, 97 (1935).

(16) J. T. Denison and J. B. Ramsey, ibid., 77, 2615 (1955).

(17) L. P. Hammett, "Physical Organic Chemistry," McGraw-Hill Book Co., New York, N. Y., 1940, pp. 76-78, 123 184-194.

TABLE II

QUANTITIES DERIVED FROM SHEDLOVSKY TREATMENT

	Solute[a]	T, °C.	$\Lambda°$, mhos cm.²/mole	$10^5 K_{exp}$, moles/liter	$\Delta F°_{exp}$[b] kcal./mole	$\Delta H°_{exp}$[b] kcal./mole	Scatter about Shedlovsky line,[e] %
1	Tri-m-C₆H₅	-8.93	157	1.94	+5.70		±1.40
	Tri-m-C₆H₅	+0.12	159	1.36	+6.09	-5.62	1.08
2	Di-m-C₆H₅	-8.93	162	3.10	+5.44		1.14
	Di-m-C₆H₅	+0.12[d]	163	2.22	+5.82	-5.80	0.77
3	Mono-m-C₆H₅	-8.93	177	4.63	+5.24		1.22
	Mono-m-C₆H₅	+0.12	184	3.07	+5.64	-6.54	1.30
4	Unsubstd.	-17[e]	168	13.0	+4.56		2.14
	Unsubstd.	-8.93	188	6.69	+5.05	-11.2	1.24
	Unsubstd.	0.00[e]	207	4.15	+5.48	-7.53	1.41
5	Mono-m-methyl	0.00[e]	201	9.53	+5.02		0.85
6	Mono-m-t-butyl	-8.77	173	32.3	+4.23		0.94
	Mono-m-t-butyl	0.00[e]	200	17.3	+4.73	-10.2	0.78
7	Mono-p-C₆H₅	-8.93	172	42.4	+4.08		0.55
	Mono-p-C₆H₅	+0.12[d]	189	24.1	+4.52	-9.02	0.74
8	Mono-p-t-butyl	-8.85	177	101	+3.63		0.64
	Mono-p-t-butyl	0.00[e]	192	72	+3.93	-5.58	0.43
9	Mono-p-methyl	0.00[e]	196	77	+3.89		1.05
10	Di-p-C₆H₅	-8.90	168	147	+3.42		.50
	Di-p-C₆H₅	+0.10	181	105	+3.72	-5.40	.74
11	Tri-p-C₆H₅	+0.10	177	310	+3.13		.66
12	Di-p-t-butyl	0.00[e]	191	330	+3.10		1.33

[a] Solutes are indicated as derivatives of triphenylchloromethane as in Table I. [b] Calculated from the relationship, $\Delta F°_{exp} = -RT \ln K_{exp}$, and eq. 3. [c] In terms of the ordinate, $1/\Lambda S(z)$. [d] Cf. ref. 2b for conductance data. [e] Cf. ref. 2a for conductance data.

in both $\Delta H°_1$ and $\Delta H°_2$. For the remainder of the series (compounds 6–12), insofar as they are known, $\Delta H°_{exp}$ and $\Delta F°_{exp}$ vary in opposite directions. Here, the contribution of $\Delta H°_1$ is presumably diminishing and the limit where $\Delta H°_{exp}$ equals $\Delta H°_2$ is approached.

Confirmation of these conclusions requires a knowledge of values of K_1 and K_2 and the corresponding thermodynamic quantities. Spectroscopic measurements with solutions of triphenylchloromethane in sulfur dioxide solution have indicated[18] that, for this solute at $1 \pm 0.3°$, $K_2 \geqslant 3 \times 10^{-3}$. Lacking further experimental information, we are limited to estimation of these quantities on the basis of theory.[19] The results[3] of the investigation of KCl, KBr, KI and (CH₃)₄NBr enable a small amount of progress to be made in this direction. Since Bjerrum's equation, with a taken equal to the sum of ionic radii has been shown to yield unusually good agreement with values of K_{exp} for these spherical ions in sulfur dioxide solution, it is possible to predict ion pair dissociation

(18) P. D. Bartlett and R. E. Weston, Jr., ONR Technical Report No. 6 under Project No. NR-056-095, Contract No. N5 ori-76, Task XX, April 10, 1952.

(19) Although the analysis represented by eq. 2 is capable of accommodating available information, it is recognized that it does not constitute a unique interpretation. The data are, for instance, also consistent with the notion that the ions of each solute at a given temperature associate in only one way. The species so formed would, for the weakest electrolytes, closely approximate a normal covalent molecule, for the strongest a Bjerrum ion-pair. For intermediate cases the carbon-chlorine bond would have varying degrees of ionic character in excess of that characteristic of the normal amount for this bond. This hypothesis is, in principle, experimentally distinguishable from that of eq. 2, but not via conductance data. Equation 2, however, permits quantitative, theoretical speculation which is not possible with the alternative model. This, to be sure, constitutes a hazard as well as an advantage for eq. 2.

constants for such solutes with considerable confidence. A triphenylcarbonium ion, however, does not have spherical symmetry and information on the relationship between Bjerrum's equation and the behavior of analogous non-spherical ions in this medium is not yet available. A speculative approach to this question can be made by postulating a basis for selecting equivalent Bjerrum radii for these cations. For this purpose, it is proposed that these cations occupy the spherical spatial region defined by the largest van der Waals radius about the center of gravity of the ion.[20] Approximate estimates of these radii can be made conveniently with the aid of Fisher–Hirschfelder–Taylor models. These are listed in Table III along with corresponding values of $K_{Bjerrum}$ at 0° and $\Delta H°_{Bjerrum}$ at $-5.2°$ calculated by means of eqs. 7 and 8.[3,21] Values of K_1 calculated from eq. 2 by identifying K_2 with these $K_{Bjerrum}$ values are also tabulated. These quantities prove to be consistent with equation 2 and the experimental data. Thus, $K_{Bjerrum}$ values are all greater than the corresponding values of K_{exp}, the difference becoming small for the

$$K^{-1}_{Bjerrum} = (4\pi N/1000)(\epsilon^2/DkT)^3 Q(b) \quad (7)$$

$$\Delta H°_{Bjerrum} = R(1 - LT)[3 + e^b/Q(b)b^3] \quad (8)$$

stronger electrolytes for which it has been suggested that K_{exp} approaches K_2. In addition, $\Delta H°_{Bjerrum}$ varies but little for this series and takes values less exothermic than $\Delta H°_{exp}$ for the strongest electrolyte.

The fact that values of K_{exp} for trityl chloride

(20) This suggestion differs from that offered some time ago.[2a] The earlier proposal is not yet subject to quantitative elaboration.

(21) Cf. H. S. Harned and B. B. Owen, "Physical Chemistry of Electrolytic Solutions," Reinhold Publ. Corp., New York, N. Y., 1950, pp. XIII–XXVII, for meaning of symbols

Table III

Theoretical Equilibrium Quantities

Solute[a]	r_+, Å.	$10^3 K_{Bjerrum}$[b,c] at 0° moles/l.	$10^3 K_1$[b,d]	$\Delta H°_{Bjerrum}$ at −5.2°, kcal./mole
1 Tri-m-C$_6$H$_5$	10.8	5.76	2.37	−2.09
2 Di-m-C$_6$H$_5$	10.2	5.26	4.24	−2.03
3 Mono-m-C$_6$H$_5$	8.8	4.22	7.33	−1.93
4 Unsubstd.	7.0	3.14	13.4	−1.89
5 Mono-m-CH$_3$	7.1	3.19	30.7	−1.89
6 Mono-m-t-Bu	8.1	3.78	47.9	−1.90
7 Mono-p-C$_6$H$_5$	9.2	4.50	56.3	−1.95
8 Mono-p-t-Bu	8.3	3.90	225	−1.91
9 Mono-p-CH$_3$	7.9	3.65	268	−1.89
10 Di-p-C$_6$H$_5$	10.8	5.78	222	−2.10
11 Tri-p-C$_6$H$_5$	11.8	6.75	865	−2.23
12 Di-p-t-Bu	9.0	4.36	3230	−1.94

[a] Substituents on the triphenylcarbonium structure are indicated, e.g., di-m-C$_6$H$_5$ signifies

$$C_6H_5-C^+ \begin{cases} -C_6H_5 \\ -C_6H_5 \end{cases}$$
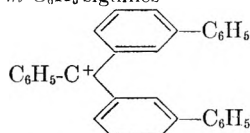
[b] For exact temperature cf. Table II. [c] Calculated with $a = r_+ + 1.8$. [d] Calculated by solving eq. 2 for K_1 and assuming $K_{Bjerrum} = K_2$.

and the mono-, di- and tri-substituted compounds, respectively, differ by quite unequal factors when the substituent is p-t-butyl or p-phenyl has been referred to previously.[2b] As expected, with m-phenyl as substituent the factors differ much less. The ratios $(K_{exp})_{n+1}/(K_{exp})_n$, where n equals the number of like substituents are, at 0°, for p-t-butyl 17.3, 4.6, for p-phenyl 5.8, 4.35, 2.95 and for m-phenyl 0.74, 0.72, 0.61 (with n in the order 0, 1, 2). The corresponding sets of ratios based on K_1 values, rather than K_{exp}, are much more nearly constant for all three substituents. These are 16.8, 14.4 for p-t-butyl,[22] 4.2, 3.9, 3.9 for p-phenyl, and 0.55, 0.58 and 0.56 for m-phenyl. It thus appears that $\Delta F°_1$ varies by almost identical increments for each substituent of a given type. Streitwieser[23] has carried out molecular orbital calculations of delocalization energy (DE) for several covalent molecules and their cations of the present series and has reported ΔDE ($DE_{ion} - DE_{molecules}$) values corresponding to the ionization process which decrease by virtually the same amount for each m-phenyl and increase by almost equal amounts for each p-phenyl group. Thus there appears to be a close relationship between ΔF_1 values and potential energy differences. Quantitative correspondence is not found, $|\Delta\Delta DE|$[24] being 0.03 kcal./mole for each m-phenyl and about 0.38 kcal./mole for each p-phenyl while the corresponding average values of $|\Delta\Delta F_1|$ are 0.31 and 0.76 kcal./mole respectively.

It is also apparent that values of K_1 adhere more closely than do values of K_{exp} to the relevant form of Hammett's relationship, Equation 9,[25] where K and K_0 are equilibrium constants for substituted and parent compounds, n is the number of sub-

stituents, and ρ and σ are the Hammett reaction and substituent parameters, respectively. Since

$$\log K/K_0 = \rho n \sigma \qquad (9)$$

σ values for p-alkyl groups and p-phenyl are known to vary with the reaction,[26] this correspondence is best observed with the data for successive introduction of identical substituents.

If ρ is arbitrarily determined by employing σ values for no substituent (0.000) one, two and three m-phenyls (+0.06, +0.12, +0.18),[27] m-CH$_3$ (−0.069)[28] and m-t-butyl (−0.120)[28] in conjunction with K_1 values, it is found to be −4.410 with a standard deviation from the least squares line of 0.095 and a correlation coefficient equal to 0.999.[29]

From this and the remaining K_1 data, the σ values for p-phenyl, p-t-butyl and p-methyl are found[29] to be −0.135, −0.269 and −0.289, respectively. The high negative magnitudes of these quantities (Jaffé gives +0.009, −0.197 and −0.170, respectively) can be ascribed to the importance in stabilizing the cation of resonance distribution of positive charge into these groups. Values of σ that are considerably more negative than those tabulated by Jaffé have been calculated in a related fashion for the groups p-(CH$_3$)$_2$N-, p-NH$_2$-, p-CH$_3$O-, p-CH$_3$- and p-Cl- from spectroscopically estimated equilibrium constants for the hydrolysis of p-substituted triphenylcarbonium ions.[30] For p-methyl, σ was found to be −0.270.

Numerous data on ionization equilibria of derivatives of triphenylchloromethane in solution in nitroalkanes,[31] nitroaromatics[32] and acetic and formic acid[33] have been reported by A. G. Evans and his associates. Comparison of their results with the data relating to sulfur dioxide solution has not been attempted in this discussion because of uncertainty as to the significance of their conclusions on ion-pair dissociation. Thus, with nitro compounds as solvents, they report that dissociation to free ions is not detectable. On the basis of conductivity data extensive dissociation would be expected with solutions in nitromethane[34] and nitrobenzene[35] at concentrations cited by these workers.[36,37] Equally perplexing is their report[33] that in acetic acid solution at 17° ($D_{20} = 6.15$) the ion pair tri-p-tolyl-carbonium chloride has a dissociation constant

(22) The tri-p-t-butyl compound[2a] is now regarded as too highly dissociated to permit accurate evaluation of K_{exp}.

(23) A. Streitwieser, J. Am. Chem. Soc., 74, 5288 (1952).

(24) On the basis of $\beta = 20$ kcal./mole; cf. C. A. Coulson, "Valence," Oxford University Press, London, 1952, pp. 239–240.

(25) H. H. Jaffé, Chem. Revs., 53, 249 (1953).

(26) E. Berliner, M. C. Beckett, E. A. Blommers and B. Newman, J. Am. Chem. Soc., 74, 4940 (1952); E. Berliner and L. H. Liu, ibid., 75, 2417 (1953); E. Berliner and L. H. Altschul, ibid., 74, 4110 (1952).

(27) N. N. Lichtin and H. P. Leftin, ibid., 74, 4207 (1952).

(28) Ref. 25, p. 222.

(29) Cf. Ref. 25, pp. 253–254, for procedures employed in calculations.

(30) N. C. Deno and A. Schriesheim, J. Am. Chem. Soc., 77, 3051 (1955).

(31) A. Bentley and A. G. Evans, J. Chem. Soc., 3468 (1952); A. G. Evans, J. A. G. Jones and G. O. Osborne, Trans. Faraday Soc., 50, 16 (1954); ibid., 470; J. Chem. Soc., 5343 (1954).

(32) A. G. Evans, A. Price and J. H. Thomas, Trans. Faraday Soc., 50, 568 (1954).

(33) A. G. Evans, A. Price and J. H. Thomas, ibid., 51, 481 (1955).

(34) C. P. Wright, D. M. Murray-Rust and H. Hartley, J. Chem. Soc., 199 (1931); R. C. Miller and R. M. Fuoss, J. Am. Chem. Soc., 75, 3076 (1953).

(35) C. R. Witschonke and C. A. Kraus, ibid., 69, 2476 (1947).

(36) The ion pair dissociation constant reported for (C$_6$H$_5$)$_3$-C$^+$HgCl$_3^-$ in nitromethane at 17°, namely, 2.39 × 10^{-5} mole liter (J. W. Boyles, A. G. Evans and J. R. Jones, J. Chem. Soc., 206 (1955)) is remarkably small also.

(37) Cf. B. B. Smith and J. E. Leffler, J. Am. Chem. Soc., 77, 1700 (1955), for evidence of the instability of solutions of trityl chloride in nitromethane.

equal to about 6×10^{-7} mole/liter while in formic acid ($D_{16} = 58.5$) the dissociation of triphenylcarbonium chloride is detectable but its "extent is too small for quantitative estimation."

Acknowledgment.—This work was supported by a Frederick Gardner Cottrell Grant from The Research Corporation and by the National Science Foundation under Grant NSF-G 436. The di- and tri-p-phenyl derivatives of trityl chloride were prepared and analyzed by Mr. Michael J. Vignale. "Super-pure" magnesium was a gift of the Dow Chemical Company.

CONDUCTANCES OF POTASSIUM THIOCYANATE AND TETRA-n-BUTYLAMMONIUM IODIDE IN ACETONE AT SEVERAL TEMPERATURES WITHIN THE RANGE 25 TO −50° [1a,b]

By Paul G. Sears, Eugene D. Wilhoit and Lyle R. Dawson

Department of Chemistry, University of Kentucky, Lexington, Kentucky

Received August 17, 1955

The conductances of potassium thiocyanate and tetra-n-butylammonium iodide in acetone have been measured at 25° and at ten-degree intervals between 20 and −50°. Limiting equivalent conductances and dissociation constants have been determined by the Shedlovsky extrapolation method. The results for each salt in acetone indicate that dissociation increases with decreasing temperature and that the logarithm of the limiting equivalent conductance is a linear function of the reciprocal of the absolute temperature.

Introduction

Acetone is among the few solvents for which dielectric constant data are known for temperatures as low as −50°. Since the availability of this information is necessary for a theoretical treatment of conductance data, it was selected as an electrolytic solvent for a conductance study at low temperatures. Acetone is a volatile liquid of low viscosity having a dielectric constant of 20.7 which has been used as a solvent in several earlier conductance studies at 25°. These studies have shown that electrolytes in this solvent generally have dissociation constants of approximately 10^{-3}. The purpose of this investigation has been to study the variations of the conductances and the dissociation constants of potassium thiocyanate and tetra-n-butylammonium iodide in acetone at lower temperatures ranging to −50°.

Experimental

1. Purification of Solvent.—J. T. Baker Analyzed reagent acetone was refluxed for several hours over Activated Alumina and then was fractionated through an efficient column at atmospheric pressure. The middle fractions which were retained had the following properties at 25°: conductivity, 2×10^{-8} ohm^{-1} cm.$^{-1}$; density, 0.7845 g./ml.; viscosity, 3.02×10^{-3} poise; and dielectric constant, 20.7.

2. Purification of Salts.—Reagent grade potassium thiocyanate was recrystallized twice from distilled water. The best commercial grade of tetra-n-butylammonium iodide obtainable was recrystallized twice from ethanol-ether mixtures. Both salts were dried to constant weight in a vacuum oven at 70°.

3. Apparatus and Procedure.—Four conductance cells (two each of numbers 4943 and 4944, Type A, Leeds and Northrup Catalog EN-95) were used in the conductance measurements. The constants of these cells with lightly platinized electrodes were based upon the intercomparison of resistances with a cell for which the constant was determined using 0.01 demal potassium chloride solutions according to the method of Jones and Bradshaw.[2] A Jones conductivity bridge with an oscillator and an amplifier capable of producing 500, 1000 or 2000 cycles per second was used to measure resistances which were observed to show no significant frequency dependence.

The temperature of the solutions in the conductance cells was regulated by a manually-controlled thermostat consisting of a five-gallon Dewar flask filled with denatured alcohol which was cooled by the addition of powdered Dry Ice. Temperatures were measured with three total-immersion thermometers which are compared frequently against two thermometers calibrated by the National Bureau of Standards. Measurements were made at 25° and at each ten-degree interval between 20 and −50°. In all cases the temperature control was effective within 0.2 degree.

Two independent series of solutions covering the concentration range of 1-30 $\times 10^{-4}$ N were prepared for each salt by the weight dilution of stock solutions with all material transfers made in a dry box. Suitable buoyancy corrections were applied to all weights. The concentrations were converted from a weight to a volume basis on the assumption that the densities of the dilute solutions were equal to that of the solvent at a given temperature.

Three size-25 Ostwald–Cannon–Fenske viscometers were used to make triplicate determinations of the viscosity of acetone at each temperature. Calibrations of the viscometers were based upon the viscosity of water as 1.002 centipoise at 20°.[3] The change of a viscometer constant with temperature was calculated using the equation of Cannon and Fenske.[4] Kinetic energy corrections were considered to be negligible.

At each temperature the conductivity of the salt was obtained by subtracting the conductivity of the solvent from that of the solution. Data pertinent to the density, viscosity and dielectric constant of acetone which were used in the calculations are presented in Table I. The values of the necessary fundamental constants were taken from the latest report of the Subcommittee on Fundamental Constants.[5]

Results

Corresponding values of the equivalent conductance, Λ, and the concentration in gram equivalents per liter, C, for one of the two independent series of solutions for each salt are presented in Tables II and III. Data for the confirmatory series of solu-

(1) (a) Presented at the 128th Meeting of the American Chemical Society in Minneapolis, September, 1955; (b) based in part on research performed under a contract with the U. S. Army Signal Corps.

(2) G. Jones and B. C. Bradshaw, *J. Am. Chem. Soc.*, **55**, 1780 (1933).

(3) J. R. Swindells, J. R. Coe and T. B. Godfrey, *J. Research Natl. Bur. Standards*, **48**, 1 (1952).

(4) M. R. Cannon and M. R. Fenske, *Ind. Eng. Chem., Anal. Ed.*, **10**, 297 (1938).

(5) F. D. Rossini, F. T. Gucker, Jr., H. L. Johnston, L. Pauling and G. W. Vinal, *J. Am. Chem. Soc.*, **74**, 2699 (1952).

<div style="display:flex">
<div>

Table I

Some Physical Properties of Acetone at Temperatures within the Range 25 to −50°

Temp., °C.	Density,[7] g./ml.	Viscosity, poise × 1000	Dielectric[8] constant
25	0.7845	3.02	20.7
20	.791	3.18	21.2
10	.802	3.51	22.2
0	.814	3.91	23.3
−10	.825	4.37	24.4
−20	.836	4.96	25.6
−30	.846	5.67	26.8
−40	.857	6.57	28.1
−50	.868	7.77	29.5

tions for each salt have been deposited with the American Documentation Institute.[6]
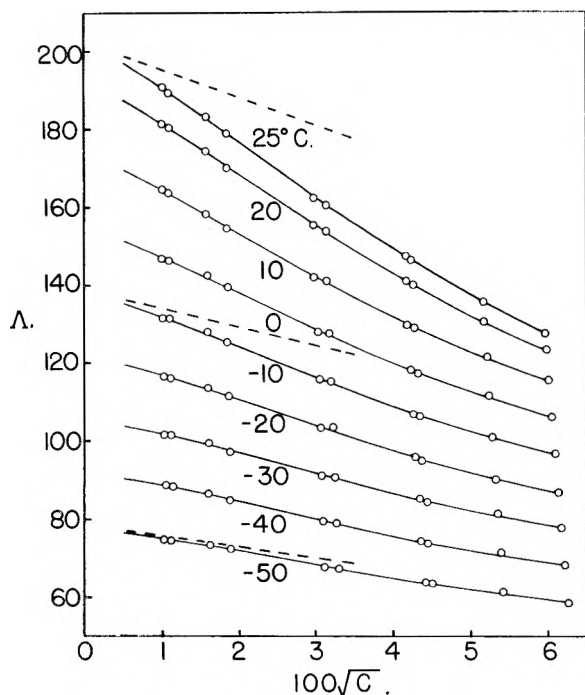
Fig. 1.—Equivalent conductance of potassium thiocyanate in acetone as a function of the square root of the concentration. Dashed lines represent Onsager slopes.

Discussion

A plot of the equivalent conductance of potassium thiocyanate in acetone as a function of the square root of the concentration is shown in Fig. 1 for each of the temperatures at which the study was made. A corresponding figure for tetra-n-butylammonium iodide has been omitted because of similarities in the behavior of the two salts. It may be observed from Fig. 1 that plots for the various temperatures differ only in the magnitude of displacement along the ordinate and in the slope which increases with increasing temperature. The plots

(6) Material supplementary to this article has been deposited as Document number 4671 with the ADI Auxiliary Publications Project, Photoduplication Service, Library of Congress, Washington 25, D. C. A copy may be secured by citing the Document number and by remitting in advance $1.25 for photoprints or $1.25 for 35 mm. microfilm, by check or money order payable to: Chief, Photoduplication Service, Library of Congress.

(7) F. J. Shell, Dissertation, University of Kentucky, 1953.

(8) A. A. Maryott and E. R. Smith, National Bureau of Standards Circular 514, August 10, 1951.

</div>
<div>

Table II

Equivalent Conductance of Potassium Thiocyanate in Acetone at Temperatures within the Range 25 to −50°

$C \times 10^4$ (a) 25°	Λ	$C \times 10^4$ (b) 20°	Λ	$C \times 10^4$ (c) 10°	Λ
0.9971	191.0	1.005	181.6	1.019	164.7
3.264	178.5	3.291	169.9	3.337	154.5
8.771	162.2	8.843	155.5	8.966	141.7
17.85	145.8	18.00	140.2	18.25	129.1
26.57	135.7	26.79	130.9	27.16	121.7
(d) 0°		(e) −10°		(f) −20°	
1.035	146.2	1.049	131.1	1.063	116.0
3.387	139.4	3.433	125.3	3.479	111.3
9.100	127.3	9.224	114.9	9.346	102.5
18.52	116.5	18.77	105.9	19.02	95.0
27.57	111.8	27.94	101.2	28.32	89.9
(g) −30°		(h) −40°		(i) −50°	
1.075	101.7	1.089	88.2	1.103	74.7
3.520	97.9	3.566	84.9	3.612	72.1
9.458	90.5	9.581	78.8	9.704	67.1
19.25	84.2	19.50	73.6	19.75	63.0
28.65	81.5	29.03	71.3	29.40	61.1

Table III

Equivalent Conductance of Tetra-n-butylammonium Iodide in Acetone at Temperatures within the Range 25 to −50°

$C \times 10^4$ (a) 25°	Λ	$C \times 10^4$ (b) 20°	Λ	$C \times 10^4$ (c) 10°	Λ
0.5440	173.9	0.5485	165.4	0.5561	150.0
1.748	168.0	1.762	160.2	1.787	145.5
5.034	158.5	5.076	151.4	5.146	137.9
10.41	147.3	10.50	140.9	10.64	128.6
16.48	139.7	16.61	134.0	16.85	122.4
(d) 0°		(e) −10°		(f) −20°	
0.5644	134.7	0.5721	120.6	0.5797	106.8
1.814	130.8	1.838	117.4	1.863	103.7
5.223	124.1	5.294	111.4	5.365	98.9
10.80	115.9	10.95	104.3	11.09	92.6
17.10	109.9	17.33	98.0	17.56	89.2
(g) −30°		(h) −40°		(i) −50°	
0.5866	93.5	0.5942	80.3	0.6019	67.7
1.885	90.9	1.909	78.2	1.934	66.0
5.429	86.7	5.499	74.7	5.570	63.1
11.23	81.3	11.37	70.2	11.52	59.4
17.77	78.8	18.00	66.7	18.23	57.5

are non-linear and have limiting slopes which are appreciably more negative than those calculated for a completely dissociated electrolyte; consequently, evaluation of the limiting equivalent conductance, Λ_0, by direct extrapolation of the Λ *versus* $\sqrt{C}$ plots would be subject to considerable error.

The limiting equivalent conductance and dissociation constant for each salt were determined by the Shedlovsky extrapolation equation.[9] Shedlovsky plots for tetra-n-butylammonium iodide in acetone are shown in Fig. 2. The method of least-squares was used to calculate the values of the limiting equivalent conductances and the dissociation constants. Data pertinent to these are presented in Tables IV and V for potassium thiocya-

(9) T. Shedlovsky, *J. Franklin Inst.*, **225**, 739 (1938).

</div>
</div>
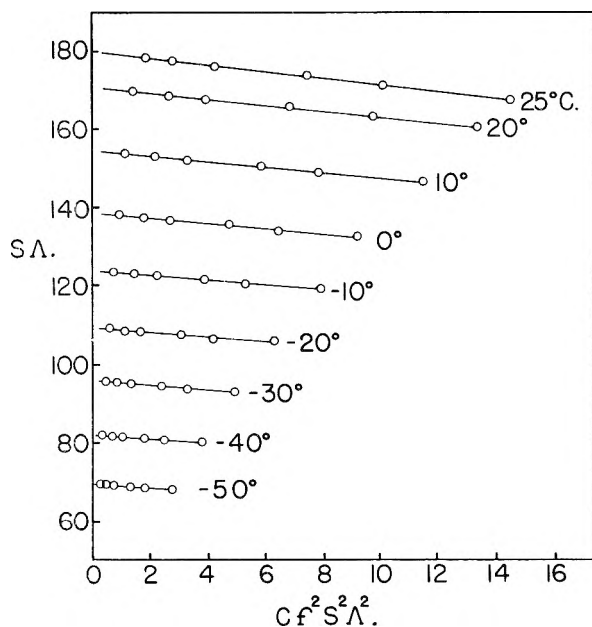
Fig. 2.—Shedlovsky plots for tetra-n-butylammonium iodide in acetone.

nate and tetra-n-butylammonium iodide, respectively.

TABLE IV

LIMITING EQUIVALENT CONDUCTANCE, DISSOCIATION CONSTANT AND CONDUCTANCE–VISCOSITY PRODUCT FOR POTASSIUM THIOCYANATE IN ACETONE

Temp., °C.	Λ_0	$K \times 10^3$	$\Lambda_0\eta_0$
25	202.2	3.4	0.611
20	191.6	3.8	.609
10	173.7	4.2	.610
0	154.4	5.2	.604
−10	138.1	6.0	.604
−20	122.2	6.8	.606
−30	106.7	8.5	.605
=40	92.3	9.6	.606
−50	78.1	10.9	.607

Reynolds and Kraus[10] have reported also the limiting equivalent conductances and dissociation constants for these two salts in acetone at 25°. Their values of 201.6 and 179.4 ohm^{-1} cm.^{2} equiv.$^{-1}$ for the limiting equivalent conductances and 3.8 × 10^{-3} and 6.5 × 10^{-3} for the dissociation constants of potassium thiocyanate and tetra-n-butylammonium iodide, respectively, indicate relatively good agreement with our data.

Figure 3 shows linear plots of the logarithm of the

(10) M. B. Reynolds and C. A. Kraus, *J. Am. Chem. Soc.*, **70**, 1097 (1948).

TABLE V

LIMITING EQUIVALENT CONDUCTANCE, DISSOCIATION CONSTANT AND CONDUCTANCE–VISCOSITY PRODUCT FOR TETRA-n-BUTYLAMMONIUM IODIDE IN ACETONE

Temp., °C.	Λ_0	$K \times 10^3$	$\Lambda_0\eta_0$
25	180.2	6.1	0.544
20	171.2	6.8	.544
10	155.2	7.7	.545
0	139.3	8.5	.545
−10	124.7	9.6	.545
−20	110.1	10.8	.546
−30	96.4	11.8	.547
−40	82.8	13.6	.544
−50	69.8	15.5	.542

limiting equivalent conductance *versus* the reciprocal of the absolute temperature. Calculations reveal that the slopes of these parallel plots are almost numerically equal to that of a plot of the logarithm of the viscosity of acetone *versus* $1/T$. This apparent equivalence of the temperature coefficients of conductance and viscosity is reflected in a constant conductance–viscosity product for each salt. Obviously, at low concentrations, there is little or no change in the effective sizes of the solvodynamic units over the temperature range.
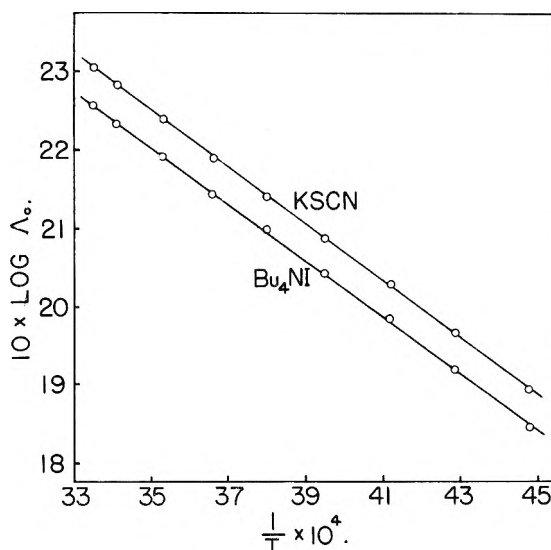
Fig. 3.—Limiting equivalent conductances of potassium thiocyanate and tetra-n-butylammonium iodide in acetone as a function of the reciprocal of the absolute temperature.

The data in Tables IV and V show that the dissociation constant for each salt increases with decreasing temperature. Probably this is a consequence of the greater dielectric constant of the solvent at lower temperatures.

COMPLEX IONS IN MOLTEN SALTS.   IONIC ASSOCIATION AND COMMON ION EFFECT[1]

BY ERVIN R. VAN ARTSDALEN

Chemistry Division, Oak Ridge National Laboratory,[2] Oak Ridge, Tennessee

Received August 17, 1955

The concepts of complex ion and ideality are considered in the case of molten salt solutions.   Freezing point depression measurements in molten sodium nitrate as solvent are used to determine the nature and number of ions into which several solutes dissociate.   It is demonstrated that a number of salts of relatively simple oxy-acids as well as many other simple salts are stable and remarkably ideal in solution in molten sodium nitrate.   Partial dissociation and complex ion formation are shown to exist at high dilution in the case of lead(II) chloride, copper(II) chloride, cadmium chloride, zinc chloride and cadmium bromide.   The important species in the solutions appear to be those with zero, two and four chlorines per +2 metal ion.   The occurrence of the common ion effect is amply substantiated with these compounds and chloro anions containing the +2 metal exist even at low concentrations.   Reactions are proposed which account for the results and equilibrium constants are calculated for these reactions.

Molten salts are generally good Faraday-type conductors of the electric current and as such may be looked upon as very concentrated electrolytes. However, molten salt solutions lack the complication of the presence of water or other polar molecules as solvent and in a certain sense this makes them simpler of theoretical treatment.   In another sense they are more complicated because of the closeness of approach of charged ions to one another and on this basis one may anticipate, despite high temperature, that there will be considerable complex ion or ion pair formation.   It is hoped that detailed study of molten salts will contribute to more complete understanding of concentrated electrolytes.

Phase diagrams of numerous binary salt systems show that complex compounds frequently exist in the solid state.   It is of considerable importance to inquire how stable these compounds are in the liquid state.   A rough indication of their stability is given by the sharpness of the peak in the phase diagram which indicates complex formation.   It is particularly interesting to learn whether such complex compounds produce complex ions which are stable in molten salts.   A natural question to ask is whether those complex ions containing halogens which are stable in aqueous solutions are also stable in molten salt solution.

Before considering experimental information which relates to these questions, the definition of a complex ion should be considered in connection with molten salts.   We shall consider a complex ion to be a kinetic entity with a lifetime long compared with the time of molecular vibrations.   Thus, we do not consider as a complex ion or ion-pair two ions which in the fleeting instant of a molecular vibration find themselves closer together than would be the case over a time average of a few micro- or milli-seconds.   This concept does not preclude the possibility or indeed the likelihood that extensive exchange of individual atoms takes place between complex ions.   Nor does it imply that there may not be equilibria between associated and dissociated complex ions.   However, we feel that anything which should be considered as a complex

ion must show the usual so-called colligative properties.

Electrical conductance data of molten salt mixtures have frequently been used in conjunction with phase diagram information to support the idea that complex ions do exist in many mixtures.   It is reasonable to expect that when simple ions associate to form a large complex ion with lowered mobility the electrical conductance should decrease. However, the mere fact that one observes a minimum in conductance in a mixture should not be taken alone as evidence for the existence of complex ions in the melt as has been pointed out by Van Artsdalen and Yaffe.[3]

It is possible to use cryoscopic measurements to determine the number of ions (or other particles) into which a "molecule" of solute dissociates in a given molten solvent provided solid solutions do not interfere.   The theory is that of the classical Raoult–Van't Hoff freezing point depression law. All foreign particles in any particular solvent depress its freezing point, but solute ions which are the same as those of the solvent do not depress. This has been amply substantiated by a number of investigators; the most recent work has been by Kordes and associates,[4] Darmois and associates[5] and Van Artsdalen,[6] who discussed the basic behavior.   It has been established that many simple salts produce lowering of the freezing point which depends linearly upon their concentration in the solvent.   In many cases this linearity holds to quite high concentrations.   The author has shown[6] that sodium chloride is strictly linear to the eutectic composition (about 7 mole per cent.) when dissolved in sodium nitrate.   It would thus appear that simple salt solutions form very nearly ideal mixtures with activity coefficients close to unity (although the possibility exists that the activity coefficients vary linearly with concentration[6a]). Indeed, it is to be expected that molten salt solu-

(1) Presented at the Ion Pair Symposium, 128th meeting of the American Chemical Society, Minneapolis, Minn., September 14, 1955.

(2) Operated by Union Carbide Nuclear Company for the Atomic Energy Commission under Contract W-7405.

(3) E. R. Van Artsdalen and I. S. Yaffe, THIS JOURNAL, **59**, 118 (1955).

(4) E. Kordes, W. Bergmann and W. Vogel, *Z. Elektrochem.*, **55**, 600 (1951); E. Kordes, G. Ziegler and H. Proeger, *ibid.*, **58**, 168 (1954).

(5) E. Darmois and M. Rolin, *J. chim. phys.*, **47**, 176 (1950); Y. Doucet, J. LeDuc and G. Pannetier, *Compt. rend.*, **236**, 1018 (1953), and other papers in *Compt. rend.*

(6) E. R. Van Artsdalen, *J. Tenn. Acad. Sci.*, **29**, 122 (1954).

(6a) This question could be settled if adequate vapor pressure measurements were available for molten salt solutions. Unfortunately, there are practically no such data in the literature.

tions, in the absence of complex ion formation, should be much more nearly ideal than aqueous solutions for the ions of almost any salt will resemble ions of another salt much more than they resemble water or other polar molecules.

It is well known that certain metal halides form complex ions of moderate stability in aqueous solution, for example the halides of cadmium, lead and copper. The following study involves a detailed investigation of the stability of complex chlorides of lead(II), copper(II), cadmium and zinc in molten sodium nitrate and molten potassium nitrate.

Experimental

Materials.—All chemicals were highest quality C.P. reagents obtained commercially and used without further purification. Freezing points of the cryoscopic solvents, $NaNO_3$ and KNO_3, showed that these were of very high purity. All substances were dried to constant weight at about $140°$ and stored in desiccators before use. In the case of those substances which were obtained as hydrates, e.g., $CdCl_2\cdot2.5H_2O$, $CuCl_2\cdot2H_2O$, after the salts were heated to constant weight an analysis for chloride was made to check that the stoichiometric composition was correct.

Apparatus.—Freezing points were determined on salt melts contained in an approximately $1^3/_4''$ i.d. Pyrex test-tube which was heated with a Marshall tube furnace which contained an extra stainless steel liner to smooth thermal gradients and increase the heat capacity. The stirrer was a screw-type propeller blade which operated at approximately constant speed sufficient to produce vigorous stirring both laterally and vertically.

A platinum-platinum, 13% rhodium single-junction thermocouple encased in a thin-wall quartz tube was the temperature sensing element. This thermocouple junction was placed in a reproducible position near the middle of the melt. The output of the thermocouple was nearly completely bucked out through a White potentiometer and the small unbalance fed through an L&N Microvolt amplifier, the output of which was placed on a 10 mv. range Speedomax Recorder. An over-all amplification factor of 200 was achieved so that the full 10 inch scale on the recorder chart corresponded to 50 microvolts or approximately $5°$ in the temperature range in question. With this setup cooling curves were traced directly on the recorder chart. Voltages were obtained from this chart and the known bucking potential and the temperature calculated from the voltage at the freezing point. Tests showed that purposely impressed bucking voltage fluctuations several times those experienced during measurements caused undetectably small errors in temperature determination. This arrangement using the microvolt amplifier gave an exceedingly constant gain and measurements of temperature could be made to $0.005°$.

A semi-automatic recording Mueller Bridge with a platinum resistance thermometer was used in some of the earlier work. The sensitivity and reproducibility with this instrument were the same as with the thermocouple.

Procedure.—Two hundred grams of previously dried sodium nitrate (weighed to 0.1 g.) was melted and two freezing point cooling curves were taken. A uniform cooling rate, reproducible from run to run, was quite essential to obtain satisfactory freezing points. Therefore, a fixed heater current was passed through the furnace for a predetermined time interval beginning a certain number of minutes after the onset of first freezing. In this way a uniform temperature rise was achieved above the melting point for each freezing point determination and reproducible cooling rates (ca. 0.8 to 0.9°/min.) were obtained. Following the check of pure solvent, suitable amounts of solute (weighed to 0.0001 g.) were added in successive increments and their freezing points determined. In any one melt usually four to six separate additions of solute were made. Repeated measurements were made with fresh melts. The freezing points were determined from the cooling curves and could be estimated to $0.005°$. In general the reproducibility of freezing points of replicate experiments was about $0.01°$.

Results

Freezing point depression measurements in

molten sodium nitrate were made for a considerable series of salts. A plot was made of the freezing point depression against molal concentration for each solute salt and the slope of the plot was determined analytically. Data for a number of salts which gave linear plots are summarized in Table I. The slope of these curves is clearly the freezing point depression constant ($\kappa = RT_0^2/1000L_0$) of the Raoult–Van't Hoff law

$$\Delta T_i = \nu_i \frac{RT_0^2}{1000L_0} m_i = \nu_i \kappa m_i \qquad (1)$$

where ΔT_i is the freezing point depression, ν_i the number of ions into which one "molecule" of solute i dissociates, R the gas constant per mole, T_0 the freezing point of the pure solvent in degrees absolute, L_0 the heat of fusion per gram of pure solvent and m_i the concentration of solute in moles per 1000 g. of solvent. It will be noted that when sodium ion or nitrate ion are dissociation products of the solute they cause no depression of the freezing point of sodium nitrate since they are not foreign ions in the melt. The data of Table I clearly show that all potassium salts produce too little lowering of the freezing point compared with other salts.

FREEZING POINT DEPRESSION IN SODIUM NITRATE

1 Foreign ion		2 Foreign ions		3 Foreign ions	
Salt	$\kappa(\text{deg.})^a$	Salt	$\kappa(\text{deg.})$	Salt	$\kappa(\text{deg.})$
NaCl	15.0^b	LiCl	29.8	$CaCl_2$	45.4
Na_2CO_3	14.8	CsCl	31.4	$SrCl_2$	44.8
Na_2SO_4	15.1	KCl	(28.5)	$BaCl_2$	44.5
$NaBrO_3$	15.0	$KBrO_3$	(28.0)	K_2CO_3	(42.7)
Na_2WO_4	15.1	KIO_3	(29.0)	K_2SO_4	(41.3)
Na_2MoO_4	15.0			$K_2Cr_2O_7$	(41.7)
$Pb(NO_3)_2$	15.2				
$LiNO_3$	15.1				44.9 ± 0.3
KNO_3	(13.5)				

$$15.0 \pm 0.1$$

^{a} Average per foreign ion $15.0 + 0.1$. ^{b} Average of 5 runs.

Phase equilibrium studies[7] indicate that potassium nitrate and sodium nitrate form solid solutions, with potassium nitrate being about 10% as soluble in the solid sodium nitrate phase as in the liquid. The freezing point depression data presented here are in accord with this result. In a previous publication[6] it was shown that when solid solutions are formed the Raoult–Van't Hoff law can be modified to use the effective concentration of solute, i.e., the difference between solubility in liquid and solid phases. If all ions which do not form solid solutions give a freezing point depression constant of $15.0°$ one computes from the data of Table I (seven K salts) that the potassium ion gives a freezing point depression of $13.5 \pm 0.2°$. This is (very close to) a 10% reduction and is consistent with the approximately 10% solid solubility of potassium nitrate in sodium nitrate.

A depression constant in sodium nitrate of $15.0°$ per mole of foreign ions per 1000 g. of solvent agrees well with the prediction from a calorimetrically measured heat of fusion by Goodwin and Kalmus,[8] who reported 45.3 cal./g. for L_0. When this is substituted into equation 1 using $305.8° = 579°K.$

(7) "International Critical Tables," Vol. 4, E. W. Washburn, ed., McGraw–Hill Book Co., Inc., New York, N. Y., 1928, p 69.

(8) H. M. Goodwin and H. T. Kalmus, Phys. Rev., **28**, 1 (1909).

for the melting point of sodium nitrate as determined in the present studies, one computes that the depression constant is 14.7°. The agreement is evidence that the salt solutions are very nearly ideal in the concentration ranges studied.

It is evident that many oxy-anions are stable in molten sodium nitrate at its melting point. Thus Table I shows that carbonate, sulfate, bromate, iodate, tungstate, molybdate and dichromate ions give normal freezing point depression. Potassium chromate is almost ideal, though it shows a very slight curvature.

A number of solutes show pronounced deviations from ideality in lowering the freezing point of sodium nitrate. Data for lead(II) chloride, copper(II) chloride, cadmium chloride, zinc chloride and cadmium bromide are presented in Fig. 1. The dashed lines marked 1X and 3X show the depression which would be produced by solutes giving one and three foreign particles (ions), respectively, per molecule. The simplest explanation of the behavior of these salts is that they are considerably less than completely dissociated in molten sodium nitrate. If $CdCl_2$ remained as molecules in $NaNO_3$ the freezing point depression would follow the curve 1X. Partial dissociation gives a curve lying between dashed curves 1X and 3X as is observed in Fig. 1. These salts exhibit this same effect in aqueous solution, with tendency to associate into complex ions with excess halide ions. The relative order of dissociation observed from freezing point lowering in molten sodium nitrate is about the same as that in aqueous solution, where lead chloride dissociates more than cadmium chloride and cadmium bromide is still less dissociated than the chloride.
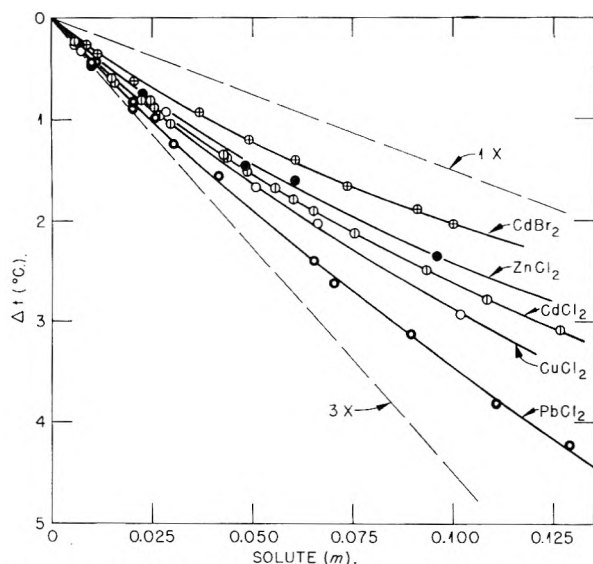
Fig. 1.—Freezing point depression by certain halides in sodium nitrate.

A study was made of the effect of added excess chloride on the freezing point depression by these salts. All of the added excess chlorides exhibit ideal behavior; i.e., they show complete dissociation. The results are plotted in Figs. 2, 3 and 4 for cadmium chloride, lead chloride and zinc chloride, respectively. In these plots the freezing

point depression (ΔT) is the additional depression caused by the cadmium chloride, lead chloride or zinc chloride over and beyond that by the added excess chloride. It is evident that there is a pronounced "common ion effect." The dissociation of cadmium, lead or zinc chlorides is repressed by the addition of chloride ion from any completely dissociated chloride. This "common ion effect" is independent of the nature of the cation of the excess chloride in the concentration ranges reported here; it depends only on the concentration of added common ion (chloride).

More detailed studies were made with cadmium chloride[9] than with the other salts, so their behavior will be considered in terms of cadmium chloride. In the first place, the fact that in the presence of 0.2 m NaCl or 0.109 m $CaCl_2$ (0.218 m Cl^-) the depression by $CdCl_2$ is less than that for a single undissociated molecule (dashed line 1X) indicates that some chloride is removed from solution to form one or another chlorocadmium complex anion. Secondly, the important observation is made that the addition of a little cadmium chloride to sodium nitrate containing 0.627 m NaCl actually raises the freezing point. From this we conclude that an anionic complex is formed which contains at least four chlorine atoms, since the rise of the freezing point can only be the result of removing more than one Cl^- ion per $CdCl_2$ "molecule" dissolved. The subsequent decrease in the freezing point is explained as resulting from the gradual decrease in excess chloride ion as the amount of dissolved $CdCl_2$ increases, since Cl^- is being used to form anionic complexes with $CdCl_2$.

It immediately became of interest to attempt to calculate constants for the various equilibria which one might postulate as existing in these solutions. The first reactions considered were

$$CdCl_2 = CdCl^+ + Cl^- \qquad (2)$$
$$CdCl^+ = Cd^{++} + Cl^- \qquad (3)$$
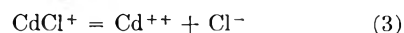
The assumption was made that at very low total $CdCl_2$ concentration reaction (2) was essentially complete to the right, and so one could calculate an equilibrium constant for reaction (3) from the observed depression of the freezing point. This constant could then be used to compute the dissociation constant for reaction (2) from freezing points at higher concentration taking into account both reactions 2 and 3. However, dissociation constants calculated in this way were found to be very markedly concentration dependent, so much so in fact that the method was abandoned.

Next an attempt was made to calculate a dissociation constant for the over-all dissociation of cadmium chloride according to the equation

$$CdCl_2 = Cd^{++} + 2Cl^- \qquad (4)$$
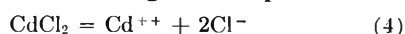
This met with success; the values of the dissociation constant remained constant within experimental error (random fluctuations only) over the entire concentration range studied with the pure salt in the absence of excess chloride, i.e., up to 0.15 m.

(9) Phase diagram studies made in this Laboratory show that there is a eutectic (m.p. 292–293°) in the $CdCl_2$–$NaNO_3$ system at about 8.5 mole % $CdCl_2$. The system was investigated to about 22 mole % $CdCl_2$ with no evidence for the formation of solid solutions.
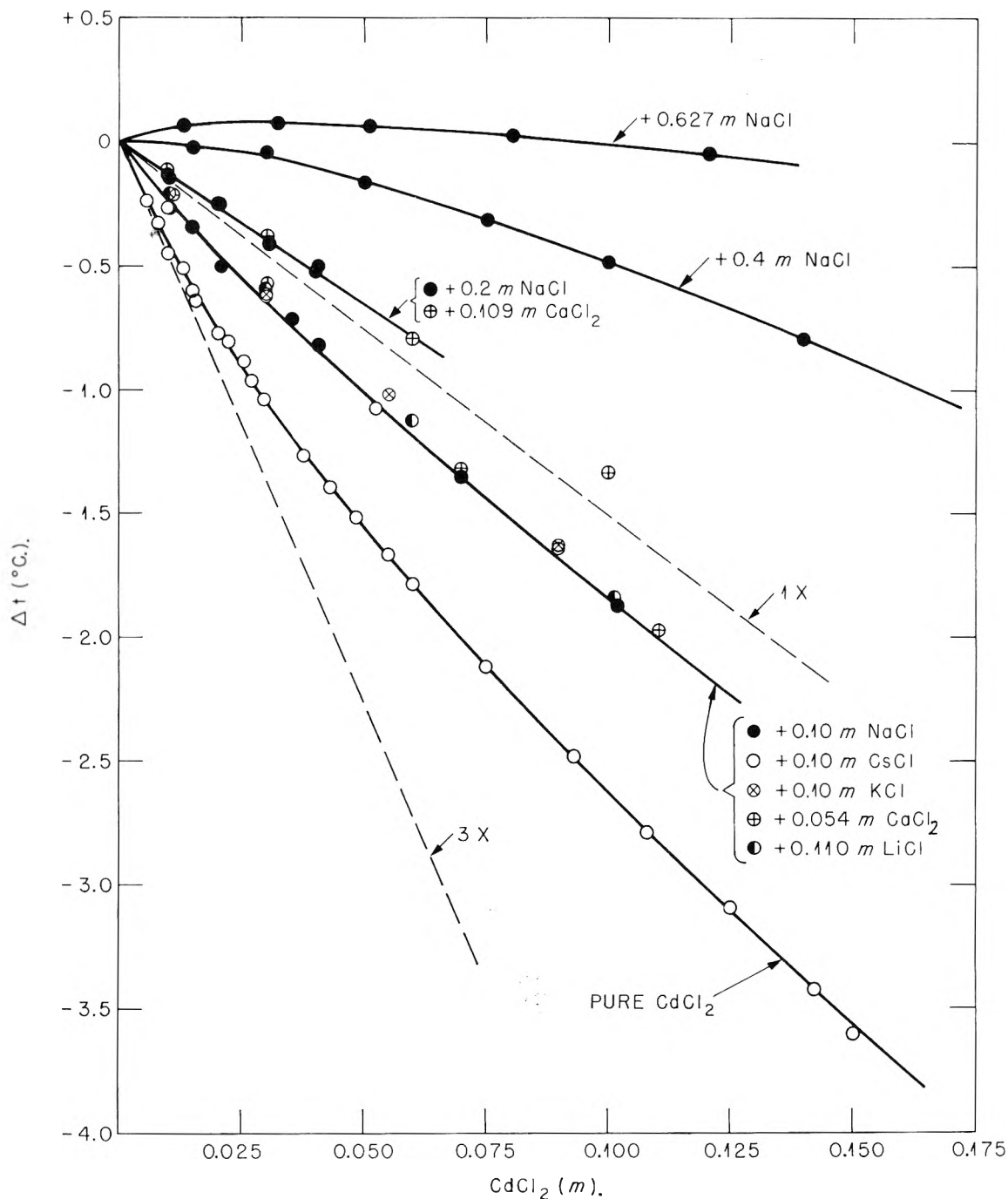
Fig. 2.—Effect of added chlorides on the freezing point depression by cadmium chloride in sodium nitrate.

This seems to indicate that the $CdCl^-$ ion is not thermodynamically important in these solutions, though it is certainly reasonable to postulate that dissociation and association proceed through it as an intermediate product. Using the value for K_{20}, it is a direct matter to calculate a constant for the anionic association reaction

$$CdCl_2 + 2Cl^- = CdCl_4^= \qquad (5)$$

from freezing point data in the presence of added sodium chloride.[10] The values computed for these

(10) The equations used to calculate the equilibrium constants were

$$K_{20} = \frac{(Cd^{++})(Cl^-)^2}{(CdCl_2)} = \frac{(w - a - b)(w - a)^2}{(3a + b - w)}$$

which simplifies to

$$K_{20} = \frac{(w - a)^3}{(3a - w)}$$

in the absence of excess Cl^-, and

$$K_{24} = \frac{(CdCl_4^=)}{(CdCl_2)(Cl^-)^2} =$$
$$\frac{2a[2K_{20} + (w - a)^2] - (w + a - b)[K_{20} + (w - a)^2]}{(w + a - b)(w - a)^4}$$

where a = initial formal $CdCl_2$ concentration, b = initial added chloride concentration (twice formal concentration for $CaCl_2$), and w = concentration of "particles" from freezing point measurement. Concentrations are in moles per 1000 g. of solvent. The computed values of K_{20} agreed whether from data in the presence or absence of excess Cl^-.
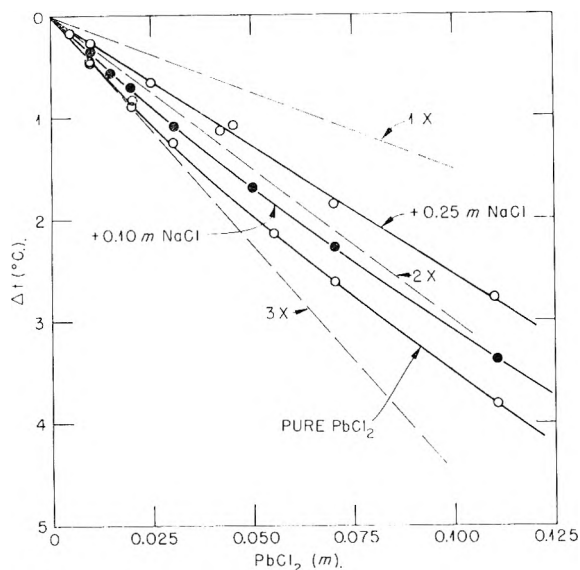
Fig. 3.—Effect of added sodium chloride on the freezing point depression by lead(II) chloride in sodium nitrate.

Fig. 4.—Effect of added sodium chloride on the freezing point depression by zinc chloride in sodium nitrate.

constants for several salts in molten sodium nitrate are given in Table II. The nomenclature is such that the subscript on K denotes both the process and the number of chlorines involved. The first digit of the subscript denotes how many chlorines there are in the starting material of the reaction while the second digit shows the number of chlorines in the cadmium product of the reaction. Thus, K_{20} is the equilibrium constant for reaction 4 as written, while the association shown in reaction 5 has K_{24} as its equilibrium constant. Because of the small amount of anionic complexing in the case of $PbCl_2$, it was not possible to compute a very reliable value for K_{24} in this case. The constants in Table II are the average computed from all experimental freezing point depressions for the particular salt. The deviations shown in the table are standard deviations computed in the usual way. In the case of cadmium chloride, K_{24} given in Table II is the average value obtained with all of the different added excess chlorides shown in Fig. 2. There was no significant difference depending on the nature of the cation, which is evident also from Fig. 2.

Table II
Equilibrium Constants in Molten NaNO₃

Salt	K_{20}		K_{24}	K_{02}	K_{04}
$PbCl_2$	0.033	$\pm$ 0.005	(0.2)	30	(6)
$CdCl_2$	.0031	$\pm$ .0004	4.4 $\pm$ 0.8	320	1410
$ZnCl_2$	.0026	$\pm$ .0002	5.1 $\pm$ 0.2	380	1940
$CdBr_2$	.00035	$\pm$ .00011	...		2900

The equilibrium constant K_{04} for the reaction

$$Cd^{++} + 4Cl^- = CdCl_4^{=} \qquad (6)$$
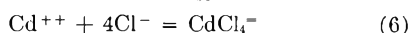
is a derived value only, obtained by multiplying K_{02} times K_{24}. Actually if one attempts to calculate K_{04} from the experimental points on the assumption that reaction (6) actually obtains and that essentially no $CdCl_2$ "molecules" or better termed associated double ion pairs exist in the solution, K_{04} is found to vary by more than two orders of magnitude depending on both the initial
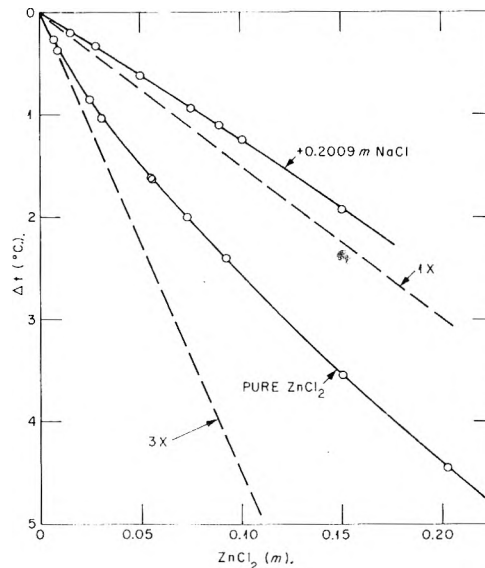
concentration of $CdCl_2$ and added chloride. Therefore, it is clear that this reaction does not represent the actual state of affairs in the solution. On the other hand, the fact that K_{20} and K_{24} are independent of concentration is evidence that reactions (4) and (5) do in fact represent over-all processes which occur in these solutions.

It is probably significant that these calculations show that Cd^{++} associates with even numbers only of Cl^- to form double ion pairs or complex ions. This suggests that more or less "chemical binding" is involved in holding the complexes together rather than mere electrostatic charge.

Solutions of lead chloride and cadmium chloride in molten potassium chloride and sodium chloride have been investigated previously. Phase diagrams are available and Bloom and Heymann[11] have studied electrical conductivity. They find some correlation between conductance and compound formation in the high concentration ranges. Electrical conductance of the system lithium chloride-cadmium chloride has been reported by Bloom, et al.,[12] who found only smooth changes of conductance with changing composition.

Hildebrand and Rhule[13] used e.m.f. measurements to investigate the activity of molten lead chloride upon dilution with potassium chloride. They interpreted their results on the assumption that complex chlorolead anions exist in solution. Recently Lantratow and Alabyshev[14] using similar techniques have investigated the activity of lead chloride and cadmium chloride dissolved at high concentration in molten alkali and alkaline earth halides. They concluded that both lead chloride and cadmium chloride are extensively associated

(11) H. Bloom and E. Heymann, *Proc. Roy. Soc. (London)*, **A188** 392 (1947).

(12) H. Bloom, I. W. Knaggs, J. J. Molloy and D. Welch, *Trans. Faraday Soc.*, **49**, 1458 (1953).

(13) J. H. Hildebrand and G. C. Rhule, *J. Am. Chem. Soc.*, **49**, 722 (1927).

(14) M. L. Lantratow and A. F. Alabyshev, *J. Appl. Chem. URSS*, **26**, 263, 353 (1953).

with chloride ions in molten chloride solutions. They also observed some specific cation effects at high concentrations.

All prior studies were made with high concentrations of cadmium or lead chlorides dissolved in other halides. No third component was used which might be considered as a solvent. The results reported here really represent a rather different study. Dilute solutions of the appropriate chlorides have been studied in what may be looked upon as a non-reacting solvent. No specific cation effects, of the type reported by Lantratow and Alabyshev, were detected in the quite dilute solutions investigated here. One observes solely a common ion effect considering association of Cd^{++} to form a series of ion-pairs and complex ions. But actually one should not anticipate finding specific cation effects at concentrations well below one molal, since the solution is mostly sodium nitrate, which will largely determine its charge effects, swamping out those of the added chloride.

A few preliminary results have been obtained with cadmium chloride dissolved in molten potassium nitrate (melting point 335°). There are some difficulties in these measurements because

potassium nitrate does not behave as well as sodium nitrate when used as a cryoscopic solvent. Cadmium chloride in molten potassium nitrate shows increasing ionic association with rising concentration and exhibits a common ion effect of about the same order of magnitude observed in sodium nitrate. It appears, however, at the higher temperature of freezing potassium nitrate that cadmium chloride is slightly less associated and complexed than in freezing sodium nitrate.

It is clear that our results show behavior in molten salt solutions which in many ways is analogous to that of aqueous solutions. The degree of association in molten salts is very roughly of the same magnitude as that observed in aqueous solutions at comparable concentrations of chlorides. Further studies of the common ion effect and ionic association are in progress in this Laboratory, not only by the freezing point method but by means of electrochemical and other techniques.

DIPPING ELECTRODES FOR PRECISION CONDUCTIMETRY

BY ORMOND V. BRODY[1] AND RAYMOND M. FUOSS

Contribution No. 1328 from the Sterling Chemistry Laboratory, Yale University, New Haven, Conn.

Received August 17, 1956

Two designs of dipping electrodes are described, one glass insulated and one Teflon insulated. The former involves only two simple platinum wire–Pyrex seals and the latter has no glass–metal seals. The electrodes are flat rings of bright platinum, mounted on an insulating tube; the electrode assembly fits into a cylindrical cell compartment which is only slightly larger than the outer diameter of the electrodes. The electrolyte is located in the annular space between the insulator and the cylinder; by varying electrode spacing and/or thickness of electrolyte layer, cell constants in the range 0.3–4.0 cm.$^{-1}$ are readily obtained. The electrode assembly is carried on a $\overline{\text{S}}$ fitting; electrodes are thus interchangeable. The lead to the lower electrode is shielded by the cylindrical lead to the top electrode; both run inside the central insulating tube. Consequently Parker effect is negligible until very high cell resistances are reached. Both designs give good frequency characteristics and ratios of various pairs of cells are reliable to about 0.02%.

Introduction

Nichol and Fuoss[2] recently described an electrode design for precise determination of conductance in solutions of high resistance, which has the advantages of easy construction, interchangeability and excellent frequency characteristics. The design is, however, restricted practically by its geometry to cell constants smaller than about 0.1 cm.$^{-1}$. With the conventional standardizing solutions, which have specific conductances in the range $10^{-2} - 10^{-4}$, such a cell gives too low a resistance to be measured with precision, and hence the cell constant must be determined by comparison with a cell which has a higher constant. It would naturally be desirable to have a simple design for the comparison cells as well as for the measuring cells.

High resistances with highly conducting solutions have usually been obtained in the past by connecting two electrode compartments with a tube of small cross section. It is possible to make a cell

of this type without glass–metal seals, but the design has other disadvantages. Another method of decreasing solution cross-section between electrodes is to confine the solution into the annular space between two concentric tubes. If the inner tube, which contains the leads to the electrodes, is made large enough, the capacity from the leads to the solution can be made so small that the Parker effect becomes negligible over a wide range of cell resistance. The purpose of this paper is to describe two cell designs which are based on the above principle, which cover the cell constant range between about 0.3 and 4.0. One design involves two simple platinum–Pyrex seals (10–15 mil wire through glass tubing) and the other uses Teflon as insulation. Both sets of electrodes are dipping electrodes, carried on standard taper supports; hence they can be interchanged with electrodes of different cell constants or be placed in solution reservoirs of different volumes.

Experimental

Glass Insulated Design.—The construction of the glass cell is shown in Fig. 1A. The electrodes are discs cut from

(1) Du Pont Postdoctoral Research Fellow, 1954–1955.

(2) J. C. Nichol and R. M. Fuoss, THIS JOURNAL, **58**, 696 (1954).

bright[3] platinum, 12 mil (0.3 mm.) thick. The diameter of the central hole is only slightly larger than the diameter of the inner glass tube (18 mm. or greater), and the outer diameter is 1.5-3.0 mm. smaller than the inner diameter of the outer tube. The inner tube is sealed to a ⚲ section; in Fig. 1A, a male section is shown carrying the electrode
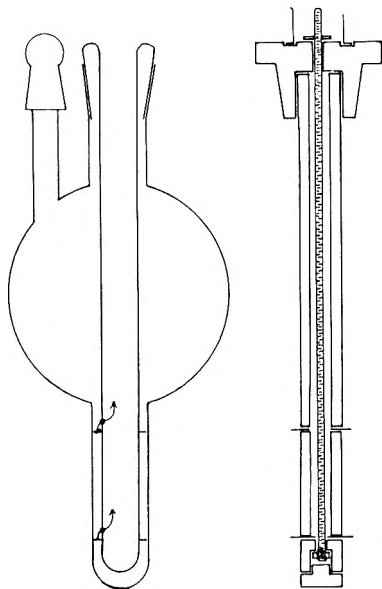
Fig. 1.—Glass insulated conductance cell, left; Teflon insulated cell, right.

assembly, because we could then interchange glass and Teflon insulated electrodes in the same vessel. Our final design for the glass insulated electrodes carries the electrodes on a female section, in order to reduce the hazard of contamination of the cell contents. A small hole is blown in the inner tube at a suitable point and then a platinum ring with lead wire attached (10–15 mil platinum) is slipped over the tube. The wire has a glass bead about 2 cm. from the electrode; the bead is sealed into the hole. Then 6 small bulges (3 above and 3 below) at 120° intervals are blown in the tube; these serve to brace the electrode firmly in position. No attempt is made to seal the electrode to the inner tube; when the bulges are blown, the glass is just hot enough to work, but not hot enough to stick to platinum. The tube usually cracks if the glass wets the platinum. Then three more bulges are blown just above the position desired for the lower electrode, which is then slipped on and attached in a similar fashion. (Glass studs at 120° intervals above and below the electrodes can be attached to protect the platinum against accidental bending.) A piece of Teflon tubing is then slid over the lead to the bottom electrode; before insertion, this tubing is wrapped with copper foil and then another Teflon tube is placed over the foil. The lead from the top electrode is soldered to the copper foil at the top, so that one electrode lead is electrically a shield for the lead to the other electrode. The copper shielding extends to the level of the upper electrode. There is a small capacity from the lower electrode lead to the solution in the space between the cell walls and the electrodes, and hence there is present a capacity–resistance series element which shunts the cell and therefore should produce a Parker effect. But by choice of a large diameter for the inner tube, the impedance of the capacity is so large that no Parker effect appears until the cell resistance is well over 10,000 ohms.

Teflon Insulated Design.—The electrodes are bright platinum discs, 0.9375 in. (2.38 cm.) in diameter, with a central hole 0.375 in. (0.95 cm.) in diameter. They are clamped between sections of Teflon tubing (Fig. 1B) machined from 0.75 in. (1.91 cm.) Teflon rod. A short length of platinum wire is welded to each electrode, and then short flexible

copper leads are soldered to the platinum wires. The copper lead for the upper electrode is soldered into a groove in the inner brass tube (0.375 in. outside diameter, 1/32 in. wall); the brass tube serves as a shield for the other lead, and stiffens the assembly. (This tube is omitted in Fig. 1 in order to simplify the drawing. It rests on a Teflon washer which insulates it from the lower platinum electrode.) It is connected by a short length of copper wire to the outside of a General Radio panel connector (874 P13) which is screwed to the Teflon cap as shown. The lead for the lower electrode is soldered into a groove in the central brass post (³/₁₆ in. diameter); the post is both central lead and the tie-bolt which holds the assembly together. The bottom nut is protected by a Teflon plug as shown. This plug is machined a bit oversize and is chilled before inserting; on warming to room temperature, it forms a gas-tight seal. The grooves in the brass tube and post are wide enough so that the platinum wires can be folded into them when the unit is assembled. The electrodes are used in vessels similar to that shown in Fig. 1A for concentration or dilution runs; for intercomparison of two sets of electrodes, a U-tube with ⚲ ends is convenient. Obviously the cell constant can be varied over a wide range by varying the distance between electrodes and/or the width of the annular space between the Teflon tubing and the inner wall of the cylindrical electrode compartment. The latter should be long enough to permit the top electrode to be immersed to a depth of at least 1 cm. into the cylindrical section.

One practical precaution in handling Teflon must be mentioned: its temperature coefficient of expansion (5.5 × 10^{-5}) is much larger than that of glass, and a Teflon plug placed in a warmer glass joint will always freeze. It can be easily released, however, by allowing the apparatus to stand in a refrigerator or a cold room for 20–30 min. The assembly must not be allowed to get too cold, however, because too much shrinkage will loosen the electrodes. No hysteresis in dimensions due to moderate temperature changes has been observed; on inserting electrodes at variable room temperature into solution at 25.00°, the resistance always comes back to the same value within 0.01%. Teflon has two transitions, one centering around 20° and the other around 30°; the total volume change amounts to 1.23%.[4] Ideally, therefore, Teflon assemblies should always be kept around 25°.

If the ends of the Teflon sections are machined smooth and the electrodes are flat, no solution is trapped between the Teflon–platinum surfaces. This was checked by letting an electrode assembly stand in alcoholic picrate solution ($\kappa \approx 10^{-3}$) overnight, rinsing with ethanol and then inserting in conductance ethanol. No decrease of resistance was observed.

Preliminary Experiments.—All electrical measurements were made using a bridge circuit which has already been described[5]; usually data were taken at 500, 1000, 2000 and 5000 cycles. Solutions of potassium chloride or acetic acid in water were used for some of the comparisons; for those with the Teflon cell, alcoholic solutions of tri-n-propylammonium picrate were used. The Teflon cell cannot be used with aqueous solutions, because water does not wet Teflon, and fine air bubbles cling to the Teflon cylinder. Their presence alters the cell constant in an erratic fashion by about ±0.1%.

The cell constant varies somewhat with the position of the electrode assembly in the ground joint, as shown in Fig. 2 for several cells. Here resistance is plotted against angle of rotation from an arbitrary reference mark. It will be noted that each electrode assembly has two positions in which resistance is quite insensitive to angular rotation (the maximum and the minimum of the curve). One of these is selected as the working position and appropriate reference marks are made on the ground joint and the electrode assembly. Reproducibility of replacement of electrodes is shown by the following typical case: resistances on successive replacements were 1729.2, 1729.6, 1729.5 and 1729.6 ohms. The resistance is completely insensitive to depth of liquid above the top electrode, provided the latter is at least 1 cm. below the level at which the container flares away

(3) Polarization is naturally greater with bright electrodes than with platinized, but adsorption is far greater with the latter. Since polarization errors can be eliminated by extrapolation, while no simple means of avoiding sorption errors is available, polarization was accepted as the lesser evil.

(4) H. A. Rigby and C. W. Bunn, Nature, **164**, 583 (1949); F. A. Quinn, Jr., D. E. Roberts and R. N. Work, J. Appl. Phys., **22**, 1085 (1951).

(5) H. Eisenberg and R. M. Fuoss, J. Am. Chem. Soc., **75**, 2914 (1953)
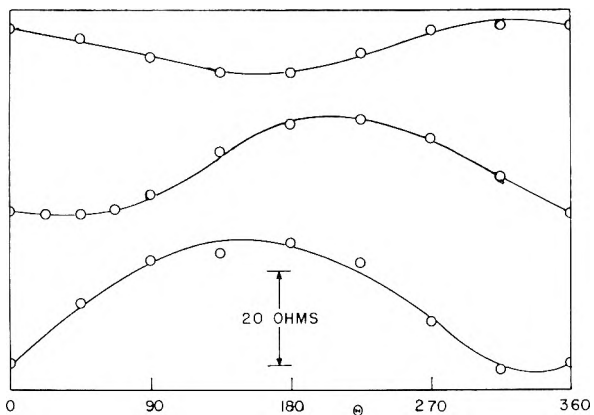
Fig. 2.—Dependence of cell resistance on rotation of the electrode assembly;   approx. total resistances: 13,900 ohms, 1500 ohms and 2400 ohms.

from the cylindrical cell compartment. The latter must, of course, be completely filled with solution.

Discussion

The frequency characteristics of two glass insulated electrode assemblies are shown in Figs. 3A
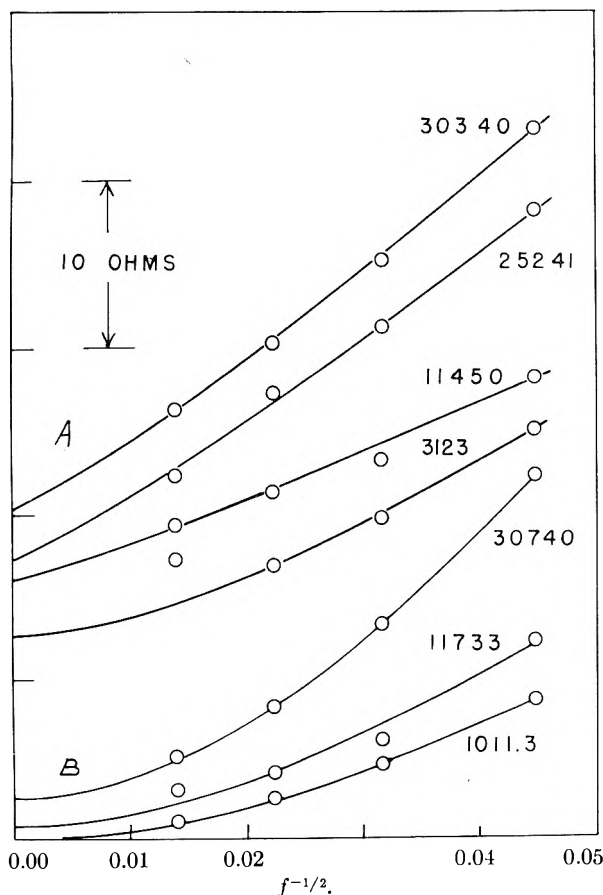
Fig. 3.—Frequency characteristics of a glass cell (k = 3.43), A; of a Teflon cell (k = 0.48), B.

and 4, where resistance is plotted against $f^{-1/2}$; f = frequency. The ordinate scale is the same for all of the curves; the absolute resistance is obtained by adding the number shown to the right of a given curve to the ordinate value. It will be seen that each cell has a working range of at least a tenfold change in resistance, over which a reliable extrap-
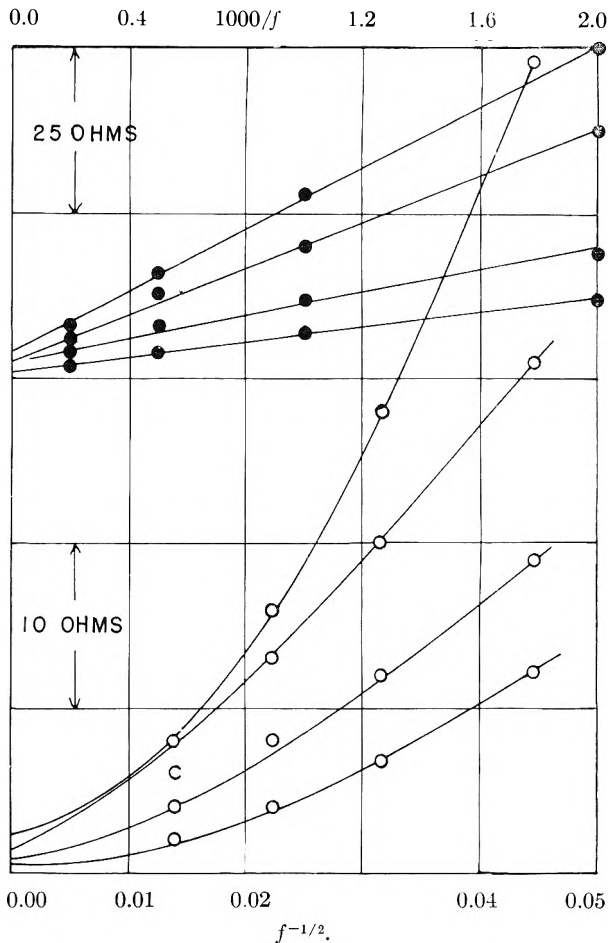
Fig. 4.—Frequency characteristics of a glass cell (k = 0.61); lower curves, R $vs.$ $f^{-1/2}$; upper curves, R $vs.$ f^{-1}; approx. total resistances: 31,000 ohms, 19,500 ohms, 14,000 ohms and 5,900 ohms.

olation to infinite frequency can be made. If $x = f^{-1/2}$, it was found[2] that

$$R = R_\infty + ax + bx^2$$

Depending on the cell and the solution, one of the frequency terms is often negligible[6]; for the examples shown in Fig. 4, the ax term is negligible, and a reciprocal frequency curve is better for extrapolation as illustrated by the solid circles for the cell with a constant of approximately 0.61 (abscissa scale at top of figure). Figure 3B shows the frequency characteristics of a Teflon insulated electrode assembly; it likewise has a wide working range. At higher resistances, the Parker effect begins to appear; the R $vs.$ $f^{-1/2}$ curves become concave-down (and useless for extrapolation).

Table I demonstrates the reproducibility of cell ratios, using various combinations of cells. The first two columns identify the cells compared and give approximate cell constants; T indicates Teflon insulation, G, glass insulation, N, Nichol–Fuoss design and J Jones–Bollinger[7] design. Resistances with various solutions are given in the next two columns and the last column gives the resist-

(6) J. C. Nichol and R. M. Fuoss, J. Am. Chem. Soc., **77**, 198 (1955).

(7) Grinnell Jones and G. M. Bollinger, ibid., **53**, 411 (1931).

ance ratio. Quality of the cells, as indicated by the constancy of the ratio, is completely satisfactory.

TABLE I
CELL COMPARISONS

Cells	Resistances	Ratio
4.59 T, 1.48 G	58685, 19004	3.0880
4.59 T, 1.48 G	6119.5, 1981.6	3.0881
1.48 G, 0.31 G	5337.0, 1113.7	4.7921
1.48 G, 0.31 G	17667, 3686.5	4.7923
1.48 G, 0.31 G	44444, 9269	4.7940
0.31 G, 0.04 N	3054.0, 419.70	7.2766
0.31 G, 0.04 N	40065, 5506.5	7.2759
10.6 G, 1.04 J	9358, 922.1	10.149
10.6 G, 1.04 J	34682, 3418.4	10.146
1.04 J, 0.24 J	3418.4, 792.2	4.3150
1.04 J, 0.24 J	11883, 2753.0	4.3164

Another test of the design was made as follows. By direct comparison with an Erlenmeyer cell[8] which had been calibrated using standard potassium chloride solutions (k = 2.6268), a Nichol–Fuoss cell was found to have a constant equal to 0.042639 (resistance ratio, 414.54/25,538). Using two glass insulated cells of the type shown in Fig. 1 as intermediates, the following sequence of data (resistances extrapolated to infinite frequency, after correcting for lead resistance and decade-box errors) were obtained: Erlenmeyer/G_1 = 5126.0/2902.3, $k(G_1)$ = 1.4873; G_1/G_2 = 5337.0/1113.7, $k(G_2)$ = 0.31037; G_2/N = 3054.0/419.70, $k(N)$ = 0.042654. The agreement between direct and indirect methods is excellent.

(8) C. A. Kraus and R. M. Fuoss, *J. Am. Chem. Soc.*, **55**, 21 (1933).

THE APPARENT STABILITY CONSTANTS OF IONIC COMPLEXES OF VARIOUS ADENOSINE PHOSPHATES WITH MONOVALENT CATIONS

By Rex M. Smith[1,2] and Robert A. Alberty

Chemistry Department, University of Wisconsin, Madison, Wisconsin

Received August 17, 1955

The apparent stability constants of the Li$^+$, Na$^+$ and K$^+$ complexes of adenosine 5-mono-, -di-, -tri- and -tetraphosphate and orthophosphate[3] have been measured at 25° at 0.2 ionic strength. Equations have been derived for calculating the stability constants from pH measurements of solutions containing these weak acids and the various cations. The stability constants have been calculated on the basis of the assumption that tetra-n-propylammonium cations do not form complexes. In each case a single value of the stability constant was found to represent the data from 25 to 100% replacement of the tetra n-propylammonium halide by the other 1–1 electrolyte. The stability constants are found to be in the order expected from electrostatic considerations, that is, Li$^+$ > Na$^+$ > K$^+$ > (CH$_3$)$_4$N$^+$ > (C$_2$H$_5$)$_4$N$^+$ and AQP^{-5} > ATP^{-4} > ADP^{-3} > P^{-2} > AMP^{-2}.

Introduction

There are 1, 2, 3 and 4 strongly ionized groups, respectively, for the adenosine phosphates AMP,[3] ADP, ATP and AQP. The ionization of the terminal group in each compound occurs in the neutral pH range. The first titrations of AMP were carried out by Wassermeyer[4] and of ATP by Eirich and Fitz[5] and by Lohmann.[6] Alberty, Smith and Bock[7] determined the apparent ionization constants of AMP, ADP and ATP preparations of high purity in 0.15 M sodium chloride using a glass electrode. Melchior[8] determined the apparent ionization constants of ADP and ATP in sodium bromide, potassium bromide and tetraethyl ammonium bromide solutions at 0.2 ionic strength using a hydrogen electrode in a cell without liquid junction. Lower values of the apparent acid dissociation constants are obtained in solutions of the tetraalkyl ammonium halides in comparison with

solutions of the alkali halides. Melchior[8] calculated stability constants for complexes of Na$^+$ and K$^+$ with ADP and ATP on the assumption that no complex is formed by (C$_2$H$_5$)$_4$N$^+$. It has been known for some time that sodium and potassium phosphate buffers having the same ratio of primary phosphate to secondary phosphate have significantly different pH values, and Scatchard and Breckenridge[9] have discussed the detailed interpretation of this observation. Knowledge of the extent to which various phosphate compounds exist in the form of complex ions is important for the interpretation of the effects of various cations, particularly Mg^{++} and Ca^{++},[10] on biological reactions of these compounds.

The apparent pK_a' value for a weak acid determined from a titration at a constant ionic strength is related to the thermodynamic pK_a value by the relation

$$pK_a' = pK_a + \log (f_{A^{-z}}/f_{HA^{1-z}}) \qquad (1)$$

where $f_{A^{-z}}$ and $f_{HA^{1-z}}$ are the activity coefficients of the basic form and of the conjugate acid, respectively. It would be expected on the basis of the Debye–Hückel[11] theory that the pK_a' values for the dissociation of the phosphate compounds would be smaller than the thermodynamic pK_a value

(1) This paper comprises a portion of a thesis presented by Rex M. Smith in partial fulfillment of the requirements for the degree of Doctor of Philosophy in the Graduate School of the University of Wisconsin, June, 1955.

(2) Pure Oil Fellow, 1953–1955.

(3) Throughout this article symbols will be used for phosphate, P, and adenosine-5-tetraphosphate, AQP, triphosphate, ATP, diphosphate, ADP, and monophosphate, AMP.

(4) H. Wassermeyer, *Z. physiol. Chem.*, **179**, 238 (1928).

(5) F. Eirich and W. Fitz, *Biochem. Z.*, **256**, 115 (1932).

(6) K. Lohmann, *ibid.*, **254**, 391 (1932); **282**, 120 (1935).

(7) R. A. Alberty, R. M. Smith and R. M. Bock, *J. Biol. Chem.*, **193**, 425 (1951).

(8) N. C. Melchior, *ibid.*, **208**, 615 (1954).

(9) G. Scatchard and R. G. Breckenridge, This Journal, **58**, 596 (1954).

(10) R. M. Smith and R. A. Alberty, in preparation.

(11) P. Debye and E. Hückel, *Physik. Z.*, **24**, 185 (1923).

and would decrease with increasing ionic strength as is observed. At constant ionic strength the highest pK_a' values are obtained using solutions of the tetraalkylammonium halides. Intermediate pK_a' values are obtained for solutions of the alkali halides and still lower pK_a' values are obtained for solutions containing alkaline earth halides.[10] The pK_a' values of the phosphate compounds are found to be in the order $(n\text{-}C_3H_7)_4N^+ > (C_2H_5)_4N^+ > (CH_3)_4N^+ > K^+ > Na^+ > Li^+ > Ca^{++} > Mg^{++}$. The shift in the pK_a' values and, in fact, of the whole titration curve can be explained in terms of the formation of complexes or ion pairs between the various cations and the anions of the phosphate compounds.

Experimental

The samples of AMP, ADP and ATP which had been chromatographically purified, were obtained from Pabst Laboratories and the Sigma Chemical Company. The AQP[12] was obtained from the Sigma Chemical Company (lot numbers 25–607, 617, 618). There was no evidence in any of the titration curves of impurities in these preparations.

The titration curves were obtained by use of a Beckman No. 9001 model RX pH amplifier which was used in conjunction with a Minneapolis-Honeywell Brown Electronik strip chart recorder. A Beckman glass electrode and a saturated calomel electrode were used. The side arm of the calomel electrode was opened so that a very slight flow of saturated KCl took place through the tip so that diffusion of solution into the salt bridge was prevented. The outward flow of KCl was so small that no significant change of the ionic strength or composition of the solution being titrated occurred during the course of a titration. The electrodes and a temperature compensator connected to the pH amplifier were enclosed in a metal box with four hollow sides through which water from a thermostat was circulated.

The titrant was delivered with a motor-driven microburet which utilizes a synchronous motor to drive a constant diameter plunger into a reservoir of mercury. The titrant was displaced by the mercury through a capillary into the solution being titrated. A three-way stopcock mounted on the capillary tube connected to a reservoir of titrant so that the buret could be refilled without removing it from the solution. During the titration the pH was continuously recorded as a function of volume of titrant added. There are several references in the literature concerning automatic potentiometric titration apparatus similar to that used in this research.[13,14]

The solutions were effectively stirred during the course of the titration by bubbling a stream of nitrogen through the solution. The nitrogen was first saturated with water vapor by bubbling it through a solution of the same ionic strength and temperature as the solution being titrated.

Several of the titrations were carried out manually using a Cambridge research model pH meter equipped with a shielded glass electrode and a saturated calomel electrode. The titrant was delivered with a Sholander type[15] microburet. The Cambridge research model pH meter was also used with a "sleeve-type" glass electrode to measure differences in pH between various solutions.

The pH meters were standardized on the paH scale with National Bureau of Standards buffers.[16]

In order to keep the ionic strength nearly constant, relatively dilute solutions of the phosphate compounds, approximately $10^{-3}\,M$, were titrated in the presence of $0.2\,M$ 1–1 electrolyte, and a relatively concentrated titrant, usually $1\,M$, was used.

Treatment of Data

If a metal ion which complexes predominately with the more basic form of a weak acid is added

(12) I. Lieberman, *Physik Z.*, **77**, 3373 (1955).

(13) J. J. Lingane, *Anal. Chem.*, **20**, 235 (1948); **21**, 497 (1949).

(14) J. B. Neilands and M. D. Cannon, *ibid.*, **27**, 29 (1955).

(15) P. F. Sholander, G. A. Edwards and L. Irving, *J. Biol. Chem.* **148**, 495 (1943).

(16) U. S. Dept. of Commerce Nat. Bur. Stds., LC993, Aug., 1950.

to a buffer solution of the weak acid, a reduction in pH will be observed. In the case of phosphate compounds higher pK_a' values are obtained for solutions of tetraalkyl ammonium halides than for alkali halides, and the pK_a' values increase slightly with increasing size of the alkyl substituents. The magnitude of the reduction in pH of a buffer solution caused by the replacement of tetraalkyl ammonium halide by metal halide at constant ionic strength may be used to calculate the stability constant of the complex formed if it is assumed that: (1) the tetraalkyl ammonium cation for which the highest pK_a' value is obtained does not form a complex, (2) this pK_a' value is a constant at a constant ionic strength, and (3) the acidic form of the weak acid does not form a complex with the metal ion.

The pH of the phosphate solution containing a completely dissociated salt of the cation which is assumed not to form complexes is given by

$$pH_1 = pK_a' + \log \frac{a}{1-a} \qquad (2)$$

where a is the fraction of the compound in the basic form. For convenience let $y = $ antilog $(pK_a' - pH_1)$ so that $y = (1-a)/a$. The pH of the phosphate solution which contains metal ions which form a complex MA will be given by

$$pH_2 = pK_a' + \log \frac{a(A)_T - (MA^{1-z}) + \delta(H^+)}{(1-a)(A)_T - \delta(H^+)} \qquad (3)$$

where $(A)_T$ is the total concentration of the weak acid and $\delta(H^+)$ is the change in hydrogen ion concentration resulting from the shift in the dissociation equilibrium. Since the pK_a' values of the terminal phosphate groups are of the order of 10^{-7} and $(A)_T$ is about $10^{-3}\,M$, $\delta(H)^+$ is negligible for a shift in pH of as much as 2 units around pH 7. For convenience let $x = $ antilog $(pK_a' - pH_2)$.

Since

$$(A)_T = (A^{-z}) + (HA^{1-z}) + (MA^{1-z}) \qquad (4)$$

$$x = \frac{(1-a) + (1-a)\dfrac{(HA^{1-z})}{(A^{-z})} + (1-a)\dfrac{(MA^{1-z})}{(A^{-z})}}{a + a\dfrac{(HA^{1-z})}{(A^{-z})} - (1-a)\dfrac{(MA^{1-z})}{(A^{-z})}} \qquad (5)$$

The apparent stability constant K' is defined by

$$K' = \frac{(MA^{1-z})}{(M^+)(A^{-z})} \qquad (6)$$

where the parentheses represent concentrations. The apparent ionization constant is defined by $K_a' = \gamma_{H^+}(H^+)(A^{-z})/(HA^{1-z})$ where $\gamma_{H^+}(H^+)$ represents antilog $(-pH)$ and γ_{H^+} is the activity coefficient of H^+ which is assumed constant at constant ionic strength. If this expression and equation 6 are introduced into equation 5, and the numerator and denominator are divided by $(1-a)$

$$x = \frac{1 + \gamma_{H^+}\dfrac{(H^+)_2}{K_a'} + K'(M^+)}{\dfrac{a}{(1-a)}\left[1 + \gamma_{H^+}\dfrac{(H^+)_2}{K_a'}\right] - K'(M^+)} \qquad (7)$$

Introducing $x = \gamma_{H^+}(H^+)_2/K_a'$ and $y = (1-a)/a$, equation 7 becomes

$$x = \frac{1 + x + K'(M^+)}{\dfrac{1+x}{y} - K'(M^+)} \qquad (8)$$

which may be rearranged to

$$\frac{x - y}{(M^+)y} = K' \quad (9)$$

If the data available are pK_a' values obtained from titration curves, so that $y = 1$, equation 10 reduces to

$$\frac{x - 1}{(M^+)} = K' \quad (10)$$

This special equation has been derived by Trevelyan, Mann and Harrison[17] who studied the binding of magnesium ions by glucose phosphate and orthophosphate.

The effect of complex formation of the above type is to cause the complete titration curve for an acidic group to be displaced along the pH axis without change in shape. Equation 3 may be written in the form

$$pH = pK_a' + \log \frac{(A^{-z})}{(A)_T - (A^{-z})[1 + K'(M^+)]} \quad (11)$$

or

$$pH = pK_a' - \log [1 + K'(M^+)] +$$
$$\log \frac{[1 + K'(M^+)](A^{-z})}{(A)_T - [1 + K'(M^+)](A^{-z})} \quad (12)$$

Thus the mid-point of the titration will occur at the pH at which $[1 + K'(M^+)] (A^{-z}) = (A)_T - [1 + K'(M^+)](A^{-z})$, and the pH at the mid-point will be $pK_a' - \log [1 + K'(M^+)]$. Cannan and Kibrick[18] used equation 12 for calculating stability constants for complexes of carboxylic acids and divalent cations.

Experimental Data

The data of Table I show the effect of various halide salts upon the pK_a' values at 25° and 0.2 ionic strength. The mean uncertainty in these values which were determined using the recording pH meter is ±0.02. It will be noted that the pK_a' values increase with the size of the cation except that there is no detectable difference between the values for P, AMP and ADP when the cation is $(n\text{-}C_3H_7)_4N^+$ or $(C_2H_5)_4N^+$. In the case of ATP and AQP the difference was small but reproducible. On the basis of the assumption that complexes are formed between the cations and the more basic forms of the phosphate compounds, these data indicate that the affinity of the various cations for the phosphate compounds is $Li^+ > Na^+ > K^+ > (CH_3)_4N^+ > (C_2H_5)_4N^+$ in all cases. The magnitudes of the changes in pK_a' in going

TABLE I

pK_a' Values for the Terminal Phosphate Groups of the Adenosine-5-phosphates at 25° and 0.2 Ionic Strength

Cation	$(n\text{-}C_3H_7)_4N^+$	$(C_2H_5)_4N^+$	$(CH_3)_4N^+$	K^+	Na^+	Li^+
P	6.92	6.92	6.87	6.71	6.67	6.61
AMP	6.45	6.45	6.40	6.32	6.29	6.19
ADP	6.68	6.68	6.62	6.40	6.36	6.10
ATP	6.95	6.91	6.76	6.48	6.41	6.02
AQP	7.27	7.23	7.06	6.58	6.46	6.04

(17) W. E. Trevelyan, P. E. F. Mann and J. S. Harrison, *Arch. Biochem. Biophys.*, **39**, 440 (1952).
(18) R. K. Cannan and A. Kibrick, *J. Am. Chem. Soc.*, **60**, 2391 (1938).

from Li^+ to $(n\text{-}C_3H_7)_4N^+$ are in the order AQP > ATP > ADP > P > AMP.

The fact that the differences between pK_a' values in $(n\text{-}C_3H_7)_4N^+$ and $(C_2H_5)_4N^+$ salts are so small suggests that stability constants for metal ion–phosphate complexes may be calculated by assuming that $(n\text{-}C_3H_7)_4N^+$ or $(C_2H_5)_4N^+$ does not complex with the phosphate compounds. Since reproducible differences were found between $(C_2H_5)_4N^+$ ion and $(n\text{-}C_3H_7)_4N^+$ ion in the data for ATP and AQP it seemed desirable to repeat the measurements with $(n\text{-}C_4H_9)_4N^+$ ion. Unfortunately, the solubility of $(n\text{-}C_4H_9)N^+$ is only 0.0701 M at 25°.

The values of $(x - y)/(My^+)$ given in Table II were obtained in experiments in which 25, 50, 75

TABLE II

$(x - y)/(M^+)y$ Values (in M^{-1}) at 25° and 0.2 Ionic Strength Assuming $(n\text{-}C_3H_7)_4N^+$ is not Bound

Salt % ionic strength	KCl	P NaCl	LiCl
25	3.0 ± 1.1	3.5 ± 1.1	4.6 ± 1.2
50	3.2 ± 0.6	4.0 ± 0.6	5.5 ± 0.7
75	3.1 ± 0.5	4.0 ± 0.5	5.2 ± 0.6
100	3.1 ± 0.4	4.0 ± 0.4	5.3 ± 0.5
Av.	3.1 ± 0.4	4.0 ± 0.4	5.2 ± 0.5

Salt % ionic strength	KCl	AMP NaCl	LiCl
25	1.7 ± 1.0	3.0 ± 1.1	4.0 ± 1.1
50	1.5 ± 0.5	2.9 ± 0.6	4.1 ± 0.7
75	1.5 ± 0.4	2.8 ± 0.4	4.1 ± 0.5
100	1.6 ± 0.3	2.9 ± 0.4	4.1 ± 0.4
Av.	1.6 ± 0.3	2.9 ± 0.4	4.1 ± 0.4

Salt % ionic strength	KCl	ADP NaCl	LiCl
25	5.7 ± 1.3	7.0 ± 1.3	
50	5.5 ± 0.8	6.6 ± 0.8	
75	5.5 ± 0.6	6.6 ± 0.6	
100	5.4 ± 0.5	6.7 ± 0.5	14 ± 0.9
Av.	5.5 ± 0.5	6.7 ± 0.5	14 ± 0.9

Salt % ionic strength	KCl	ATP NaCl	LiCl
25	12.2 ± 1.0	14.0 ± 1.0	
50	11.9 ± 0.6	14.0 ± 0.6	
75	11.7 ± 0.5	14.4 ± 0.5	
100	10.5 ± 0.4	14.5 ± 0.4	37.5 ± 2.0
Av.	11.5 ± 0.4	14.3 ± 0.4	37.5 ± 2.0

or 100% of the total ionic strength of 0.2 was made up of KCl, NaCl or LiCl, the remainder being due to $(n\text{-}C_3H_7)_4NBr$. The indicated uncertainties in the $(x-y)/(M^+)y$ values were calculated on the assumption that differences in pH values between any two solutions could be reproduced within 0.02 pH unit. The independence of the $(x-y)/(M^+)y$ values of the percentage of the ionic strength contributed by the metal halide shows that only a single constant is required to represent the data. This is in accord with equation 9 which was derived on the assumption that a single complex with the more basic ion of the phosphate compound is formed. Equation 9 identifies the values in Table II as the apparent stability constants of the complexes at the total ionic strength used. The aver-

age values of the stability constants given in the last line are weighted by a factor inversely proportional to the uncertainty. These values are summarized in Table III together with corresponding values calculated from experiments in which the remainder of the ionic strength was made up by $(C_2H_5)_4NBr$. The differences between the apparent stability constants calculated on the basis of the assumption that $(n\text{-}C_3H_7)_4N^+$ and $(C_2H_5)_4N^+$ are not bound are negligible in the case of P, AMP and ADP, and they are only slightly greater than the experimental error in the case of ATP and AQP.

TABLE III

APPARENT STABILITY CONSTANTS (K IN M^{-1}) OF ALKALI CATION COMPLEXES OF ADENOSINE-5-PHOSPHATES AT 25° AND 0.2 IONIC STRENGTH

Cation	Assuming $(n\text{-}C_3H_7)_4N^+$ is not bound		
	K^+	Na^+	Li^+
P	3.1 ± 0.4	4.0 ± 0.4	5.2 ± 0.5
AMP	1.6 ± 0.3	2.9 ± 0.4	4.1 ± 0.4
ADP	5.5 ± 0.5	6.7 ± 0.5	14.0 ± 0.9
ATP	11.5 ± 1.0	14.3 ± 0.4	37.5 ± 2.0
AQP predt.	21.3 ± 3.6	28.6 ± 4.6	78.5 ± 7.9
AQP exptl.	19.5 ± 1.0	27.2 ± 1.4	80.0 ± 3.5

Cation	Assuming $(C_2H_5)_4N^+$ is not bound		
	K^+	Na^+	Li^+
P	3.0 ± 0.4	3.9 ± 0.4	5.2 ± 0.5
AMP	1.8 ± 0.3	2.2 ± 0.2	4.1 ± 0.4
ADP	4.5 ± 0.5	5.4 ± 0.4	14.0 ± 0.9
ATP	8.5 ± 0.6	11.0 ± 0.7	33.5 ± 2.0
AQP	17.2 ± 1.0	24.2 ± 1.4	72.0 ± 3.5

The stability constants for the Na^+ and K^+ complexes of ADP and ATP agree within the indicated uncertainty with the values obtained by Melchior[3] at 0.2 ionic strength assuming $(C_2H_5)_4N^+$ ion does not form complexes. Melchior reported that there seemed to be no significant difference between the binding of sodium and potassium ions, but it was found in this research that the complexes with Na^+ were always more stable than those with K^+, including the weak complexes of AMP and P. The difference between Na^+ and K^+ was even more pronounced in the case of the highly charged AQP. It would be expected from electrostatic theory and the crystal radii that K^+ would form weaker complexes than Na^+ which in turn would form weaker complexes than Li^+, as actually observed.

Discussion

In the interpretation of data such as those reported in this paper, the question arises as to whether the observed effects should be attributed to changes in the activity coefficients at constant ionic strength,[19] or to the formation of complex ions. The alkali metal ions are not usually involved in the formation of complexes in aqueous solutions, but in the case of highly charged negative ions there is the possibility that complexes of the ion-pair type may be formed. The fact that a single stability constant represents the data so well from 25 to 100% replacement of the $(n\text{-}C_3H_7)_4N^+$ halide with

alkali halide supports the idea that a single complex ion is formed. This hypothesis is also supported by the fact that the values of the various stability constants are in the relative order that would be expected from electrostatic theory based on the crystal radius of the cations and charge of the anions. The smaller the ion and the higher the charge, the more stable the complex that is formed. A few moving boundary experiments were carried out to determine the constituent mobility,[20,21] of ATP in buffers containing various cations. The constituent mobilities at 0.2 ionic strength were found to decrease in the order $(C_2H_5)_4N^+$, K^+, Na^+, Li^+ as predicted on the basis of the stability constants.

Although P^{-2} and AMP^{-2} have the same net charge, AMP^{-2} binds protons about one third as strongly as P^{-2}, and so it would be expected, as is actually observed, that AMP^{-2} would bind other cations less strongly.

Although the Bjerrum[22] theory of ionic association involves assumptions which are not satisfactory in the present case, it is of interest to compare the results of that theory with the present experimental data. The values of the association constants in Table III were used to calculate the distance between the centers of the two ions forming the ion pair at their distance of closest approach.[23] These values increase in the order P, AMP, ADP, ATP and AQP. This is the order expected from the actual size of these ions, whereas the order of increasing stability constants AMP, P, ADP, ATP, AQP is different. The distances between centers calculated from the Bjerrum theory for the K^+ complexes increase from 1.09 to 3.73 Å. for P to AQP, for the Na^+ complexes from 0.98 to 3.35 Å. and for the Li^+ complexes from 0.87 to 2.20 Å. These values increase in the order Li^+, Na^+, K^+, the order of increasing crystal radii, rather than in the order of increasing distances of closest approach obtained from data for strong 1–1 electrolytes using the Debye–Hückel theory.

The stability constants for the alkali metal ion complexes of orthophosphate were also determined at 0°. For K^+, Na^+ and Li^+ the values are 1.2 ± 0.3, 1.2 ± 0.3 and $2.1 \pm 0.3 M^{-1}$, respectively. The ΔH and ΔS values calculated assuming that ΔH of formation is independent of temperature are about 6 kcal. mole^{-1} and 24 cal. deg.$^{-1}$ mole^{-1} for all three complexes. As expected[24] the entropy changes are positive as is often found for association reactions in solution.

It is of considerable interest to determine whether the pK_a' values for AQP and the stability constants for the AQP complexes are of the magnitude to be expected for a linear tetraphosphate since the literature data[12] does not indicate whether the four phosphate residues in this compound are in a chain or are divided between two positions on the ribose residue. Since there is a regular increase in the apparent stability constants (K') for the series of

(19) H. S. Harned and B. B. Owen, "The Physical Chemistry of Electrolytic Solutions," Reinhold Publ. Corp., New York, N. Y., 1949, p. 466.

(20) R. A. Alberty, J. Am. Chem. Soc., **72**, 2361 (1950).

(21) R. A. Alberty and E. L. King, ibid., **73**, 517 (1951).

(22) N. Bjerrum, Kgl. Danske Vidensk. Selskab., **7**, No. 9 (1926).

(23) R. M. Fuoss and C. A. Kraus, J. Am. Chem. Soc., **55**, 1919 (1933).

(24) E. L. King, J. Chem. Education, **30**, 71 (1953).

linear phosphates AMP, ADP and ATP, the values for K' for AQP were predicted using the equation $K' = na + n^2b$ and n^3c where n is the number of phosphate residues. The values of a, b and c were calculated from the apparent stability constants for AMP, ADP and ATP, and the values of K' for AQP listed as "predicted" in Table III were obtained by letting $n = 4$. The uncertainty indicated is that caused by K' being either too high or too low for AMP, ADP and ATP by the indicated uncertainties. The fact that in all cases the experimental values fall in the expected range supports the linear structure for the phosphate chain of AQP.

A comparison of the pK_a' values also offers evidence for the linear structure. On the basis of the quite regular increases in pK_a' values in the series AMP, ADP and ATP, it was predicted that the values of pK_a' for AQP would be 7.26 in $(n$-$C_3H_7)_4NBr$ and 7.14 in $(C_2H_5)_4NBr$. Since appreciable concentrations of complexes are formed in the case of K^+, Na^+ and Li^+, this simple extrapolation procedure is inadequate, and it is necessary to consider, in addition, the expected increase in the stability constants of the complexes formed. The values for pK_a' for AQP in 0.2 M KCl, NaCl and LiCl predicted on the basis of the predicted pK_a' value in $(n$-$C_3H_7)_4NBr$ and the predicted stability constants in Table II are 6.57, 6.43 and 5.92, respectively. Thus the pK_a' values for AQP obtained experimentally agree within the experimental uncertainties with the values expected for a linear phosphate.

CONCENTRATED SALT SOLUTIONS. I. ACTIVITY COEFFICIENTS OF SODIUM THIOCYANATE, SODIUM IODIDE AND SODIUM PERCHLORATE AT 25°

By M. L. MILLER AND C. L. SHERIDAN

Contribution from the Stamford Laboratories, Research Division, American Cyanamid Company, Stamford, Conn.

Isopiestic vapor pressure measurements at 25° have been extended to near saturation for NaCNS, NaI and NaClO₄. With these data, values of the osmotic coefficients and activity coefficients up to near saturation have been computed.

I. Introduction

Although the behavior of aqueous solutions of 1-1 electrolytes has been intensively investigated in the dilute and moderately concentrated range (up to 5 m) there have been fewer measurements in very concentrated solution (above 5 m). This is in part due to the limited number of salts which form such concentrated solutions and in part to a lack of interest in the field of very concentrated solutions.

The isopiestic vapor pressure method developed by Robinson and Sinclair[1] and perfected by Robinson[2] is admirably suited for the measurement of activity coefficients in very concentrated solutions. By this method, measurements have been made on LiCl[3] up to 15 m, LiBr[4] to 20 m and NH₄NO₃[5] to 26 m. Three other salts whose solubility extends up into the very concentrated range are NaSCN, NaI and NaClO₄. Measurements on these salts have, heretofore, been carried only as far as KCl or NaCl could be used as a reference salt, *i.e.*, to 4, 5 or 6.5 m.[2,6,7]

As a part of a study of concentrated salt solutions

in this Laboratory, we have extended the vapor pressure measurements on these three salts up to near saturation. For this purpose, we have used sulfuric acid as a reference electrolyte and the vapor pressure measurements of Shankman and Gordon[8] as standard. Other properties of the concentrated solutions of these salts which we have measured and which will be reported in forthcoming papers of this series are: viscosity, density, electrical conductivity and diffusion.

II. Experimental

Method of Measurement.—The method of measurement was a somewhat modified version of that of Robinson and Sinclair.[1] A 10″ glass desiccator was used for the tests. This contained a ³/₈″ stainless desiccator plate into which had been drilled 4 circular depressions ¹/₄″ deep to hold the solution cups. The solution cups, two each for salt solution and sulfuric acid, were low-form glass weighing bottles 2.5 inches wide and 1″ high (outside closure). Solutions were weighed into these bottles which were placed in the depressions on the desiccator plate. The covers were placed beside the bottles. This could be done very rapidly. The desiccator was sealed with silicone lubricant. The whole apparatus was placed on a rocking platform in a constant temperature room at 25 ± 1°. Vacuum was not used because it was found not to shorten the equilibrating time which ranged from 3 days to 2 weeks. Approximately half of the measurements were made with distillation into the sulfuric acid and half with distillation out of it. After equilibrium had been attained, all solutions lost weight on successive weighings. The relatively long time required to reach equilibrium resulted from the use of glass

(1) R. A. Robinson and D. A. Sinclair, *J. Am. Chem. Soc.*, **56**, 1830 (1934).

(2) R. A. Robinson, *ibid.*, **57**, 1161, 1165 (1935).

(3) R. A. Robinson, *Trans. Faraday Soc.*, **41**, 756 (1945).

(4) R. A. Robinson and H. J. McCoach, *J. Am. Chem. Soc.*, **69**, 2244 (1947).

(5) B. F. Wishaw and R. H. Stokes, *Trans. Faraday Soc.*, **49**, 27 (1953).

(6) R. A. Robinson, *J. Am. Chem. Soc.*, **62**, 3131 (1940).

(7) J. H. Jones, THIS JOURNAL, **51**, 516 (1947).

(8) S. Shankman and A. R. Gordon, *J. Am. Chem. Soc.*, **61**, 2370 (1939).

instead of metal cups.[2] The long equilibration time was preferred to the risk of corrosion from sulfuric acid.

Preparation of Solutions.—In working with concentrated solutions of salt, it was found convenient to establish a precise curve for density *versus* concentration and to use this in determining the concentration of solutions[3] subsequently made up.

Sodium Thiocyanate.—Three different samples of sodium thiocyanate were used, namely, (1) J. T. Baker analyzed; (2) J. T. Baker analyzed, recrystallized from ethanol; (3) Mallinkrodt C.P. Density values for samples 2 and 3 were found to fall (within 0.04%) on the smooth curve for sample 1. Therefore, J. T. Baker analyzed was used without further purification for the vapor pressure work. Densities were determined at 29.87 ± 0.02° by conventional pycnometric techniques. The temperature of the bath was measured on a platinum resistance thermometer calibrated at the National Bureau of Standards. The concentrations of samples for density work were determined by both gravimetric and volumetric methods. These analyses agreed to ±0.1%. Density values are given in Paper II of this series.

Sodium Iodide.—Sodium iodide solutions were made up without additional purification from reagent salt supplied by City Chemical Corporation. Concentrations were determined gravimetrically, and also by measuring the density and referring to the density data in International Critical Tables (at 30° corrected by a small factor to 29.87°). The agreement between the concentrations as measured by these two methods was taken as evidence that the salt was of sufficient purity. This procedure was considered safer than attempting to dry a salt as labile as sodium iodide.

Table I
Concentrations of Isotonic Solutions

Salt	Molality of salt, moles/1000 g. H₂O	Molality of sulfuric acid, moles/1000 g. H₂O
Sodium thiocyanate	4.40	3.06
	6.40	4.51
	7.22	4.80
	8.36	5.77
	10.30	6.86
	12.44	7.80
	14.11	8.50
	15.20	9.12
	17.86	10.15
	19.01	10.85
Sodium iodide	3.94	2.32
	7.10	5.16
	9.19	6.54
	9.29	6.89
	11.90	7.96
	12.72	8.52
Sodium perchlorate	15.14	7.65
	16.25	8.11
	10.85	5.81
	6.14	3.88

Table II
Activity and One Minus Osmotic Coefficients

Moles/1000 g. H₂O, m	NaSCN γ	NaSCN 1 − φ	NaI γ	NaI 1 − φ	NaClO₄ γ	NaClO₄ 1 − φ
1	[0.712]	+0.031	[0.736]	+0.009		
2	.751	−0.029	.820	−0.079		
3	.82	.093	1.05	.180		
4	.92	.154	1.25	.274	[0.626]	+0.009
5	1.03	.219	1.72	.358	.649	−0.025
6	1.16	.285	2.23	.443	.676	.056
7	1.31	.355	2.88	.523	.706	.083
8	1.49	.422	3.68	.597	.736	.107
9	1.69	.484	4.69	.667	.77	.134
10	1.90	.538	5.94	.733	.81	.156
11	2.03	.578	7.4	.784		
12	2.30	.602	9.0	.821	.89	.202
13	2.46	.619				
14	2.63	.627			.97	.246
15	2.8	.633				
16	2.9	.638			1.06	.286
17	3.1	.642				
18	3.2	.644				

Sodium Perchlorate.—Sodium perchlorate solutions were made up by weight from sodium perchlorate ("anhydrous") supplied by City Chemical Corporation. The salt was dried to constant weight in an oven at 110°. No further purification was attempted. Examination of the salt by ultraviolet emission spectroscopy[9] showed the presence of not over 0.1% of any one of 38 metal or metalloid impurities looked for.

III. Results

Table I gives the concentrations of the isotonic solutions of sodium thiocyanate, sodium iodide and sodium perchlorate as measured against sulfuric acid. In calculating activity coefficients from these data, reference values at 1 m were taken from the compilation of Robinson and Stokes[10] for sodium thiocyanate and sodium iodide. For sodium

perchlorate, the reference value at 4 m was taken from the same compilation. Randall and White's equation[11] for computing activity coefficients from vapor pressure was used to get γ

$$\log \frac{\gamma_m}{\gamma_1} = \frac{-h}{2.3} + \frac{h_1}{2.3} - \int_0^m \frac{h}{m} \, dm \qquad (1a)$$

$$= \frac{-h}{2.3} + \frac{h_1}{2.3} - 2 \int_0^{m^{1/2}} \frac{h}{m^{1/2}} \, dm^{1/2} \qquad (1b)$$

Here γ_m is the activity coefficient at molality (g. per 1000 g. water), m, and γ_1 is the same quantity at the reference molality, 1 m (or 4 m). $h = 1 - \phi$ where ϕ is the osmotic coefficient. At these high concentrations the integral in equation 1 contributes an important part to γ. It was therefore

(9) Kindly carried out by Mr. W. L. Dutton of this Laboratory.

(10) R. A. Robinson and R. H. Stokes, *Trans. Faraday Soc.*, **45**, 612 (1949).

(11) M. Randall and A. McL. White, *J. Am. Chem. Soc.*, **48**, 2514 (1926).

evaluated graphically from two plots, one of h/m versus m and one of $h/m^{1/2}$ versus $m^{1/2}$ as in equations 1a and 1b. The values of γ so computed and of ϕ are summarized in Table II.

Discussion of Results

The behavior of these salts in highly concentrated solutions is an extension of their behavior at low concentrations and shows nothing unexpected.

CONCENTRATED SALT SOLUTIONS. II. VISCOSITY AND DENSITY OF SODIUM THIOCYANATE, SODIUM PERCHLORATE AND SODIUM IODIDE

BY M. L. MILLER AND M. DORAN

Contribution from the Stamford Laboratories, Research Division, American Cyanamid Company, Stamford, Conn.

Viscosities of solutions of NaSCN, NaClO$_4$ and NaI from low concentrations up to saturation (or above) have been measured at 0, 30 and 50°. Using absolute rate theory, free energies, entropies and heats of activation of viscous flow have been calculated at 30°. These values have been interpreted to mean that at high concentration the three salts studied take on quasi-crystalline short range local order. This interpretation is supported by computation of excess partial molal entropies.

I. Introduction

Theoretical treatments of aqueous salt solutions have been confined to the dilute or moderately dilute region (not over 4 N). The range 6 N or above is largely an uncharted wilderness containing few experimental outposts. It seems reasonable to expect that a valid theoretical treatment, when it comes, may well stem from a theory of molten salt behavior rather than from a theory of the infinitely dilute solution. With this in mind, we should look for evidence, in the properties of very concentrated aqueous electrolyte solution of the beginning of short range local order. In the very concentrated ranges, we should also expect to find that ion size plays a predominant role in determining solution properties.

Some evidence for the existence of at least short range local order in concentrated salt solutions has already been found in studies of (a) density,[1,2] and (b) vapor pressure.[3]

Since 1936, there have been a number of attempts to use the quasi-crystalline concept as a basis for a theory of the liquid state. (See reference 4 and references quoted therein.) Although somewhat declining in favor as applied to pure liquids,[5] the concept of quasi-crystalline local order has much more to recommend it in the field of highly concentrated salt solutions (see Duttra[6]).

Eyring and associates[7] have used, with much success, the concept of quasi-crystalline structure in correlating the properties of pure liquids. Their methods are available for use in the study of concentrated aqueous salt solutions.

In this work, we have measured the viscosity of sodium thiocyanate, sodium perchlorate and sodium iodide solutions at 0, 30 and 50° from zero

per cent. to near (or sometimes above) saturation. Although there is a large amount of viscosity data in the literature, there is very little on aqueous solutions above 5 N and even less in this concentrated range at two or more temperatures. Among 1-1 salts only ammonium nitrate and silver nitrate, measured by Campbell and Kartzmark[8] and Campbell, Gray and Kartzmark[9] at 25, 35 and 95° and the data on lithium chloride in "The International Critical Tables" meet the above requirements.

II. Experimental

Preparation of Solutions.—The source of the salts and the preparation and assay of solutions was the same as in previous work on vapor pressure.[10]

Measurement of Viscosity.—Viscosity measurements were made using conventional techniques. Timing was by an electric timer registering to 0.1 second. Two viscometers, an Ostwald and a Cannon-Fenske type, were used. To guard against instrument error and to be sure that shear effects were not entering at higher concentrations, several of the more concentrated solutions were measured in both viscometers.

For a measurement, 5 ± 0.15 ml. was introduced into a viscometer and the amount weighed. The exact volume at the temperature of measurement was calculated from the density. Use of a weighed amount of solution was necessary to ensure sufficient precision. Because the volume, especially at high concentrations, was rarely accurately 5 ml., it was corrected to 5.00 ml. by a calibration curve prepared for each viscometer. The correction for a difference of 0.15 ml. never amounted to more than 0.8% of the flow time. Viscometers were calibrated to correct for turbulent flow and drainage using water, and 20 and 40% sucrose[11] solutions as standards.

Sucrose solutions were prepared by weight and their concentrations checked by measurement of the index of refraction. Viscosity values for sucrose solutions were taken from the work of Bingham and Jackson.[12]

The calibration equation was assumed to be of the form

$$\eta/d = At - B/t$$

where t is the flow time, d is density and η is absolute viscosity in centipoise.

(1) H. S. Harned and B. B. Owen, "The Physical Chemistry of Electrolyte Solutions," 1st Ed., Reinhold Publ. Corp., New York, N. Y., 1943, p. 259.

(2) A. F. Scott, THIS JOURNAL, **35**, 3379 (1931).

(3) R. H. Stokes and R. A. Robinson, *J. Am. Chem. Soc.*, **70**, 1870 (1948).

(4) J. S. Rowlinson and C. F. Curtiss, *J. Chem. Phys.*, **19**, 1519 (1951).

(5) J. H. Hildebrand, *Disc. Faraday Soc.*, **15**, 9 (1953).

(6) M. Duttra, *Proc. Natl. Inst. Sci. India*, **19**, 183 (1953).

(7) S. Gladstone, K. J. Laidler and H. Eyring, "The Theory of Rate Processes," McGraw-Hill Book Co., New York, N. Y., 1941, 1st Edition.

(8) A. N. Campbell and E. M. Kartzmark, *Can. J. Chem.*, **30**, 128 (1952).

(9) A. N. Campbell, A. P. Gray and E. M. Kartzmark, *ibid.*, **31**, 617 (1953).

(10) M. L. Miller and C. L. Sheridan, THIS JOURNAL, **60**, 184 (1956).

(11) Glycerol solutions, commonly recommended as calibrating liquids, proved too hygroscopic.

(12) E. C. Bingham and R. F. Jackson, *Bull. Bur. Stds.*, **14**, 59 (1918-19).

Temperature Control.—The temperature at 0° was maintained by a well-stirred ice-bath. At 29.87° a thermostat regulated to 29.87 ± 0.02°, as measured by a platinum resistance thermometer calibrated at the National Bureau of Standards, was used. The temperature of the 50° bath was measured on a mercury thermometer also calibrated at the National Bureau of Standards.

Density Measurements.—Density values over the wide concentration and temperature range needed in this work are available for sodium iodide only.[13,14] They had to be determined for sodium perchlorate[15] and sodium thiocyanate.

Densities were measured with both 10- and 25-ml. pycnometers using standard procedures. They are precise to ±0.0005 density unit. This is more than adequate for the purpose at hand.

III. Results

The densities of sodium thiocyanate and sodium perchlorate are represented by the Masson equation as shown below

For NaSCN to nearly saturation at

0°
$$d = 0.9999 + 0.04823N - 0.003472N^{3/2} \quad \sigma = 0.0004$$
29.87°
$$d = 0.9957 + 0.04137N - 0.001600N^{3/2} \quad \sigma = 0.0005$$
50.1°
$$d = 0.9880 + 0.03857N - 0.000861N^{3/2} \quad \sigma = 0.0005$$

An alternative equation at 50.1° is

$$d = 0.9880 + 0.03778N - 0.0002084N^2 \quad \sigma = 0.0002$$

For NaClO$_4$ through and including 60% solution, at 0°

$$d = 0.9999 + 0.08749N - 0.00422N^{3/2} \quad \sigma = 0.0007$$
29.87°
$$d = 0.9957 + 0.07919N - 0.00185N^{3/2} \quad \sigma = 0.0005_5$$
49.3°
$$d = 0.9884 + 0.07558N - 0.000883N^{3/2} \quad \sigma = 0.0003_5$$

N equals moles per liter at the temperature designated and σ is the average difference between observed and calculated densities.

The observed viscosities are shown in Fig. 1 and in Tables I, II and III.* Concentrations are expressed as moles per 1000 g. of solvent and viscosities as relative viscosities, i.e.

$$\frac{\text{Flow time of soln. (cor.)}}{\text{Flow time of water (cor.)}} \times \frac{\text{Density of soln.}}{\text{Density of water}}$$

It will be observed that at low and moderate concentrations, the relative viscosity, as is common with aqueous salt solutions is greater at 50° than at 0°. This means that the temperature coefficient of viscosity is less for the solution than for water.

At 5-6 N the relative viscosity curves for sodium thiocyanate, shown in Fig. 1, cross each other and fan out. Thereafter, the relative viscosity at 0° is greater than at 50°. The relative viscosity–concentration curves for sodium perchlorate and sodium iodide behave in much the same way. With sodium perchlorate, the relative viscosity–concentration curves at different temperatures (not shown) cross each

(13) W. Geffcken, Z. physik. Chem., **B5**, 81 (1929).

(14) (a) A. F. Scott and E. J. Durham, THIS JOURNAL, **34**, 1424 (1930); (b) A. F. Scott and W. R. Frazier, ibid., **31**, 459 (1927).

(15) The densities of Wirth and Collier (H. E. Wirth and F. N. Collier, Jr., J. Am. Chem. Soc., **72**, 5292 (1950)) cover only the range 0 to approximately 6 N at 25°.

* Tables I, II and III referred to in this paper may be obtained by ordering Document No. 4773, from the American Documentation Institute, Library of Congress, Washington 25, D. C., remitting in advance by check or money order $1.25 for microfilm or $1.25 for photoprint.
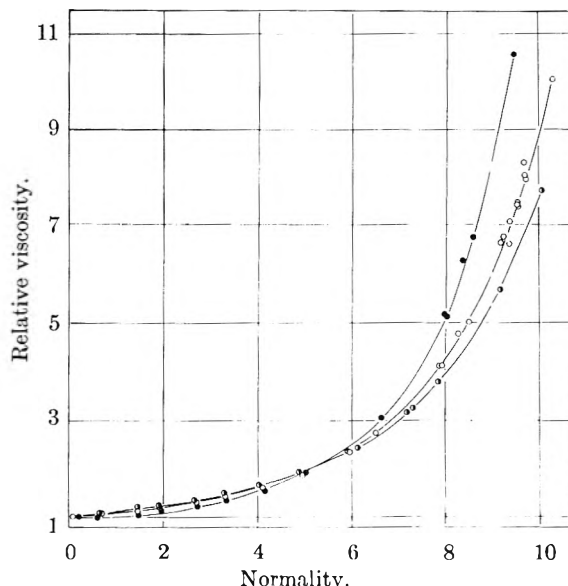
Fig. 1.—Relative viscosity of NaSCN solutions as a function of normality: ●, 0°; ○, 29.87°; ◑, 50.1.

other at 5-6 N. With sodium iodide this crossover is at 7-8 N. Examination of data in the literature shows that with lithium chloride the relative viscosity–concentration curves at different temperatures remain very close together from 8-11 N and do not fan out appreciably until around 13 N.[16] The measurements of Campbell and Kartzmark, and Campbell, Gray and Kartzmark[8,9] on two nitrates show that at saturation at 25 to 35° the relative viscosity–concentration curves of silver nitrate at different temperatures are approaching each other while those of ammonium nitrate are far apart.

IV. Discussion

Eyring[7] points out that since viscous flow can be thought of as a process in which a molecule jumps from a position which it is occupying into a hole, it can be treated as a rate process. Therefore, the absolute rate theory can be used to interpret viscosity (on pure liquids) and to compute free energies and entropies of activation for viscous flow. Similarly, we can, *in a purely formal way*, regard a solution of 1 N (or 2 N, 3 N, etc.) NaSCN as a single entity and compute over-all energies and entropies of activation for its viscous flow.

For unassociated liquids, the plots of ln η (where η is absolute viscosity) *versus* $1/T$ give straight lines from whose slope the energy of activation for viscous flow $\Delta E^{\ddagger}$ can be calculated, i.e.

$$\Delta E^{\ddagger} = R \left(\frac{d \ln \eta}{d(1/T)} \right)$$

For associated liquids, the plots of ln η *versus* $1/T$ are not linear, i.e., $\Delta E^{\ddagger}$ varies with temperature. In Fig. 2 ln η has been plotted against $1/T$ for sodium thiocyanate solutions at 0, 1, 2 . . . . . 10 N. Values for the viscosity at even normalities at each

temperature were obtained by interpolation in large plots of the type of Fig. 1. From the slopes read off the curves in Fig. 2 (and similar plots for sodium perchlorate and sodium iodide) values of $\Delta E^{\neq}$ have been obtained.
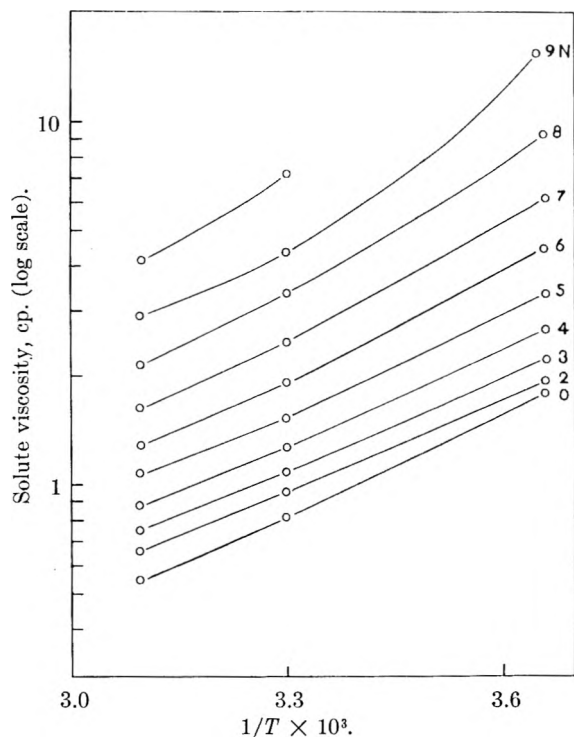
Fig. 2.—Temperature dependence of the viscosity of NaSCN solutions.

Values of the free energy of activation for viscous flow, $\Delta F^{\neq}$, have been computed from the equation[13]

$$\Delta F^{\neq} = RT \ln \frac{V \eta}{hL}$$

Here V is the molal volume of the moving unit, h is Planck's constant and L is Avogadro's number. V was computed from the density as an average value for the solution as a whole, assuming complete ionization.[17]

Assuming that the measured $\Delta E^{\neq}$ is identical with $\Delta H^{\neq}$, the heat of activation of viscous flow, the entropy of activation, $\Delta S^{\neq}$, can be computed from the relationship

$$\Delta F^{\neq} = \Delta H^{\neq} - T \Delta S^{\neq}$$

The values of $\Delta E^{\neq}$, $\Delta F^{\neq}$ and $\Delta S^{\neq}$ for the three salts under investigation are summarized in Table IV.

Examination of the figures in this table brings out some interesting relationships. In water there is a small entropy of activation of viscous flow, due to the necessity of breaking hydrogen bonds,[7] which is decreased by adding salt. With NaSCN, NaClO₄, and to a lesser extent with NaI the entropy of activation of viscous flow starts to rise around 6 N and increases rapidly with concentration. This entropy of activation can be visualized as resulting from the necessity for the disrup-

(17) If the number of moles of water in one liter of solution equals B and the number of moles of sodium ion plus moles of thiocyanate ion equals 2 N, then $V = 1000/(B + 2 N)$.

tion of some sort of short range local order in the solution before flow can take place.[18]

TABLE IV

FREE ENERGY, ENTROPY AND HEAT OF ACTIVATION OF VISCOUS FLOW

Salt	Moles per liter of soln., N	$\Delta F\ddagger$, kg. cal.	$\Delta H\ddagger$, kg. cal.	$\Delta S\ddagger$, e.u.
Water	0	2.17	3.89	5.7
NaSCN	2	2.27	3.63	4.5
	3	2.36	3.70	4.4
	4	2.46	3.70	4.1
	5	2.58	3.93	4.5
	6	2.72	4.12	4.6
	7	2.88	4.44	5.2
	8	3.08	4.78	5.6
	9	3.30	5.70	7.9
	10	3.55	8.18	15.3
NaClO₄	2	2.26	3.54	4.2
	3	2.34	3.67	4.4
	4	2.45	3.67	4.0
	5	2.59	3.71	3.7
	6	2.78	4.00	4.0
	7	2.97	4.68	5.6
	8	3.19	5.25	6.8
	9	3.45	8.70	17.3
	9.5	3.59	9.85	20.7
NaI	2	2.22	3.40	3.9
	3	2.28	3.55	4.2
	4	2.35	3.55	4.0
	5	2.46	3.65	3.9
	6	2.59	3.90	4.3
	7	2.75	4.32	5.2
	8	2.92	4.42	5.0
LiCl	10.75	3.38	4.68	4.3
	13	3.72	8.50	15.7

If order has to be destroyed before flow can take place in these highly concentrated solutions, this means order is present in them.

If the concentration at which the viscosity concentration curves cross each other is thought of as marking the concentration where this local ordering becomes significant, we can conclude that the larger the anion ($ClO_4^- > SCN^- > I^-$) the lower the concentration at which this order begins to manifest itself. With nitrates there is no evidence for this sort of order and with lithium chloride it does not appear until around 11 to 12 N.

Although the viscosity behavior of the concentrated salt solutions studied here can be interpreted as evidence for the existence of some sort of order, viscosity furnishes no clue as to whether this is ordering of the ions, analogous to molten salts, or ordering of the water, as in hydration.

The sign of the partial molal entropy of the constituents of the solution, calculated by the method

(18) Such order is not to be thought of as, in any sense, crystalline order. If the environment of any ion is observed over a long period of time, a high degree of local order in the arrangement of its neighbors would be observed and might extend over many ionic diameters but would not extend throughout the entire system as in a crystal. This order would be characterized by an alternate layering of plus and minus charges in the neighborhood of any positive ion and a corresponding alternate layering of minus and plus charges in the neighborhood of any negative ion.
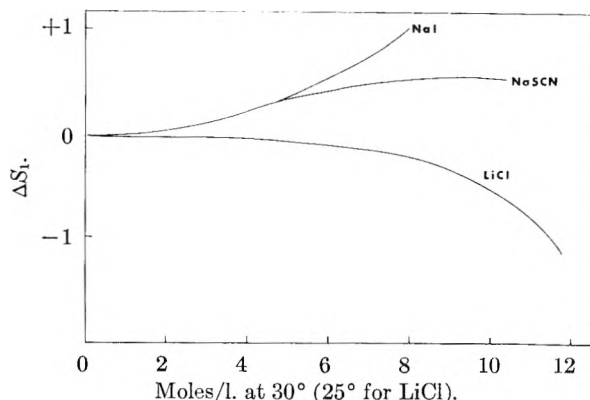
Fig. 3.—Excess partial molal entropy of water in concentrated salt solutions.

Fig. 4.—Excess partial molal entropy of salts in concentrated solutions.

of Frank and Robinson,[19] helps to decide between these two possibilities. To calculate the partial molal entropy of the constituents of the solutions, vapor pressures and heats of dilution are needed at high concentrations. Such data are available for sodium thiocyanate,[10,20] sodium iodide[10,20] and lithium chloride.[20] For sodium perchlorate the vapor pressures are available[10] but not the heats of dilution.

Following Frank and Robinson, the excess partial molal entropy of water $\Delta S_1^{\ddagger}$, and of salt, $\Delta S_2^{\ddagger}$, in solutions of sodium thiocyanate, sodium iodide and lithium chloride up to concentrations near saturation have been computed. These values for $\Delta S_2^{\ddagger}$ are plotted in Fig. 4. From this plot we see that for concentrated sodium thiocyanate solutions

(19) H. S. Frank and A. L. Robinson, *J. Chem. Phys.*, **8**, 933 (1940).

(20) F. D. Rossini, D. D. Wagman, W. H. Evans, S. Levine and I. Joffe, "Selected Values of Chemical Thermodynamic Properties," U. S. Dept. of Commerce, National Bureau of Standards, 1952.

$\Delta S_2^{\ddagger}$ is negative, indicating more order of the solute in concentrated solution than in the infinitely dilute reference solution. Sodium iodide behaves like sodium thiocyanate but to a lesser degree. This is consistent with its viscosity behavior. In contrast to these two salts, solutions of lithium chloride show a positive $\Delta S_2^{\ddagger}$ and a negative $\Delta S_1^{\ddagger}$. At 11 N. where the viscosity behavior began to show up some arrangement in the solution, the $\Delta S_1^{\ddagger}$ for water in the lithium chloride solution is rapidly becoming very negative. The little order in lithium chloride solutions at high concentrations is, therefore, associated with the solvent (hydrated lithium ion) while the more pronounced order in sodium perchlorate, sodium thiocyanate and sodium iodide solutions is associated for the most part with the solute.

Acknowledgment.—The authors are indebted to G. Yates for carrying out many of the density and viscosity measurements reported here.

CONCENTRATED SALT SOLUTIONS. III. ELECTRICAL CONDUCTANCE OF SOLUTIONS OF SODIUM THIOCYANATE, SODIUM IODIDE AND SODIUM PERCHLORATE

By M. L. MILLER

Contribution from the Stamford Laboratories, Research Division, American Cyanamid Company, Stamford, Conn.

The electrical conductance of solutions of sodium thiocyanate, sodium perchlorate and sodium iodide has been measured at 0, 30 and 50° from 1 N to saturation. At higher concentrations, the conductances of all three salts (all sodium salts) appear to be approaching a common limit. This suggests that as the concentration increases more and more of the current is being carried by the sodium ions. Comparison of the energy of activation for conductance with the energy of activation of viscous flow is consistent with this view.

I. Introduction

Preceding papers in this series[1,2] have reported measurements of the viscosity, density and vapor pressure of aqueous solutions of sodium thiocyanate, sodium perchlorate and sodium iodide from 1 N to saturation at 0, 30 and 50°. The present paper deals with the electrical conductivity over the same concentration and temperature range.

Although there is a very large amount of conductance data in the literature, there are very

few measurements on aqueous 1-1 salt solutions in the region above 8 N and fewer still at these high concentrations at two or more temperatures. There are the measurements of Campbell and Kartzmark[3] and Campbell, Gray and Kartzmark[4] at 25, 35 and 95° on silver nitrate and ammonium nitrate and some data on lithium chloride in "International Critical Tables."

(1) M. L. Miller and C. L. Sheridan, THIS JOURNAL, **60**, 184 (1956).
(2) M. L. Miller and M. Doran, *ibid.*, **60**, 186 (1956).

(3) A. N. Campbell and E. M. Kartzmark, *Canadian J. Chem.*, **30**, 128 (1952).
(4) A. N. Campbell, A. P. Gray and E. M. Kartzmark, *ibid.*. **31**, 617 (1953).
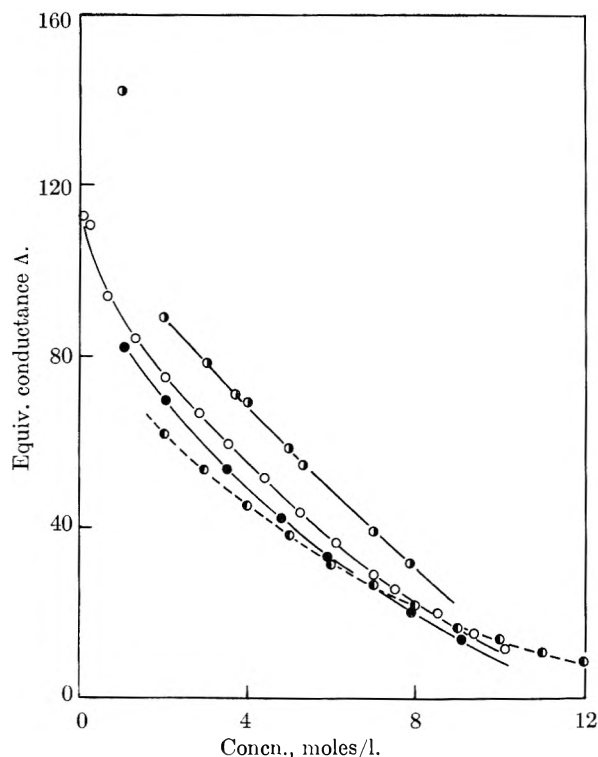
Fig. 1.—Equivalent conductance at 29.9°: ○, NaSCN; ●, NaClO₄; ◐, NaI; ◑, LiCl (25°).

Fig. 2.—Equivalent conductance at 0 and 50°: ○, NaSCN; ●, NaClO₄; ◐, NaI.

Conductance measurements on the three salts, sodium thiocyanate, sodium perchlorate and sodium iodide, show that as the concentration increases the equivalent conductances of all three salts, all of them sodium salts, are approaching a common limit. This limit is lower than the limit approached by lithium salts (if such a limit exists for lithium salts) and suggests that as the concentration increases the sodium ion is taking over more and more of the conductance.

This conclusion is consistent with measurements of self-diffusion in sodium thiocyanate solutions made in this Laboratory.[5]

The equivalent conductance viscosity product is remarkably constant considering the wide concentration range covered (from 0.2 to 18.7 m for sodium thiocyanate).

II. Method

1. **Solutions.**—Solutions were made up and assayed by methods already described.[1,2].

2. **Temperature.**—Conductance measurements were made in an oil-bath regulated to ±0.02°. The temperatures at 29.92° and at near 50° were checked against a thermometer calibrated by the National Bureau of Standards. At 0° the cell was immersed in a narrow rectangular trough of oil which had been precooled overnight in an ice-box. This oil trough was immersed in a large well-packed ice-bath. After the assembly came to temperature, 2–3 hours, the conductance remained constant indicating good temperature stability.

3. **Conductance. a. Bridge.**—Conductance was measured on the precision conductance bridge designed by E. E. Lineken.[6] It is a shielded, fixed ratio arm bridge with a modified Wagner grounding device similar to the apparatus described by Shedlovsky.[7] The precision of balancing was

(5) To be reported.

(6) Bound Brook Division of American Cyanamid Company, Bound Brook, New Jersey.

(7) T. Shedlovsky, *J. Am. Chem. Soc.*, **52**, 1793, 1806 (1930).
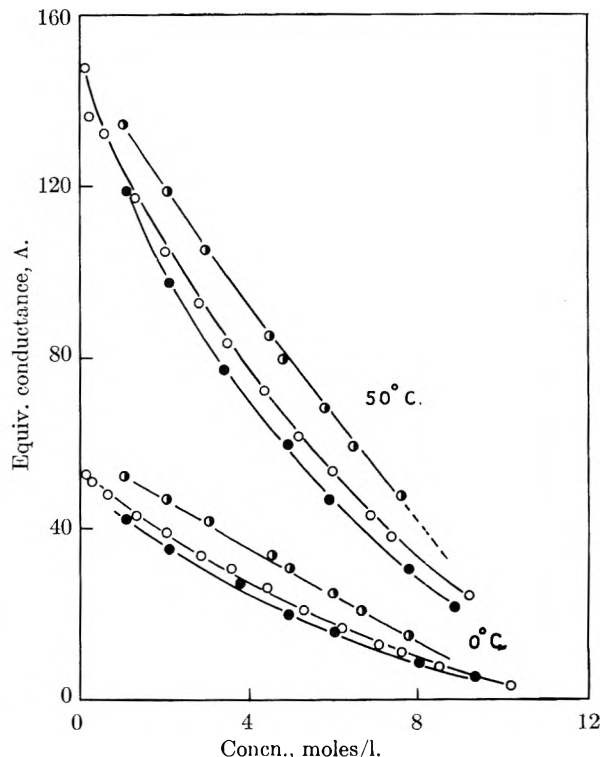
to better than four significant figures. A frequency of 1000 cycles was used in the measurements.

b.—Because of the high conductance of these concentrated solutions, it was necessary to use capillary cells. Two cells with different capillary diameters were used. They consisted of a length of capillary tubing about 13 cm. long with a capillary diameter about 1 mm. Since the cells were calibrated against KCl, it was not necessary to measure these dimensions. The capillaries were attached to J-tubes containing smooth platinum electrodes, by rubber stoppers. Because substantially all of the effective resistance was in the capillary, the positioning of the stopper was unimportant. Rubber is not attacked by the solutions used. Measurements with the two capillary cells used for most of the work agree, in general, to within 0.03%. A few of the more dilute preparations were measured in a conventional Washburn cell with platinized electrodes.

III. Data

The results are summarized in Tables I through IV which are self-explanatory.*

IV. Discussion

1. **Specific Conductance.**—The maximum in the specific conductance, κ, as the salt concentration is raised, is characteristic of electrolytes and has long been known. It is rather remarkable that, if we start with a cube of 10 N NaSCN, and replace part of the NaSCN (a conductor) with water (a non-conductor) the conductance of the cube goes up. This calls to mind some of the modern work on crystals where adding an impurity loosens the structure (produces vacancies) and increases the conductance.

2. **Equivalent Conductance.**—Figures 1 and 2 plot the equivalent conductance, Λ. The most

interesting thing about these plots is the fact that at each temperature the equivalent conductance curves of the three salts, *all of them sodium salts*, seem to be converging to a common limit. Examination of conductance data on lithium chloride in "International Critical Tables" indicates that the common limit to which the conductance of the sodium salts is converging is below that for the lithium salts (if such a limit exists for lithium salts). This suggests that in these concentrated sodium salts more and more of the current is being carried by a common unit, the sodium ion. If we accept the idea that these very concentrated aqueous salt solutions exhibit quasicrystalline local order, this is not unreasonable. Confirmation of this interpretation could be obtained by measuring transference numbers in very concentrated salt solutions.

3. Equivalent Conductance Viscosity Product. —Walden's rule states that the equivalent conductance viscosity product, $\Lambda\eta$, for an ion or salt is approximately constant and independent of solvent and temperature. This relationship follows directly from Eyring's absolute rate theory,[8] *if viscosity and conductance proceed by the same mechanism.* This can be seen if, *in a purely formal way we write*, Λ for a 1-1 salt as[9]

$$\Lambda = \frac{V_c^{2/3}F^2}{RT} e^{-\Delta F_c^{\ddagger}/RT} \qquad (1)$$

where F is the faraday, V_c the volume of the moving unit and $\Delta F_c^{\ddagger}$ the free energy of activation for conductance. In a similar way, viscosity can be written as

$$\eta = \frac{hN}{V_v} e^{\Delta F_v^{\ddagger}/RT} \qquad (2)$$

where $\Delta F_v^{\ddagger}$ is the free energy of activation for viscous flow, V_v is the volume of the moving unit and N is Avogadro's number. Thus, if the free energy and the moving units are the same in both processes

$$\eta\Lambda = F^2 hN/RTV^{1/3} \qquad (3)$$

The values of $\Lambda\eta$ for sodium thiocyanate solution at different concentrations are shown in Fig. 3. Plots for sodium iodide and sodium perchlorate are so similar that they have not been included. The small spread in the $\Lambda\eta$ values considering the wide concentration range is surprising. Nevertheless, the observed variations are much greater than experimental error and follow consistent trends. This could be a result of oversimplification in the formalized treatment or it could mean that either the assumptions that $V_c = V_v$ or $\Delta F_c^{\ddagger} = \Delta F_v^{\ddagger}$ (or both) are breaking down.

The drop in $\Lambda\eta$ with concentration in the early part of the curves in Fig. 2 can be attributed to an increase in the volume of the moving unit as the concentration of salt is increased since volume occurs in the denominator of equation 3.

The rise in $\Lambda\eta$ from 6 N is less easily dealt with.

(8) S. Glasstone, K. J. Laidler and H. Eyring, "The Theory of Rate Processes," McGraw–Hill Book Co., New York, N. Y., 1941, 1st Edition.

(9) It is to be understood that the expressions in equation 1 and 2 are purely formal. Strictly speaking, the right-hand side of each should be replaced by a sum of terms referring to the anion, the cation and the solvent, together with interaction terms.
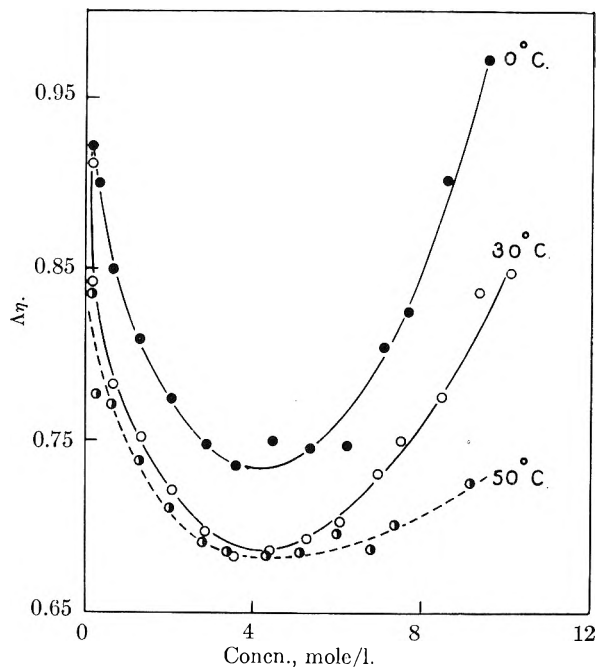
Fig. 3.—Equivalent conductance viscosity product for NaSCN: ○, 29.92°; ●, 0.0°; ◑, 52.25°.

It could mean that in this region viscosity and conductance are proceeding by different mechanisms.

If as the curves in Fig. 1 lead us to suspect, this is the region where the sodium ion is taking over more and more of the conductance as the concentration increases this fact is sufficient to account for the rise in $\Lambda\eta$ since in viscous flow both ions must be moving together.

The dependence of $\Lambda\eta$ on temperature is, of course, implicit in equation 3.

4. Energy of Activation of Conductance.—If viscous flow and conductance proceed by a different mechanism at high concentrations, this fact should show up in differences in the energy of activation.

We have, therefore calculated $\Delta H_c^{\ddagger}$ the heat of activation for the conductance of sodium thiocyanate sodium perchlorate and sodium iodide at 30° from the slopes of plots of ln Λ against $1/T$.

Values of $\Delta H_c^{\ddagger}$ at 30° are given in Table V. This table also includes, for comparison, values of $\Delta H_v^{\ddagger}$ the heat of activation of viscous flow at 30°. This last quantity was taken from a previous study.[2]

TABLE V

ENERGY OF ACTIVATION FOR DIFFERENT SALTS

	NaSCN		NaClO₄		NaI	
Salt/N	$\Delta H_c^{\ddagger}$	$\Delta H_v^{\ddagger}$	$\Delta H_c^{\ddagger}$	$\Delta H_v^{\ddagger}$	$\Delta H_c^{\ddagger}$	$\Delta H_v^{\ddagger}$
2	3.64	3.63	3.64	3.54	3.64	3.40
3	3.64	3.70	3.74	3.67	3.64	3.55
4	2.64	3.70	3.84	3.67	3.64	3.55
5	3.84	3.93	4.04	3.71	3.74	3.65
6	3.84	4.12	4.04	4.00	3.84	3.90
7	4.00	4.44	4.19	4.68	3.94	4.32
8	4.55	4.78	4.56	5.25	4.04	4.42
9	4.88	5.70	4.77	8.70	...	...
10	5.10	8.18	5.20	9.85	...	...

It will be seen from this table that through 5 to 6 N $\Delta H_c^{\ddagger} = \Delta H_v^{\ddagger}$. In this region conductance and viscosity may, therefore, be proceeding by the same

mechanism. At higher concentrations $\Delta H_v{}^{\ddagger}$ rises faster than $\Delta H_c{}^{\ddagger}$. Previous work has shown[2] that at these concentrations there is a relatively high positive entropy of activation of viscous flow which we have interpreted as evidence for the presence of short range local order.

Viscous flow would have to disturb the whole structure while conductance could avoid disturbing the arrangement of the big anions if it shifted more and more to cationic conductance. Therefore, conductance would not be expected to have as high an entropy of activation as viscosity.

THE DECOMPOSITION OF HYPONITRITES OF CALCIUM AND STRONTIUM

By Trambaklal Mohanlal Oza and Vasantrai Trambaklal Oza

The Inorganic and Physical Chemistry Laboratory, The M.R. Science Institute, Gujarat College, Ahmedabad, and The Institute of Science, Bombay, India

The decomposition of SrN_2O_2 and $CaN_2O_2 \cdot H_2O$ is studied by the application of heat and by exposure to carbon dioxide. The thermal decomposition products are similar to those of $SrN_2O_2 \cdot 5H_2O$ and $CaN_2O_2 \cdot 4H_2O$, respectively. The effect of carbon dioxide varies with the salt and the dryness of the sample. The results suggest that reactions (1) $MN_2O_2 = MO + N_2O$ (1) and $3MN_2O_2 = 2MO + M(NO_2)_2 + 2N_2$ (2), which appear to be simultaneous, are the characteristic reactions of the decomposition.

In a previous study we investigated the thermal decomposition of calcium hyponitrite tetrahydrate[1]; this work was undertaken to determine the role of water in the decomposition. Sodium hyponitrite which decomposes *in vacuo* at about 300°, produces no nitrous oxide[2-4] whereas the pentahydrate under the same conditions produces nitrous oxide.[1] Carbon dioxide displaces nitrous oxide almost quantitatively from sodium hyponitrite[3] and in the presence of water nitrous oxide is formed from the anhydrous salt.[4] The fact that carbon dioxide decomposes barium hyponitrite has been reported by Kirschner.[5]

The present paper describes (a) the decomposition of anhydrous strontium hyponitrite and of calcium hyponitrite monohydrate and (b) the action of carbon dioxide on the hydrates of these salts.

Our results indicate that the state of hydration of the hyponitrite has little influence on the nature of the decomposition products, but that the relative amounts of these products are affected by the conditions of the decomposition. Carbon dioxide acts on the hyponitrites to a variable extent, but it may have no effect, if the salt has been intensively dried.

Experimental

Materials.—Strontium hyponitrite pentahydrate was prepared according to Partington and Shah[4]; dehydration *in vacuo* at 150° for 0.5 hour gave the anhydrous salt.

Anal. Calcd. for $SrN_2O_2 \cdot 5H_2O$: H_2O, 37.8; Sr, 59.4; N, 18.97. Found: H_2O, 38.6; Sr, 59.47; N, 19.08.

Calcium hyponitrite monohydrate precipitated when calcium nitrate dissolved in absolute alcohol was mixed with $Na_2N_2O_2 \cdot 5H_2O$ in a drop of water in the cold; the precipitate was washed with alcohol and ether, and dried in a vacuum desiccator.

Anal. Calcd. for $CaN_2O_2 \cdot H_2O$: Ca, 35.28; N, 23.73. Found: Ca, 35.4; N, 23.75.

Like the tetrahydrate, the substance could not be dehydrated without decomposition.

Analyses.—The gases from all the experiments and the residue from the calcium salt were analyzed as described in Oza and Oza.[1] The residue of the strontium salt was

tested only for nitrate by the phenolsulfonic acid reagent; nitrate was found absent in all experiments.

Table I shows that the dehydration of strontium hyponitrite for various periods of time has no influence on the products of the decomposition. The gas evolved consisted of a fairly constant mixture of nitrous oxide and nitrogen; no nitric oxide was present. The hydrated salt[6] gave similar results. From the last column of the table it is evident that the decomposition residue contained little hyponitrite.[7]

Table I

Decomposition of SrN_2O_2 at 300 in 0.5 Hr. after Dehydration by Exposure to P_2O_5 *in vacuo* at 150° for Varying Periods

Expt. no.	Mass, g.	Time of exposure to P_2O_5, hr.	Evolved gas, ml.			Gas evolved on treatment of residue with water, ml.[a]
			Total	N_2O	N_2	
1	0.1050	1	6.4	62.5	37.5	0.4
2	.1075	2	6.6	59.1	40.9	0.5
3	.1089	3	7.0	60.0	40.0	0.5
4	.1200	4	8.9	66.3	33.7	0.7

[a] The gas was absorbed in cold alcohol.

As in the case of the tetrahydrate, the quantity of the calcium hyponitrite monohydrate decomposed has a similar effect on the gas evolved (Table II).

In the experiments summarized in Table III, the salts, which were coated on glass beads to increase the surface, were exposed to carbon dioxide in an evacuated apparatus. The gas, which was pumped off through potassium hydroxide, was analyzed after removal of the carbon dioxide. The quantity of gas evolved, which was low with the ordinary dry calcium salt, was appreciable with the moistened salt. Under identical conditions exposure to carbon dioxide caused almost quantitative displacement of nitrous oxide from the dry sodium salt; when, however, the sodium salt was intensively dried *in vacuo* over P_2O_5 in the system for 24 hours prior to exposure to dry carbon dioxide, the effect was slight.

In general it has been reported that dry carbon dioxide[2,4,8] or dry air[9] has little effect upon dry hyponitrite salts, but that they are slowly converted to the carbonate upon exposure to air.[2,4,5,10]

(1) T. M. Oza and V. T. Oza, *J. Chem. Soc.*, 909 (1953).
(2) E. Divers, *ibid.*, **47**, 97 (1899).
(3) T. M. Oza, *J. Ind. Chem. Soc.*, **21**, 71 (1944).
(4) J. R. Partington and C. C. Shah, *J. Chem. Soc.*, 2071 (1931).
(5) A. Kirschner, *Z. anorg. Chem.*, **16**, 424 (1898).

(6) T. M. Oza and S. A. Patel, *J. Ind. Chem. Soc.*, **31**, 523 (1954).
(7) T. M. Oza, V. T. Oza and N. L. Dipali, *ibid.*, **28**, 15 (1951).
(8) A. Thum, Inaug. Diss. Prague, 1893.
(9) J. R. Partington and C. C. Shah, *J. Chem. Soc.*, 2589 (1932).
(10) W. Zorn, "Die Untersalpetrigsaure und deren Organischen Derivate," Heidelberg, 1879.

TABLE II

DECOMPOSITION OF $CaN_2O_2 \cdot H_2O$ IN STAGES

Expt. no.	Mass, g.	Residue, g.			Gas evolved[a,b] 1st stage				2nd stage				3rd stage			
		$Ca(NO_2)_2$	CaO	$Ca(NO_3)_2$	Total	NO	N_2O	N_2	Total	NO	N_2O	N_2	Total	NO	N_2O	N_2
5	0.1000				18.9	2.4	9.2	5.3								
						(14.0)	(54.4)	(31.5)								
6	0.1599				5.3	0.8	2.4	2.1	6.05	0.7	2.8	2.5	15.4	1.5	10.1	3.8
						(15.1)	(45.3)	(39.6)		(11.6)	(46.3)	(41.3)		(9.7)	(65.5)	(24.7)
7	0.2170	0.00495	0.0881	0.0460	14.5	1.55	7.2	5.3	8.5	0.6	6.0	1.9	11.2	0.8	7.8	2.6
		(3.7 × 10⁻⁵)	(5.2 × 10⁻⁴)	(2.0 × 10⁻⁴)		(10.7)	(50.0)	(39.3)		(7.0)	(70.0)	(23.0)		(7.1)	(70.0)	(23.0)

[a] Parentheses give g. mol. or percentages.   [b] The gas was collected as formed in three consecutive lots.

TABLE III

EXPOSURE OF HYPONITRITES TO CARBON DIOXIDE IN EVACUATED SYSTEM

Expt. no.	Hyponitrite, g.		Condition of hypo-nitrite	Evolved gas,[a] ml.
8	$CaN_2O_2 \cdot 4H_2O$	0.0500	Dry	0.7
9	$CaN_2O_2 \cdot 4H_2O$	.0500	Moist	1.6
10	$Na_2N_2O_2$	.0192	Dry	4.1
11	$Na_2N_2O_2$	.0730	Carefully dried	0.4
12	$SrN_2O_2 \cdot 5H_2O$	.1025	Dry	3.8

[a] The gas was absorbed in cold alcohol.

Discussion

These results show that the production of nitrous oxide and nitrogen during decomposition is characteristic of hyponitrites. Their production, in the case of the anhydrous salt, may be due to the reaction

$$CaN_2O_2 = CaO + N_2O \qquad (1)$$

and

$$3CaN_2O_2 = 2CaO + Ca(NO_2)_2 + 2N_2 \qquad (2)$$

which may be simultaneous, for the products of the one reaction are not likely to affect the course of the other. In the case of the anhydrous sodium salt, reaction (2) is almost quantitative, while (1) is absent[2-4]; the hydrated sodium salt decomposes according to both reactions.[1] Although nitrous oxide is not produced during the decomposition of anhydrous sodium hyponitrite, it is formed in the presence of carbon dioxide and water.[4] In the case of the calcium salt this effect of carbon dioxide and water is not completely absent (Table III). The production of nitric oxide from the calcium salt has been shown[1,6] to arise from the decomposition of the nitrite, produced as in (2), with the simultaneous formation of nitrate; our observation that in the case of the strontium salt, neither nitrate nor nitric oxide were detected supports this mechanism. The decomposition of hyponitrous

acid[11,12] is similar to that of calcium hyponitrite; the nitric oxide and nitric acid found can arise from the decomposition of nitrous acid formed by a reaction similar to (2). Nitric acid is also a product of the reaction of acids with the hyponitrites of the alkali and alkaline earths; presumably the first step is the formation of hyponitrous acid which then decomposes as described above.

Thus, equations 1 and 2 seem to represent characteristic reactions of hyponitrites and hyponitrous acid undergoing decomposition. As carbon dioxide is isosteric with nitrous oxide, it can displace the latter if the conditions permit.

The variations in the proportions of nitrous oxide and nitrogen observed at various stages of the decompositions must depend on the structure of the decomposing substance. The formation of the observed decomposition products cannot be explained in terms of the structure of hyponitrous acid as usually represented,[13] HO–N:N–OH, and if the cleavage is assumed to occur at the double bond, the formation of even nitrous oxide and water is not satisfactorily explained. The formation of the nitrite, the oxide and nitrogen becomes explicable if it is assumed that the hyponitrous acid molecule exists in more than one form and that one or the other form may dominate depending on the conditions.

The existence of hyponitrites in more than one form was postulated by Ray.[14,15] At present two forms of oxyhyponitrites are known,[13] the α-oxyhyponitrite and the β-oxyhyponitrite of sodium.

(11) A. Hantzsch and L. Kaufmann, Ann., 292, 317 (1896).

(12) P. C. Ray and A. C. Ganguli, J. Chem. Soc., 91, 1866 (1907).

(13) C. C. Addison, G. A. Gamlen and R. Thompson, ibid., 338 (1952).

(14) P. C. Ray, ibid., 71, 1194, 349 (1897).

(15) P. C. Ray and A. C. Ganguli, ibid., 91, 1399 (1907).

THE EFFECT OF SURFACE COVERAGE ON THE SPECTRA OF CHEMISORBED CO[1]

By R. P. Eischens, S. A. Francis and W. A. Pliskin

Beacon Laboratories, The Texas Company, Beacon, New York

Received July 8, 1955

An *in situ* cell was constructed and modifications made in a spectrometer so that the infrared spectra of chemisorbed molecules could be obtained over a wide range of sample temperatures and gas pressures. The effect of varying the surface coverage was studied for carbon monoxide chemisorbed on silica-supported Pd, Ni and Pt. The spectra of carbon monoxide on Ni and Pd showed an increase in the number of bands with increasing surface coverage indicating that these samples were heterogeneous. The changes in the spectra of $C^{12}O$ and $C^{13}O$ on Pt which are observed as the surface coverage is varied are attributed to interaction effects.

Introduction

Many fundamental catalyst studies have been concerned with determining the reason for the generally observed decrease in heat of chemisorption as surface coverage increases. Attempts have been made to explain this phenomenon on the basis of surface heterogeneity,[2] repulsive interactions between adsorbed atoms[3] and changes in work function of the adsorbent surface induced by the adsorbed gas.[4] Observation of the effect of surface coverage on the infrared spectra of chemisorbed carbon monoxide provides a new method of attack on this problem.

Some pertinent information can be obtained from the number of bands in the spectra at a single stage of surface coverage as shown in the original spectra of chemisorbed CO.[5] However, these single stage spectra do not reveal the relative strength of bonding for the chemisorbed CO contributing to each band or the effect of interaction on the band positions. To obtain this information the spectra of chemisorbed CO were studied as a function of surface coverage over silica-supported Pt, Pd and Ni. Isotope shift data were also obtained using chemisorbed $C^{13}O$.

In order to carry out this work efficiently it was necessary to design apparatus in which the infrared spectra could be obtained while the samples were subjected to a wide range of temperatures and pressures. Successful development of this *in situ* apparatus not only makes it possible to study the effect of surface coverage but also opens the way to infrared studies of chemisorbed molecules while reactions are in progress.

Experimental Method

In Situ Cell.—The main difficulty in the design of an *in situ* cell is imposed by the limitation that the beam path cannot be obstructed by glass or other materials which are not transparent to infrared radiation. Windows of CaF_2 or other salts which pass infrared radiation in the wave length regions of primary interest must be sealed to the body of the cell. Ideally, this seal should be able to withstand high temperatures so that the entire cell can be baked out to remove residual gases. However, the salt plates crack easily under stress and it is difficult to match the thermal expansion of the salt with that of any material which is suitable for the body of the cell. Because of these diffi-

culties it was necessary to compromise on the design and construct a cell in which the salt-glass seal could be kept cool while the sample was heated.

The *in situ* cell is shown in Fig. 1. It has 50 mm. diameter CaF_2 windows, A, which are sealed to the cell body with glyptal resin. The sample, B, is supported inside a tungsten-wound quartz furnace, C, by a 25 mm. CaF_2 plate, D. A 35 mm. CaF_2 plate is used as a gas convection shield, E, to protect the top window from the hot gases rising from the furnace. The shield is not sealed to the cell so it can expand and contract freely with changes of temperature. The shield is not necessary at pressures lower than one cm. The sample temperature is measured by a Pt–Pt, Rh thermocouple, F, which has its junction, G, in a slot in the CaF_2 plate which supports the sample. The entire furnace can be lowered out of the cell for sample changing by opening the standard taper joint, H, which is sealed with Apiezon W wax, and disconnecting the clamps, L, which hold the heating wire leads, I. The cell is evacuated and gas admitted through J. It is held in place by clamps around J and K. The cell has been used at sample temperatures as high as 540° and it probably could go up to 800°. The CaF_2 windows are cooled with an air jet when the cell is used at high temperatures.

Modification of the Perkin–Elmer Spectrometer.—In the conventional Perkin–Elmer spectrometer the infrared beam travels horizontally when passing through the sample. The horizontal beam is a disadvantage when solid catalyst samples are used because the face of the salt plate holding the sample must be in a vertical position and it is difficult to keep the sample from falling off. Another disadvantage of the conventional spectrometer is that there is only a 4 in. space for the sample cell between the infrared source housing and the monochromator. This is not long enough to accommodate an *in situ* cell which requires that the salt windows be kept cool while the sample is heated.

To overcome these disadvantages a Perkin–Elmer spectrometer equivalent to Model 12C was modified by mounting an additional source unit containing globar, plane mirror and spherical mirror above the spectrometer. The beam travels downward vertically from the spherical mirror in the upper source unit and is focused on the sample at a point approximately midway between the upper and lower source units. A plane mirror making an angle of 45° with the horizontal bedplate of the spectrometer reflects the beam on to the spherical mirror in the lower source unit, after which the beam follows a normal path through the spectrometer. Changes in the optics associated with this modification make it possible to have a space of 10 in. for the *in situ* cell.

Preparation of Samples.—The preparation of samples used in this work was essentially the same as reported in the initial development of the technique for observing the infrared spectra of gases chemisorbed on metals.[5] The metals were dispersed by making pastes from solutions of metal salts and non-porous silica. The pastes were dried at room temperature and pressed manually into a thin layer on a 25 mm. CaF_2 plate. The sample thickness was of the order of 0.012 g./cm.[2] and the concentration of metal after reduction was 7.4–9.1% by weight.

The CaF_2 plate holding the sample was inserted into the quartz furnace and the cell assembled as shown in Fig. 1. The sample was dried under vacuum at temperatures in the 100–200° range and then reduced in H_2 at 200–350°.

Figure 2 is an electron micrograph of a silica-supported

(1) This paper was presented at the AAAS Conference on Catalysis and at the Ohio State University Symposium on Molecular Structure and Spectroscopy in June 1955.

(2) H. S. Taylor, This Journal, **30**, 145 (1926).

(3) J. K. Roberts, *Proc. Roy. Soc. (London),* **A152**, 445 (1935).

(4) M. Boudart, *J. Am. Chem. Soc.,* **74**, 3556 (1952).

(5) R. P. Eischens, W. A. Pliskin and S. A. Francis, *J. Chem. Phys.,* **22**, 1786 (1954).
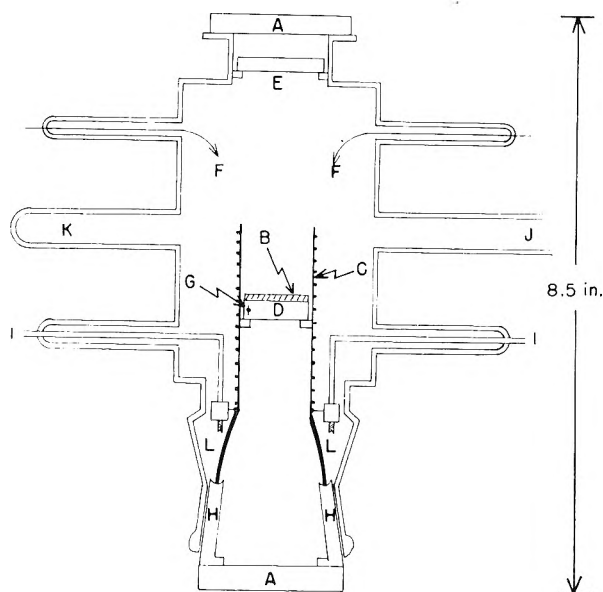
Fig. 1.—*In situ* cell for infrared study of chemisorbed gases.

Fig. 2.—Electron micrograph of platinum (9.1 wt. %) on Cab–O–Sil.

platinum sample.[6] This shows the platinum particles as dark spots dispersed on the lighter silica. These particles are too small to allow conclusions as to their shape. Direct measurement from the electron micrograph shows that the diameters of these particles fall in the range 40–100 Å. with an average of about 70 Å. Determination of the crystallite size by X-ray line broadening gave values of 80 and 90 Å. in two different trials[7]. At room temperature this sample chemisorbed 16.4 cc. of CO per gram of Pt. This corresponds to one molecule of CO for every seven atoms of Pt in the sample. If it is assumed that this result means that one out of seven Pt atoms is on the surface of the particles the particle size can be calculated. The assigned size will depend on the shape assumed for the particle and the crystal face exposed. If the particle is assumed to be a cube with (100) faces exposed the edge is calculated as 85 Å. Assumption of an octahedron with (111) faces exposed leads to a value of 105 Å. for the edges. The resolution of the electron microscope is not good enough to distinguish whether the Pt particles are spheres, cubes or octahedra. The agreement between the crystallite size determined by X-ray and the particle size determined by the electron micrograph and chemisorption measurements shows that the particles are single crystals. Single crystals of Pt would be either cubes or octahedra if they were large enough to be well formed. Since it is not known whether single crystals of this size would be well formed it is not possible to come to a firm conclusion regarding the shape of the particles. Extensive work has not been carried out to determine the nature of the Pd and Ni samples. It is assumed that they are similar to the Pt sample in that the metal is concentrated in small particles rather than being evenly distributed on the carrier surface.

The sample preparation is a critical step in obtaining spectra of chemisorbed CO. The basic problem is to obtain a sample which will transmit a usable amount of infrared radiation and which at the same time has sufficient area so that the absorption bands of the chemisorbed CO will be measurable. In the case of non-metallic adsorbents one can often work in a spectral region where the adsorbent is relatively transparent, so that satisfactory spectra can be obtained if the scattering losses are reduced by the use of small particles. However, metals absorb strongly in the infrared region, so there was considerable doubt when the work was started whether it was possible under any circumstances to obtain usable samples. This work has shown that satisfactory spectra can be obtained when metallic particles having dimensions of 100 Å. or less are dispersed in a medium consisting of non-porous spheres of silica having diameters in the 150–200 Å. range.

---

(6) This electron micrograph was obtained by H. M. Allred of this Laboratory.

(7) The X-ray work was done by P. H. Lewis of this Laboratory.
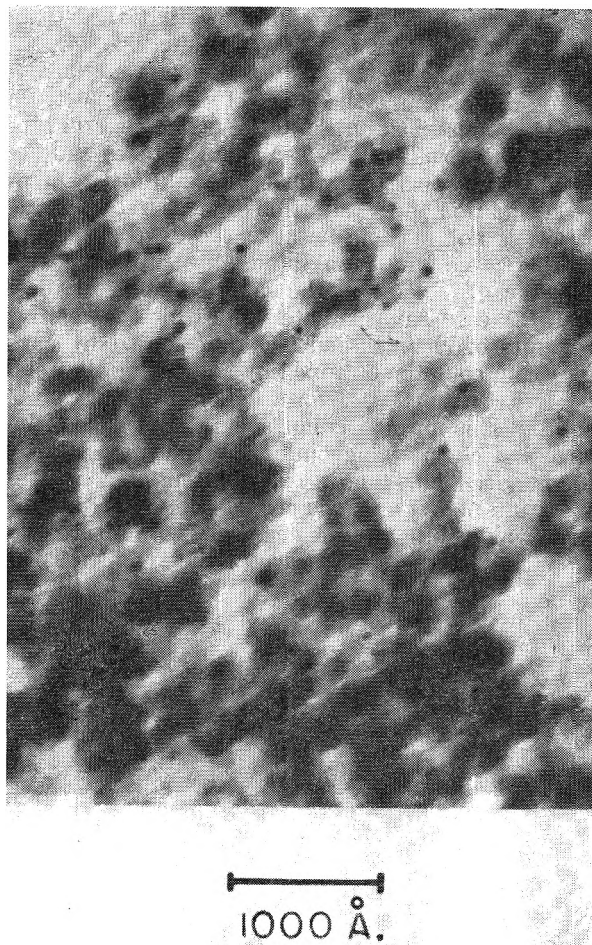
Recording of Spectra.—Spectra were obtained in the 2.5–7.5 μ region using a CaF_2 prism. The sample cell was left in the beam at all times and backgrounds were determined on either the oxidized or reduced samples. In most cases conditions were sufficiently stable so that reproducible background spectra could be obtained over a period of several hours, and even days in many cases. For the best samples the transmission near 5 μ with no chemisorbed CO was about 6%, although many samples were studied for which the transmission at this position was as low as 2%. Because of the low transmission of the samples slit widths of about 0.2 mm. were required at 5 μ in order to obtain a signal-to-noise ratio of about 200. The corresponding spectral slit width is about 0.02 μ.

Results and Discussion

Spectra of CO on Pd.—The spectrum of CO on Pd has more than one band and makes possible a study of surface heterogeneity based on the effect of fractional surface coverage, θ, on the rate of growth of the bands. Under equilibrium conditions if all of the bands increase at the same relative rate as θ increases, it would be known that the position of the band was not a function of bonding strength and that the factors which produce a multiple band spectrum are not related to surface heterogeneity. A difference in the growth rate would indicate that the surface was heterogeneous and that the first bands to appear were associated with the most strongly bonded CO. A third possibility is that an increase in θ would produce new bands coupled with the disappearance of bands formed at

low coverages. This would show that the structure of the chemisorbed CO was a function of θ.

Figure 3 shows the results of experiments designed to determine the effect of θ on the spectrum of CO chemisorbed on Pd at 25°. The general procedure was to add the CO in small batches and determine the spectrum after each addition. Direct determination of θ by addition of measured amounts of CO is not feasible because the dead space, including a volume in a liquid N_2 trap, is nearly 2,000 cc. (S.T.P.) and the sample chemisorbs less than 0.1 cc. Approximate values for the relative amounts of chemisorbed CO represented by each spectrum could be obtained by comparing the total integrated intensities of the bands for each spectrum. This method is not accurate because of interaction effects which influence the intensities of the bands. This factor will be discussed when the spectrum of CO on Pt is considered. Fortunately exact values of θ are not necessary to interpret the results when the spectra are of the type shown in Fig. 3.
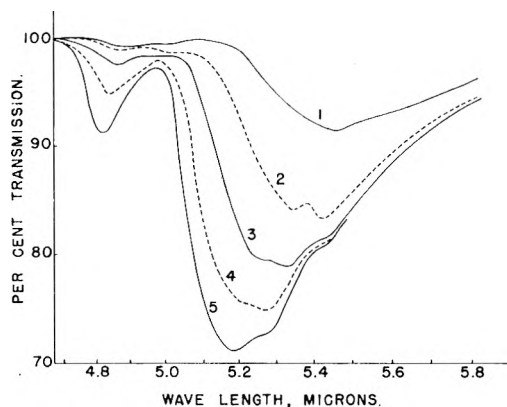
Fig. 3.—Spectra of CO chemisorbed on Pd as influenced by surface coverage with curves numbered according to increasing surface coverage.

Spectrum 1 shows that a band at 5.45 μ is the first to appear. In the second spectrum a band appears at 5.3 μ. New bands at 4.85 and 5.2 μ are evident in the third spectrum. These develop in the fourth and fifth spectra with the 4.85 μ band having proportionally more growth than the 5.2 μ band. Although there is some overlapping, it can be seen that the longer wave length bands are detectable first and in some cases may be complete before the shorter wave length bands are detectable. Evacuation removes the bands in the reverse order of their appearance.

The spectral evidence that the number of bands increases with surface coverage shows that the Pd surface is heterogeneous. This heterogeneity appears to be the type in which the surface is divided into a relatively few portions which differ from each other but which are relatively homogeneous within themselves. On this basis each band represents a homogeneous portion. It is plausible to identify these portions with the major crystal faces.

The spectra in Fig. 3 divide themselves into two parts with the region near 5 μ serving as the dividing line. In the spectra of metal carbonyls bands in the 4.8–5.0 μ region have been attributed to CO bonded through the carbon to single metal atoms.

Data are available for carbonyls of nickel,[8] iron,[9,10] cobalt,[11] manganese[12] and rhenium.[12] On this basis it appears that the 4.8–5.0 μ bands in the chemisorption spectra are due to CO bonded to a single surface atom. This structure will be referred to as linear CO. In the case of iron nonacarbonyl,[9] iron tetracarbonyl[10] and dicobaltoctacarbonyl[11] bands are also found in the 5.4–5.5 μ region and are assigned to CO bridged between two metal atoms, so it is reasonable to attribute the 5.4–5.5 μ bands in the chemisorption spectra to bridged CO. There is no previous experience on which to interpret the bands in the 5.0–5.4 μ region but the pattern of change produced by increasing surface coverage suggests that these bands should be assigned to bridged CO rather than to CO bonded to a single metal atom.[5] This interpretation implies that only the band at 4.83 μ in Fig. 3 is due to linear CO. This CO may be adsorbed on the single sites left vacant by the random pairing of the atoms adsorbing bridged CO.

The CO contributing to the 4.83 μ band is weakly held. The spectra in Fig. 3 represent an increase in pressure from 10^{-4} to 0.1 mm. The 4.83 μ band becomes more intense if the pressure is increased further. It is removed immediately if the pressure is reduced to 10^{-4} mm. The spectrum of CO on Pt also has a band near 4.83 μ. The CO contributing to this band is strongly bonded. This shows that the band position for linear CO on different metals is not a measure of the chemisorption bond strength.

The spectra of CO chemisorbed on Pd as well as the spectra discussed later of CO on Ni show that the positions of the bands due to bridged CO are sensitive to bond strength. Spectra of linear CO on Pd, Ni and Pt show little or no sensitivity of band position to bond strength. Since the closest distances between the metal atoms is the same on all major crystal faces of Pd (f.c.c.), the strength of bonding could affect the angle between the two metal–carbon bonds of bridged CO through variation in the length of the metal–carbon bond. There is some previous indication that the band position of bridged CO is sensitive to this angle.[9]

Spectra of CO on Ni.—The effect of decreasing θ on the spectrum of CO on Ni is shown in Fig. 4. Spectrum 1 was obtained at room temperature at a pressure of 0.1 mm., spectrum 2 after pumping at 10^{-4} mm. for 12 minutes and 3 after 2 hours and 25 minutes. When the pump-off rate at 25° became inconveniently slow the temperature was increased to 100° for 4 and 150° for 5.

The 5.0 μ region serves as a dividing line between bands due to linear and bridged CO as was observed with CO on Pd. The longer wave length bridged CO is the most strongly held. Spectrum 5 shows evidence of two bands in the short wave length region (<5.0 μ). In spectrum 1 the band at 4.82 μ

(8) B. L. Crawford, Jr., and P. C. Cross, *J. Chem. Phys.*, **6**, 525 (1938).

(9) R. K. Sheline and K. S. Pitzer, *J. Am. Chem. Soc.*, **72**, 1107 (1950).

(10) R. K. Sheline, *ibid.*, **73**, 1615 (1951).

(11) J. W. Cable, R. S. Nyholm and R. K. Sheline, *ibid.*, **76**, 3373 (1954).

(12) E. O. Brimm, M. A. Lynch, Jr., and W. Sesny, *ibid.*, **76**, 3831 (1954).
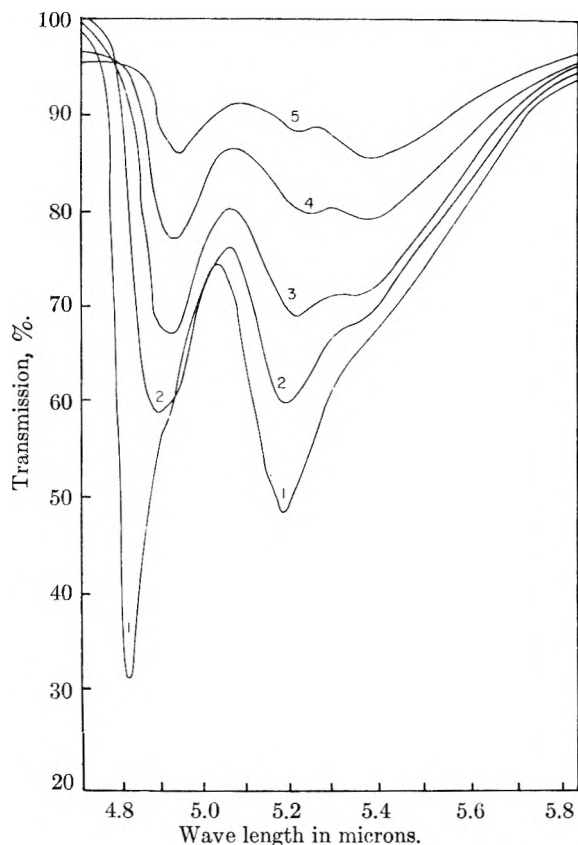
Fig. 4.—Effect of prolonged evacuation on spectra of CO chemisorbed on Ni with curves numbered according to decreasing surface coverage.

is the most intense while the 4.90 μ band is most intense at lower coverages. Addition of Ni(CO)$_4$ to the system produced a sharp band at 4.85$_3$ μ so neither of the two bands can be accounted for by assuming that nickel carbonyl was present on the surface. This point is substantiated by the fact that any nickel carbonyl which may have been formed would be expected to be frozen into the adjacent liquid nitrogen trap. The possibility that the 4.90 μ band results from a single CO on a Ni atom while the 4.82 band is due to more than one CO on a single atom was considered. Evidence for this would be provided if the 4.90 μ band increased with decreasing coverage. There is an indication that the 4.90 μ band is more intense in spectrum 2 than in spectrum 1. However, the bands are too close together to warrant a firm conclusion on this point so the possibility that the short wave length bands are sensitive to the strength of bonding cannot be ruled out in this case.

As the CO was removed by pumping at 100° a new band appeared at 4.56 μ. This band increased at 150° and disappeared at 300°. The significance of this band has not been established. High temperature work with CO on Ni is complicated by the fact that the Ni may be oxidized or carbided.

The evidence concerning surface heterogeneity indicated by the effect of θ on the spectrum of CO chemisorbed on Ni apparently is subject to the interpretation previously discussed for CO on Pd. It should be noted that the bands in Figs. 3 and 4 show a slight shift to shorter wave lengths as the amount of CO on the surface is increased. This shift

is attributed to interaction effects which will be discussed in connection with the spectrum of CO on Pt.

Spectra of CO on Pt.—The method of studying surface heterogeneity which was used for Pd and Ni is not applicable to Pt because the spectrum of CO on Pt has only one intense band and this band is in the short wave length region. Since it cannot be assumed that the wave length positions of bands due to linear CO are sensitive to variations in bond strength, no conclusion regarding the heterogeneity of the Pt is warranted from the fact that the spectrum shows only a single sharp band. To circumvent this difficulty surface coverage experiments were conducted with a mixture of C^{12}O and C^{13}O on the theory that the isotope shift (the displacement of the band caused by substitution of C^{13} for C^{12}) would provide information pertinent to the surface heterogeneity problem.

Figure 5 shows the spectrum of a chemisorbed mixture of C^{12}O and C^{13}O (ratio 1.7:1) at 25° with a pressure of 2 mm. It is assumed that under these conditions the Pt surface is fully covered with chemisorbed carbon monoxide. This assumption will be discussed later. The band near 4.82 μ is due to linear C^{12}O and the band at 4.97 μ is due to the corresponding structure for C^{13}O. There were no other bands although in some Pt samples a band near 5.4 μ, attributed to bridged CO, has been observed.[5]
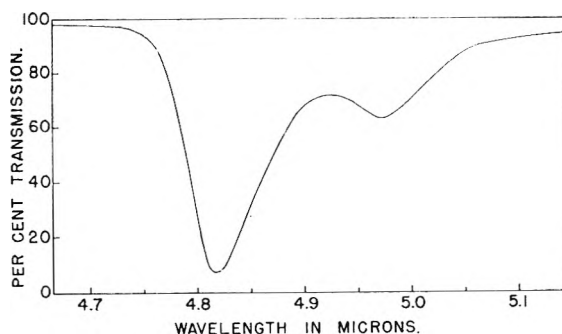
Fig. 5.—Spectrum of C^{12}O and C^{13}O chemisorbed on platinum.

It was expected that the isotope shift data would make possible the calculation of force constants for the metal–carbon and carbon–oxygen bonds. The force constant measures the resistance of the bond to change in length from its equilibrium value and an increase in the force constant is associated with an increase in bond strength. A theoretical treatment of the vibrations of the metal–C–O system was carried out. In this treatment it was assumed that the system was comparable to a linear XYZ type molecule,[13] but the mass of the metal was assumed to be infinitely large. Only the stretching vibrations were considered and interactions between the M–C and the C–O bonds were neglected. Theoretically the results of these calculations make it possible to relate the force constants to the ratio of the wave length positions of the chemisorbed C^{13}O and C^{12}O. These relations for the case where the chemisorbed C^{12}O band is near

(13) G. Herzberg, "Infrared and Raman Spectra," D. Van Nostrand Co. Inc., New York N. Y., p. 173.

TABLE I

Effect of Pumping on the $C^{12}O$ and $C^{13}O$ Bands of Carbon Monoxide

Total time,[a] hr.	Band positions, μ $C^{12}O$	$C^{13}O$	Isotope shift ratio	Absorbance[b] $C^{12}O$	$C^{13}O$	Ratio of absorbances[c]	θ[d]
0	4.842[e]	5.023	1.037	1.334	0.164	8.1	1.00
0.07	4.855	5.019	1.034	1.112	.188	5.8	0.93
0.83	4.871	5.019	1.030	0.826	.203	4.1	.77
2.0	4.875	5.018	1.029	.748	.206	3.6	.72
5.5	4.880	5.019	1.029	.637	.200	3.2	.66
9.1	4.884	5.022	1.028	.559	.185	3.0	.58
12.7	4.887	5.023	1.028	.498	.173	2.9	.52
21.2	4.889	5.021	1.027	.392	.149	2.6	.40
26.5	4.893	5.022	1.026	.318	.128	2.5	.32
29.9	4.893	5.019	1.026	.290	.117	2.5	.30
36.5	4.897	5.019	1.025	.231	.101	2.3	.24
45.5	4.896	5.017	1.025	.177	.078	2.3	.18
51.9	4.895	5.022	1.026	.139	.062	2.2	.14

[a] Cumulative pump-off time at 200° and 10^{-4} mm. pressure. At zero time CO pressure was 2 mm. [b] Absorbance = log transmission of background/transmission of sample. [c] Actual ratio of $C^{12}O$ to $C^{13}O$ was 1.7/1. [d] Values of θ were determined from a separate experiment in which the CO was burned off with O_2. [e] The reason for the 0.02 μ difference in this value of the wave length for the $C^{12}O$ band at full coverage and those shown in Figs. 5 and 8 has not been established.

4.83 μ, as is true when Pt is the adsorbent, are shown in Fig. 6. Although calculated for the 4.83 μ band these curves may be used over the range in position of this band which is observed experimentally for Pt without markedly affecting the conclusions. On the basis of the curves in Fig. 6 it would be expected that the isotope shift ratio would increase with increasing strength of bonding between the carbon monoxide and the Pt.
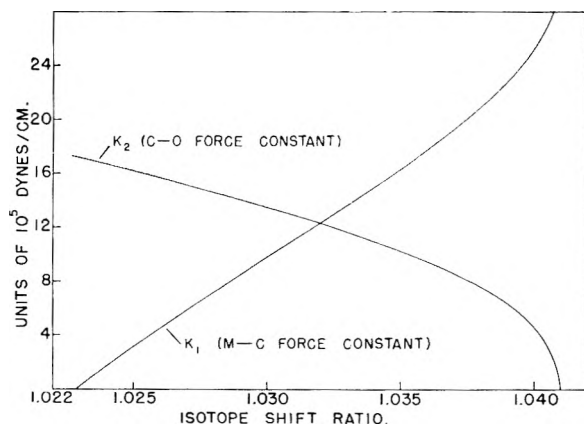
Fig. 6.—Calculated relations between force constants and isotope shift ratio for a 4.83 μ band of $C^{12}O$ chemisorbed on metals.

Table I gives the results of an experiment in which a chemisorbed mixture of $C^{12}O$ and $C^{13}O$ was pumped off at 200° over a period of two days. The following observations can be made from these data.

1. Initially the absorbance ratio for the $C^{12}O$ and $C^{13}O$ bands is much larger than the actual ratio of the numbers of $C^{12}O$ and $C^{13}O$ molecules. The ratio decreases with decreasing coverages to a value of 2.2 which is only slightly higher than the actual ratio of 1.7.

2. The absorbance of the $C^{12}O$ band decreases with time with the most rapid change occurring during the first five hours.

3. The absorbance of the $C^{13}O$ band increases during the first five hours and then decreases for the rest of the experiment.

4. The isotope shift ratio decreases rapidly dur-

ing the first five hours and then decreases slowly. The isotope shift changes are due to an increase in the wave length of the $C^{12}O$ band—the $C^{13}O$ band position remains constant, within the limits of experimental accuracy, during the entire experiment. The isotope shift value for low surface coverage is about 1.026.

The artificially high initial ratio of the absorbance, the increase in the absorbance for the $C^{13}O$, and the decrease in the isotope shift ratio show that it is not possible to treat the Pt–C–O system as an ordinary molecule as was done in the calculations leading to Fig. 6. Evidently it is the inability to assess the influence of the adsorbed molecules on each other that invalidates this approach. Despite the fact that the data in Fig. 6 cannot be used directly they are of critical importance in showing that the changes in the spectra of CO on Pt produced by varying θ are due to interaction effects rather than to surface heterogeneity.

If it is assumed that the interaction effects are negligible at low values of θ, Fig. 6 can be used to determine the order of the Pt–C and the C–O bonds. An isotope shift ratio of 1.026 indicates force constants of 4.5×10^5 dynes/cm. for the Pt–C bond and 16×10^5 dynes/cm. for the C–O bond. These values correspond to a single bond between the platinum and carbon and a triple bond between the carbon and oxygen.

Figure 7 shows kinetic data for the removal of chemisorbed CO from Pt at 10^{-4} mm. and 200°. The absorbances (log scale) for the $C^{12}O$ and $C^{13}O$ bands are plotted as a function of the pump-off time. After five hours good straight lines are obtained. If it is assumed that over the linear portion the absorbance is directly proportional to the amount of chemisorbed CO, this part of the curve indicates that the removal of chemisorbed CO follows the simple first-order rate law.

The deviation from the straight line could be due solely to changes in absorbance per molecule or to this effect plus an initially high rate of pump-off. Therefore Fig. 7 by itself is not sufficient to determine the range of θ over which the simple first-order rate law is followed.
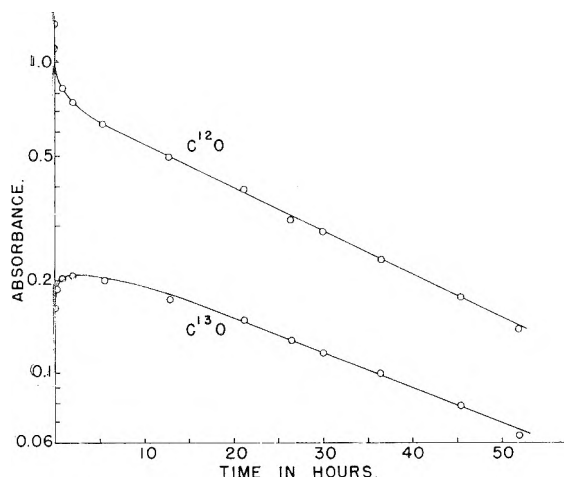
Fig. 7.—Effect of pumping time at 200° on the absorbance (log scale) of $C^{12}O$ and $C^{13}O$ chemisorbed on platinum.

Fig. 8.—Effect of surface coverage on the absorbance and wave length of $C^{12}O$ chemisorbed on platinum.

In order to get values for the absorbance and wave length positions of the bands as a function of θ, experiments were conducted in which the chemisorbed CO was removed by oxidation rather than by pumping. This was done by starting at full coverage and adding small batches of O_2 to convert the chemisorbed CO to CO_2 which could be removed from the system by freezing into a liquid nitrogen trap. After a batch of O_2 was added the reaction was followed with a thermocouple gage until the pressure fell to the level observed before the addition. The spectra were recorded after the reaction was complete. At 200° it required less than a minute to consume batches of O_2 sufficient to oxidize 10% of a monolayer.

Determination of the position and intensity of the bands corresponding to full coverage was a critical factor in this experiment. At 25° the band was not sensitive to pressure in the range 2 to 10^{-4} mm. From this it was assumed that complete coverage was attained at this temperature. In order to reach the state of full coverage it was necessary to expose the sample to a pressure of 2 mm. of CO at 200° for $1/2$ hour in order to ensure removal of chemisorbed O_2. After this treatment the temperature was lowered to 25° and the gaseous CO pumped off at 10^{-4} mm. The apparatus was then closed off and the temperature brought back up to the oxidation temperature. The increase in temperature decreased the band intensity and increased the gas pressure. The first batch of O_2 was evidently consumed in oxidizing the gaseous CO since the pressure was decreased to the pump-off value and there was no change in the band. This shows that at least 10% of the chemisorbed monolayer was desorbed while increasing the temperature from 25 to 200°.

Figure 8 shows the results of oxidation experiments at 200° in which normal CO was removed. In the first run the absorbances are indicated by triangles and the wave lengths by squares. In the second run the absorbances are indicated by filled circles and the wave lengths by open circles. The differences between these two runs will be discussed later. The wave length for the $C^{12}O$ band is shown on the right ordinate and the absorbance on the left. The horizontal portions of the curves start-

ing at $\theta = 1$ result from the fact that the part of the monolayer which has been desorbed in raising the temperature from 25 to 200° remains in the system. The curve is horizontal because the amount of chemisorbed CO does not change while the gaseous CO is being oxidized.
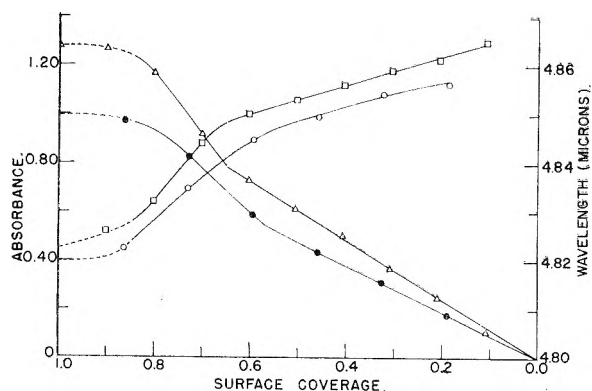
After the gaseous CO is used up, further addition of O_2 decreases the amount of chemisorbed CO. The θ values were calculated from the amount of O_2 required to remove the chemisorbed CO. It was assumed that no oxygen was permanently chemisorbed until the CO was removed. This assumption was based on the consideration that oxygen and CO could not be chemisorbed at the same time in an equilibrium state while the CO_2 was being removed from the system. In following the reaction by observation of the band intensities it was found that the decrease in intensity coincided with the decrease in pressure as measured by the thermocouple gage. There was no evidence for changes in band intensity after reaching the minimum pressure. This shows that the oxygen is not rapidly chemisorbed followed by a slow reaction between chemisorbed oxygen and chemisorbed CO. Attempts were made to follow the band intensity as a function of time after addition of O_2. At 200° the reaction was complete in a few seconds and was too fast to be followed quantitatively. A qualitative conclusion from this aspect of the work was that the reaction is slightly slower in the ranges $\theta = 1.0$–0.8 and 0.2–0 than it is in the middle range.

In Fig. 8 the absorbances and wave lengths are not a linear function of θ and the absorbance per molecule of adsorbed $C^{12}O$ is markedly increased above $\theta = 0.65$. This shows that at least part of the deviation from linearity in Fig. 7 is due to the increased absorbance per molecule of $C^{12}O$. When the absorbance values for a curve similar to Fig. 8, obtained by oxidation of the $C^{12}O$–$C^{13}O$ mixture, are applied to Fig. 7 it is concluded that the linear portion extends from a maximum of about $\theta = 0.66$ down to $\theta = 0.1$ (measurements below $\theta = 0.1$ are not reliable because of the small intensity of the bands).

By combining the information obtained from Figs. 7 and 8 it has been established that at least part of the deviation from linearity in Fig. 7 is due to a variation in the absorbance values. Further consideration leads to the conclusion that this is not the only factor and that an initially high rate of

pump-off is also important. This can be shown by plotting the logarithm of the θ values shown in Table I against the pump-off time. This curve is linear from the lowest coverages measured up to $\theta = 0.78$. The slope is much larger from $\theta = 0.78$ to $\theta = 1$. It is plausible to assume that the initial pump-off is high because the interaction effects are repulsive. Further study is required to determine the significance of the fact that the break in the absorbance vs. θ curve occurs near $\theta = 0.66$ while the break in the log θ vs. pump-off time occurs near $\theta = 0.78$.

Figure 8 presents data from two oxidation experiments which were run over the same sample. In order to explain the difference between these runs it is necessary to consider the sequence in which experiments were conducted on this sample. After the pump-off of the chemisorbed $C^{12}O$–$C^{13}O$ mixture at 200° (Fig. 7) the next experiment was an oxidation of the $C^{12}O$–$C^{13}O$ mixture at 200°. This was followed by the oxidation of normal CO at 200° which produced the curves indicated by the squares and triangles in Fig. 8. At this point an investigation of the effect of oxidation temperature was undertaken. Oxidation runs were carried out at 150, 175 and 250°. After the 250° run the sample which formerly chemisorbed 0.11 (S.T.P.) cc. of CO, as calculated from the amount of O_2 required to oxidize it, chemisorbed only 0.08 cc. The run indicated by the circles and filled circles in Fig. 8 was conducted after the 250° oxidation. Apparently oxidation at 250° produced a change in the Pt sample. It is unlikely that 250° would be high enough to affect the Pt and it is more reasonable to assume that the increased rate of oxidation caused localized overheating which was not indicated by the thermocouple.

The two runs in Fig. 8 follow the same general pattern. However, it appears that the break occurs at a lower value of θ (0.6 or 0.55) in the second run. If the decrease in the amount of chemisorbed CO from 0.11 cc. to 0.08 cc. was not accompanied by a decrease in Pt area so that the decrease of 0.03 cc. was due to leaving part of the surface uncovered, the break would shift to higher values of θ. This makes it appear that the decrease in the amount of chemisorbed CO is accompanied by a decrease in the Pt area, perhaps by redistribution of the exposed crystal faces.

The evidence presented here shows that the unusual spectral changes produced by changes in θ are due to interactions between chemisorbed molecules. These interactions produced changes in the wave length positions of the absorption bands and in the absorbance per molecule. These effects are most pronounced at values of $\theta > 0.66$. At coverages less than $\theta = 0.66$ interactions are also present but the effects are smaller in magnitude. Evidence for this is furnished by the changes in wave length position of the $C^{12}O$ band in Table I and in Fig. 8 and by changes in the $C^{12}O$–$C^{13}O$ absorbance ratio in Table I.

The fact that the interactions are most important at large values of θ indicates that they are not of the type which would result from changes in the work function of the surface.[4] It is believed that they

are of a type which can be expressed by the introduction of an interaction term between adjacent CO molecules in the potential energy expression.[14] This results in the coupling of the motions of adjacent molecules. In the case of two $C^{12}O$ molecules the results would be two new vibrational modes with the molecules vibrating in-phase in the high frequency mode and out-of-phase in the low frequency mode. Only the high frequency mode would be capable of absorbing infrared radiation. In the case of one $C^{12}O$ and one $C^{13}O$ molecule the coupling is less effective since their zero-order frequencies are different. The new modes would be an in-phase mode involving predominantly $C^{12}O$ at the higher frequency and an out-of-phase mode involving predominantly $C^{13}O$ at a lower frequency. The in-phase mode will have the higher intensity. It is believed that this type of picture can explain the effects of surface coverage on the spectra of CO on Pt and that these effects predominate over any surface heterogeneity effects. This type of interaction is expected to be most important at large values of θ. Experiments are planned in which the ratio of $C^{12}O$ and $C^{13}O$ will be varied over a wide range in order to test this hypothesis more fully.

Conclusions

The work reported here was designed to determine the relative importance of surface heterogeneity, interaction between adjacent molecules, and changes in the work function of the surface by a study of the infrared spectra of chemisorbed CO as a function of surface coverage. As a corollary to the stated objective the utility of the infrared technique as a tool for the study of metal surfaces was being evaluated.

The increase in the number of bands in the spectra of CO on Pd and Ni with increasing surface coverage shows that these samples are heterogeneous. However, there is no evidence for the type of heterogeneity which would result from a continuous distribution of bonding energies over the surface sites. The heterogeneity indicated by the spectra of CO on these metals is that in which the surface is divided into two or three major components which must be considered individually in the distribution of sites. Each component is subject to interaction effects. This behavior is similar to that expected from the exposure of more than one crystal face.

There is no evidence of either type of heterogeneity for the Pt sample. The changes in the spectra of chemisorbed CO observed upon variation of the surface coverage are due solely to interaction effects. These interactions are between adjacent adsorbed molecules since the effects are largest at large values of θ. There is no evidence for interaction effects of the type associated with changes in the work function of the surface.

In evaluating the infrared technique as a tool for studying the nature of metal surfaces it is evident that it has produced evidence which is novel and

(14) A similar explanation has been used by Decius for the effects of isotope substitution on the spectra of certain crystals: J. C. Decius, J. Chem. Phys., 22, 1941 (1954); 22, 1946 (1954).

informative. In some respects the evidence is conclusive and in others conflicting. Despite the latter difficulty it is clear that this technique will prove to be extremely important in the study of adsorption and catalysis.

THE RELATIONSHIP BETWEEN ADSORPTION KINETICS AND THE DEFECT SOLID STATE

By T. J. Gray and P. W. Darby

The New York State College of Ceramics at Alfred University, Alfred, New York

Received July 11, 1955

Whereas, the qualitative relationship between defect structure and catalysis is becoming more widely accepted, the fundamental problems which exist in establishing any exact correlation are not generally appreciated. An attempt is made to assess those relationships obtained at the surface of an oxide during adsorption and desorption of oxygen. Kinetics are developed and ambiguities discussed and assessed. The method of developing detailed kinetics from a study of variations in semi-conductivity is demonstrated.

Introduction

The early observations of the effect of the adsorption of gases on the semiconductivity of certain systems described by Dubar[1,2] have been extended to a systematic study of adsorption kinetics on various systems in the work of Gray and co-workers.[3-10] Other groups, particularly that of Anderson,[11-14] have studied similar effects, although not from the aspect of a kinetic study.

In developing the kinetic relationships certain fundamentals must be considered and it is at this stage that an initial difficulty of interpretation arises.

From the current theories relating to impurity semi-conduction it would appear that there should exist a relationship between the number of additional defects produced or destroyed in a semi-conducting medium during the adsorption of gas of suitable characteristics. From a statistical consideration it may be deduced that in a generalized form the number of free current carriers is related to the number of defects as

$$\frac{n(N - N_e + n)}{N_e - n} = V \left(\frac{2\pi mkT}{h^2}\right)^{3/2} e^{-E/kT} \quad (1)$$

after de Boer and van Geel[15] and Nijboer[16] where

(1) L. Dubar, *Compt. rend.*, **192**, 341 (1931).

(2) L. Dubar, *Ann. phys.*, **9**, 5 (1938).

(3) T. J. Gray, *Nature*, **162**, 260 (1948).

(4) W. E. Garner, T. J. Gray and F. S. Stone, *Proc. Roy. Soc.*, *(London)*, **A197**, 294 (1949).

(5) T. J. Gray, *ibid.*, 314 (1949).

(6) W. E. Garner, T. J. Gray and F. S. Stone, *Reactions dans l'etat solide*, Paris (1949).

(7) W. E. Garner, T. J. Gray and F. S. Stone, *Trans. Faraday Soc. Disc.*, **8**, 246 (1950).

(8) T. J. Gray and S. D. Savage, *ibid.*, 250 (1950).

(9) T. J. Gray, *ibid.*, 331 (1950).

(10) T. J. Gray, "Semi-conducting Materials," Butterworths, London, 1951.

(11) J. S. Anderson and M. C. Morton, *Trans. Faraday Soc.*, **43**, 185, 194 (1947).

(12) D. J. M. Bevan, J. P. Shelton and J. S. Anderson, *J. Chem. Soc.*, 1729 (1948).

(13) D. J. M. Bevan and J. S. Anderson, *Trans. Faraday Soc. Disc.*, **8**, 238 (1950).

(14) J. S. Anderson and N. N. Greenwood, *Proc. Royal Soc. (London)*, **A215**, 353 (1952).

(15) J. H. de Boer and W. C. van Geel, *Physica*, **2**, 286 (1935).

(16) B. R. A. Nijboer, *Proc. Phys. Soc.*, **51**, 575 (1939).

n = no. of free electrons (carriers) excited into the conduction band at temp. T

N = no. of impurity levels in volume V

N_e = no. of electrons

E = the energy required to raise an electron from an impurity level to the conduction band

m, k and h have their usual significance

This is the generalized expression for a real crystal in which one may expect to find defects frozen into the lattice so that the number of defects exceeds the number of electrons. In the idealized case where $N = N_e$ then the expression reduces to

$$\frac{n}{\sqrt{N - n}} = (2) \, V^{1/2} \left\{ \left(\frac{2\pi mkT}{h^2}\right) \right\}^{3/4} e^{-E/2kT} \quad (2)$$

the factor (2) being introduced to cover the exigency of an impurity level containing paired electrons. Now if $n \ll N$ we have

$$\frac{n}{V} = (2) \sqrt{\frac{N}{V}} \left\{ \frac{2\pi mkT}{h^2} \right\}^{3/4} e^{-E/2kT} \quad (3)$$

which is the conventional Fowler–Wilson[17] expression.

If, however, the case of real crystals is considered and the same assumption is made that $n \ll N_e$ there are two limiting possibilities according as $n \ll N - N_e$ or $n \gg N - N_e$. If $n \ll N - N_e$ we have approximately

$$n = \frac{N_e}{N - N_e} V \left\{ \frac{2\pi mkT}{h^2} \right\}^{3/2} e^{-E/kT} \quad (4)$$

while if $n \gg N - N_e$

$$n = \sqrt{N_e V} \left\{ \frac{2\pi mkT}{h^2} \right\}^{3/4} e^{-E/2kT} \quad (5)$$

From this it might be deduced that at T_c for $n = n - N_e$ there would be expected to be a change in slope of the log σ against $1/T$ plot of two.

However, the complexity does not end here since there is the ambiguity as to the state of degeneracy. In the case of a large number of impurity centers (of the order 0.1%) it would be anticipated that ionization was considerable so that the assumption $n \ll N_e$ no longer holds. In this case a direct proportionality will exist at any given temperature be-

(17) A. H. Wilson and R. H. Fowler, *Proc. Royal Soc. (London)*, **A133**, 458 (1931); **A134**, 277 (1932); "Statistical Mechanics," Cambridge, 1936.

tween the number of free current carriers and the number of defects.

It has long been appreciated following the work of Fritsch,[18] Hartmann,[19] Meyer and Neldel[20] and others that the activation energy for the production of free current carriers, decreases with increase in the concentration of defects. Thus in the case of zinc oxide the variation in concentration of interstitial zinc occasions a change in activation energy from 0.6 to 0.01 e.v. while in certain circumstances a positive coefficient of resistance may be observed. The work of Lark–Horovitz[21] and Bardeen[22] together with the extensive work of Shockley[23] has clearly established the significance of impurity concentration. Under conditions of high impurity concentration the extra current carriers and impurity centers function as a degenerate electron gas. Hence, under these conditions, pseudometallic behavior may be anticipated.

A temperature may be defined dividing the condition of degenerate from non-degenerate systems.

$$T = \left(\frac{3}{\pi}\right)^{2/3} \frac{h^2}{8km^*} n_D^{2/3} = 4.2 \times 10^{-11} \left(\frac{m}{m^*}\right) n_D^{2/3} \,^\circ K. \quad (6)$$

or

$$kT = 21.6 \times 10^{-10} \left(\frac{m}{m^*}\right) n_D^{2/3} \text{ e.v.} \quad (7)$$

where n_D is the number of electrons for a degenerate condition. According as the material under consideration falls into the non-degenerate or degenerate category there is again an ambiguity as to whether the number of free current carriers should be taken as proportional to the root of the number of defects or directly to that number. The importance of these effects in terms of modification to mean free time, mobility and Hall coefficient is considered in the Conwell–Weisskopf[24] and Johnson–Lark–Horovitz[25] treatment of the non-degenerate and degenerate cases, respectively.

It will be apparent from this very brief summary that it is of the utmost importance to investigate the experimental data observed during the adsorption and desorption of appropriate gases on semiconducting materials on the basis of all reasonable possibilities. The object of this appreciation is to indicate the different types of formal kinetics which can be deduced from the most probable models and to develop a kinetic treatment with the minimum of ambiguity.

Experimental

The experimental results now to be considered were derived after the method described by Gray.[5] The method already has been described in some detail and an outline only is necessary for present consideration. Variations in semi-conductivity were determined for thin films of oxides in the range 300–2500 Å. prepared from evaporated films of metals of limiting purity (99.9997%) deposited on the inner

surface of a hard glass cylinder which had been subjected to vigorous degassing technique including rare gas ion bombardment. The glass cylinder carries four ring electrodes of thermal pure platinum foil fused into the surface of the glass and connected by thermal pure platinum leads to the measurement system. Thermocouples are provided on each electrode. Measurements of resistance are made at zero and low alternating frequencies by potentiometric and Wheatstone or modified Schering bridge methods, respectively.

Changes in conductivity during the adsorption and desorption of oxygen and other gases are observed against time for clearly defined conditions of pressure and temperature. Within defined limits of temperature and pressure, highly reproducible (approximately 0.1%) characteristics are observed. By an extended study adsorption isotherms and activation energies may be deduced.

The routine for measurements is vigorously maintained. Under closely defined conditions the films are evacuated at a pressure of below 10^{-7} mm. of mercury by high speed mercury diffusion pumps, the reaction tube being protected from mercury vapor by several liquid oxygen traps in tandem. Evacuation is continued until a stationary value of conductivity is obtained, usually about 30–40 hours, when a precision of 0.1% is obtained over a series of experiments. This is referred to as the evacuated condition of surface. Gas is then admitted at a given pressure and the adsorption followed with time at a fixed temperature ($\pm0.01°$) in terms of conductivity change and amount of gas adsorbed until a constant value of conductivity is obtained. In certain cases this is not possible since a continuous change in conductivity with time obeying a zero order law is observed after the initial stages. In these cases adsorption is continued until the zero-order rate is clearly defined. Such characteristics are observed chiefly where the lattice dimensions of the oxides are such as to permit a considerable degree of oxygen solubility.

When the absorption is terminated the system is subjected to a high vacuum, below 10^{-7} mm. of mercury being achieved within a half minute. Pumping continues with high speed pumps capable of approximately 180 l./sec. at this degree of vacuum. It has been found imperative to employ pumps of this very high capacity in order to achieve maximum reproducibility. The change in conductivity is observed during the desorption process and additionally the amount of gas desorbed is periodically measured by backing the high-speed diffusion pumps with a suitable triple-jet mercury diffusion circulating pump presenting the desorbed gas directly into a calibrated volume with a precision McLeod gage attached. However, since the volume of gas is extremely small it is quite feasible that this "desorption" process may in fact be completed by the building into the lattice of some of the adsorbed oxygen. The minute change in oxidation state thus occasioned is not determinate by any conventional technique and does not constitute any significant drift in semi-conducting properties in the actual samples investigated.

Repetition of measurements on individual films subjected to a progressive annealing correlates specific activity with the state of surface while repetition over different films yields information on specific activity as a (qualitative) function of the details of the method of preparation. The wide variation of specific activities obtainable for only minor variations in surface area establishes the specificity of certain selected sites as a predominant feature of the adsorption process. Simultaneous conventional measurements are made whenever possible.

The most detailed information relates to the copper, zinc, manganese and nickel oxide systems and in all cases correlation is made with corresponding measurements obtained by a variety of methods on loose powders of the materials. Much of this work has been described in the work of Garner and Stone.[4-7,26,27]

Fundamental Considerations.—It is not the object of this appreciation to consider a specific oxide system but rather to develop certain generalizations which may clarify the interpretation of the experimental measurements.

A typical plot for the change in conductivity against

(18) O. Fritsch, *Ann. Physik*, **22**, 375 (1935).
(19) W. Hartmann, *Z. Physik*, **102**, 709 (1936).
(20) W. Meyer and H. Neldel, *Phys. Z.*, **38**, 1014 (1937).
(21) K. Lark-Horovitz, *Phys. Rev.*, **69**, 258 (1946).
(22) G. L. Pearson and J. Bardeen, *ibid.*, **75**, 865 (1949).
(23) W. Shockley, "Electrons and Holes in Semi-conductors," D. Van Nostrand Co., New York, N. Y.
(24) E. Conwell and V. F. Weisskopf, *Phys. Rev.*, **69**, 258A (1946); **77**, 389 (1950).
(25) V. A. Johnson and K. Lark-Horovitz, *ibid.*, **71**, 374 (1947).

(26) F. S. Stone and P. F. Tiley, *Trans. Faraday Soc. Disc.*, **8**, 254 (1950).
(27) W. E. Garner, F. S. Stone and P. F. Tiley, *Proc. Roy. Soc. (London)*, **A211**, 472 (1952).

time in the case of nickel oxide is shown in Fig. 1. This displays a constant initial conductivity characterizing the highly evacuated film to which precise return can be made after adsorption and desorption within certain limits of temperature and pressure. At point (A) oxygen at a given pressure is admitted to the film and the change in conductivity observed against time. By the point (B) adsorption is complete and desorption will normally be performed a short time after this point. Prolonged exposure to oxygen in this condition results in small but significant permanent change in the oxidation state leading to irreproducible results. This is avoided by preventing prolonged exposure. Presumably this effect is due to the building in of the adsorbed oxygen into the surface zone. The difference in chemical characteristic of the "adsorbed" oxygen with residence time has been discussed by Garner, Gray and Stone.[7]

Superimposed on Fig. 1 is an adsorption plot (modified scale) in the case of a particular sample of nickel oxide where oxygen solubility was occurring and a typical change from initial adsorption stage to continuous zero-order solubility characteristic is observed.

Analysis from such curves will now be considered on the basis of various models and employing several different assumptions for the relationship between increase in conductivity and the amount of oxygen adsorbed. These results will be considered by direct formulation from the experimental points and also in a differential form employing tangential plot methods from the graphical "fair curve."

Various stages have been described for the adsorption of oxygen on oxides. These are summarized as follows, considering a p-type oxide such as Cu_2O.

$$O_2 + Me^+ \rightleftharpoons O_2^- + (Me^{2+})\oplus \tag{8}$$

$$O_2 + 2Me^+ \rightleftharpoons 2O^- + 2(Me^{2+})\oplus \tag{9}$$

$$O^- - Me^+ \rightleftharpoons O^= + (Me^{2+})\oplus \tag{10}$$
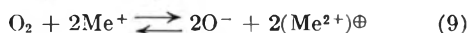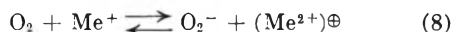
where $\oplus$ represents a positive hole. On the basis of energetics the first of these is unlikely and incomplete. There is insufficient energy available to dissociate oxygen molecules on the molecular ion basis. However, in the second equation this is overcome by the energy made available in the formation of O^- ions. The probability of the formation of these has been demonstrated by susceptibility measurements (Gray[28]). The third equation indicates the stage which covers the building in of the oxygen into the oxide lattice. These are considered to be of the most pertinent expressions and can now be considered in terms of the kinetics of adsorption derived by semi-conductivity measurements which are related to the positive holes generated during these reactions.

Derivation of Graphical Plots

The Adsorption Process.—According to the primary assumptions the formal kinetics for the adsorption of oxygen on semi-conducting oxides vary somewhat in detail. It has been clearly established that there is a direct correlation between the rate of adsorption of oxygen and the change in semi-conductivity as determined experimentally. It is now necessary to examine the correlation in detail to determine if possible the most reasonable and accurate correlation.

The rate of adsorption of O_2 is a function of the number of vacant sites present in the surface and the possible expressions which will be considered are those for first-order, second-order and exponential relationships. These relationships have been derived by many authors making direct measurements of the amount of oxygen adsorbed.

First order:

$$\frac{dN_t}{dt} = k(N_\infty - N_t) \tag{11}$$

(28) T. J. Gray, "Summer Scholl on Catalysis," Bristol, England, 1953.
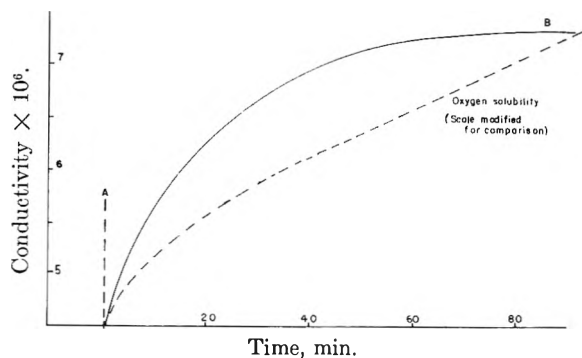
Fig. 1.—Adsorption of oxygen on oxides.

Second order:

$$\frac{dN_t}{dt} = k(N_\infty - N_t)^2 \tag{12}$$

Exponential:[29]

$$\frac{dN_t}{dt} = ae^{-\alpha N_t} \tag{13}$$

where N_t = number of oxygen atoms adsorbed at time t and N = total number of adsorption sites on the surface (i.e., number of oxygen atoms adsorbed at time $t = \infty$), k, a and α are constants. On integration, equation 11 becomes

$$\log_e (N_\infty - N_t) = kt + \text{const.} \tag{14}$$

On the basis of the change in conductivity of the specimen arising from the increased number of impurity centers it is reasonable to correlate the number of oxygen ions on the surface with the change in number of impurity sites. The difference in possible mechanism involved would introduce a factor of two on the total number which is indistinguishable in the theoretical calculation for the increase in number of impurities owing to greater uncertainty in other variables.

If the relationship between conductivity and the number of impurity centers is given by

$$\sigma = k\sqrt{N}, \text{ then } N_t = \sigma_t^2/K^2$$

Substitution for N_t and N_∞ in equation 14 gives

$$\ln (\sigma^2 - \sigma_t^2) = kt + \text{const.}' \tag{15}$$

Replacing specific conductivity by the actual conductivity measured gives

$$\ln (\lambda_\infty^2 - \lambda_t^2) = kt + \text{const.}'' \tag{16}$$

Alternatively, if the condition $\sigma \alpha N$ is applicable, then the final expression will be

$$\ln (\lambda_\infty - \lambda_t) = kt + \text{const.}''' \tag{17}$$

Thus a plot of log $(\lambda_\infty^2 - \lambda_t^2)$ vs. time should be linear if σ is proportional to root of N, whereas log $(\lambda_\infty - \lambda_t)$ against time ought to be obeyed when the proportionality is direct. The slope will give a measure of the rate of change of conductivity with time on the basis of a first-order relationship.

(29) An exponential relation was first introduced into adsorption kinetics by Zeldovich and Roginsky[30] and further developed by Elovich.[31,32] In a number of recent papers this exponential relation has been referred to as the Elovich equation. The two terms are used synonymously in the present text.

(30) (a) Ya. Zeldovich, Acta Physicochim. URSS, 1, 449 (1934); (b) S. Roginsky and Ya. Zeldovich, ibid., 1, 554, 595 (1934).

(31) S. Elovich and S. Roginsky, ibid., 7, 295 (1937).

(32) S. Elovich and G. M. Zhabrova, Zhur. Fiz. Khim., 13, 1761, 1775 (1939).

In order to plot these expressions the value of λ_∞ must be known. With slow processes, this may be difficult to determine accurately. Furthermore, the logarithmic scale means that one cannot get as accurate a picture as would be desirable for the initial stages of the adsorption processes. Most important of all, if complex kinetics are involved during the process of adsorption, it is open to question whether the experimental λ_∞ value or a derived value should be employed.

By substituting λ^2 or λ for N_t in equation 11 we obtain either

$$\frac{d\lambda_t^2}{d_t} = k(\lambda_\infty^2 - \lambda_t^2) \qquad (18)$$

or

$$\frac{d\lambda_t}{dt} = k(\lambda_\infty - \lambda_t) \qquad (19)$$

The order of the reaction can be determined by plotting the tangential relation $d\lambda_{t^2}/dt$ against λt^2 or d_t/dt against λt. In either case K is given by the slope.

In order to investigate the possibility of a second-order relationship it is necessary to consider equation 12

$$\frac{dN_t}{dt} = k(N_\infty - N_t)^2$$

Using the same treatment as for the first-order expressions we have

$$\frac{1}{\lambda_\infty^2 - \lambda_t^2} = Kt + \text{const.} \qquad (20)$$

or

$$\frac{1}{\lambda_\infty - \lambda_t} = Kt + \text{const.} \qquad (21)$$

Using the alternative tangential plots

$$\frac{d\lambda_{t^2}}{dt} = k(\lambda_\infty^2 - \lambda_t^2)^2 \qquad (22)$$

$$\frac{d\lambda_t}{dt} = k(\lambda_\infty - \lambda_t)^2 \qquad (23)$$

the slopes may be deduced giving K.

The exponential relation (13) can be tested by plotting $\log (dN_t)/dt$ against N_t, that is, either $\log (d\lambda_t^2)/dt$ against λ_t^2 or $\log (d\lambda_t)/dt$ against λ_t. Alternatively, the integrated form of the equation may be plotted, as has been done, by a number of previous workers. The integrated form has been studied here in order to compare results with generalizations made by Taylor and Thon.[33] The integrated form is

$$N_t = \frac{2.3}{\alpha} \log (t + t_0) - \frac{2.3}{\alpha} \log t_0 \qquad (24)$$

where

$$t_0 = 1/\alpha a$$

In addition to considering these various possibilities, it is essential to consider the significance of the actual conductivity determined experimentally. The previous considerations assume that λ is homogeneous and remains so during the adsorption process. Such an assumption is valid on the basis of a model for the specimen having bulk con-

(33) H. Austin Taylor and N. Thon, *J. Am. Chem. Soc.*, **74**, 4169 (1952).

ductivity together with a surface conductivity providing that the surface conductivity alone varies during the process of adsorption and that the surface conductivity is always much greater than the bulk conductivity. This condition should hold throughout the entire adsorption process although the validity is not seriously impaired if the initial conductivity of the highly evacuated surface is of the same order of magnitude as the bulk conductivity (considering only P-type oxides at this juncture). Alternatively, if there is only one conductivity region, this conductivity must vary uniformly throughout both the bulk and surface as adsorption proceeds. This latter assumption is not likely to hold in the temperature region over which these studies are made since mobilities in the bulk are very small below the Tammann temperature. On this basis it is reasonable to consider a model in the case of P-type oxides for which there is a surface zone having a conductivity significantly higher than the bulk of the material, the conductivity of which varies with the amount of oxygen adsorbed. Associated with this surface region is a zone of bulk material substantially unaffected during the adsorption process. This model originally put forward by Gray[28] can now be considered in relation to the complication of the kinetic derivation.

If bulk conductivity were always negligible with respect to the surface conductivity, then λ (surface) $\simeq \lambda$ (measured) and no further considerations are necessary. However, consider the case in which the bulk conductivity is not a negligible quantity. If in the limiting condition the initial specific conductivity of a surface which has been subjected to prolonged evacuation can be taken as equal to the bulk conductivity, it is possible to consider the various kinetic relationships which now obtain

$$\lambda = \lambda(s) + \lambda(b)$$

where λ is the measured conductivity and $\lambda(b)$ is the bulk contribution to conductivity while $\lambda(s)$ is the increased conductivity of the surface zone. At zero time $\lambda(s) \simeq 0$. If λb is assumed to remain constant throughout the process of adsorption

$$\lambda(s)_t - \lambda(s)_0 = \lambda_t - \lambda_0 = \Delta\lambda$$

In this case the plots of λ (measured) will give the same results as if λ(surface) were plotted. Using the relationship $\lambda^2 \propto N$, instead of using the expression

$$\frac{d\lambda_{t^2}}{dt} = K(\lambda_\infty^2 - \lambda_t^2)$$

the plot

$$\frac{d\lambda(s)_t^2}{dt} = K(\lambda_\infty(s)^2 - \lambda(s)_t^2) \qquad (25)$$

should be used for a first-order process.

This develops as

$$\frac{d}{dt}(\lambda_t - \lambda_b)^2 = K\{(\lambda_\infty - \lambda_b)^2 - (\lambda_t - \lambda_b)^2\}$$

If λ_b is equal to the total conductivity at time $t = 0$, i.e., $\lambda_b = \lambda_0$

$$\frac{d(\lambda_t - \lambda_0)^2}{dt} = K\{(\lambda_\infty - \lambda_0)^2 - (\lambda_t - \lambda_0)^2\} \qquad (26)$$

and a linear plot for $d(\lambda_t - \lambda_0)/dt$ against $(\lambda_t - \lambda_0)^2$ will indicate a first-order process.

If $\lambda_b \gg \lambda_0$, the expression reduces to that of equation 18.

A second-order relationship is given by

$$\frac{d(\lambda_t - \lambda_0)^2}{dt} = K\{(\lambda_\infty - \lambda_0)^2 - (\lambda_t - \lambda_0)^2\}^2 \quad (27)$$

and can be plotted as

$$\sqrt{\frac{d(\lambda_t - \lambda_0)^2}{dt}} \text{ against } (\lambda_t - \lambda_0)^2$$

The exponential plot must also be corrected for the effect of the bulk conductivity if the square root conductivity relationship is applicable. On this basis it may be shown that the required plot is

$$(\lambda_{st}^2 - \lambda_{s0}^2) \text{ vs. log } (t + t_0) \quad (28)$$

Now

$$\lambda_{st}^2 - \lambda_{s0}^2 = (\lambda_t - \lambda_b)^2 - (\lambda_0 - \lambda_b)^2$$

and if

$$\lambda_b = \lambda_c, \text{ then } \lambda_{st}^2 - \lambda_{s0}^2 = (\lambda_t - \lambda_0)^2$$

whereas if

$$\lambda_b \ll \lambda_0, \text{ then } \lambda_{st}^2 - \lambda_{s0}^2 = \lambda_t^2 - \lambda_0^2$$

The Desorption Process.—Always accepting the possible complexity of the desorption process through the building in of oxygen, similar considerations apply for the case of the adsorption process. On the basic assumption that the rate of desorption of oxygen is a function of the number of sites still occupied, we have

$$\frac{-dN_t}{dt} = k(N_t - N_\infty) \quad (29)$$

$$\frac{-dN_t}{dt} = k(N_t - N_\infty)^2 \quad (30)$$

or

$$\frac{-dN_t}{dt} = ae^{-\alpha N_t} \quad (31)$$

for the formal kinetics as previously considered. Similar relationships are obtained as follows allowing for bulk and surface conductivity.

First-order desorption, either

$$\frac{-d\lambda_t^2}{dt} = k(\lambda_t^2 - \lambda_\infty^2) \quad (32)$$

or

$$\frac{-d\lambda_t^2}{dt} = k(\lambda_t - \lambda_\infty) \quad (33)$$

Second-order desorption, either

$$\frac{-d\lambda_t^2}{dt} = K\{(\lambda_t - \lambda_b)^2 - (\lambda_\infty - \lambda_b)^2\}^2 \quad (34)$$

and if $\lambda_b \ll \lambda_\infty$, this reduces to

$$\frac{-d\lambda_t^2}{dt} = K(\lambda_t^2 - \lambda_\infty^2)^2 \quad (35)$$

or if $\lambda_b \simeq \lambda_\infty$

$$\frac{-d\lambda_t^2}{dt} = K\{(\lambda_t - \lambda_\infty)^2\}^2 \quad (36)$$

Results and Their Interpretation

A very large number of experimental results are available covering the semi-conductivity changes during the adsorption and desorption of oxygen and other gases on oxide systems of extremely high purity. The copper, nickel, manganese and zinc oxide systems have been studied in detail and the results

from the first three oxides will be considered. The case of zinc oxide is opposite in character since this is an N-type oxide as opposed to P-type in the other cases and it will not be considered at this juncture. The effect of adsorption of oxygen is in the opposite sense as affecting conductivity, that is, the conductivity diminishes on the adsorption of oxygen.

As the results obtained are highly reproducible under the critically defined conditions of the experimental technique, a limited number of results can be accepted as typical of a very large number of experiments derived from research progressing over more than eight years. Two such results are displayed in Fig. 1, which illustrates the cases of simple, uncomplicated adsorption of oxygen and the significant difference observed when solubility of oxygen occurs.

The Adsorption of Oxygen on a Surface Not Showing Any Complicating Zero-order Effect.—Considering first the case where the experimental adsorption indicates no complication by oxygen solubility. First-order adsorption kinetics are plotted in Fig. 2 which is a plot of equation 16 together with the corrected plot (eq. 27) necessary if the derived model of a surface and bulk contribution is employed where the conductivity prior to adsorption is essentially the bulk conductivity of the specimen.
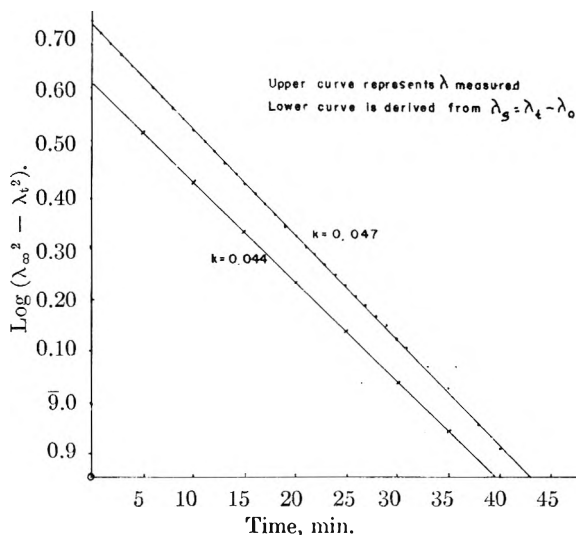
Fig. 2.—First-order plot on λ^2 kinetics for oxygen on NiO at 295°.

No plot is given for equation 17, the corresponding relation for $\lambda \propto N$ kinetics. It has been shown (Gray and Savage[3]) that both logarithmic relations fit the results equally well in the case of Cu_2O and this conclusion has been substantiated from results in certain other systems. The linear plot obtained indicates a first-order adsorption process but does not make it possible to distinguish between $\lambda^2 \propto N$ and $\lambda \propto N$ kinetics. The equation is obeyed equally well in the two limiting cases considered in Fig. 2; namely, $\lambda_b \ll \lambda_0$, $\lambda_b \simeq \lambda_0$, with the value of the first-order rate constant, K, varying by about 6% for these limiting conditions.

In Fig. 3, the tangential plots are given for $\lambda^2 \propto N$ kinetics, corresponding to the equations 18 and 22,
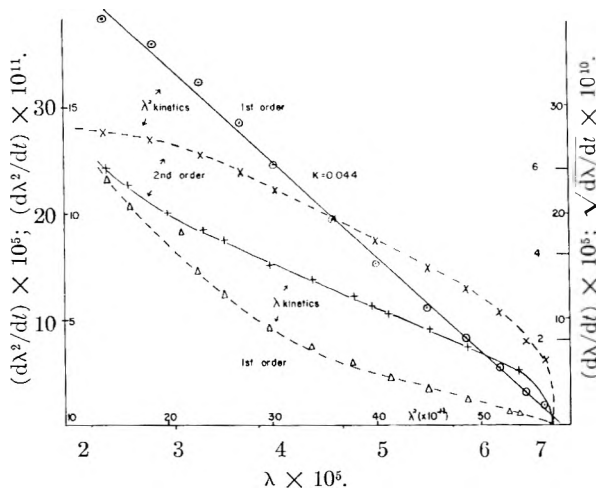
Fig. 3.—Tangential plot for adsorption of O_2 on NiO at 295°.

together with the corresponding plots for $\lambda \propto N$ kinetics as expressed in equations 19 and 3. Although not indicated with maximum clarity in the examples given, neither the plot for first-order nor that for second-order kinetics on the $\lambda \propto N$ basis holds satisfactorily throughout the total adsorption in the majority of experimental determinations. The results obtained suggest an initial second-order process followed by a first-order stage. The relative proportion of these varies with the type of oxide and the absolute activity of the specimens. In other words, it appears to be significantly structure sensitive. For NiO, with kinetics based on $\lambda^2 \propto N$, the first-order plot is frequently linear throughout; in this particular case the intercept gives $\lambda^2 = 57.6 \times 10^{11}$ as compared with the experimental value of 56.2×10^{11}. The second-order plot is definitely non-linear in this particular case. However, for copper oxide, a second-order process is always present under the experimental conditions in use.

Figure 4 shows the tangential plots for kinetics after correcting for bulk conductivity as considered in equations 26 and 27. It will be observed that the second-order plot is still non-linear. For the first-order relationship, there is an initial increase in the rate of change of conductivity, followed by a linear region. The linear portion gives the same rate constant and equilibrium conductivity value as did the uncorrected plot.
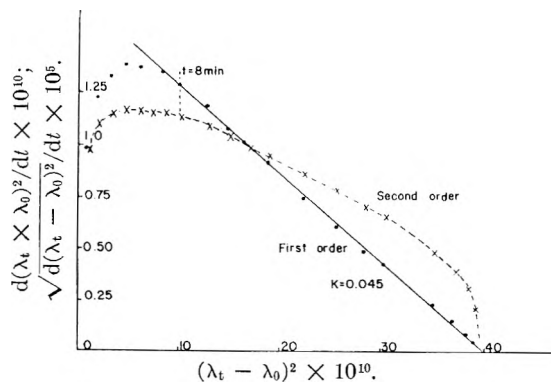
Fig. 5 shows the exponential plots for $\lambda \propto N$ kinetics, and for the uncorrected and corrected $\lambda^2 \propto N$. In all three cases, a linear Elovich plot is obtained only over a limited time interval from the start of the adsorption. It is very important to appreciate that the expression does not describe the whole reaction, an increasing deviation from linearity always appearing as the absorption proceeds.
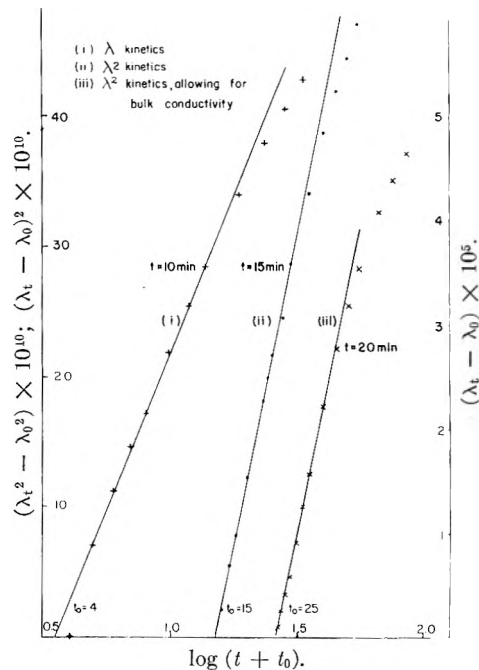
Fig. 5.—Exponential plots for adsorption of O_2 on NiO at 295°.

The experimental results so far considered have been those for a typical reproducible experiment in a series performed over a range of temperature and pressure. The particular experiment considered was studied at the maximum temperature and pressure for the series. Under such conditions a very high order of reproducibility can be achieved as is illustrated in Fig. 6 for constant temperature and closely similar oxygen pressures (four values between 6.3×10^{-2} mm. and 5.6×10^{-2} mm.). However, on lowering the pressure, it is observed from detailed analysis that both the first-order

Fig. 4.—λ_s^2 kinetics.
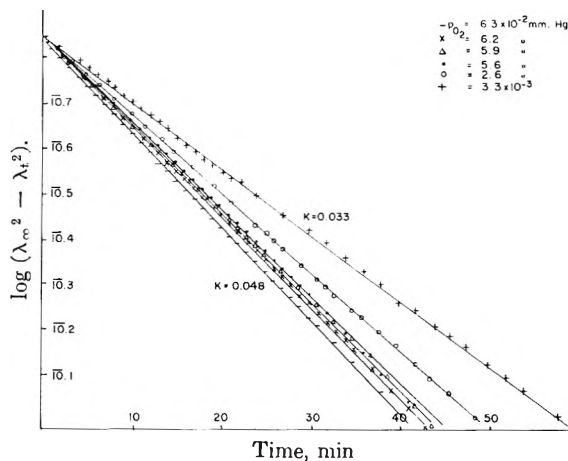
Fig. 6.—Adsorption of O and NiO at 295°.

logarithmic and tangential plots deviate from linearity (toward higher order) at the start of the adsorption. Over this region a second-order relationship fits the results more satisfactorily. A similar effect is observed when the temperature is lowered, pressure being kept at the maximum value. This phenomenon has been observed for MnO, NiO and Cu_2O systems, the extent of second-order region being greater in the copper oxide case.

The consideration of formal adsorption kinetics is incomplete without an examination of the pressure dependence of the adsorption process and the derivation, where possible, of the activation energies of the rate controlling stage. In spite of the apparent change in complexity as the temperature and pressure are lowered it is still possible to consider these relationships in respect of the predominant process.[34] In Fig. 7 the rate constants derived by such treatment are plotted against pressure as standard isotherms for the systems, Cu_2O, MnO and NiO. These isotherms are then compared on the basis of log K against log p which gives linear results suggesting a Freundlich type isotherm.
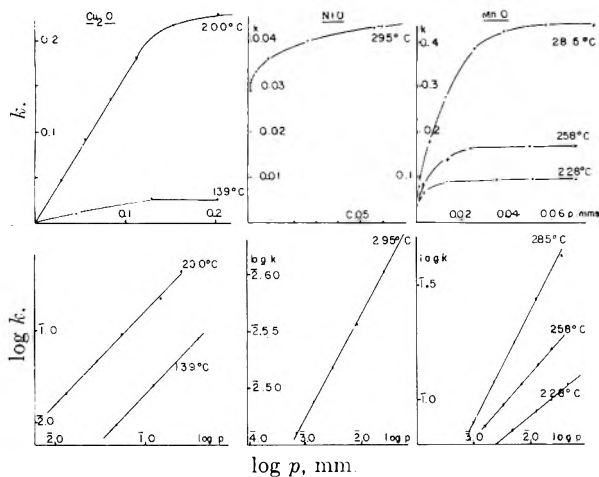
Fig. 7.—Top, variation of rate constant k with pressure at constant temperature; bottom, Freundlich isotherms corresponding to respective k/p curves.

For all three systems, activation energies have been calculated and Fig. 8 shows the relationship for nickel oxide. Superimposed is a plot of log $a/\Delta\lambda^2$ against $1/T$, where a is the constant in the Elovich equation and $\Delta\lambda^2 = \lambda_\infty^2 - \lambda_0^2$. The linearity of this latter plot indicates that the Elovich equation can give an apparent activation energy for the initial rate of reaction. Further analysis of the Elovich λ^2 plots by the method of Taylor and Thon indicates that the constants t_0, α, qt_0 vary with temperature and pressure as they have observed. In the case under consideration, however, it has already been demonstrated that the exponential relation is not of fundamental significance but only a general approximation for the initial stages of the process.

(34) A logarithmic plot for the variation in rate of adsorption with pressure over the range 6×10^{-2} mm. to 3×10^{-3} mm., at constant temperature, is given in Fig. 6.
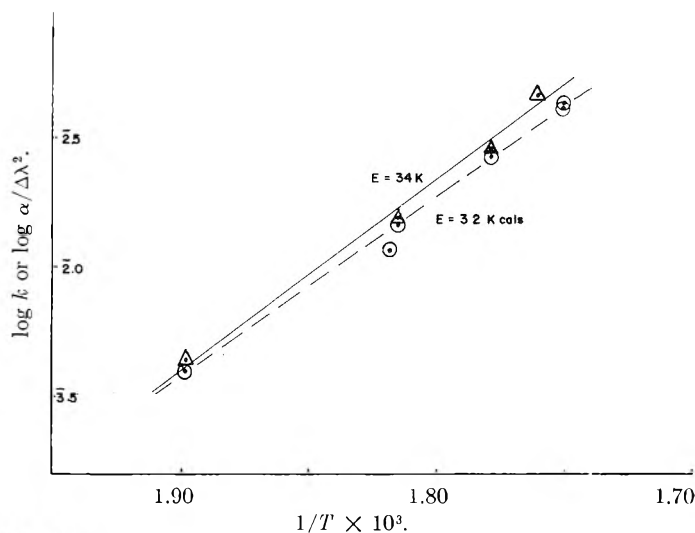
Fig. 8.—Activation energy for the adsorption of O_2 on NiO; first-order λ^2 kinetics, $\bigcirc$; Elovich exponential law $\triangle$.

Adsorption of O_2 on Surface Showing Superimposed Zero-order Effect.—Corresponding more closely to the type of relationship studied by Taylor and Thon is that for adsorption complicated by zero-order process, as shown in Fig. 1. Such characteristics are encountered more particularly in oxides where the lattice parameters are such as may tolerate appreciable oxygen solubility in the oxide. This is found to be the case with the manganese oxide system and to a lesser extent in the nickel oxide system.

Figure 9 gives plots for the first- and second-order kinetics ($\lambda^2 \propto N$) after subtracting for the zero-order effect. The composite curve can be analyzed into an initial second-order period, quickly leading to a first-order period, with a zero-order process occurring simultaneously and continuing after the first-order change has concluded.
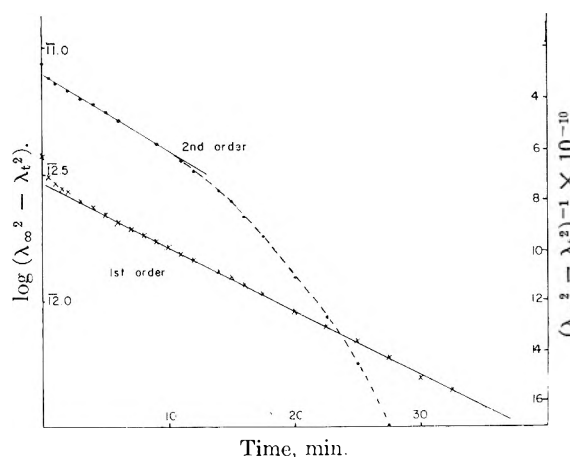
Fig. 9.—Adsorption kinetics for film, allowing for zero-order conductivity change.

The Elovich plot for this adsorption is given in Fig. 10 and holds more satisfactorily in this case than for the less complicated adsorption which reached an equilibrium value in a finite time. That is to say, the exponential plot is a better over-all approximation for the complex order process than for one obeying a single order kinetics, or a combi-
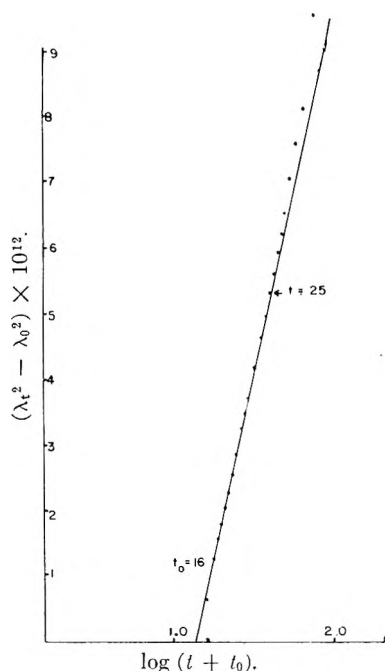
Fig. 10.—Elovich plot for O_2 adsorption on NiO when a complicating zero-order effect is actually present.

nation of two processes. However, it is probable that the detailed analysis into separate types is of greater significance where this can be performed as in the technique under consideration.

Desorption of Oxygen from Oxide Surfaces.— There is considerably greater difficulty in a full analysis for the desorption process largely arising from experimental difficulties. In the lower temperature ranges the desorption is very protracted, sometimes taking many days. Even at the higher temperatures it is normally found necessary to desorb at 10^{-8} mm. of mercury for 36–48 hours to obtain a reproducible stationary state of surface. This means that even the 0.1% accuracy achieved in the conductivity measurements leaves some margin for discrepancy over this time period.

For nickel oxide a detailed study has been made of the possible plots (1st, 2nd, 4th and exponential) for $\lambda \propto N$ and $\lambda^2 \propto N$ kinetics. From the results it would appear that the process is most probably second-order, and $\lambda \propto N$ kinetics gives a better plot than $\lambda^2 \propto N$. There is evidence for an initial fourth-order desorption under certain conditions for copper oxide (Gray and Savage[8]) and this may be observed in some instances with manganese oxide (Macmillan[35]). Subsequently, the kinetics for both these oxide systems is best represented by second-order, $\lambda \propto N$ plots. The exponential plot has been observed to hold over a very limited portion of the NiO desorption plots, but, on the basis of $\lambda^2 \propto N$ kinetics, results with copper oxide indicate the exponential relation to be the most suitable; though a fourth-order relation is also possibly justified (Derry, Garner and Gray[36]). Temperature and pressure effects probably define the range in which such complications occur but at present the experimental evidence, although extensive, is

(35) R. B. Macmillan, Ph.D. Thesis, University of Bristol, 1951·
(36) R. Derry, W. E. Garner and T. J. Gray, "Paris Conference on Catalytic Materials," 1954.

inadequate to define exact conditions. Additionally, when adsorption is performed above a few millimeters oxygen pressure a first-order relationship occasionally has been observed.

Proposed Model for an Oxide Surface.— On the basis of these investigations and the detailed analysis of the kinetics of the adsorption and desorption of oxygen, the model which most accurately accounts for the experimental evidence is that of a two-zone system. This model is envisaged as comprising a surface zone which may in some cases be restricted to a few molecular layers from the surface, either internal or external, or may in other cases extend to a depth of several hundred layers. Beneath this surface zone there is a bulk temperature range at present under consideration, that is substantially below the Tammann temperature. It follows that the relative thickness of the surface zone is likely to be temperature dependent and will certainly be structure sensitive, particularly with respect to method and temperature of preparation. In this surface zone the concentration of defects will be significantly different, in general, from the concentration in the bulk and will be subject to variations according to the state of adsorption and desorption of ions on the surface.

From considerations of semi-conductivity it is generally assumed that the conductivity at zero and low alternating frequencies is largely that of the surface of grains or crystallites. This may be related, according as they are ionized to a small or large extent, respectively. On this basis changes in conductivity occurring during the process of adsorption and desorption of oxygen on an oxide can be correlated directly in terms of defects produced. This in effect constitutes a justification for the use of semi-conductivity measurements in the study of adsorption kinetics.

Following the detailed consideration of the results obtained from the investigation of changes in semi-conductivity during the adsorption and desorption processes it appears that a surface which has been subjected to very prolonged evacuation may approximate to the same defect concentration as the bulk material. In these conditions the number of defects in the surface zone will be small and it is possible to develop satisfactory formal kinetics on the basis of the conductivity being related to the number of defects as $\lambda^2 \propto N$. When the surface is saturated with oxygen the zone possesses pseudo-metallic characteristics owing to the very high concentration of defects which may be considered as substantially completely ionized. Then the kinetics can be developed on the basis of direct proportionality existing between the conductivity of the surface zone and the concentration of defects in that zone. This appears to hold at least over the initial portion of the desorption process and might be anticipated to complicate the later stages of the adsorption process.

Additional Observations.— The early zone of second-order kinetics appears to be highly structure sensitive and varies considerably from oxide to oxide. Certain generalizations are observed although they have not been fully substantiated in all cases.

1. The second-order adsorption region does not appear to arise to a measurable extent when the oxide is capable of dissolving oxygen; in other words, if the lattice parameter is sufficient to allow oxygen penetration of the surface zone to an appreciable extent the second-order region is reduced to a very small proportion of the total.

2. As the "activity" of the material is increased the second-order region diminishes but may be increased on a particular sample by annealing, a process which reduces specific activity.

3. The lower the temperature the greater the extent to which the second-order adsorption is observed. If for any particular sample the temperature is raised to an extent that sintering is commencing, the second-order reaction has in general almost disappeared only to reappear on cooling.

SEMI-CONDUCTIVITY AND CATALYSIS IN THE NICKEL OXIDE SYSTEM

By T. J. GRAY AND P. W. DARBY

Contribution from The New York State College of Ceramics at Alfred University, Alfred, New York

Received July 11, 1955

The kinetics of adsorption processes on nickel oxide have been studied as a function of the changes in conductivity which they produce. It is demonstrated that the complex adsorption and reaction processes occurring over the oxide ion be satisfactorily studied by this method and a model is developed envisaging the adsorption and dissociation (or electron transfer process) occurring on certain preferred sites which are probably surface dislocations. A relationship between catalytic activity and defect concentration is anticipated and qualitatively demonstrated. Correlation of the results of this investigation with the work of other authors leads to an interpretation of the variations of results which are generally experienced. This fact is entirely consistent with the proposed model. Acceptance of a complex model is stressed rather than the ready acceptance of an oversimplified model.

Introduction

The relationship between catalytic activity and the defect solid state is now widely accepted. This relationship forms the basis of the methods developed by Gray[1] and co-workers at Bristol and subsequently followed elsewhere. The particular aspect on which most attention has been focused is the variation of semi-conductivity during the adsorption, desorption or reaction of gases on a solid surface. By such a study the kinetics of the individual stages of the adsorption and reaction process can be studied and in conjunction with magnetic measurements (Gray[2]), a detailed model can be established. Certain ambiguities exist in the correlation and are discussed elsewhere (Gray and Darby[3]). It is only by the acceptance of these ambiguities and the general complexity of the catalytic process that a realistic model can be established. In particular, it is of the utmost importance to appreciate that the systems are not normally equilibrium systems and that dynamic conditions must be considered.

In the particular case of nickel oxide the electrical conductivity was subject to the critical attention of Le Blanc and Sachse[4] who observed the color changes when the method of preparation or after treatment was varied. Although early views postulated the formation of intermediate oxide phases the work of Lunde[5] established that NiO was the only stable phase and any "excess" of oxygen was present as lattice deficiency of nickel. A study of the oxygen dependence of semi-conductivity indicated that the material behaves as a normal p-type semi-conductor. However, there is evidence that under certain reducing conditions the material may give an unstable n-type oxide, probably interstitial nickel (Igaki[6]).

The early work of Wagner and Baumbach[7] indicated a pressure dependence of conductivity which has frequently been quoted. However, many other authors obtained varying results and the formal representation employed is obviously of limited validity. It is apparent from the work of Hogarth,[8] Igaki[6] and others that no simple relationships exist. de Boer and Verwey[9] are responsible for the generally accepted view that the oxygen excess is accommodated by a change in effective oxidation state consequent on the formation of positive holes due to oxygen excess. There is a marked discrepancy in the temperature coefficient for the conduction process and numerous authors who have studied this system[6-8, 10-13] report values from 0.3 e.v. to as high as 2.0 e.v. depending on the temperature range, method of preparation, purity and the gas atmosphere employed. These variable results will be considered later.

Many investigations have been made of the adsorption of various gases on nickel oxide, particu-

(1) T. J. Gray, *Nature*, **162**, 260 (1948); *Proc. Roy. Soc. (London)*, **A197**, 314 (1949); *Disc. Faraday Soc.*, No. 8, 331 (1950).

(2) T. J. Gray, Summer School, Bristol, 1953.

(3) T. J. Gray and P. W. Darby, THIS JOURNAL, **60**, 201(1956).

(4) M. Le Blanc and H. Sachse, *Z. Elektrochem.*, **32**, 58 (1926); **32**, 204 (1926); *Ber.*, **82**, 133 (1931); *Physik Z.*, **32**, 887 (1931).

(5) G. Lunde, *Z. anorg. allgem. Chem.*, **163**, 345 (1927).

(6) K. Igaki and S. Takeuchi, *J. Japan Inst. Metals*, **148**, 16 (1950).

(7) H. H. Baumbach and C. Wagner, *Z. physik Chem.*, **B24**, 59 (1934).

(8) C. A. Hogarth, *Nature*, **161**, 60 (1948); *Proc. Phys. Soc.*, **B64**, 691 (1951).

(9) J. H. de Boer and E. J. W. Verwey, *ibid.*, **49**, Ex. 59 (1937).

(10) R. W. Wright and J. P. Andrews, *ibid.*, **62A**, 446 (1949).

(11) M. G. Harwood, N. Herzfeld and S. L. Martin, *Trans. Faraday Soc.*, **46**, 650 (1950).

(12) M. Foex, *Bull. soc. chim. France*, D, 373 (1952).

(13) F. J. Morin, *Phys. Rev.*, **93**, 1199 (1954).

Fig. 1.—Temperature coefficient of conductivity of NiO.

larly those of Roginsky.[14] Dell[15] has studied the extent and heat of adsorption of gases on nickel oxide while the kinetics of gas reactions over nickel oxide have been considered by many authors. Of particular interest in association with the present study is the work of Schwab[16] who extended the controlled valency principle to the modification of nickel oxide employed as a catalyst material and demonstrated clearly the activation energy variations which can be produced in simple catalytic processes by a change in defect concentration.

The present investigation was an extension to earlier work on other oxide systems and aims at correlating the changes in conductivity during the adsorption and desorption of various gases over nickel oxide with the kinetic processes involved. From these considerations a model for the catalyst surface has been developed which satisfactorily accounts for its known properties.

Experimental

The general method of study is similar to that already described by Gray.[1] A film of extremely pure metal is evaporated from an electrolytically plated axial tungsten filament onto the inner surface of a hard glass cylinder bearing four platinum conduction electrodes equipped with thermocouples. Thorough degassing of the grease-free system prior to the evaporation of the metal is performed by prolonged evacuation at 10^{-8} mm. and a temperature of 400°. Ion bombardment in a helium atmosphere ensures a satisfactorily clean substrate. Subsequent oxidation of the metal film is performed under conditions whereby the oxidation process may be studied, the oxygen being admitted by diffusion through silver. When the metal film has been oxidized to the required condition, temperature coefficients of conductivity are determined under hard vacuum conditions, and then changes in conductivity with the adsorption of gases are studied over a range of temperatures and pressures so selected by preliminary experiments that no drift in characteristics is obtained. Under these conditions a complete kinetic survey is made using both direct and alternating current measurements of conductivity and orthodox measurements for pressure or volume changes.

Results

Temperature Coefficient of Conduction Process. —The NiO surface is characterized, following controlled evaporation and oxidation, by measuring

(14) S. Z. Roginsky and T. F. Tsellinskaya, *Zhur. Fiz. Khim.*, **21**, 919 (1947); *Acta Physicochim., U.S.S.R.*, **14**, 225 (1944); *Zhur. Fiz. Khim.*, **22**, 1360 (1948).

(15) R. M. Dell, Ph.D. Thesis, Bristol, 1953; R. M. Dell and F. S. Stone, *Trans. Faraday Soc.*, **50**, 501 (1954).

(16) G. M. Schwab, Symposium, Paris, 1954 (in press, *J. Soc. Chem. Phys.*); G. M. Schwab and J. Block, *Z. physik. Chem.*, **1**, 42 (1954).

the change in conductivity with temperature, (a) after evacuation at the oxidizing temperature, (b) in the presence of oxygen at a pressure of 10^{-2} to 10^{-1} mm. and, (c) when reduced by limited amounts of either hydrogen or carbon monoxide. Results for a particular series are plotted in Fig. 1, while Table I contains values of ϵ, as calculated from the equation

$$\lambda = Ae^{-\epsilon/kT}$$

and determined from plots of log λ against $1/T$ on the several films. There is no discontinuity or change of slope in any of the temperature coefficients obtained but the activation energies are structure-sensitive.

TABLE I

TEMPERATURE COEFFICIENT OF CONDUCTIVITY

Film	E_λ (evacuated) in kcal.	E_λ (oxygenated) in kcal.	E_λ (reduced) in kcal.	Note
1	10	8		
4	11.1	10.1	24.4	Reduction with H₂ at 200°
4	9.2	7.7	19.2	After inc. in oxidation state and reduction with CO at 430°
5	14.3 10.0–9.3– 8.3			Progressive inc. in oxidation state (stationary values)
5	8.1 7.6	7.8	11.3	Reduction with CO at 430°
5	9.3	7.8		Over-all reduction of oxidation state

Adsorption of Oxygen on Nickel Oxide.—An increase of conductance consequent on the adsorption of oxygen is the typical behavior of a p-type semiconductor, and the rate of this conductivity change has been investigated over the temperature interval 200 to 300°. The kinetics for the process have been exhaustively studied, according to the possibilities considered in the preceding paper (Gray and Darby) and shown to be essentially first order for a series of experiments at 295° and 6×10^{-2} mm. pressure, obeying the relation

$$\frac{d\lambda^2}{dt} = K(\lambda_\infty^2 - \lambda_t^2)$$

where λ_∞ represents the conductivity at saturation.

On lowering the pressure, it is observed, from detailed analysis, that both the first-order logarithmic and tangential plots deviate from linearity (toward higher order) at the start of the adsorption. A second-order relation fits the initial portion of the curve more satisfactorily, as shown in Fig. 2 for a pressure of 2×10^{-2} mm. A subsequent first-order stage realized the experimentally observed endpoint, being similar to the results achieved with copper and manganese oxides. A similar effect is obtained when the temperature is lowered, as demonstrated in Fig. 3, for a temperature of 277°. This feature of an initial second-order process changing to a first-order process is characteristic of all the oxides so far investigated although the relative extent of the processes differ considerably and is certainly structure sensitive. The pressure dependence of adsorption process and apparent ac-
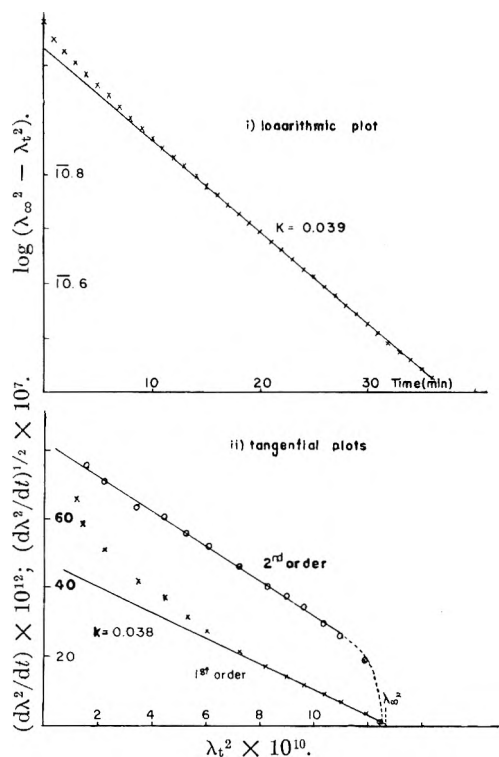
Fig. 2.—Adsorption of O_2 on NiO at 295°; $P = 2 \times 10^{-2}$ mm.

tivation energy of rate-controlling stages of adsorption data has been considered in the preceding paper. The variation in the rate of adsorption with pressure at constant temperature indicates a saturation of the effective sites with oxygen. The first-order velocity constant, K, has been determined for

a series of adsorptions on a film of constant activity and a value of 32 kcal./mole is obtained for the apparent activation energy.

Desorption of Oxygen from Nickel Oxide.— Figures 4, 5 and 6 summarize the kinetic studies for the desorption process. In Fig. 4, the tangential plots for the first-, second- and fourth-order processes are compared for $\lambda \propto N$ kinetics, and in Fig. 5, the same plots are given for $\lambda^2 \propto N$ kinetics. These results indicate a second-order process with the former plot being valid under these conditions. This conclusion has been verified over a large number of desorption plots. The exponential relation is plotted in Fig. 6, and only holds over a very limited region of the desorption process.

The rate of desorption at a given temperature is a function of the pressure employed during the adsorption process. The value of the rate constant, K', where $-d\lambda/dt = K'(\lambda_t - \lambda_\infty)$, depends critically upon the actual conductivity values, and a function of $K'\Delta\lambda$, where $\Delta\lambda = \lambda_0 - \lambda_\infty$, is found to give reproducible results. Values of $K'\Delta\lambda$ and pressure are given in Table II and plotted in Fig. 7.

The rate of desorption at temperatures less than 295° is extremely slow and indicates an apparent activation energy for desorption of the order of 60 kcal./mole.
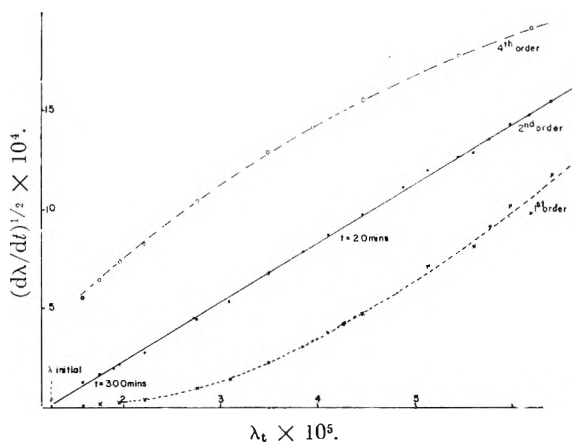
Fig. 4.—Desorption of O_2 from NiO at 295°; 2nd order tangential plot.

Fig. 3.—Adsorption of O_2 on NiO at 277°; $P = 6 \times 10^{-2}$ mm.

Initial conductivity

$\lambda^2 \times 10^{10}$; $(\lambda_t - \lambda_\infty)^2 \times 10^{10}$.
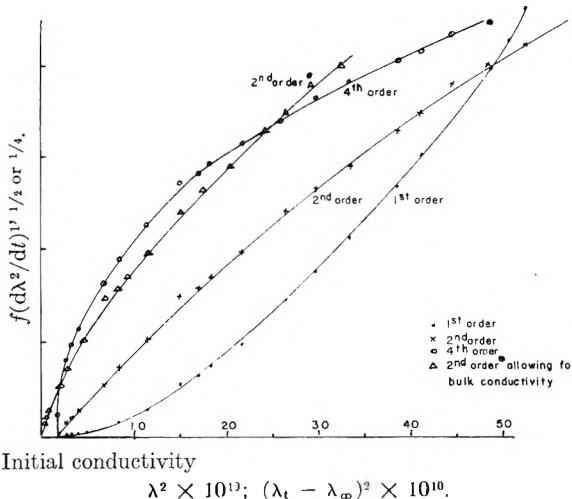
Fig. 5.—Desorption of O_2 from NiO at 295° (λ^2 kinetics)
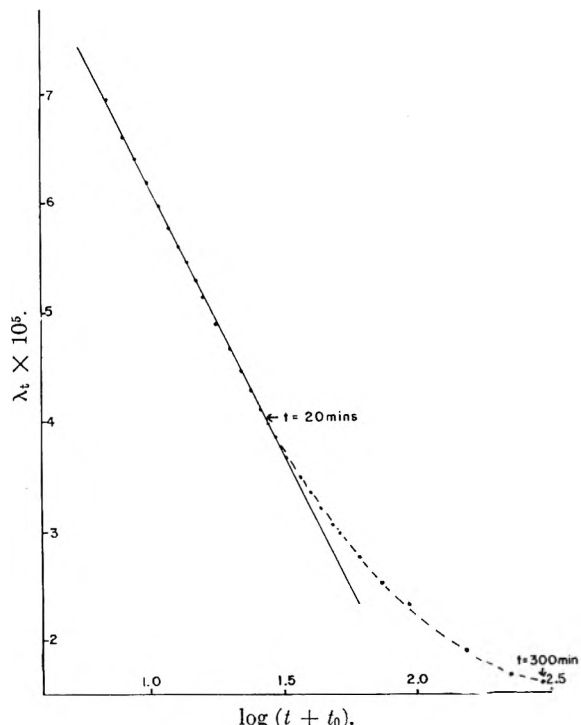
Fig. 6.—Elovich plot for the desorption of O_2 from NiO at 295°.
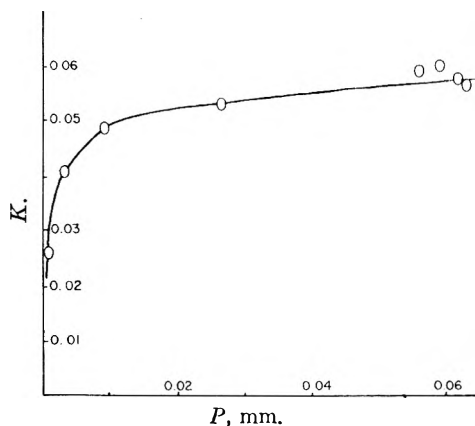
Fig. 7.—Variation of K with pressure at 295° desorption.

Fig. 8.—R.F. discharge applied during O_2 adsorption at 427°.

No readings of resistance can be taken while the discharge is being applied since the measuring devices are affected, but as soon as the discharge is interrupted, the conductivity begins to fall, and in time the normal rate of adsorption is resumed. Figure 9 shows the effect that a radio frequency discharge in the oxygen atmosphere has on the conductivity of an oxygen-covered surface which has reached its equilibrium value. The conductivity is increased as before and on removing the discharge the conductivity is slowly restored to its original value. However, after prolonged treatment, the stationary value of conductivity may be permanently altered. This may be due to oxygen being built into the lattice by this procedure.
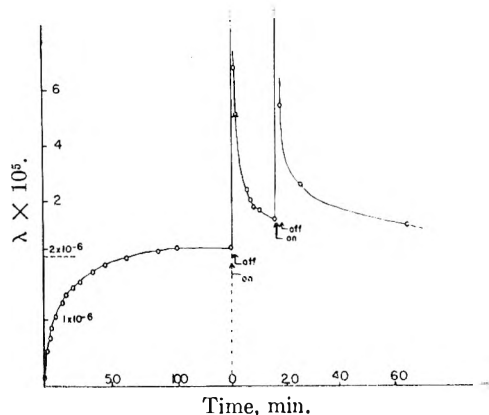
Fig. 9.—R.F. discharge applied to surface saturated with O_2 at 250°.

This effect has been shown to be due predominantly to the oxygen atoms by removing the ions using an electric field and magnetic deflection. It has been extensively employed in the oxidation of those highly annealed films of metal which, in a state of limiting purity, are extremely difficult to oxidize at temperatures up to 500°. By the use of atomic oxygen the rate of oxidation can be increased by several orders of magnitude.

Effect of "Active" Oxygen.—The rate of change of conductivity is very greatly increased by the atomization and ionization of the oxygen gas above the film during the adsorption process. Such an effect is demonstrated in Fig. 8, which shows the normal increase in conductivity with time being suddenly accelerated when a discharge is applied.

Effect of Adsorbed H_2 and CO on the Conductivity of NiO.—Conductivity changes consequent on the adsorption of H_2 and CO on NiO at various temperatures have been determined. Both gases are adsorbed irreversibly and initially give a decreased conductivity. The lowest temperature at which hydrogen has any observable effect on the conductivity is 140°, while for CO a temperature of 200° is necessary. Reduction of the bulk oxide with H_2 occurs at 340°, but no reduction with CO is observed at temperatures up to 430°.

TABLE II

RATES OF DESORPTION OF OXYGEN FROM NiO AT 295°

Pressure of adsorbed gas (mm.)	Rate constant K', for desorption	$K'\Delta\lambda$
0.0634	912	0.0569
.0623	1404	.0579
.0592	2540	.0602
.0561	5960	.0593
.0262	1880	.0528
.0088	2825	.0488
.0033	4190	.0408
.00076	17300	.026

Reactions of Gases Over Nickel Oxide. A.

$$2H_2 + O_2 \longrightarrow 2H_2O$$
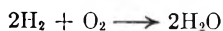
For "less active" film, reaction is only observed at elevated temperatures, but on a sufficiently active film, reaction proceeds readily at room temperature. Rate measurements have even been confined to the range $-21°C$. to $137°$ because of the great speed of reaction at higher temperatures. Both pressure and conductivity changes have been followed for different states of the surface (evacuated, oxygenated and partially reduced oxide), the product being continuously removed by condensation into a liquid oxygen trap. The apparent reaction order is one-half. Using the equation $-dp/dt = K(P_t - P)^{1/2}$ to obtain values for the rate constant K, an activation energy 3.4 kcal./mole is found over the range 0 to $137°$. Data is contained in Table III and in Fig. 10.

TABLE III

Pressure change p (mm.)	Time of half change (min.)	Initial rate $-dp_0/dt$	log $(-dp_0/dt)$	log (Δp)
0.0454	5.8	0.0050	$\bar{3}.699$	$\bar{2}.657$
.0605	7.05	.0062	$\bar{3}.792$	$\bar{2}.782$
.0863	7.3	.0072	$\bar{3}.857$	$\bar{2}.936$
.1000	8.2	.0079	$\bar{3}.898$	$\bar{1}.000$
.1250	9.2	.0082	$\bar{3}.914$	$\bar{1}.097$
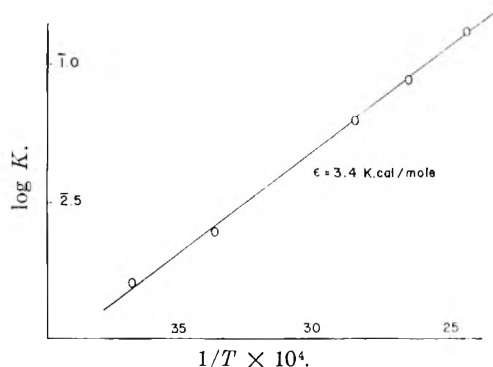
Fig. 10.—Activation energy for reaction $2H_2 + O_2 \rightarrow 2H_2O$.

The dependence of rate on the partial pressures of the individual gases has been determined by varying each component separately. It has been established that the rate of reaction is independent of the hydrogen pressure and proportional to the square root of the oxygen pressure. Whenever an excess of oxygen over stoichiometry is contained in the reaction mixture, the rate of reaction is apparently zero order. If the film is first saturated with oxygen at $300°$ and then cooled to room temperature, after pumping off oxygen the general characteristics for the reaction are unaltered but the rate of reaction is three times as great as over the surface evacuated at a high temperature ($300°$). Alternatively, after reduction with CO at $300°$, the rate of reaction at room temperature is considerably reduced, being only one-tenth of the value for an evacuated surface.

B.—
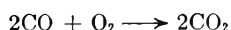
$$2CO + O_2 \longrightarrow 2CO_2$$

This reaction has been studied in the range $200°$ to $300°$, where conductivity and pressure changes can be followed simultaneously. A typical plot for a reaction at $295°$ is given in Fig. 11. The conduc-
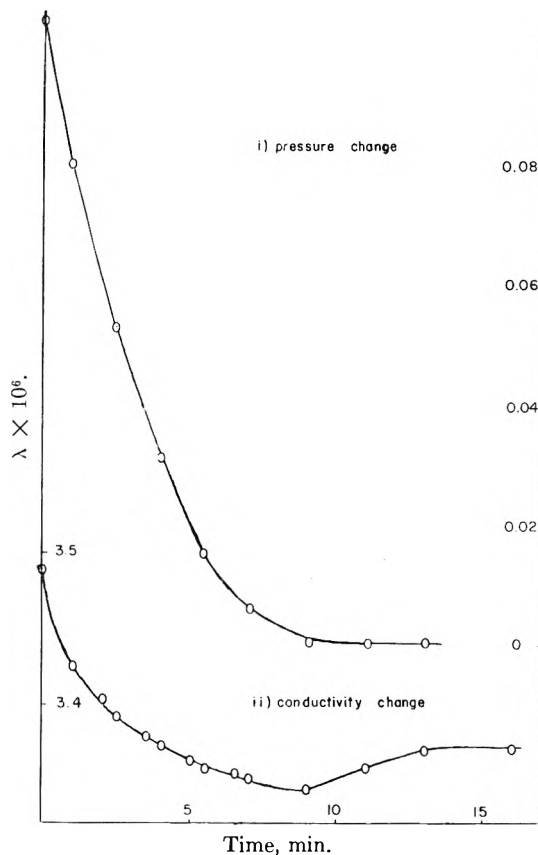
Fig. 11.—$2CO + O_2 \rightarrow 2CO_2$ over NiO at $295°$.

tivity always falls to a minimum and then increases. If an excess of oxygen is used in the gas mixture, the conductivity still falls initially, but then rises beyond its original values as the oxygen adsorption on NiO succeeds the oxidation of CO. The order of reaction has been determined to be one-half and a value of 20 kcal./mole is obtained as the apparent activation energy, as shown in Fig. 12. The dependence of the reaction rate on the partial pressures indicates that the rate is independent of CO pressure. When an excess of oxygen is present, the rate of oxidation increases throughout the reaction. While the initial rates are not strictly reproducible,
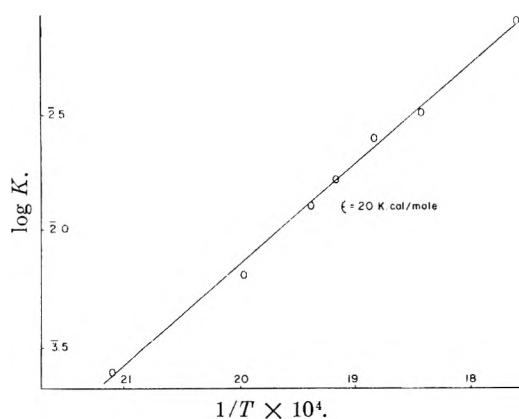
Fig. 12.—Activation energy for reaction $2CO + O_2 \rightarrow 2CO_2$ over NiO.

the maximum rates generally are. In consequence, the dependence of the initial rate on the oxygen pressure cannot be satisfactorily decided. By comparison with the hydrogen–oxygen case, it may be anticipated that the rate of reaction depends solely on the square root of the oxygen partial pressure.

Discussion

Temperature Coefficient of Conductivity.—The activation energy, E, required to produce a positive hole from the defect structure can be derived from the temperature coefficient of the conduction process, according to the approximate relation

$$\sigma = N^{1/2} ev \left(\frac{2\pi m KT}{h^2}\right)^{3/4} e^{-E/2kT}$$

σ = conductivity
N = number of impurity levels
e = electronic charge
v = mobility

The conditions necessary for this relation hold; namely, (i) the number of free electrons, n, is less than N, (ii) n is sufficiently small that the system is non-degenerate, (iii) that $E >> 2KT$ are satisfied here.

The results obtained have suggested that the values of E (equal to twice the E_x plotted experimentally) depend on the previous history of the film to a considerable extent. The activation energy over an evacuated surface has been found to fall from 1.24 to 0.8 e.v.; and appears to be gradually approaching the value of 0.67 e.v. recorded for an oxygen-covered surface, suggesting that some irreversible oxygen uptake occurs during a series of adsorptions and desorptions of gas. Partial reduction of the oxide surface increases the activation energy to as much as 2 e.v. These effects may be interpreted in terms of a model in which the activation energy is a composite of the energy for a bulk region reduced by a surface zone having under oxygen saturated conditions quasi-metallic properties with an almost zero activation energy, the thickness of this surface zone being temperature-dependent and structure sensitive.

A number of authors have presented data relating to the activation energy of conductivity for NiO. The relevant information is summarized in Table IV.

The effects of heating in air or *in vacuo* have not been sufficiently emphasized by the various authors. Those samples prepared at high temperatures *in vacuo* and for which the conductivity measurements have been made without removal from vacuum may be expected to have a composition close to stoichiometric NiO. The values 1.2 to 1.8 e.v. (Harwood, Herzfeld and Martin) and 1.25 e.v. (Takeuchi and Igaki) for samples thus treated agree well with the value of 1.25 e.v. obtained by the present authors on a freshly oxidized NiO film where the composition is expected to be very nearly stoichiometric NiO.

Samples heated at a high temperature in air or in oxygen and then cooled in such an atmosphere, have smaller temperature coefficients and, below 300°, have values of E between 0.3 and 1.1 e.v. The actual values are influenced by the temperatures of preparation, as is indicated in the results of Foex which suggest that samples prepared below

TABLE IV
COLLECTED RESULTS OF ACTIVATION ENERGY OF CONDUCTIVITY CHANGE IN NiO

Details of prep. of NiO	Activation energy values (e.v.)	Ref.
	0.95–1.17 (300–600°)	7
Heating Ni strip in air at 1000°	1.88–2.16 (300–700°)	10
Heating NiO pellet in air at 1000°, measure in air	0.90–0.96 (500–830°)	11
Heating NiO pellet *in vacuo* at 1000°, measure *in vacuo*	1.24–1.82 (850–1280°)	11
Oxidizing Ni wire at 1000° measuring at different P_{O_2} values	For P_{O_2} = 0, 1.25 P_{O_2} = 1 at., 0.63 (500–1000°)	6
Decompn. of Ni(NO₃)₂ At 500°	0.72 (below 250°) 0.63 (above 250°)	12
At 600°	0.80 (below 250°) 0.49 (above 250°)	
At 1400°	1.11 (below 250°) 0.55 (above 250°)	
"Green" NiO	P_{O_2} = 10⁻³ mm., 0.66 = 100 mm., 0.80 (200–550°)	8
"Black" NiO	0.55 (20–550°)	
Evap. film of Ni oxidized to NiO, heated to max. 300°	1.92 (above 190°) 0.58 (below 190°) (*in vacuo*)	Derry (Ph.D. Thesis, Bristol 1954)
Similar evap. films heated to max. of 400°	0.78–1.25 (below 300° (*in vacuo*) 0.67 (below 300°) P_{O_2} = 10⁻² mm.	Present authors
Thermal decompn. of carbonate or oxalate with sintering at 1100° and more in reducing atm.	Measured in air 0.85–0.93 (80–700°)	13
Thermal decompn. of Ni(NO₃)₂, sintered at 1200° in oxygen atm.	0.69 (20–250°)	13
Single crystal NiO	0.75 (20–300°)	13

500° should not show any change in activation energy at 250°. These results are in accord with the hypothesis of Nijboer[17] who postulated that, on cooling from a high temperature, defects would be frozen into the lattice. From this concept, Nijboer developed a theory which predicted that a change in slope of the temperature coefficient would occur at a certain temperature and that the activation energy below this temperature would be exactly one-half of its value above this temperature.

The conclusion reached from this analysis is that for nickel oxide, free from foreign impurities, the activation energy is due to a single-type-impurity conduction and for stoichiometric NiO will be at least 1.25 e.v., and possibly even as high as 2.0 e.v. Experimental values will depend critically on the temperature of preparation and gas atmosphere present during preparation and measurement. The structure-sensitive low temperature activation energy is a composite of a constant activation energy for the bulk material modified by an activation energy for the surface zone, variation in the latter ac-

(17) B. R. A. Nijboer, *Proc. Phys. Soc.*, **51**, 575 (1939).

counting for the variation in the experimental values.

Evidence for this concept is provided in results on manganese oxide where a change in slope of the temperature coefficient of conductivity occurs at about 120°. Below this temperature the activation energy over an evacuated surface is considerably reduced, and disappears completely for an oxygen covered surface. This is interpreted as the surface conduction predominating in this temperature range to such an extent that the bulk conductivity is negligible in comparison. It is thought that the observation of such an effect in manganese oxide alone among the oxides studied may be due to a combination of a higher specific resistance and a larger temperature coefficient is the average.

Oxygen Adsorption and Semi-conductivity of Nickel Oxide.—The reversible chemisorption of oxygen on a nickel oxide surface has been demonstrated over the temperature range 200–300°, the conductivity change on adsorption obeying a unimolecular law, indicating that the rate-determining step in the surface process is of first order. The corresponding desorption stage involves a rate-determining step of second order.

The form of the curve, expressing the rate of change of conductivity on oxygen adsorption with pressure of adsorbed gas, resembles a Freundlich isotherm, and the approach of the rate constant to a limiting value is interpreted as being a saturation of the available sites on the surface with oxygen. The process of adsorption may be divided into several distinct stages, ending with the formation of an oxygen ion on the surface. The various stages may be considered as the initial adsorption, the dissociation of adsorbed molecules and the surface diffusion of gas atoms or ions, with or without solution in the interior. Any one of these stages may be rate determining, though the over-all rate may be determined by several of these stages.

In a kinetic study based on semi-conductivity measurements, only those stages involving electron transfer are of immediate significance. The theoretical considerations have been discussed previously (Gray and Darby). Activation energies deduced from kinetics determined in this manner are in general designated "apparent" activation energies. The temperature coefficients for the oxides in a stationary state (E_t) represent the energy necessary for the production of a current carrier. However, the apparent activation energy, E_r, deduced from the reaction kinetics is related to the over-all process of adsorption dissociation, diffusion and building into the lattice complicated by a change in E_t between the initial and final stationary states. In a typical adsorption of oxygen on nickel oxide E_t commences approximately 18 kcal. for the evacuated surface and falls to approximately 15.6 kcal. for the oxygen saturated surface while the corresponding apparent activation energy for the reaction process is experimentally 32 kcal./mole. In certain instances where second-, first- and zero-order reactions can be followed consecutively by both conductivity and gas adsorption measurements, then this apparent activation can be further broken down into its component parts. Sufficient

experimental results are not at present available to justify amplification at this juncture.

The dissociation of molecular oxygen in the gaseous phase requires 117 kcal./mole. If the gas is chemisorbed in an atomic or ionic form, it is important to know whether the act of adsorption requires an activation energy. Roberts and Anderson[18] have found that oxygen is chemisorbed very rapidly on UO_2 at liquid air temperature and that the number of molecules adsorbed is about one-half of the number of N_2 molecules physically adsorbed by the same surface. The adsorption of oxygen thus has the characteristics of an unactivated process, yet the gas is bound in atomic form. Stone and Tiley,[19] studying the adsorption of oxygen on Cu_2O at room temperature, obtain a $p^{1/2}$ relationship, suggesting that dissociation has occurred prior to the rate-determining step, and that an equilibrium $O_2 \rightleftarrows 2O$ is established on the surface.

There is strong evidence that initially the ion formed is O^- and not O^{2-} or O_2^- since only the O^- is formed exothermically (approx. 8 e.v.). Subsequently, another electron may be extracted from the surface for the formation of O^{2-} which is only stable in a strong electric field. In the interior of the oxide O^{2-} is stabilized by the strong field of the cations, but at the surface, the positive force field may be inadequate for stability. Magnetic susceptibility measurements on cuprous oxide (Fensham[20]), showed that when O_2 was adsorbed, the susceptibility first increased to a maximum then fell to its original value (within the experimental error). The magnitude of the change was such that it could only be accounted for if either O, O^- or both were formed. The subsequent decrease in x is interpreted as $O^- \rightarrow O^{2-}$ for which the rate will increase with the temperature, a fact which was verified by Fensham. The adsorption of oxygen is accompanied by an electron transfer producing O^- ions and positive holes, the former confined to the surface, the latter diffusing to some extent, into the interior, leaving a negative charge at the surface. The potential gradient thus set up aids in the diffusion of Ni^{2+} to the surface, and O^- is built into the surface as O^{2-} ions. This is essentially similar to the oxidation process as considered by Mott and Cabrerra.[21] From a series of experiments for adsorptions on NiO at room temperature, Dell and Stone[15] have concluded that the high reactivity of adsorbed oxygen toward CO and CO_2 is associated with the O' ion or oxygen atom since conversion to O^{2-} is very slow at room temperature.

Considering the nickel oxide system further, the adsorption is probably a rapid equilibrium process, the equilibrium being determined by the pressure of oxygen. The availability of Ni^{2+} ions is probably the most important rate-determining factor and will depend on the extent to which conversion to Ni^{3+} has occurred; a stationary value of equilibrium occurs when all the available Ni^{2+} sites in the surface region are saturated. The diffusion step may

(18) L. E. J. Robert and J. S. Anderson, *Rev. Pure App. Chem.* (*Australia*), **2**, 1 (1952).

(19) F. S. Stone and P. Tiley, *Disc. Faraday Soc.*, No. 8, 254 (1950).

(20) P. J. Fensham, Ph.D. Thesis, Bristol, 17 (1952).

(21) N. F. Mott and N. Cabrera, *Repts. Progr. Phys.*, **12**, 163 (1949).

also be activated and the increase in the rate of change of conductivity with increased oxygen pressure may be a function of the diffusion rate; more oxygen is available on the surface and so the chance of meeting an Ni^{2+} ion is increased. The reaction of oxygen with an Ni^{2+} ion can be represented in several ways

(a)
$$O_2 \rightleftarrows 2O$$
$$O + Ni^{2+} \rightleftarrows O^- + Ni^{2+\oplus}$$
$$O^- + Ni^{2+} \rightleftarrows O^{2-} + Ni^{2+\oplus}$$

(b)
$$O_2 + 2Ni^{2+} \rightleftarrows 2O^- + 2Ni^{2+\oplus}$$
$$2O^- + 2Ni^{2+} \rightleftarrows 2O^{2-} + 2Ni^{2+\oplus}$$

(c)
$$O_2 + Ni^{2+} \rightleftarrows O_2^- + Ni^{2+\oplus}$$
$$O_2^- + Ni^{2+} \rightleftarrows 2O^- + Ni^{2+\oplus}$$
$$2O^- + 2Ni^{2+} \rightleftarrows 2O^{2-} + 2Ni^{2+\oplus}$$
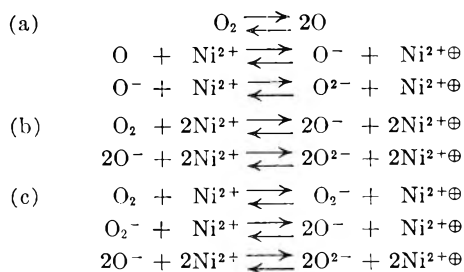
where $Ni^{2+\oplus}$ represents a positive hole. The third of these possibilities is not very likely since the initial step is energetically improbable. Considering possibility (a), for a steady concentration of oxygen atoms on the surface, the availability of Ni^{2+} becomes rate determining, leading to a first-order rate expression for the conductivity change with time. In (b) the initial step will be of second order while in both cases the subsequent step leading to the formation of O^{2-} ions is first order.

Since a combination of second- and first-order kinetics are actually observed the second proposal is favored. This is also in accord with the desorption process where we have

$$2O^{2-} + 2Ni^{2+\oplus} \rightleftarrows 2O^- + 2Ni^{2+}$$
$$2O^- + 2Ni^{2+\oplus} \rightleftarrows O_2 + 2Ni_2^+$$
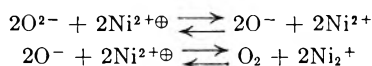
the latter being second order and rate determining as observed experimentally.

In conditions where the first stage of the adsorption process becomes very rapid the over-all kinetics are of first order. This is the case at higher temperatures and with very active films. The results obtained correspond very nearly with those on cuprous oxide and manganese oxide where second-order kinetics are followed by first order, the extent to which each occurs being temperature, pressure and structure sensitive. In the case of many films of cuprous oxide the first stage

$$O^2 + 2Cu^+ \rightleftarrows 2O^- + 2Cu^{++}$$
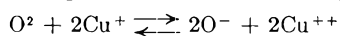
is rate determining over most of the reaction while in others the extent of the reaction over which the second-order relationship holds can be varied as low as 10% of the total reaction.

By developing a composite model for a two-zone system as considered elsewhere (Gray and Darby) it can be established that successive reactions of this character would account exactly for the observed changes in the conductivity. Owing to the complexity of the model and the difficulty in determining experimental values at lower temperature it has not been possible to obtain exact quantitative verification of this hypothesis.

Reactions of Gases over Nickel Oxide.—The rate of reaction of hydrogen over nickel oxide is such as to restrict measurements to temperatures below about 140°. It has been established that the apparent activation energy is 3.4 kcal./mole which

is significantly smaller than that for the oxygen adsorption process which would be anticipated from the results obtained at higher temperatures as being approximately 18 kcal./mole. The great increase in rate occurring over an oxygen saturated surface indicates that the dissociation of oxygen is probably rate determining and the reaction may be considered as taking place simultaneously with the first stage of adsorption process

$$O_2 + 2Ni^{2+} \rightleftarrows 2O' + 2Ni^{2+\oplus}$$
$$O' + Ni^{2+\oplus} + H_2 \rightleftarrows H_2O - Ni^{2+}$$
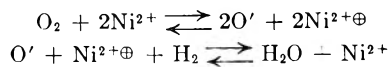
the latter having a much lower activation energy than the second stage of the oxygen adsorption process.

In the case of the oxidation of carbon monoxide no appreciable reaction occurs below 200°. Above this temperature the initial rate depends on the square root of the oxygen pressure, is independent of the carbon monoxide pressure and has an activation energy of 21 kcal./mole.

Dell anticipated the work of Parravano[22] who has indicated that there are two regions with different activation energies for this reaction. Below 180° the activation energy is given as 2 kcal. and above this temperature as 18 kcal. The discrepancy between these results and those obtained in the present research lies in the nature of the material. Since these thin films are significantly more active than the powders used by Parravano, the CO_3 complex which Dell has demonstrated as being stable to approximately 180–200° does not decompose to desorb CO_2 and hence there is no significant reaction once the active sites are saturated. It is interesting to observe that the activation energy for the reaction above 200° is in satisfactory agreement with the values obtained by Dell[15] and Schwab.

The reaction can be understood as deriving from the initial adsorption and dissociation of oxygen followed by the reaction of the carbon monoxide with the O^- ion.

$$O_2 + 2Ni^{2+} \rightleftarrows 2O' + 2Ni^{2+\oplus}$$
$$CO + O' + Ni^{2+} \rightleftarrows CO_2 + Ni^{2+}$$
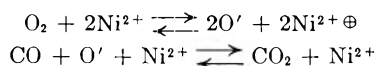
So
$$\frac{d(CO_2)}{dt} = \frac{K(CO)(O')(Ni^{2+\oplus})}{(Ni^{2+})}$$
$$= K'(CO)(O_2)^{1/2}$$

Since
$$(O') \alpha \frac{(O_2)^{1/2}(Ni^{2+})}{(Ni^{2+\oplus})}$$

Experimentally it is found that the rate is proportional to the root of the oxygen pressure which indicates that the former reaction must be rate determining. Additionally the decrease in conductivity indicates the extent to which this is more rapid than the oxygen adsorption and dissociation, the conductivity only recovering when the excess of oxygen takes control.

The further significance of this approach to the problem is indicated by the work of Schwab[16] and Parravano[22] who applied the principle of controlled valency to increase or decrease the equilibrium number of $Ni^{2+\oplus}$ positive holes present. They

(22) G. Parravano, *J. Am. Chem. Soc.*, **75**, 1448 (1953).

were able to show that an increase in number of positive holes caused by the introduction of Li^+ ions correspond with a decrease in the activation energy for the oxidation of carbon monoxide to about 12 kcal./mole, whereas a reduction in this number by the introduction of Cr^{3+} ions raised the activation energy to 24–26 kcal./mole.

Conclusion

It has been established that the adsorption of oxygen on nickel oxide is a complex process best described by two expressions covering the adsorption of molecular oxygen and dissociation to O^- ion followed by a second stage in which the oxygen reverts to the O^{2-} state. Both of these occur accompanied by a change in semi-conductivity which may be used to determine the detailed kinetics. The most probable kinetics evolved are consecutive second- and first-order reactions, the relative significance being structure, temperature and pressure sensitive. The general model gave qualitative agreement with the reactions between gases over the oxides while the variations due to oxidation state or controlled valency emphasize the significance of the defect state in catalytic reactions.

THE CONDUCTANCES OF SOME SIMPLE ELECTROLYTES IN AQUEOUS SUCROSE SOLUTIONS AT 25°

By Jean M. Stokes and R. H. Stokes[1]

Contribution from the Chemistry Department of the University of Western Australia, Nedlands, Western Australia

Received July 11, 1955

The conductances of seven uni-univalent electrolytes in 10 and 20% aqueous sucrose solutions are measured at concentrations up to ~0.05 N. The concentration-dependence is accurately described by the modified Onsager equation proposed by Robinson and Stokes[2]; the ion size parameters required are the same in the sucrose solutions as in water. The limiting equivalent conductances are determined, and their ratios to the corresponding values in water are found to be nearly independent of the nature of the salt. These ratios are however not equal to the ratios of the fluidities of the sucrose solutions and water.

Introduction

A major difficulty in the theoretical treatment of conductance and diffusion in concentrated electrolyte solutions arises from uncertainty about how to allow for the effect of the changing viscosity of the solution on the mobility of the ions. Recent developments of the interionic attraction theory have largely removed the restriction of its range of validity to the "limiting-law" region below 0.01 N, at least in the case of uni-univalent electrolytes, and the viscosity problem now takes on increasing importance. We are therefore making a series of investigations aimed at elucidating the relation between viscosity and ionic mobility. The present paper deals with conductance in aqueous sucrose solutions, sucrose having a marked effect on the viscosity; later work will deal with other added non-electrolytes in a similar way, and with the effect of high salt concentrations on the mobility of non-electrolytes in diffusion.

Experimental

Most of the conductance measurements here reported were made with a Leeds & Northrup Jones conductance bridge, but those on potassium chloride in 20% sucrose and on sodium chloride in 10 and 20% sucrose were made earlier using a bridge built up from a calibrated Pye P.O. box. Subsequent checks with the Jones bridge showed that these earlier results were correct within 0.03%, which is remarkably good considering that the P.O. box can hardly have been designed as an a.c. bridge. The conductance cells were of orthodox design, except that the troublesome mercury-filled lead-in tubes were eliminated, heavy silver wires being welded to the platinum wires beyond the seals and taken through glass tubes to well separated points above the thermostat level. Lead resistances were measured and allowed for. The cells being of Pyrex, some difficulty was experienced in producing completely tight seals to the platinum electrodes; this was overcome by introducing a small amount of "Araldite"[3] thermosetting resin on the side of the seal remote from the cell contents and polymerizing it *in situ*. The cells were used in a 25° oil-thermostat of 90-l. capacity, controlled by a toluene-filled regulator consisting of a helix of 4 meters of copper tubing of 8 mm. internal diameter, joined by "Araldite" to a glass portion with the usual mercury contacts. This type of regulator has a very rapid response and easily maintains a constancy of 0.002°.

The cells were calibrated with the Jones and Bradshaw[4] 0.01 and 0.1 demal potassium chloride solutions. Since nearly all the literature data of the past twenty years are based on these standards, which are given in terms of the old International Ohm unit of resistance, the conductances reported here are *not* converted to the new absolute ohm basis. Frequency-dependence was negligible in the range 500–2000 cycles/sec.

Materials.—Doubly distilled water with a specific conductivity 1.2×10^{-6} ohm^{-1} cm.$^{-1}$ was used throughout. A.R. sucrose was dried in a vacuum desiccator and used without further purification to make solvents containing 10.00 and 20.00% of sucrose by weight. The composition of these was checked by accurate density measurements. The sucrose solutions were prepared in 1-kg. batches and used within a day or two of preparation, being stored in a refrigerator when not in actual use. The specific conductivity of each batch was measured and allowed for in the usual way. It was however relatively high, about 4×10^{-6} ohm^{-1} cm.$^{-1}$ for the 10% solutions and 6×10^{-6} ohm^{-1} cm.$^{-1}$ for the 20% solutions. Later, commercial loaf sugar was used in place of the A.R. material; this gave a specific conductivity about 50% higher, but the densities and viscosities were indistinguishable from those of the A.R. material,

(1) Chemistry Department, University of New England, Armidale, New South Wales.

(2) R. A. Robinson and R. H. Stokes, *J. Am. Chem. Soc.*, **76**, 1991 (1954). See also Robinson and Stokes, "Electrolyte Solutions," Butterworths, 1955.

(3) Ciba Pty., Basle.

(4) G. Jones and B. C. Bradshaw, *J. Am. Chem. Soc.*, **55**, 1780 (1933).

as were the equivalent conductivities obtained using it. The comparatively high solvent conductivity precluded useful measurements at concentrations below 0.005 N, where the solvent correction was already about 1% of the measured conductivity; but the present state of theory is such that reliable extrapolations can be made from the region studied without the need for measurements at extreme dilutions.

Potassium Chloride.—B.D.H. "Analar" salt was once recrystallized from conductivity water, and dried first in a vacuum desiccator and then overnight at 400°.

Sodium Chloride.—The "Analar" salt was dried in the furnace at 400°. Results were indistinguishable from those obtained with a sample further purified by precipitation by HCl gas.

Potassium Bromide.—The "Analar" salt was once recrystallized, dried in a vacuum desiccator and then at 400°.

Potassium Iodide.—The "Analar" salt was once recrystallized, dried in a vacuum desiccator and then at 120° overnight.

Potassium Nitrate.—The "Analar" salt was once recrystallized, dried in a vacuum desiccator, then in the oven at 120° and finally at 240°.

Silver Nitrate.—A freshly opened sample of the "Analar" salt was recrystallized and dried in the dark in a vacuum desiccator for some days. When nearly dry the salt was pulverized in an agate mortar and dried to constant weight in the vacuum desiccator. Oven-drying, even at 120°, caused a brownish discoloration.

Lithium chloride was made by passing carbon dioxide through a solution of laboratory grade lithium hydroxide, then dissolving the carbonate in freshly distilled hydrochloric acid. The solution was filtered off from a slight excess of undissolved carbonate, boiled for some time and allowed to crystallize. The crystals were quickly filtered off on a sintered funnel. A stock solution of this product was analyzed for chloride by potentiometric titration.

The purity of these salts was checked by comparing the conductivity of aqueous solutions of known concentration (usually 0.05 N) with the values given in the literature.[5-8] Agreement was within 0.03% except in the cases of potassium bromide where our results were 0.07% *lower* than those of Shedlovsky[7] but 0.10% *higher* than those of Jones and Bickford,[8] and of silver nitrate where our value was 0.05% lower than that of Shedlovsky whose material was fused.

From the pure dry salts or from the stock solution in the case of lithium chloride, solutions were prepared containing a few parts per cent. of salt in solvents consisting of 1 part sucrose to 9 and 4 parts, respectively, of water by weight. From these, solutions of the concentrations shown in Table I were made by weight dilution with the 10 or 20% sucrose solutions. The densities of these final solutions, required for the calculation of the molarity, were obtained as follows: from the International Critical Tables, the density increment for the addition of a small percentage of the salt to pure water at 25° was found. It was then assumed that the same increment would hold for the addition of the salt to a sucrose solution. Pycnometric checks in a few cases verified that this procedure gave densities correct within 0.02% at the highest concentrations used for the conductivity measurements. (Even if the errors were greater than this, they would not affect the Λ^0 values, as the error would extrapolate out.)

Results and Limiting Conductances

Table I gives the equivalent conductivities at the experimental concentrations. The concentration dependence can be described accurately, except for potassium nitrate, by the equation[2]

$$\Lambda = \Lambda^0 - \frac{B_1\Lambda^0 + B_2}{1 + Ba\sqrt{c}}\sqrt{c} \qquad (1)$$

where B_1, B_2 and B are theoretical constants involving solvent properties and the temperature,

(5) T. Shedlovsky, *J. Am. Chem. Soc.*, **54**, 1411 (1932).

(6) B. B. Owen and H. Zeldes, *J. Chem. Phys.*, **18**, 1083 (1950).

(7) Unpublished but quoted by D. A. MacInnes, "Principles of Electrochemistry."

(8) G. Jones and C. F. Bickford, *J. Am. Chem. Soc.*, **56**, 602 (1934).

TABLE I

Equivalent Conductivities of Salts in Aqueous Sucrose Solutions at 25°

c, mole/l.	Λ, ohm^{-1} mole^{-1} cm.^{2}	c, mole/l.	Λ, ohm^{-1} mole^{-1} cm.^{2}
A, solvent, 10% sucrose			
LiCl		KI	
0.05129	81.30	0.05064	108.76
.03076	83.46	.02713	111.24
.012811	86.34	.009317	114.72
.004544	88.96	.005638	115.97
NaCl		KNO$_3$	
0.10983	86.53	0.04582	103.23
.07088	88.69	.03194	105.30
.03876	91.55	.02103	107.43
.011886	95.90	.009140	110.67
.006300	97.59	.006883	111.56
KCl		.005623	112.29
0.04604	109.16	AgNO$_3$	
.02890	111.23	0.05167	92.93
.009269	115.42	.03747	94.81
.004764	117.12	.01816	98.39
KBr		.008098	101.22
0.07164	108.38		
.03225	112.09		
.015616	114.81		
.008691	116.63		
B, solvent, 20% sucrose			
LiCl		KI	
0.04748	63.21	0.04563	83.68
.02666	64.94	.03198	84.74
.01748	65.99	.02158	85.83
.009470	67.42	.011061	87.41
NaCl		.006226	88.57
0.09581	67.57	KNO$_3$	
.05622	69.84	0.04822	79.59
.03577	71.27	.03029	81.57
.02157	72.86	.016555	83.84
.007430	75.25	.010042	85.17
KCl		.007056	86.08
0.05935	83.81	.003784	87.30
.04189	85.06	AgNO$_3$	
.015123	88.20	0.09899	68.00
.008515	89.68	.05260	71.34
KBr		.03026	73.70
0.07744	83.45	.02777	74.08
.03824	85.90	.02055	75.08
.02559	87.10	.013894	76.32
.012900	89.14	.008497	77.66
.007309	90.30		

given in Table II. In order to determine Λ^0, this equation is rearranged to

$$\Lambda^0 = \Lambda + \frac{B_1\Lambda + B_2}{1 + (Ba - B_1)\sqrt{c}}\sqrt{c} \qquad (2)$$

The best value of the ion size parameter a is then found by trial. Just as in the case of the Debye–Hückel activity coefficient formula, this "best value" depends slightly on the range of concentration covered by the data used in its determination. However, deviation plots, in which the right-hand side of equation 2 is plotted against the molarity c,

TABLE II

SOLVENT PROPERTIES AND CONSTANTS OF EQUATIONS 1 AND 2 FOR 25°

d = density, ϵ = dielectric constant, η = viscosity.

	Water	10% Sucrose	20% Sucrose
d, g. ml.$^{-1}$	0.99707	1.03679[a]	1.07940[a]
ϵ	78.5$_4$	76.2$_0$[b]	73.6$_6$[b]
η, poise	0.008937	0.01183[c]	0.01704[d]
B_1, mole$^{-1/2}$ l.$^{1/2}$	0.2289	0.2394	0.2529
B_2, ohm^{-1} mole$^{-3/2}$ cm.^{2}, l$^{1/2}$	60.32	46.3$_2$	32.6$_7$
$10^{-8} B$, mole$^{-1/2}$ cm.$^{-1}$ l$^{-1/2}$	0.3286	0.3336	0.3393

[a] Landolt–Bornstein "Tabellen," Vol. I, Julius Springer, Berlin, 1923, p. 463. [b] C. G. Malmberg and A. A. Maryott, *J. Research Natl. Bur. Standards*, **45**, 299 (1950). [c] This research. [d] E. C. Bingham and R. F. Jackson, *Bull. Bur. Stds.*, **14**, 59 (1918–1919).

show that for the present concentration range of about 0.005 to 0.05 M the same a parameter is valid for the sucrose solutions as for water as solvent. (In this range, a change of 0.1 Å. in a makes a detectable difference to the constancy of the Λ^0 values.) The a values used here are up to 0.5 Å. greater than those found in an earlier investigation of solutions in water, in which the concentration range was 0.0001 to 0.01 or 0.02 M. The Λ^0 values obtained by equation 2 for solutions in water, using literature data between 0.005 and 0.05 M, are in some cases a little different from the accepted values. While the discrepancy is not serious, it suggests that the Λ^0 values obtained for the sucrose solutions may be subject to errors of about 0.05%.

Potassium nitrate and silver nitrate, both in water and in the sucrose solutions, do not conform as accurately to equation 2 as do the alkali halides; this effect is attributed to ion association. Satisfactory Λ^0 values can however be obtained by using equation 2 as an extrapolation function, employing an ion size $a = 1.6$ Å.

and Jones and Bickford[8] (which are all in good agreement) were used.

Discussion

The fact that the same value of a holds for a given salt in water and in the sucrose solutions is further evidence for the soundness of equation 1. It is unlikely that the large sucrose molecule can attach itself to an ion with the firmness that the water molecule can, and though some degree of ion–sucrose interaction seems possible, it must be recognized that the sucrose molecules are greatly outnumbered by water molecules, being present in the ratio of only 1 to 76 even in the 20% solution. Hence the solvent remains essentially water. Table II shows that the dielectric constant is not greatly affected by the sucrose, though the viscosity is nearly doubled in the 20% solution. It thus seems likely that the ions retain much the same state of solvation as they have in water.

The most important conclusion to be drawn from the results is however that the reduction of the limiting mobility by a given sucrose addition is to a first approximation in the same proportion for all the ions studied: the ratio Λ^0 (sucrose)/Λ^0 (water) varies only from 0.805 to 0.814 for 10% sucrose, and from 0.615 to 0.629 for 20% sucrose. Thus all the ions are retarded to approximately the same extent. This clearly suggests that the retardation is largely of a non-specific frictional nature. It is however less than that corresponding to the change in bulk viscosity produced by the sucrose, the relative fluidities being 0.756 and 0.525 for the 10 and 20% solutions, respectively. There is rough agreement with the 0.7 power of the fluidity, as proposed long ago by Heber Green,[10] but this relation has no theoretical background. It must of course be clearly understood that this conclusion, being based on the limiting values of the equivalent conductances at infinite dilution, is not subject to any consideration of ion–ion interactions.

TABLE III

LIMITING EQUIVALENT CONDUCTANCES OF ELECTROLYTES IN SUCROSE SOLUTIONS AT 25° AND THEIR RATIOS TO CORRESPONDING VALUES IN WATER

Λ^0 = limiting equivalent conductance; a = ion size parameter (eq. 1 and 2); η = viscosity of sucrose solution; η^0 = viscosity of water.

Salt	$10^8 \times a$, cm.	Λ^0 (10% sucrose), ohm^{-1} mole^{-1} cm.^{2}	Λ^0 (20% sucrose), ohm^{-1} mole^{-1} cm.^{2}	$\dfrac{\Lambda^0 (10\%)}{\Lambda^0 \text{ (water)}}$	$\dfrac{\Lambda^0 (20\%)}{\Lambda^0 \text{ (water)}}$
LiCl	4.0	93.1$_9$	71.7$_4$	0.810$_4$	0.623$_9$
NaCl	3.8	102.7$_0$	79.3$_0$	.812$_5$	.627$_4$
KCl	3.8	121.8$_7$	94.2$_6$	.813$_5$	.629$_2$
KBr	4.4	122.8$_6$	94.5$_3$	.810$_3$	.623$_5$
KI	5.0	120.9$_7$	92.4$_4$	.804$_6$	.614$_7$
KNO$_3$	(1.6)	117.6$_5$	90.7$_0$	.811$_6$	.625$_7$
AgNO$_3$	(1.6)	107.4$_6$	82.2$_5$	.805$_6$	.616$_6$

$\eta^0/\eta = 0.756$ $\eta^0/\eta = 0.525$

The Λ^0 values for the seven salts studied are compared in Table III with those obtained for aqueous solutions in the same concentration range. The latter were calculated by equation 2 from the data of Shedlovsky, except for potassium bromide where the data of Benson and Gordon,[9] Owen and Zeldes,[6] and Jones and Bickford[8] (which are all in good agreement) were used.

That specific effects of the order of 1% are also operative is apparent from Table III. At a given sucrose content, iodide ion is more retarded than bromide, bromide than nitrate and nitrate than chloride; while among the cations the order of decreasing retardation is silver, lithium, sodium, potassium. The further consideration of these small

(9) G. C. Benson and A. R. Gordon, *J. Chem. Phys.*, **13**, 473 (1954).

(10) W. Heber Green, *J. Chem. Soc.*, **93**, 2049 (1908).

specific effects is best deferred until measurements of some transport numbers in the sucrose solutions have been completed; this will make possible the examination of the effects on a single-ion basis. Some preliminary measurements on hydrochloric acid in 10% sucrose indicate a limiting conductiv-

ity of about 357 ohm^{-1} mole^{-1} cm.^{2}, corresponding to a ratio (Λ^0 (sucrose)/Λ^0 (water)) of 0.838. It thus appears that the hydrogen ion is less retarded than other simple ions, which is consistent with the accepted view that it moves by an essentially different mechanism.

SORPTION OF AMMONIA BY DEHYDRATED POTASH ALUM

By G. W. Benson[1] and F. C. Tompkins

Chemistry Department, Imperial College of Science and Technology, London, S.W. 7

The kinetics of sorption of ammonia by dehydrated potash alum crystals has been studied between 35.6 and 57.7° in the pressure range 1–30 cm. The amount sorbed at constant pressure and temperature is a linear function of (time)$^{1/2}$ but a process either of diffusion into non-interconnecting channels or of diffusion from a network of interconnecting channels into spherical zones has proved inadequate. A theory based on the presence of two different categories of sorption sites, and the replacement of residual water by ammonia molecules, however, has proved adequate in explaining the main experimental results.

Introduction

Certain hydrated salts, on being heated *in vacuo*, lose all or part of their coördinated water molecules of hydration to give a skeleton lattice which collapses, either into an assembly of microcrystals with dimensions less than those necessary for an X-ray diffraction pattern, or into a highly disordered lattice of higher free energy than that of the corresponding microcrystalline form.[2] The structure of this product has a marked influence on the rate of dehydration[3] of the parent hydrate since loss of water proceeds preferentially at the dehydration interface, consequently further information concerning the nature of the product would undoubtedly assist in our understanding of the dehydration process.

The sorption of gases and vapors by the dehydrated solid has provided valuable data in the case of zeolites and clays[4], but there have been few investigations of the "simpler" dehydrated hydrates.[5] The entropy and enthalpy of the transition of "disordered" $CuSO_4 \cdot H_2O$ to the stable crystalline monohydrate has been investigated by Frost, *et al.*[5] Gar-

ner, *et al.*,[6] have made detailed studies of the dehydration of alums, and Bielanski and Tompkins,[7] the sorption of water vapor by dehydrated potash alum. The latter authors concluded that the rate-controlling process was the diffusion of water molecules from higher adsorbed layers but could not accurately assess, by the weighing technique employed, the number of molecules in these layers. In the present work, the uptake of sorbate has been followed by measurement of the pressure of the gaseous adsorbate and many of the difficulties associated with the use of a sensitive spiral balance have been obviated.

Experimental

Materials.—Ammonia and sulfur dioxide were purified by repeated low temperature vacuum distillation of the corresponding liquid of commercial origin. Carbon monoxide was prepared from outgassed A.R. formic and sulfuric acids and passed through traps packed with glass wool and cooled in liquid nitrogen. A.R. potash alum was recrystallized from distilled water.

Apparatus.—This was similar to that used previously[8] for obtaining sorption rates at constant pressure except that constancy was maintained automatically by a relay operating a stopcock[9] which adjusted the mercury level in a calibrated gas buret. The sorption bulb, buret and connecting tubing were maintained at constant temperature by water circulated from a thermostat. During the later stages of the investigation a constant volume apparatus was used; the rate process could be followed accurately over a few per cent. drop in total pressure so that measurements approximated to constant pressure conditions.

Results and Discussion

Using conditions of dehydration similar to those employed previously,[7] *viz.*, 16 hr. evacuation at 50°, the amount of ammonia subsequently sorbed and its rate of sorption were irreproducible, but with single crystals of similar shape and weight, reproducibility (5%) was obtained either by increasing the time to 40 hr. or by raising the temperature to

(1) Division of Mechanical Engineering, National Research Council, Ottawa, Ontario.

(2) G. B. Frost, K. A. Moon and E. H. Tompkins, *Can. J. Chem.*, **29**, 604 (1951); W. E. Garner and H. V. Pike, *J. Chem. Soc.*, 1565 (1937).

(3) J. A. Cooper and W. E. Garner. *Trans. Faraday Soc.*, **32**, 1739 (1936).

(4) R. M. Barrer, *Proc. Roy. Soc. (London)*, **167**, 392 (1938); R. M. Barrer and D. A. Ibbitson, *Trans. Faraday Soc.*, **40**, 195 (1944); R. M. Barrer, *ibid.*, **40**, 555 (1944); R. M. Barrer and D. A. Ibbitson, *ibid.*, **40**, 206 (1944); E. Rabinowitch and W. C. Wood, *ibid.*, **32**, 947 (1936); A. B. Lamb and E. N. Ohl, *J. Am. Chem. Soc.*, **57**, 2154 (1935); A. B. Lamb and J. C. Woodhouse, *ibid.*, **58**, 2637 (1936); M. G. Evans, *Proc. Roy. Soc. (London)*. **A134**, 97 (1931); A. Tiselius, *Z. physik. Chem.*, **A174**, 401 (1935); This Journal, **40**, 223 (1936); W. O. Milligan and H. B. Weiser, *ibid.*, **41**, 1029 (1937); J. Mering, *Trans. Faraday Soc.*, **42B**, 205 (1946); S. B. Hendricks, *Ind. Eng. Chem.*, **37**, 625 (1945); A. G. Keenan, R. W. Mooney and L. A. Wood, This Journal, **55**, 1462 (1951).

(5) G. B. Frost, K. A. Moon and E. H. Tompkins, *Can. J. Chem.*, **29**, 604 (1951); G. B. Frost and R. A. Campbell, *ibid.*, **31**, 107 (1953); H. W. Quinn, R. W. Missen and G. B. Frost, *ibid.*, **33**, 286 (1955); R. C. Wheeler and G. B. Frost, *ibid.*, **33**, 546 (1955); also Queen's University, Ontario, M.Sc., Theses by Moon (1948), Campbell (1950), Breck (1951), Missen (1951) and Wheeler (1951).

(6) J. A. Cooper and W. E. Garner, *Trans. Faraday Soc.*, **32**, 1739 (1936); J. A. Cooper and W. E. Garner, *Proc. Roy. Soc. (London)*, **A174**, 487 (1940); G. P. Acock, W. E. Garner, J. Milstead and H. J. Willavoys, *ibid.*, **189**, 508 (1947).

(7) A. Bielanski and F. C. Tompkins, *Trans. Faraday Soc.*, **46**, 1072 (1950).

(8) F. C. Tompkins, *ibid.*, **34**, 1469 (1938).

(9) D. M. Young, *Chemistry and Industry*, 155 (1949).

62° and evacuating for 16 hr.   These more drastic conditions led to only a slight additional loss of water of hydration.   As found previously,[7] nearly 2 moles of water per mole alum still remained in the crystal.

After sorption of ammonia, the crystals were outgassed at 62° for 16 hr., but in subsequent sorptions less ammonia was taken up, showing that the process is partly irreversible due, as shown later, to structural changes brought about in the dehydrated salt by the sorption process.   Similarly, with crystals having similar geometric forms but of different weights, the plot of the rates of sorption against crystal weight showed considerable scatter, due to slight variations of dehydration rates and in the degree of dehydration with crystal sizes.

Consequently, a master batch of small crystals was prepared so that each sample would be statistically the same.   With such samples the plot of sorption rate against weight, although displaying little scatter, was not linear.   This non-linearity is undoubtedly associated with the fact that the dehydration conditions cannot be maintained identical with different masses (e.g., due to the presence of varying transient water vapor pressures, to different local rates of heating and degrees of self-cooling, etc., for the individual crystallites).   Throughout, therefore, the same mass (0.1 g. for constant pressure, 1.0 g. for constant volume) of crystals was used and the dehydration carried out in the sorption bulb under the carefully controlled conditions given above.

Sorption Rates.—The sorption rates at four temperatures, 35.6, 42.7, 50.1 and 57.7°, were measured at constant volume over the pressure range 0–30 cm.   Some typical results at 57.7° are shown in Fig. 1 where it is seen that the amount x of ammonia sorbed is a linear function of (time, t)$^{1/2}$ after the first minute, i.e.

$$x = at^{1/2} + b \qquad (1)$$

where a is the slope of the line and b the intercept on the x-ordinate.

Now it is likely that during dehydration a series of channels to the surface by and for the escape of water molecules are formed.   If these channels are non-interconnecting then for a constant diffusion coefficient D and "one-dimensional" transport along the major axis of the channels, the amount sorbed after a time will be given for long channels by

$$x = \int J_{x=0}\, d\tau = \int_0^t -D\left(\frac{\partial c}{\partial x}\right)_0 d\tau = 2C_0\left(\frac{Dt}{\pi}\right)^{1/2} \qquad (2)$$

for $t = 0$, $x > 0$, $c = 0$; and $t > 0$, $x = 0$, $c = c_0$; $J_{x=0}$ is the flux at $x = 0$.   Equation 2 is thus consistent with the form of the experimental rate plots.   The intercept of the x–$t^{1/2}$ plot on the x-ordinate corresponds to a rapid initial adsorption on the external surface of the dehydrated crystal.   With SO_2 as adsorbate, a polar gas like NH_3 but larger in size, it was found that the amount adsorbed in the same temperature range was, however, too small for accurate measurement and very much less than the b-values for ammonia.   There was no rate process so, presumably, the sorbed sulfur dioxide is largely confined to the small external surface area of the dehydrated alum.   It seems therefore un-
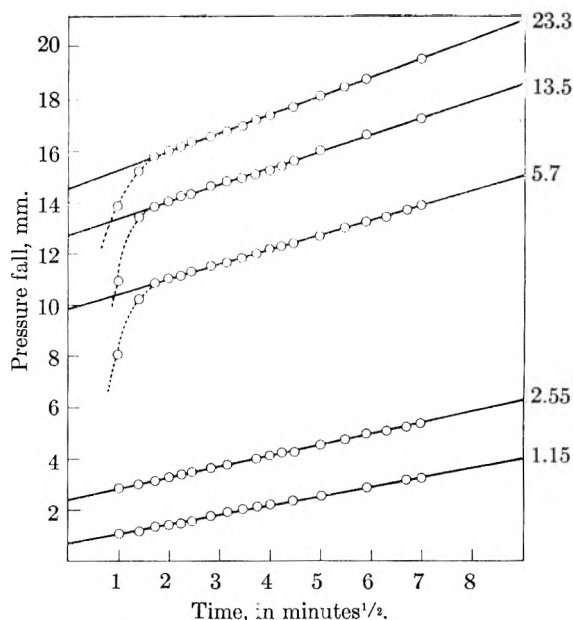
Fig. 1.—Sorption of ammonia at 57.7° at constant volume, plotted as a function of the square root of time: the mean pressure in cm. is indicated on each plot.

likely that this model of non-connecting idealized channels is correct.

Alternatively, the channels may form an interconnecting network easily accessible to the ammonia molecules, in which case some assumptions about the nature of the domains or zones within this network must be made.   On a statistical basis, the zones can be approximated by spheres particularly in view of Garner's work where spherical dehydration nuclei have been observed.   To continue quantitatively with the analysis, one must now either assume a size distribution of zones or a definite average radius of domains.   A tractable solution for diffusion of gas into these zones can be obtained if the latter alternative is chosen.   Using spherical polar coördinates and assuming a constant value for D, we may write

$$\frac{\partial c}{\partial t} = D\left\{\frac{1}{r^2}\frac{\partial}{\partial r}\left(r^2\frac{\partial c}{\partial r}\right)\right\}$$

for $t = 0$, $r < a$, $c = 0$; and $t > 0$, $r = a$, $c = c_0$ where a is the average radius of the zones, the solution has the form[10]

$$\int_0^t J_{r=a}\, d\tau = \frac{2ac_0}{\pi}\sum_{n=1}^{\infty}\frac{1}{n^2}\left\{1 - \exp\left(\frac{-Dn^2\pi^2t}{a^2}\right)\right\}$$

and has been evaluated numerically by Benson.[11]   He finds that the amount sorbed is a linear function of $(D\pi^2t/a^2)^{1/2}$ over quite a wide range of t-values for small $(D\pi^2t/a^2)^{1/2}$;   this model is therefore also consistent with the experimental results.

On this theory a considerable internal surface should be easily accessible to small molecules, such as CO.   We have, therefore measured the adsorption of this gas at liquid–air temperature and obtained a normal (type II) B.E.T. isotherm (Fig. 2) from which a surface area of 5 m.^{2} per g. adsorbent was evaluated.   No rate process subsequent to the

(10) H. S. Carslaw and J. C. Jaeger, "Heat Conduction in Solids," Clarendon Press, Oxford, 1947.
(11) G. W. Benson, Ph.D. Thesis, London University, 1952.
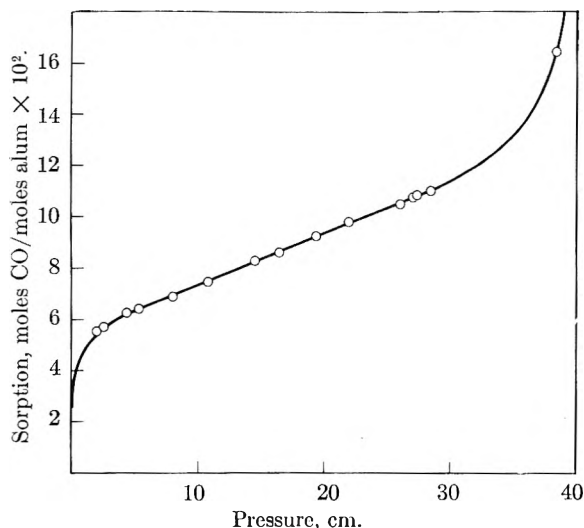
Fig. 2.—Adsorption isotherm for CO at −196°.

initial adsorption was found and the monolayer capacity per g. adsorbent was independent of the weight of dehydrated alum (*cf.* the non-linearity of the rate against weight plot using ammonia). This large internal area, easily accessible at liquid–air temperature by small molecules, is consistent with the zone theory. Such zones, assumed spherical and of equal size, would have a radius of about 3000 Å. to give a surface area of 5 m.^{2}.

On this view the intercept b on the rate curves (Fig. 1) for various constant pressures and constant temperature represents the amount of ammonia rapidly adsorbed on the internal surfaces for various equilibrium pressures. Such "isotherms" at four different temperatures are plotted in Fig. 3. They resemble type V B.E.T. plots where the sharp increase of amount sorbed over a small pressure range is ascribed to the filling of pores and capillaries of the dehydrated alum.
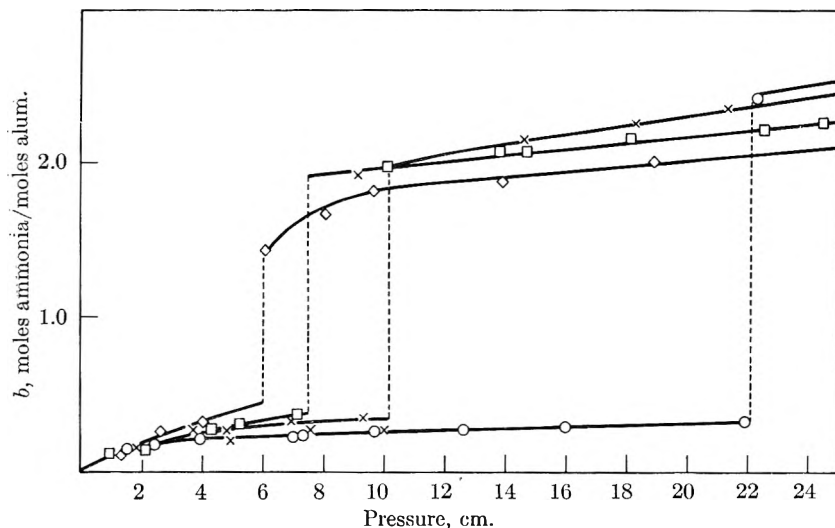
Fig. 3.—Variation of the intercept b with temperature and pressure: ◯, 35.6°; ✕, 42.7°; ◻, 50.1°; ◇, 57.7°.

Now it is reasonable to assume on the zone model that the rate of sorption is a function of the concentration of ammonia molecules in the first layer at the surface of the zones. One can therefore

visualize the building-up of higher layers (multi-layer formation) with an accompanying small mono-tonic increase in concentration in the first layer, so that despite the large increase in the total amount adsorbed, the rate of sorption increases only slightly and the rate against pressure plot shows no singularity. Nevertheless this theory is difficult to accept for the following reasons:

(i) The large abrupt increase in the value of the intercept b occurs (*cf.* Fig. 3) when a critical amount (0.3 mole/mole adsorbent) is adsorbed and this is independent of the pressure or the temperature.

(ii) The plot of the total amount sorbed at the completion of the rate process (Fig. 4) shows no similar large increase as might be expected were multilayer formation taking place.
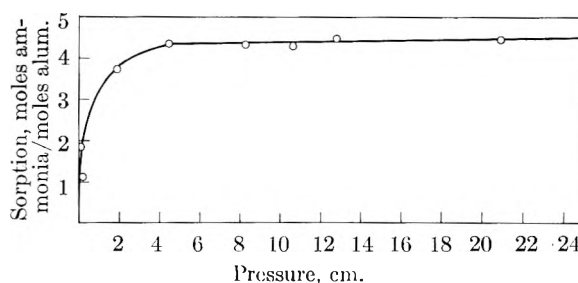
Fig. 4.—Total sorption at 50.1° as a function of pressure.

(iii) If the area deduced from the B.E.T. isotherm for CO is accepted, *viz.*, 5 m.^{2}/g., then the amount of ammonia sorbed on the internal surfaces at the critical value (0.3 mole/mole) corresponds to 6 layers and above the critical b value to nearly 50 layers. In view of the non-penetration of the sulfur dioxide molecule under comparable conditions of temperature and pressure, channels sufficiently wide for such a thick layer cannot be present.

(iv) If Fig. 3 represents a series of reversible adsorption isotherms then the "critical" pressure should increase with temperature. The reverse however is found.

Any theory based on an orthodox diffusion phenomenon thus seems improbable unless one postulates a diffusion coefficient that varies extremely rapidly with concentration in the initial stages.

Concept of Different Sorption Sites.—An alternative theory involving the concept of different types of sorption sites, however, is consistent with the experimental results. From previous work on dehydrated salts of similar type to potash alum, the dehydrated product often comprises a large number of small crystalline domains in a fairly open matrix of non-crystalline, collapsed, disordered material. There are likely to be many different sites for ammonia attachment where the energy of binding of the sorbate molecule varies with

the nature of the site. For simplicity, these sites are assumed to comprise two main categories which we shall refer to as crystalline and amorphous sites, without implying more than that these regions differ in degree of order and therefore in the sorption energy of the sites.

We recall that about 2 moles of water per mole alum still remain in the dehydration product but that under more drastic conditions these can eventually be removed. We denote sites in the amorphous material by X, and those in the crystalline material by Y; each type is in equilibrium with the same very small vapor pressure of water, i.e.

$$X + H_2O \rightleftarrows X \cdot H_2O, \quad K_1 \qquad (3)$$

$$Y + H_2O \rightleftarrows Y \cdot H_2O, \quad K_2 \qquad (4)$$

or, combining

$$Y + X \cdot H_2O \rightleftarrows X + Y \cdot H_2O, \quad K = K_2/K_1 \qquad (5)$$
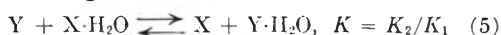
The constant K_1 is assumed large compared with K_2, i.e., K is small and the binding energy for H_2O at the X sites is greater than that at the Y sites; the hydration of the amorphous sites is therefore favored. The sorption of ammonia is therefore largely associated with the X-sites, which process disturbs the equilibrium in that more X sites are made available as sorption proceeds.

At time $t = 0$ let: ξ_0 = the number of X sites available for adsorption, N = the number of $X \cdot H_2O$ sites, the units being in terms of "moles" per mole of alum.

At time "t" let: x = number of X sites occupied by sorbed NH_3 molecules, ξ = number of free X sites. Equilibrium (5) is assumed to be maintained during the rate process so that

$$K = \frac{K_2}{K_1} = \frac{[X][Y \cdot H_2O]}{[Y][X \cdot H_2O]} = \frac{\xi(x + \xi - \xi_0)}{[Y]\{N - (x + \xi - \xi_0)\}}$$

if [Y] is sufficiently large variations in its value will have little influence on K so that it is permissible to write

$$K' = K[Y] = \frac{\xi(x + \xi - \xi_0)}{(N - x - \xi + \xi_0)} \qquad (6)$$

rearranging

$$\xi^2 + (x + K' - \xi_0)\xi - K'(N + \xi_0 - x) = 0$$

Solving this as a quadratic in ξ

$$\xi = \frac{1}{2}[(\xi_0 - K' - x) \pm \sqrt{\{(x + K' - \xi_0)^2 + 4K'(N + \xi_0 - x)\}}]$$

For small values of K' it is possible to expand this by the binomial theorem

$$\xi \simeq \frac{1}{2}[(\xi_0 - K' - x) \pm (\xi_0 - K' - x)\{1 + \frac{2K'(N + \xi_0 - x)}{(\xi + K' - x)^2}\}] \qquad (7)$$

After a short time, $x > N$ and so for a positive value of ξ the negative sign above must be considered

$$\xi = \frac{-K'(N + \xi_0 - x)}{(\xi_0 - K' - x)} \qquad (8)$$

Now the rate of sorption of ammonia is given by

$$\frac{dx}{dt} = k'[NH_3]\xi = k\xi \qquad (9)$$

where $[NH_3]$ is constant in any run since the rate

processes are measured under effectively constant pressure conditions. From equations 8 and 9

$$\frac{dx}{dt} = -k \frac{K'(N + \xi_0 - x)}{(\xi_0 - K' - x)} \qquad (10)$$

which, on integration, gives

$$x + (N + K') \log \left\{ \frac{N + \xi_0 - x}{N + \xi_0} \right\} = -kK't \qquad (11)$$

The rate of sorption will initially be large compared with the rate of the forward reaction of the equilibrium (5), so that the equilibrium is displaced and equation 11 is invalid. However, as sorption proceeds, the number of available X sites decreases until the rate of sorption is small compared with the rate of attainment of the equilibrium and the above analysis is now valid. We denote the value of ξ_0 at the new origin of time (t_0) by ξ_0'. At this time the value of ξ_0' is small compared with N, consequently since K' is also small, equation 11 takes the form

$$x' + N \log \left(1 - \frac{x'}{N}\right) = -kK't' \qquad (12)$$

Expanding the log term $(x'/N << 1)$, and neglecting terms higher than $(x'/N)^2$, then

$$x'^2/2N = kKt' \qquad (13)$$

or

$$x' = (2kK'Nt')^{1/2} \qquad (14)$$

as found experimentally. The intercept b on the x-ordinate found experimentally can now be identified with the total sorption taken place during the time interval $t = 0$ to $t = t_0$.

Now in deriving equation 14 assumptions concerning the orders of magnitude of various terms were made and it is essential that these be self-consistent.

The term $(2kK'N)^{1/2}$ is the slope a of the $t^{1/2}$ plot (Fig. 1) which has the order of magnitude 0.1 mole/mole alum (min.)$^{1/2}$. The value of N (the number of $X \cdot H_2O$ sites at $t = t_0$) in units of moles/mole alum is 2. The velocity constant k has to be sufficiently large that the initial rapid sorption process is virtually complete before the first rate measurement is made $(t = 1 \text{ min.})$. We may write

$$x = \xi_0 \{1 - \exp(-kt)\}$$

which for $k = 20$ min.$^{-1}$ is 99% complete at $t = 0.25$ min. Hence with $(2kK'N)^{1/2} = 0.1$, $k = 20$, $N = 2$.

$$K' = \frac{[X][Y \cdot H_2O]}{[XH_2O]} = 10^{-4}$$

and since $[X \cdot H_2O] + [Y \cdot H_2O] \simeq 2$ and $[XH_2O] >> [YH_2O]$, both [X] and $[YH_2O]$ are small compared with $[X \cdot H_2O]$, the assumptions $\xi_0' << N$ and $K' << N$ are justified.

In equation 9, we wrote

$$k = k'[NH_3]$$

where $[NH_3]$ is a constant for a constant pressure of ammonia but otherwise left undefined. Since the gas probably enters the solid via an adsorbed layer, the quantity $[NH_3]$ is related to the adsorption isotherm. Unfortunately no direct methods of measuring the adsorption isotherm were feasible; however, the most probable form can be deduced.
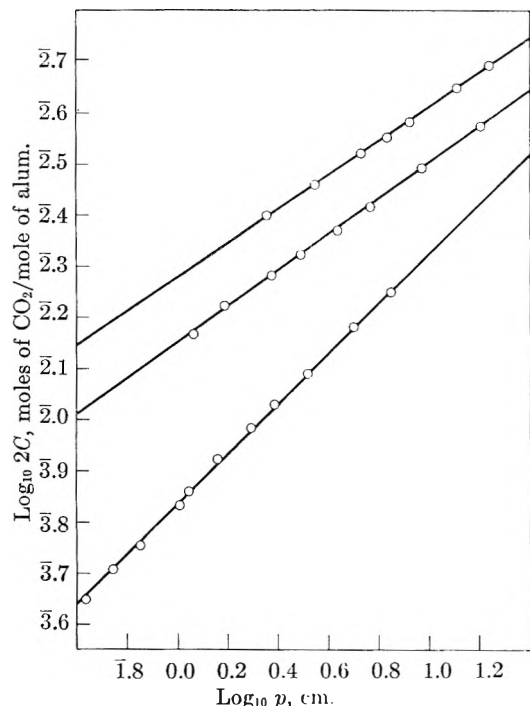
Fig. 5.—Adsorption isotherms for CO_2 at $-45.2°$ (bottom), -63.5 (middle) and $-78.2°$ (top).

Carbon dioxide was found to give adsorption isotherms of the Freundlich type (Fig. 5) while measurements on the total sorption isotherm (Fig. 4) indicate a similar relationship over the lower pressure range. These results show the feasibility of a relationship of the type

$$[NH_3] = Cp^{1/2} \qquad (15)$$

Combining equations 1, 9, 14 and 15 it follows that

$$a^2 = 2k'K'NCp^{1/2} \qquad (16)$$

The validity of this equation is seen in Fig. 6. From the slopes of these lines an apparent activation energy E of approximately 9 kcal. can be obtained. This energy term is a composite one reflecting the temperature coefficient of the product K', k' and C and is thus the algebraic sum of the activation energy of the reaction

$$X + NH_3 \longrightarrow X \cdot NH_3$$

the heat of the reaction

$$X \cdot H_2O + Y \rightleftharpoons X + Y \cdot H_2O$$

and also a term involving the heat of adsorption of ammonia at the surface.

The shape of the plots (Fig. 3) requires explanation, in particular with regard to the large abrupt
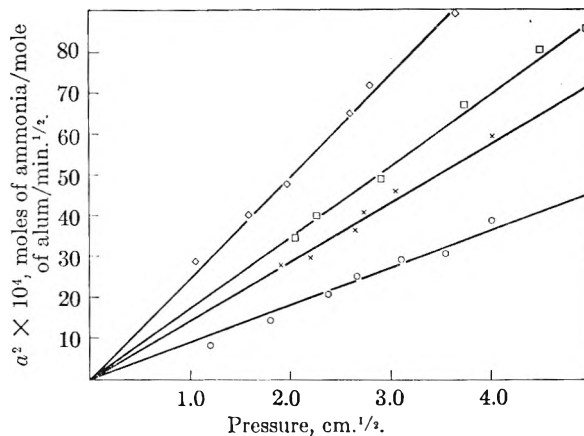
Fig. 6.—Plot of a^2 against $p^{1/2}$ at: O, 35.6°; X, 42.7; □ 50.1; ◊, 57.5°.

increase of the intercept b when 0.3 mole of ammonia per mole of alum has been sorbed. The fact that there is no corresponding discontinuity in the rate as a function of pressure (Fig. 6) indicates the occurrence of a completely independent process. Also, no discontinuity is apparent in the total amount of ammonia sorbed (Fig. 4), indicating that the process involved can proceed either very rapidly at the start of an experiment and very slowly during the approach to equilibrium (approximately 48 hours duration). An attempt was made to measure directly the critical pressure by slowly raising the pressure during an experiment and observing the pressure at which a large increase in the rate of sorption occurred. Using this technique however, no effect was observed. This and the fact that the discontinuity occurs at about the same "b" value suggest that the process is initiated by a critical quantity of sorbed ammonia and is then accelerated by the heat released during sorption. The process has, in fact, the properties of a metastable phase transition. It seems likely that this involves a disintegration of the amorphous zones and a creation of sorption sites. Similar disintegrations are obtained by the sorption of polar molecules in other systems, e.g., ammonia by chabasite[12] and water by dehydrated silica gel.[13]

Acknowledgments.—One of us (G.W.B.) would like to express his gratitude to the Ministry of Education, to the Department of Scientific and Industrial Research and to the Board of Governors of Imperial College for financial assistance which made this work possible.

(12) M. G. Evans, *Proc. Roy. Soc. (London)*, **A134**, 97 (1931).
(13) R. Zsigmondy, *Z. anorg. allgem. Chem.*, **71**, 356 (1911).

THE VISCOSITY OF AQUEOUS SOLUTIONS OF BOVINE SERUM ALBUMIN BETWEEN pH 4.3 AND 10.5[1]

By Charles Tanford and John G. Buzzell[2]

Contribution from the Department of Chemistry, State University of Iowa, Iowa City, Iowa

Received July 18, 1955

Measurements have been made of the viscosity of solutions of bovine serum albumin, as a function of concentration, pH (*i.e.*, molecular charge) and ionic strength. Between pH 4.3 and 10.5 the results may be interpreted on the basis of a compact, sparingly hydrated, undeformable protein molecule, not greatly different from a sphere. At 25°, over a considerable range of pH and ionic strength near the isoionic point, the intrinsic viscosity is 0.037, which is about 50% greater than would be expected for a sphere with 20% hydration and about equal to what would be expected for a prolate ellipsoid with the same hydration and with an axial ratio of about 3:1. (However, evidence is presented to indicate that the albumin molecule is, in fact, not a rigid ellipsoid.) As the molecular charge is increased by approaching the limits of the pH range here covered, a small increase in intrinsic viscosity occurs, which is of the order of magnitude predicted for rigid spheres by Booth's equation for the electroviscous effect. This equation also accounts for a small increase at the isoionic point in the complete absence of salt. The effect of concentration is shown to be a sum of two effects, one independent of charge or ionic strength, the other an electrostatic effect increasing roughly as the square of the charge and decreasing with ionic strength.

An experimental study of the viscosity of bovine serum albumin in aqueous solutions has been in progress in this Laboratory for two years. The results are conveniently divided into two portions: (1) those obtained in the range of pH 4.3 to 10.5, where the albumin molecule behaves as an undeformable solid particle; and (2) those obtained outside this pH range, where the albumin molecule appears to undergo transition to a flexible "expanded" form. The present paper describes the results between pH 4.3 and 10.5, concentrating especially on the effect of electrostatic charge and ionic strength, both on the intrinsic viscosity and on the concentration dependence of reduced viscosity. The results are compared with theoretical equations for the behavior of solid charged spheres or ellipsoids where such equations are available. The results outside the range of pH 4.3 to 10.5 are of interest principally because of the information they give concerning the expansion of the albumin molecule: they will be discussed in a later paper together with evidence by other experimental procedures which bear on the expansion process.

Virtually all previous studies of the viscosity of proteins have been designed to elicit specific information about protein molecules. The intrinsic viscosity has been used as a measure of hydrodynamic volume or shape; changes in intrinsic viscosity (or in reduced viscosity at low concentrations) have been used as a measure of extent of "denaturation." Only one previous experimental study, that of ovalbumin by Bull[3] has been oriented toward the underlying physical theory. Bull studied the effect of electrostatic charge and ionic strength on the reduced viscosity at low ovalbumin concentrations, interpreting it essentially as intrinsic viscosity. His result showed a very much smaller effect of charge than the then current theory predicted, and resulted in a revision of the theory by Booth.[4] The present study shows that the behavior of bovine serum albumin between pH 4.3 and 10.5 is similar in this respect to ovalbumin. It is found,

however, that there is a large effect of electrostatic charge on the concentration dependence of reduced viscosity.

Experimental

Serum Albumin.—Crystalline bovine serum albumin was obtained from Armour and Co. The material used came from lot numbers R 370295 A, N 67009, M 66909 and P 67502.

The protein was dissolved in water and the solutions were passed down an ion-exchange column as described by Dintzis.[5] The resulting stock solutions were assumed salt-free and isoionic. Their concentrations were determined by drying to constant weight at 107°.

Solutions for measurement were prepared from such stock solutions by addition of appropriate amounts of standard HCl, KOH, KCl and conductivity water. Solutions of lower protein concentration were often prepared by appropriate dilution of more concentrated solutions rather than directly from the stock solutions, primarily so as to conserve the protein. All solutions were filtered through fine fritted Pyrex glass funnels immediately preceding their introduction into a viscometer. (Centrifugation was used instead in some of the early determinations.) Their pH values were determined in a Cambridge pH meter.

Densities.—The densities at 25.0° of many of the solutions were measured with a precision of better than 0.0001 in a pycnometer of the type described by Lipkin, *et al.*[6] The densities of the solutions not subjected to measurement were calculated from those measured by interpolation.

Viscometers and their Calibration—Two types of viscometer, both of the capillary variety, were used. One of these is the Ostwald type as modified by Cannon and Fenske,[7] the other the Ubbelohde "suspended level" type.[8] The relation between viscosity and flow time for such viscometers is

$$\eta = \rho(At - B/t) \tag{1}$$

where η is the viscosity, t the flow time, ρ the density and A and B are constants. The constants A and B were determined for each viscometer used by the procedure recommended by the American Society for Testing Materials,[9] using conductivity water as the calibrating liquid. The calibrations of the Ubbelohde viscometers were also checked by measurement with sucrose solutions.[10]

The contribution of the kinetic energy term, B/t, in equation 1 was found to be essentially zero for the Cannon–Fenske viscometers used but not for the Ubbelohde type. (In each case we used the slowest-flowing models commercially available.) Ten viscometers were used in all.

The viscometers were mounted in a bath maintained at 25.0°, with a maximum variation of 0.002°. They were

(1) Presented at the 128th National Meeting of the American Chemical Society, Minneapolis, Minn., September, 1955.

(2) Abstracted from the Ph.D. thesis of John G. Buzzell, State University of Iowa, August 1955.

(3) H. B. Bull, *Trans. Faraday Soc.*, **36**, 80 (1940).

(4) F. Booth, *Proc. Roy. Soc. (London)*, **A203**, 533 (1950).

(5) H. M. Dintzis, Ph.D. Thesis, Harvard University, 1952.

(6) M. R. Lipkin, J. A. Davison, W. T. Harvey and S. S. Kurtz, Jr., *Ind. Eng. Chem., Anal. Ed.*, **16**, 55 (1944).

(7) M. R. Cannon and M. R. Fenske, *ibid.*, **10**, 297 (1938).

(8) L. Ubbelohde, *ibid.*, **9**, 85 (1937).

(9) *Am. Soc. Testing Materials, Standards*, Pt. V, 899 (1949).

(10) G. Jones and R. E. Stauffer, *J. Am. Chem. Soc.*, **59**, 1630 (1937).

mounted in such a way that the same viscometer always occupied precisely the same position in the bath. They were cleaned immediately before each filling with hot sulfuric acid–dichromate solution, rinsed numerous times to remove all traces of the acid, and dried with filtered air.

Flow times were measured to 0.001 second by means of electric timers. Solutions were allowed to come to temperature equilibrium and passed once through the capillary before any measurements were made. From three to eight flow time measurements were made on each solution, usually in duplicate (*i.e.*, using two different viscometers). Flow times were about 200 seconds for the Fenske viscometers and 100 seconds for the Ubbelohde type. Reproducibility in each case was of the order of 1 part in 2000.

Solvent viscosities, where measured, agreed with the determinations on KCl solutions made by Jones and Talley.[11] Their data are more precise than ours, however, and their values were used in all calculations. Within the limits of our experimental error, the small amount of HCl or KOH present in most of the solvents used had no effect on the viscosity.

Extrapolation to Obtain Intrinsic Viscosity.—To obtain the intrinsic viscosity as a function of electrostatic charge and ionic strength, the function

$$\eta_{red} = \eta_{sp}/c = (\eta - \eta_0)/\eta_0 c \qquad (2)$$

was evaluated at the same charge and ionic strength, but at different concentrations of protein, and extrapolated to zero concentration. In equation 2 η is the viscosity of the solution, η_0 is the viscosity of solvent, c the concentration in grams per 100 ml. of solution, and η_{sp} and η_{red}, respectively, represent specific and reduced viscosity, defined by equation 2 in accordance with custom.[12]

The "ionic strength" of a solution is here defined, as is usual in dilute protein solutions, as the total concentration of added electrolyte (all added electrolytes being univalent), regardless of the fact that some of the electrolyte ions must be bound to the protein molecules. In effect this is a compromise between two extreme procedures: that of counting a protein molecule with a net charge of Z as a Z-valent ion, which, because of the wide separation of the charges, is clearly inappropriate, and that of not counting the protein charges at all. For virtually all of the work described in this paper the major portion of the ionic strength is present as free KCl and no serious difficulty arises as a result of our assumption. This is not true, however, when measurements are extended to pH 2 or to pH 12 at low ionic strength.

To maintain constant electrostatic charge at a given ionic strength requires constant pH. The amounts of KCl and HCl or KOH in a series of measurements at different protein concentrations are thus fixed: the latter so as to maintain constant pH, the sum of the two so as to maintain constant ionic strength.

Definition of the Protein Component[13]

The use of equation 2 to define reduced viscosity, and its extrapolation to zero protein concentration, requires that all of the solutions leading to a given extrapolated reduced viscosity be capable of definition as two-component systems: a *solvent component* which remains unchanged in a given series, and a *protein component* the concentration of which is related to that of the added concentration of dry isoionic albumin. Most of our measurements are concerned with protein ions, and, for the purpose of interpretation, we shall be interested in the viscosity increment per unit concentration of such ions. The protein component, however, must be electrically neutral, and must therefore contain other ions in addition to the protein ions. The purpose of this section is to find what these ions are and to what extent they are likely to influence the viscosity.

Our discussion will be simplified if we express all concentrations in terms of moles/liter, designated by capital letters, C_i or C_i'. The experimental protein concentration, c, in grams of isoionic protein per 100 ml., is related to the corresponding concentration, C_2', in moles per liter, by a constant, $c = (M/10)C_2'$ where M is the protein molecular weight.

Four different substances are added to our solutions: water, isoionic protein, HCl or KOH (concentration C_3'), and KCl (concentration C_4'). Only two components are present, however, because the pH and the ionic strength, as previously defined, are kept constant in a given dilution series. Constant pH requires (at a given ionic strength) that there be present the same concentration of *free* HCl or KOH, C_3'', in each solution. The protein, at equilibrium at a given pH and ionic strength is combined, independently of its concentration, with a given number, n, of H^+ or OH^- ions.[14] The actual added concentration of HCl or KOH is therefore

$$C_3' = C_3'' + nC_2' \qquad (3)$$

Since, by definition, μ = constant = $C_3' + C_4'$, the added concentration of KCl is

$$C_4' = \mu - C_3' - nC_2' \qquad (4)$$

From equations 3 and 4, by placing C_2' equal to zero, we see that the *solvent component* in a given dilution series contains C_3'' molar HCl or KOH and $(\mu - C_3'')$ molar KCl.

We may now let one mole of the protein component contain 1 mole of isoionic protein, x moles of HCl or KOH, and y moles of KCl. The composition of any solution in a given dilution series is now definable in terms of the single concentration of this component, C_2, and of the concentrations present in the solvent, so that the added concentrations become

$$\left.\begin{array}{l} C_2' = C_2 \\ C_3' = C_3'' + xC_2 \\ C_4' = \mu - C_3'' + yC_2 \end{array}\right\} \qquad (5)$$

Combining equations 3 to 5 we see at once that $x = n$ and $y = -n$. One mole of protein component thus contains in addition to the isoionic protein n moles of HCl or KOH *minus n* moles of KCl, or, in other words n moles of H^+ or OH^- *minus n* moles of K^+ or Cl^-. But n moles of H^+ or OH^- are actually bound to the protein to make the protein ion. The protein component therefore corresponds to the protein ion *minus a number of K^+ or Cl^- ions equal to the number of bound H^+ or OH^- ions*.

To determine the extent to which these salt ions contribute to the experimental results we may consider the experimental η_{sp} at c = 1 g./100 cc., *i.e.*, $C_2 = 10/M$, *i.e.*, concentration of salt ions forming part of the protein component = 10 n/M. The maximum value of n reached in the present study is about 40, the molecular weight of serum albumin is 65,000,[15] so that the maximum value of the concentration of salt ions forming part of the protein component is 6 × 10^{-3}. These ions may be expected

(11) G. Jones and S. K. Talley, *J. Am. Chem. Soc.*, **55**, 624 (1933).

(12) L. H. Cragg, *J. Colloid Sci.*, **1**, 261 (1946).

(13) This section is based on a similar discussion, in connection with osmotic pressure, given by G. Scatchard, *J. Am. Chem. Soc.*, **68**, 2315 (1946).

(14) Combination with OH⁻ ions is equivalent to dissociation of H⁺ ions. The number of bound H⁺ or OH⁻ ions is essentially independent of protein concentration by actual experimental test (titration curves).

(15) J. M. Creeth, *Biochem. J.*, **51**, 10 (1952).

to make a contribution to the specific viscosity of the same order of magnitude as an equal concentration of KCl. From the results of Jones and Talley,[11] η_{sp} for KCl in the concentration range here used is $0.0052C^{1/2} - 0.014 \, C$, so that the addition or subtraction of $6 \times 10^{-3} \, M$ KCl beyond that present in the solvent leads to a change in η_{sp} of about 4×10^{-5}. The measured η_{sp}, however, is of the order of 0.040. It may therefore be concluded that the measured η_{sp} is a measure of the contribution of the protein ions only, that of the salt ions in the protein component being negligible.

Results

Figure 1 shows some typical experimental results, and straight lines drawn through the data. The slopes and intercepts of these straight lines were determined by the method of least squares. The intercepts of such straight lines are the intrinsic viscosities, the slopes represent the concentration dependence.

Table I shows all intrinsic viscosity values obtained in this way, together with the corresponding slopes. Most entries in Table I represent duplicate determinations, some, especially at the isoionic point, represent averages of two or three sets of duplicates. The mean charge $\bar{Z}$ per protein molecule was calculated from titration curves obtained
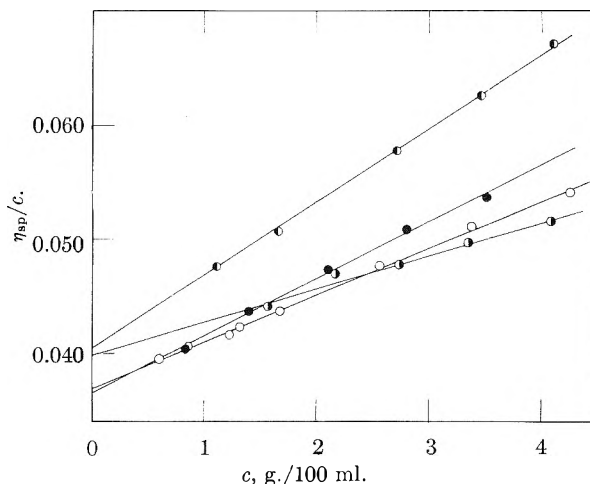
Fig. 1.—Representative data for BSA. The lines represent, respectively, isoionic BSA, $\mu = 0.001$ (●) and $\mu = 0.002$ (○), BSA at pH 8.5 and $\mu = 0.02$ (◐), and BSA at pH 9.3 and $\mu = 0.15$ (◑). Most of the points represent averages of two or more sets of measurements, in different viscometers. Slopes and intercepts were determined by least squares.

TABLE I

INTRINSIC VISCOSITIES AND SLOPES

pH	μ	$\bar{Z}$	$[\eta]$	Slope
4.3	0.01	+ 7	0.0393	0.0035
	.05	+ 8	.0372	.0032
	.15	+ 8	.0374	.0033
4.8	.01	+ 1	.0377	.0033
	.05	0	.0373	.0029
	.15	− 2	.0376	.0027
Isoionic[a]	0	0	.0406	.0054
	.001	− 1	.0362	.0050
	.002	− 1	.0369	.0040
	.01	− 4	.0361	.0035
	.085	− 8	.0382	.0025
	.15	−10	.0371	.0027
	.25	−	.0382	.0023
	.50	−	.0376	.0025
7.3	.01	−11	.0412	.0049
	.05	−16	.0383	.0030
	.10	−18	.0365	.0028
	.50	−	.0371	.0027
8.5	.02	−20	.0406	.0064
	.05	−23	.0395	.0039
	.15	−27	.0417	.0023
	.50	−	.0391	.0027
9.3	.01	−22	.043	.0161
	.02	−23	.038	.0098
	.05	−27	.041	.0039
	.15	−31	.040	.0029
10.5	.05	−39	.041	.0063
	.15	−45	.040	.0034
	.50	−	.041	.0030
3.0	.03	+47	.100	...
	.15	+46	.065	...

[a] The isoionic pH is about 5.0 in water and increases to about 5.6 at the highest chloride concentration. The increase in pH and in $\bar{Z}$ are due to chloride binding.

in this Laboratory,[16] together with chloride binding data of Coleman.[17] It was assumed that potassium ion does not bind to serum albumin in the pH range under study.

Table I shows that there is no significant effect of ionic strength on the intrinsic viscosity, $[\eta]$, at the isoionic point, except that the value in the complete absence of salt is significantly higher. The mean at all ionic strengths excluding $\mu = 0$ is 0.0369 $\pm$ 0.0010 compared to the value of 0.0406 $\pm$ 0.0007 obtained in the absence of salt. It will be seen below that an increase of this magnitude is to be expected on theoretical grounds.

The effect of pH (or charge) on $[\eta]$ is also seen to be small. The mean at all ionic strengths above 0.01, between pH 4.3 and 7.3, including all of the values at the isoionic values except those at $\mu = 0$, is 0.0371 $\pm$ 0.0009, which is not significantly different from the mean obtained from the isoionic values alone. Only above pH 7.3 does a really significant increase in intrinsic viscosity take place. Even here, it should be pointed out, the difference is very much smaller than that observed outside the range of pH 4.3 to 10.5. To illustrate this, Table I includes values of $[\eta]$ obtained at pH 3, where the positive electrostatic charge is approximately the same as the negative charge at pH 10.5, but the intrinsic viscosity is much greater.

The slopes are plotted as a function of $\bar{Z}$ (or pH) in Fig. 2. It can be seen that a single limiting value of the slope, independent of $\bar{Z}$, is approached at high ionic strength, and at each ionic strength as $\bar{Z}$ approaches zero.[18] The mean value of this limiting slope, obtained from all data at the higher ionic

(16) C. Tanford, S. A. Swanson and W. S. Shore, J. Am. Chem. Soc., in press.

(17) J. S. Coleman, Ph.D. Thesis, Massachusetts Institute of Technology, 1953.

(18) The limiting slope is not quite reached at any value of $\bar{Z}$ at $\mu = 0.01$. This is probably due to the fact that the slope is a function of $\bar{Z}^2$ rather than Z (see Discussion). The value of $\bar{Z}^2$ never becomes zero. Cf. E. J. Cohn and J. T. Edsall, "Proteins, Amino Acids and Peptides," Reinhold Publ. Corp., New York, N. Y., 1943, Chapter 20.

Fig. 2.—Slopes of viscosity plots as a function of charge at ionic strength 0.01 (◑), 0.02 (⊕), 0.05 (◒), 0.15 (○) and 0.50 (●). The limiting slope was obtained by averaging all slopes at low $\bar{Z}$ and high μ, and represents the non-electrostatic contribution to the slopes. The other curves drawn are parabolas, such that the difference between observed and limiting slopes is proportional to $(\bar{Z})^2$. It should be noted that the two points at $\mu = 0.01$, near $\bar{Z} = 0$, which fall above the corresponding parabola, probably do so because the electrostatic contribution to the slope varies as $\bar{Z}^2$ rather than $(\bar{Z})^2$. At large values of $\bar{Z}$ the difference between these quantities should not be greater than the error arising from the uncertainty in $\bar{Z}$ itself.

strengths between pH 4.8 and 8.5, is 0.00259 ± 0.00018.

This limiting slope must represent a measure of the non-electrostatic protein–protein interaction. The increase in slope above this limiting value is greatest at low ionic strength and high charge, which suggests that it represents an electrostatic protein-protein interaction.

Discussion

Comparison with Previous Work on Serum Albumins.—A number of values have been previously obtained for the intrinsic viscosity of serum albumins in the isoionic region.[19–24] They are listed in Table II, and are seen to differ greatly among themselves. This difference cannot be due to the somewhat different conditions of pH and ionic strength used, for Table I shows that these are essentially without effect. Nor can the differences be reasonably ascribed to the fact that different workers used albumin from different species of mammals, for all experience suggests that the species difference should be small. It is probable that the purity of the samples is at least in part responsible, as is indicated by the different values of [η] obtained by Neurath, *et al.*,[22] for different preparations of horse albumin. The value obtained by us agrees very closely with that of Neurath, *et al.*, for the McMeekin preparation of horse albumin. Particularly significant is the fact that it agrees well

(19) K. R. Fahey and A. A. Green, *J. Am. Chem. Soc.*, **60**, 3039 (1938).

(20) A. Polson, *Kolloid-Z.*, **88**, 51 (1939).

(21) S. Bjornholm, E. Barbu and M. Macheboeuf, *Bull. soc. chim. Biol.*, **32**, 924 (1950); **34**, 1083 (1950).

(22) H. Neurath, G. R. Cooper and J. O. Erickson, *J. Biol. Chem.*, **138**, 411 (1941).

(23) J. L. Oncley, G. Scatchard and A. Brown, THIS JOURNAL, **51**, 184 (1947).

(24) J. T. Yang and J. F. Foster, *J. Am. Chem. Soc.*, **76**, 1588 (1954).

with Yang and Foster's recent determination on bovine albumin,[25] for their albumin preparation was not purified by ion exchange. This indicates that the ion-exchange purification, which causes significant changes in the ability of serum albumin to bind anions,[17] does not have an appreciable effect on molecular-kinetic properties. Yang and Foster's data also show essentially the same pH dependence as ours; very little effect of pH between pH 4.3 and pH 7, and a sharp rise below pH 4.3.

TABLE II

INTRINSIC VISCOSITY OF SERUM ALBUMINS[a]

Investigator	Species	Conditions	[η]
Polson[20]	Horse	$\mu = 0.25, 20°$	0.049
Fahey and Green[19]	Horse	$\mu = 0.5, 25°$	.047[b]
Bjornholm, *et al.*[21]	Horse	$\mu = 0.2, 20°$	.045
Neurath, *et al.*[22]	Horse (Kekwick)	$\mu = 0.22, 25°$	.043
Oncley, *et al.*[23]	Human	$\mu = 0.15, 37°$	.042
Yang and Foster[24]	Bovine	$\mu = 0.10, 25°$	.038
Neurath, *et al.*[22]	Horse (McMeekin)	$\mu = 0.22, 25°$	.037
This paper	Bovine	...	.037

[a] All data obtained near the isoionic point. [b] This value is erroneously listed as 0.062 in several tabulations.

The Hydrodynamic Particle Equivalent to an Isoionic Serum Albumin Molecule.—Theoretical relations between viscosity and molecular size and shape have been expressed in terms of the function

$$\lim_{\varphi \to 0} (\eta - \eta_0)/\eta_0 \varphi \equiv \nu \qquad (6)$$

where φ is the fraction of the solution volume occupied by the dissolved particles. For *solid uncharged spheres*, ν is equal to 2.5 regardless of the size of the individual spheres[27]; for *solid uncharged ellipsoids of revolution*, ν increases with increasing asymmetry from 2.5 to very much larger values (593 for prolate ellipsoids and 69 for oblate ellipsoids, when the axial ratio is 100:1).[28] No theoretical values for ν are available for solid particles of other shapes.

The relation between intrinsic viscosity and ν is complicated by the fact that proteins dissolved in aqueous solution form particles containing a certain amount of solvent.[29] The specific volume of the particles therefore depends on the amount of solvation, which is not easily established experimentally. The hydrodynamic volume per gram of dry protein, v_h, may be related to the thermodynamic partial specific volume, $\bar{v}$, by the relation

$$v_h = \bar{v} + \delta_1 v_1^0 \qquad (7)$$

(25) The study of Yang and Foster was intended to obtain relative values as a measure of the expansion of albumin in acid solutions. The value given in Table II is based on data supplied in a personal communication from Dr. Foster. It has been corrected for two factors not taken into account in their work; (1) the kinetic energy term in equation 1, which they neglected, and (2) the fact that they measured intrinsic *kinematic* viscosity rather than intrinsic viscosity. The correction for the latter amounts to 0.0027,[26] that for the kinetic energy factor to about 0.002. Yang and Foster's experimental value of 0.033 thus leads to the value given in Table II.

(26) C. Tanford, THIS JOURNAL, **59**, 798 (1955).

(27) A. Einstein, *Ann. Physik*, **19**, 289 (1906); **34**, 591 (1911).

(28) R. Simha, THIS JOURNAL, **44**, 25 (1940); J. W. Mehl, J. L. Oncley and R. Simha, *Science*, **92**, 132 (1940).

(29) J. T. Edsall in "The Proteins" (H. Neurath and K. Bailey, ed.), Vol. IB, Academic Press, Inc., New York, N. Y., 1953, Chapter 7.

where δ_1 is the number of grams of solvent incorporated in the hydrodynamic particle per gram of dry protein, and v_1^0 is the specific volume of pure solvent.[30]

By equation 7 the volume occupied by c g. of unsolvated protein is $c v_h$, so that the volume fraction φ corresponding to a concentration of c g. per 100 ml. is $c v_h/100$, leading to the relation

$$100[\eta] = \nu(\bar{v} + \delta_1 v_1^0) \qquad (8)$$

As has been pointed out by Scheraga and Mandelkern,[31] equation 8 contains two unknown quantities, ν and δ_1, and both can obviously not be determined from the intrinsic viscosity. This does not mean, however, that we can obtain no information at all about the hydration and shape of the isoionic albumin molecule in solution. In the absence of high shear and resulting orientation, a sphere would presumably offer less interference to flow than a particle of equal volume with any other shape. Hence one can estimate the *maximum* amount of hydration by placing $\nu = 2.5$. The amount obtained is 0.75 g. per gram of protein. Alternatively one can place δ_1 in equation 8 equal to zero and obtain the maximum possible value of ν. The value so obtained is $\nu = 5.0$. More reasonably, one can attempt to use an experimental estimate of hydration in serum albumin and similar proteins[29,32]; a reasonable figure would seem to be $\delta_1 = 0.2$, which leads to $\nu = 4.0$, which is equivalent to the value for a prolate ellipsoid of axial ratio 3.3:1. Table III shows that similar figures are obtained if the same kind of calculation is based on diffusion coefficients or on the electrostatic interaction factor obtained from titration curves.

TABLE III

SHAPE AND SOLVATION OF SERUM ALBUMIN HYDRODYNAMIC PARTICLE

	Equiv. Sphere		Equiv. prolate ellipsoid axial ratio assuming 0.2 g. solvation/g. protein
	Radius, Å.	Solvation, g./g. protein	
Viscosity	33.7	0.75	3.3
Diffusion	34.8	0.90	4.3
Titration curves	33 ± 2	0.65	..

These data show without question that the isoionic serum albumin molecule must be very compactly folded, as are most globular proteins. One need only compare the values of ν obtained for fibrinogen (27)[29] or for typical polymers of about the same molecular weight as serum albumin (31 to

98)[33] to realize how close to a compact sphere the dissolved serum albumin molecule must be.

In this connection it is of interest to discuss the procedure suggested by Scheraga and Mandelkern[31] to obviate the ambiguity in the interpretation of intrinsic viscosity by combining intrinsic viscosities with other hydrodynamic data, such as diffusion. Diffusion constants may be related by an equation similar to equation 8, to the solvation, δ_1, and to the ratio, f/f_0 of the frictional coefficient of the actual particle to that of a sphere of the same volume and therefore the same solvation. The ratio f/f_0 is equal to 1 for a sphere and takes on larger values for other shapes. Clearly the same ambiguity arises in the interpretation of diffusion constants alone as in the interpretation of viscosities alone. However, if the two are combined, δ_1 can be eliminated. One obtains for the experimental quantity, $\beta = D[\eta]^{1/3}M^{1/3}\eta_0/kT$, where D is the diffusion constant, M the molecular weight, and k Boltzmann's constant, the value $(N/16200 \pi^2)^{1/3} \nu^{1/3} f_0/f$. Thus β gives unequivocal values of the ratio of $\nu^{1/3}$ to f/f_0. Unfortunately, we have no basis on which to judge the meaning of a particular value of this ratio. Whereas ν is equal to 2.5 for spheres, greater for asymmetric ellipsoids and presumably other non-spherical particles, and very large for chain-like polymers, and a similar progression exists for f/f_0, we have no way of judging the course of the ratio of these quantities. For spheres β is 2.12×10^6; for oblate ellipsoids it is essentially independent of the axial ratio and equal to essentially the same value as for spheres; for prolate ellipsoids it rises slowly from 2.12×10^6 to larger values (3.22×10^6 for an axial ratio of 100:1); for chain-like polymers it is a constant independent of length equal to 2.5×10^6. The regular progression with decreasing compactness is lacking.

Nevertheless, the calculation of Scheraga and Mandelkern's factor leads to a most interesting result. Using the diffusion constant of Creeth[15] and our intrinsic viscosity, as shown in a preliminary communication,[34] one obtains for β the value $(2.04 \pm 0.06) \times 10^6$. This clearly indicates at least one thing: that serum albumin cannot be successfully represented by a solid ellipsoid.

Electroviscous Effect and the Rigidity of the Albumin Molecule.—The preceding discussion has shown that near its isoelectric point the albumin molecule in solution behaves as a compact particle not very different from a sphere. As the albumin molecule becomes charged two factors arise which may increase the intrinsic viscosity. If the molecule maintains its compact shape, there will be a small increase due to electrostatic interaction with the ionic atmosphere which surrounds a protein molecule possessing a net charge. This has been called the *electroviscous effect*. The albumin molecule may, however, not maintain its compact shape. If the internal secondary bonds are sufficiently weak, or if there are numerous alternative ways of forming secondary bonds, the mutual repulsion of

(30) It has frequently been thought that equation 7 requires the assumption that the *actual* specific volume of the protein portion of the hydrodynamic particle is $\bar{v}$ and that of the solvent portion is v_1^0. This is not true, however. The only assumptions required in the derivation of equation 7 are (a) that no volume change occurs in any portion of the solvent not incorporated in the hydrodynamic particle, and (b) that the solvent incorporated in the hydrodynamic particle has the same composition as the pure solvent. The second of these assumptions is probably not applicable to proteins dissolved in salt solutions, but the fraction of the solvent volume occupied by inorganic ions in the dilute salt solutions here under consideration is so small that no appreciable error in equation 7 is likely to result.

(31) H. A. Scheraga and L. Mandelkern, *J. Am. Chem. Soc.*, **75**, 179 (1953).

(32) J. H. Wang, *ibid.*, **76**, 4755 (1954).

(33) W. Kauzmann, "The Mechanism of Enzyme Action" (W. D. McElroy and B. Glass, ed.), Johns Hopkins Press, Baltimore, Md. 1954.

(34) C. Tanford and J. G. Buzzell, *J. Am. Chem. Soc.*, **76**, 3356 (1954).

like charges may cause the molecule to take on a new configuration in which the charges are further apart and in which salt ions of the solvent may penetrate into the solvated particle. This would result in a viscosity increase due to a larger value of ν or δ_1 (equation 8), or both.

As is shown by Table I and the accompanying text, the observed increase in intrinsic viscosity is large outside the pH region under discussion in this paper, but quite small within this pH region. (It should be noted that the limits of the pH region are not determined by charge. The lower limit is at $\bar{Z} = +8$, the upper limit near $\bar{Z} = -50$). One might therefore guess that the changes within the range of pH 4.3 to 10.5 are due to the electroviscous effect alone and that no deformation of the albumin molecule occurs under these conditions. We shall accordingly compare the observed increase in intrinsic viscosity with values calculated from theoretical predictions of the magnitude of the electroviscous effect.

An equation for the electroviscous effect of solid charged spheres was first presented, without derivation, by Smoluchowski.[35] Twenty years later, Krasny-Ergen[36] derived a similar equation, differing from Smoluchowski's only by a factor of 3/2. Both these equations predict a very large electroviscous effect,[37] a result obviously incompatible with Bull's data for ovalbumin.[3] This discrepancy prompted Booth[4] to reinvestigate the problem. He found that Smoluchowski's and Krasny-Ergen's result depended on the assumption that the thickness of the ionic atmosphere is small compared to the particle radius, an assumption not applicable to ordinary protein solutions, and derived a new equation, which, rearranged to a form convenient to the present data, is

$$[\eta]_{el} = 322[\eta] \frac{\epsilon^3 Z^2 \psi(\kappa a)}{DkT\eta_0 a^2} \frac{\sum_i c_i z_i^2/\lambda_i}{\sum_i c_i z_i^2} \quad (9)$$

In this equation $[\eta]_{el}$ represents the anticipated increase in intrinsic viscosity due to the electroviscous effect, $[\eta]$ being the intrinsic viscosity at the isoelectric point, ϵ is the protonic charge, Z is the charge on the particle and a its radius, D is the dielectric constant of the solvent, and η_0 its viscosity, k is Boltzmann's constant, T is the absolute temperature, κ is the Debye–Hückel constant proportional to the square root of the ionic strength, $\psi(\kappa a)$ is a decreasing function of κa, values of which are given by Booth, the c_i are the concentrations of all inorganic ions in the solution, z_i their charges and λ_i their ionic conductances in practical units.

The electroviscous effect as calculated by equation 9 is shown in Table IV. We have used for a the radius of the equivalent sphere given in Table III, and have placed $\lambda_{K^+} = \lambda_{Cl^-} = {}^1/_2 KCl$. The calculated results are seen to compare remarkably well with the observed increases. The latter are

uniformly higher, by about a factor 2, but there is no trend with charge and ionic strength. Considering the simplicity of the model used in Booth's theory, and the fact that the uncertainty in the measurements is at least 0.001, better agreement could not have been expected.[38]

One may clearly conclude from these calculations that the albumin molecule is in fact not undergoing appreciable deformation in the range of pH 4.3 to 10.5. As a corollary, the very large increase in intrinsic viscosity shown in Table I for pH 3 implies that a marked change in size or shape has occurred at that pH.

TABLE IV

INTRINSIC VISCOSITY INCREASE DUE TO ELECTROVISCOUS EFFECT

Ionic strength	pH	$\bar{Z}$	Increase in $[\eta]$ Booth's eq.	Obsd.
0.01	7.3	−11	0.0008	0.004
	9.3	−22	.0029	.006
0.05	7.3	−16	.0005	.001
	8.5	−23	.0009	.002
	9.3	−27	.0014	.002
	10.5	−39	.0027	.004

The conclusion that no deformation of the serum albumin molecule occurs between pH 4.3 and 10.5 is confirmed by other physico-chemical measurements. For example, Creeth[15] has shown that no change in diffusion constant occurs between the isoionic point and pH 8.6; Weber[39] has shown that only minor changes occur in the polarization of fluorescence between roughly pH 4 and pH 11, the optical rotation is also relatively constant over this pH range,[40] and so is the electrostatic free energy change per unit charge as measured from titration curves.[16] All of these quantities, where measured, change markedly below pH 4 and above pH 10.5 or 11.

Our conclusion that serum albumin is not deformable between pH 4.3 and 10.5 is not in accord with the finding of Klotz[41] and co-workers, based on binding studies with neutral organic molecules, with organic anions and with calcium, that a change in configuration does occur between pH 7 and 9. However, the two points of view are not necessarily incompatible, for a rearrangement of internal bonds near the surface of the molecule could easily occur without effect on its over-all size and shape, but with considerable effect on binding properties. The data of Klotz and co-workers could also be explained if the free energy of binding in each of their studies were reduced by the presence of neutral imidazole groups. In this case their pH effects would be a reflection of the ionization equilibrium of the imidazole groups, rather than of configurational changes.

(35) M. Smoluchowski, *Kolloid. Z.*, **18**, 190 (1916).

(36) W. Krasny-Ergen, *ibid.*, **74**, 172 (1936).

(37) In comparison with the values calculated below by Booth's equation, these equations would predict an increase larger by a factor of 10,000 at the isoionic point in the absence of salt, by a factor of 100 for the data of Table III at $\mu = 0.01$, and by a factor of 20 for the data at $\mu = 0.05$.

(38) If, instead of using for a the radius of an equivalent sphere calculated from the isoionic intrinsic viscosity, one calculates the volume of the particle by equation 9 with $\delta_1 = 0.2$ and uses for a the radius of a sphere of this volume, the calculated $[\eta]_{el}$ becomes more than 50% greater than the values given in Table IV. These values would then agree even more closely with the observed values.

(39) G. Weber, *Biochem. J.*, **51**, 155 (1952).

(40) B. Jirgensons, *Arch. Biochem. Biophys.*, **41**, 333 (1952); B. Jirgensons and S. Sirotzky, *J. Am. Chem. Soc.*, **76**, 1367 (1954).

(41) I. M. Klotz, R. K. Burkhard and J. M. Urquhart, *ibid.*, **74**, 202 (1952); I. M. Klotz and J. Ayers, *ibid.*, **74**, 6178 (1952); S. Katz and I. M. Klotz, *Arch. Biochem. Biophys.*, **44**, 351 (1953).

Viscosity Increment in the Complete Absence of Salt.—Table I shows that a small increase in $[\eta]$ occurs not only as the charge is increased, but also at the isoionic point in the complete absence of salt. This effect may also be interpreted as an electroviscous effect for while the average charge at the isoionic point is zero, the average value of Z^2 is not zero,[29] a fact responsible for a number of physical phenomena of isoionic proteins at low ionic strength.[42]

Assigning a value of 10 to $\overline{Z^2}$ for serum albumin at the isoionic point, and assuming that the only inorganic ions present are the hydrogen ions required to produce the equilibrium $p\mathrm{H}$ of 5.0, we may again apply Booth's equation and calculate an increase in $[\eta]$ of 0.0009. This is somewhat smaller than the observed increase of 0.0035, but the difference is much less than the difference between results calculated and observed for ovalbumin in the absence of salt. Booth[4] states that his equation is not strictly applicable to very low values of κa.

Concentration Dependence.—It was pointed out in connection with Fig. 2 that the concentration dependence of reduced viscosity, as reflected in the slopes of plots such as those of Fig. 1, appears to contain two factors, a non-electrostatic one independent of charge or ionic strength, and an electrostatic factor depending strongly on these variables. The expanded form of Einstein's equation, or the corresponding equations of Guth,[43] suggest that

there might be significance in expressing the concentration dependence of the viscosity of macromolecular solutions by a power series of the form[44]

$$\eta/\eta_0 = 1 + [\eta]c + K[\eta]^2 c^2 + \ldots$$

if we use this equation to describe our results, we should conclude that K is the sum of two terms, $K = K_0 + K_1$, K_0 representing the non-electrostatic interaction between the dissolved particles and K_1, the electrostatic interaction. K_1 should be a function of charge and ionic strength, and should vanish when $\overline{Z^2} = 0$, or, at any value of $\overline{Z}$, where μ is sufficiently large. Rough empirical values of K_0 and K_1 may be obtained from Fig. 2. One obtains for K_0 the value of 1.88 ± 0.13, while K_1 is given approximately as $2 \times 10^{-5}\ \overline{Z^2}/\mu^{3/2}$.

It is of interest that the value of K_0 is essentially the same as that found in this Laboratory for another protein, ribonuclease, for which we obtained $K_0 = 1.92 \pm 0.12$. It is also close to the value, $K_0 = 2.26$, predicted by the equation of Guth and Gold.[43] An examination of literature data does not suggest, however, that this is a universal constant applicable to all proteins.[45]

(42) J. G. Kirkwood and J. B. Shumaker, *Proc. Natl. Acad. Sci. U.S.*, **38**, 863 (1952).

(43) E. Guth, *Kolloid-Z.*, **74**, 147 (1936); E. Guth and O. Gold, *Phys. Revs.*, **53**, 322 (1938).

(44) J. G. Buzzell, Ph.D. Thesis, State University of Iowa, 1955.

(45) The data of Polson,[20] for example, yield considerably smaller values of K_0 for a number of proteins, but a value near 2.0 is obtained from his data for serum globulin in 0.81 *M* NaCl.

HIGH TEMPERATURE HEAT CONTENT AND HEAT CAPACITY OF Al₂O₃ AND MoSi₂[1]

By B. E. Walker, J. A. Grand and R. R. Miller

Chemistry Division, Naval Research Laboratory, Washington, D. C.

The heat capacity of Al₂O₃ and MoSi₂ were derived from heat content measurements made over the range 30 to 700° for Al₂O₃, and 30 to 900° for MoSi₂. The changes in enthalpy were determined by the "drop" method and a copper-block calorimeter. The calorimeter is a modified version of one previously used and described by J. C. Southard.[2] The furnace for heating the samples is specially constructed for high temperature heat capacity work.

Introduction

The purpose of this investigation was to check the accuracy of this Laboratory's apparatus through enthalpy and heat capacity measurements on a calorimetric standard material, Al₂O₃, and to provide some useful and accurate high temperature data on a relatively new and little known material, MoSi₂, for another agency.

Experimental Apparatus

The apparatus used in these determinations is a modified version of Southard's apparatus[2] in which a capsule is heated to a desired temperature and at a given moment is dropped into a calorimeter of known heat capacity. The modifica-

tions described below were introduced principally to attain greater accuracy and ease in operation.

The copper-block calorimeter is immersed in an oil-bath, which is well insulated to prevent excessive heat leakage. The bath is controlled at 30° by a Magna-set precision thermostat, which, when used in conjunction with two motor-driven stirrers, a 50-watt nichrome heater and a copper-cooling coil, maintains the bath temperature to within ±0.005°.

The calorimeter consists of three separate copper parts, which were machined from the same bar and assembled by shrinking the inner parts into position. The calorimeter thermometer, which is a transposed bridge arrangement of two copper and two manganin resistances (270 Ω each), as suggested by Maier[3] and used by Southard,[2] is wound on the central copper piece. The heater for electrical calibration purposes is wound on the copper block that forms the receiving well. The calorimeter is protected from furnace

(1) This work was sponsored by the Materials Lab., Research Division, Wright Air Development Center.

(2) J. C. Southard, *J. Am. Chem. Soc.*, **63**, 3142 (1941).

(3) C. G. Maier, This Journal, **34**, 2860 (1930).

radiation by a double cam arrangement, which permits both cams to be opened simultaneously during a bucket drop.

The thermometer current is controlled by a NBS calibrated standard resistance and heliopot and is read on a Type B Rubicon millivolt potentiometer. The relative temperature of the calorimeter is read to 0.0002° on a shielded Type C Rubicon micro-volt potentiometer. The heat exchange rate of the calorimeter is 0.00106° per minute-degree and is reproducible from day to day to ±0.00002° per minute-degree.

The heat capacity of the calorimeter was determined in the standard manner by supplying a known quantity of heat to the calorimeter and observing the rise in temperature. The heat capacity was obtained from about thirty calibrations made before and during the enthalpy measurements and found to be 2049.35 cal./mv. with an average deviation of ±0.03%. (In this system 1 mv. is equivalent to 0.963°.)

The furnace is specially constructed for this work so that there will be an isothermal zone of considerable length and the temperatures of the containers will be accurately known. The Alundum furnace core (2.5 in. bore and 48 in. long) is wound with three platinum–10% rhodium heating elements so that a desired temperature can be obtained more quickly and to provide the long isothermal zone mentioned above Power for the heaters is supplied and controlled by several cascaded constant-voltage Sola transformers, in conjunction with a variable transformer for each heater.

A 60 in. McDanel porcelain tube fits inside the Alundum core and the thermocouples inside this tube are shielded from induced electromotive forces by a nickel screen placed between the core and the McDanel tube. Platinum–platinum–10% rhodium thermocouples are peened into the center of five high conducting gold tubes 1, $1/_2$, 6, $1/_2$ and 1 in. long. The gold tubes are spaced at equal intervals by porcelain tubes and located so that the temperature in the furnace may be read at several points. The central gold piece has two additional thermocouples attached at each end and a gold disc has been pinned to this tube so that the sample container, when drawn up into the furnace, will occupy the center and most nearly isothermal region of the furnace. The porcelain spacers and the gold tubes are grooved on their outer surfaces to allow clearance for the seven $1/_{16}$ in. diameter double-bore porcelain tubes, which contain the thermocouple leads. By suitable adjustment of the three heaters the temperature gradient of the central gold piece can be controlled within 0.1°/cm.

The thermocouples were calibrated at this Laboratory against several primary standard thermocouples from the National Bureau of Standards. The furnace temperatures are read on a Type B millivolt potentiometer and are calculated to be accurate to about ±0.05%.

Experimental Method

In brief, the method consists in heating the sample to a known temperature in the furnace; then dropping it into the calorimeter and measuring the temperature rise of the calorimeter. The furnace is considered to be at equilibrium when the change in temperature of the three thermocouples on the central gold tube is less than 0.01°/min. The temperature rise of the calorimeter is determined by the method of least squares and extrapolation back to a "zero" time computed by Dickinson's method.[4] These procedures are repeated at a number of furnace temperatures and the heat capacity can be derived by the usual methods.

The calorimeter and furnace tube are subjected to a continuous flow of argon gas to minimize the oxidation of the type 347 stainless steel containers. The effectiveness of the argon is evident from the fact that less than 6.0 mg. of oxygen were gained during the entire series of runs on the sample container.

In addition to the enthalpy measurements for the bucket containing the sample, the method also requires that measurements be made for the empty container. The heat content data obtained from type 347 stainless steel, varies slightly from the true heat content, especially at high temperatures, due to heat loss by radiation and convection during a drop and the heat content of the nichrome wire, which is attached to the container and included in a drop. When these corrections are applied, the heat content values for 347 stainless steel have an average deviation of only ±0.25%

from those found by the National Bureau of Standards.[5] The heat loss and the heat contributed by the nichrome wire, however, do not have to be accounted for in the sample runs because a bucket of similar shape, mass and composition is used, as well as the same dropping technique.

The method further requires that other conditions be nearly the same for the empty container runs as for the sample runs, such as the rate of flow of argon through the system, the thermal equilibrium of the furnace, and the time of fall of the containers from the furnace into the calorimeter. The buckets were allowed to fall freely, but due to the piston-like effect of the containers in falling, the heavier sample containers fell faster than the empty buckets. This was adjusted by attaching weights to the opposite end of the wire holding the container with sample in such a manner that its time of fall would be the same as an empty container.

The heat content measurements were all adjusted to the same temperature (30°). Small corrections, a maximum of 0.05% of the total heat measured, were made to account for the oxide formation on the bucket and for the argon gas in the bucket.

Experimental Results

In order to check the performance of the system, initial heat content and heat capacity measurements were made on the calorimetric standard material, Al_2O_3. The Al_2O_3 crystals were furnished by the National Bureau of Standards and stated to be 99.97% pure. The results were obtained from 30 to 700° over 100° intervals and are listed and compared to those attained at the National Bureau of Standards[6] in Tables I and II. The sample weighed 20.6987 g., *in vacuo*, and the type 347 stain-

TABLE I

HEAT CONTENT OF Al_2O_3

Temp., °C.	NRL $H_t - H_{30}$, cal./g.	NBS $H_t - H_{30}$, cal./g.	Cal./g. dev. NRL–NBS	% Dev. NRL–NBS
98.12	13.74	13.84	−0.10	−0.73
98.61	13.88	13.95	− .07	− .50
197.20	36.63	36.71	− .08	− .22
207.63	39.18	39.25	− .07	− .18
296.86	61.83	61.81	+ .02	+ .03
298.26	62.12	62.17	− .05	− .08
404.81	90.63	90.57	+ .06	+ .07
416.51	93.68	93.76	− .08	− .09
511.30	120.10	120.06	+ .04	+ .03
503.01	117.68	117.74	− .06	− .05
595.05	144.05	143.83	+ .22	+ .15
598.17	144.69	144.72	− .03	− .02
705.23	175.89	175.68	+ .21	+ .12
702.36	175.03	174.84	+ .19	+ .11

Mean   ±0.17%

TABLE II

HEAT CAPACITY OF Al_2O_3

Temp., °C.	NRL C_p, cal./g., °C.	NBS C_p, cal./g., °C.	% Dev. NRL–NBS
64.2	0.2020	0.2038	−0.89
150.4	.2315	.2319	−0.17
250.0	.2530	.2527	+0.12
354.1	.2669	.2671	−0.07
458.9	.2771	.2771	0.00
551.9	.2848	.2838	+0.35
650.2	.2900	.2892	+0.28

Mean   ±0.29%

(4) W. P. White, "Modern Colorimeter," Chemical Catalog Co., Inc., New York, N. Y., 1928, pp. 53–57.

(5) T. B. Douglas and J. L. Dever, NBS Report 2302, 1953.

(6) D. C. Ginnings and R. J. Corruccini, *J. Research Natl. Bur. Standards*, **38**, 593 (1947).

less steel container weighed 22.6643 g. No corrections were made for the small amount of impurities in the material.

The sample of MoSi₂ was supplied as a hot-pressed solid block and was machined to a precision fit with the 347 stainless steel container. This was done so that there would be good heat transfer from the sample to the calorimeter and thermal equilibrium in the calorimeter would be established in a relatively short period of time. The density of the sample was calculated to be 5.95 g./cc., which is 95% of the theoretical value (6.24 g./cc.).

Chemical analysis of the sample material indicated a purity of 97.8%, 1.0% iron and 0.4% excess silicon. Since it seemed most plausible that the impurities would be present as oxides, analysis for oxygen was performed by a vacuum fusion technique by the Metallurgy Division of this Laboratory. The amount of oxygen determined by this method was 0.8%, which satisfied the requirements for the presence of iron as Fe_2O_3 (1.4%) and the presence of silicon as SiO_2 (0.8%). Corrections were applied to the heat content measurements on this basis, since this seemed the most reasonable from the evidence and calculations showed that corrections based on other possible forms of the impurities would be substantially of the same order of magnitude.

Heat content and heat capacity results for MoSi₂ were completed from 30 to 900° at 100° intervals. The enthalpy values are shown in Table III and the heat capacity is indicated in Fig. 1. The sample weighed 29.6305 g. *in vacuo* and the 347 stainless steel container, 22.8911 g. The equations for heat content and specific heat of MoSi₂ in c.g.s. units are as follows

Temperature range 30 to 325°

$$H_t - H_{30}° = 0.1332t - 21.83 \log (t + 273.16) - 75.88(\pm 0.5\%) \quad (1)$$

$$C_p = 0.1332 \frac{-9.477}{t + 273.16} \quad (\pm 1.0\%) \quad (2)$$

Temperature range 325 to 875°

$$H_t - H_{30}° = 0.1404t - 31.93 \log (t + 273.16) + 50.18(\pm 0.5\%) \quad (3)$$

$$C_p = 0.1404 - \frac{13.864}{t + 273.16} \quad (\pm 1.0\%) \quad (4)$$

Although two sets of equations are given this does not necessarily indicate a break in the heat capacity curve of MoSi₂. This was only done because these two sets of equations best represented the experimental data.

It was also determined that the results agreed very well with heat content and heat capacity data for MoSi₂, as calculated from K. K. Kelley's data for molybdenum and silicon.[7] The average deviation of the experimental results from those calculated from Kelley's data was less than 0.3% for both the enthalpy and the heat capacity values. Consequently, the results give additional confirmation of Dulong and Petit's additive law of heat capacities and also provide verification of the heat content and heat capacity data on molybdenum and silicon.

(7) K. K. Kelley, Bureau of Mines Bulletin 476, 1949.
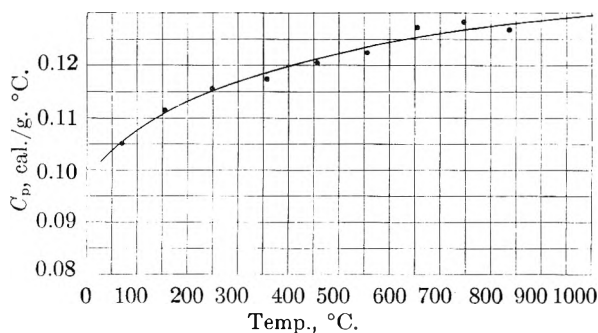
Fig. 1.—Heat capacity of molybdenum disilicide.

The results were also compared with those attained at the National Bureau of Standards.[8] The results of this investigation are about 2% higher in heat content and heat capacity than the NBS data. This may be due to differences in the samples, which, in both cases, were corrected for impurities, but are not known to be wholly in the form of the compound MoSi₂. The agreement, however, is fairly good considering the uncertainties attached to the samples, and either set of data should be applicable to most thermodynamic calculations.

TABLE III

HEAT CONTENT OF MoSi₂

Temp., °C.	$H_t - H_{30}$, cal./g. Obsd.	Calcd.	Dev. Obsd. − calcd., cal./g.	Dev. Obsd. − calcd., %
110.10	8.41	8.37	+0.04	+0.48
109.61	8.37	8.39	− .02	− .24
199.05	18.36	18.32	+ .04	+ .22
197.92	18.20	18.19	+ .01	+ .05
299.67	30.09	29.89	+ .20	+ .67
298.32	29.96	29.73	+ .23	+ .77
419.25	44.08	44.05	+ .03	+ .07
412.49	43.42	43.24	+ .18	+ .42
496.03	53.48	53.38	+ .10	+ .19
495.93	53.33	53.36	− .03	− .06
617.86	68.36	68.44	− .08	− .12
613.50	67.74	67.90	− .16	− .24
697.57	78.56	78.45	+ .11	+ .14
695.80	78.15	78.22	− .07	− .09
802.27	91.79	91.73	+ .06	+ .07
787.73	90.17	89.87	+ .30	+ .33
876.15	101.34	101.18	+ .16	+ .16
872.90	100.77	100.72	+ .05	+ .01

Mean   ±0.24%

The probable error in the present apparatus was calculated to be about ±0.3% in the enthalpy measurements and =2% in the heat capacity results. As indicated by the data, however, it appears that the above approximations are somewhat higher than is actually the case. This is probably due to the fact that the probable error was computed from the sum of all the uncertainties attached to the calibration, empty bucket and sample measurements, whereas most of these uncertainties were partially or fully cancelled out by maintaining the same techniques and procedures throughout the investigation.

(8) T. B. Douglas and W. Logan, *J. Research Natl. Bur. Standards*, **53**, 91 (1954).

INTERMETALLIC COMPOUNDS BETWEEN LITHIUM AND LEAD. I. THE STRUCTURES OF Li₃Pb AND Li₇Pb₂

By Allan Zalkin and William J. Ramsey

The crystal structures of Li_3Pb and Li_7Pb_2 have been determined. The Li_3Pb cell is face-centered cubic with $a = 6.687$ Å.; the Li_7Pb_2 cell is hexagonal with $a = 4.751$ Å. and $c = 8.589$ Å. Two other compounds with Li/Pb mole ratios of approximately 2.5 and 4.0 have been characterized by cooling-curve data and by X-ray diffraction patterns. The arrangement of the atoms in Li_3Pb is similar to that in lithium metal with the appropriate number of lithium atoms replaced by lead atoms; Li_7Pb_2 has a similar but slightly modified arrangement.

Introduction

The phase diagram of the lithium–lead system has been determined by Grube and Klaiber,[1] and Czochralski and Rassow.[2] The phase diagram indicates the existence of five intermetallic compounds, LiPb, Li_5Pb_2, Li_3Pb, Li_7Pb_2 and Li_4Pb. More recently Wilson[3] has investigated the electrical properties of LiPb; the structure of this compound has been treated by Nowotny,[4,5] Gundermann,[6] and Dehlinger.[5] Heats of formation of alloys of various compositions have also been determined.[7]

Rollier and Arreghini[8] have reported the structure of a compound, $Li_{10}Pb_3$, which they state corresponds to the melting point maximum in the system ascribed to Li_7Pb_2 by other workers. It has been found here that in the range of compositions where the Li/Pb atom ratio is between 4.0 and 2.5, four phases could be distinguished by X-ray diffraction analysis. Since these four phases corresponded in number to the four compounds previously reported, it was deemed desirable to investigate the structure of these phases. The results of this investigation are reported below.

Experimental

Reagents.—Lithium metal containing between 0.1 and 1% sodium, obtained from Metal Hydrides, Inc., was used. "Analytical Reagent" grade lead metal, obtained from Mallinckrodt Chemical Company and vacuum melted to remove the oxide coating, was used.

Apparatus.—The apparatus used in preparing the intermetallic compounds comprised essentially the following: a quartz tube to contain either an inert atmosphere or vacuum; an iron crucible to contain the melt, a thin walled can to protect the quartz from lithium vapor, and a thermocouple well, all made of Armco iron; and a resistance heater. Cooling curves were obtained with a recording potentiometer.

Procedure.—Various compositions of lead–lithium alloys were prepared in the following way. In an argon filled drybox, a sample of lithium metal weighing about 10 g. was cleaned, weighed and melted in an Armco iron crucible. While the lithium was liquid, an Armco iron thermocouple well was inserted, and the lithium was allowed to cool and solidify. A previously weighed sample of lead metal was then placed in the crucible containing lithium. This crucible was placed in an Armco iron protecting crucible, the thermocouple was inserted into the thermocouple well, and the apparatus described above was completely assembled.

The apparatus was then removed from the dry-box and attached to a manifold. As the sample was heated in an argon atmosphere, the lithium melted, and very soon thereafter reaction between the metals took place. Temperature increases on the order of 400° on reaction were not unusual. Two or three cooling curves were run to check the phase composition and homogeneity of the sample. In general, the cooling curves agreed well with the phase diagram of Grube and Klaiber.[1]

Once each sample had cooled, it was removed from the apparatus. A part was ground and loaded into capillaries, and a portion was analyzed chemically. The chemical analyses corresponded within a few per cent. (relative) to the amounts weighed out for each sample.

X-Ray Diffraction and Structure

In the range of compositions investigated, powder diffraction patterns indicated the presence of four distinct phases which occurred in the ranges of compositions in which the phase diagram predicts the existence of four compounds.

Li₃Pb.—X-Ray diffraction powder patterns showed the presence of a compound that is isomorphous with β-Li_3Bi and β-Li_3Sb.[9]

Li_3Pb is face-centered cubic with a cell constant of $a = 6.687 \pm 0.003$ Å., $Z = 4$, X-ray density = 5.06 g./cc., space group $O_h^5 - Fm3m$.

The following positions are suggested[10]

$$4Pb \quad \text{in } 4(a) \ 0,0,0; \text{ plus face centering}$$
$$4Li(I) \quad \text{in } 4(b) \ {}^1/_2, {}^1/_2, {}^1/_2; \text{ plus face centering}$$
$$8Li(II) \quad \text{in } 8(c) \ {}^1/_4, {}^1/_4, {}^1/_4; \ {}^3/_4, {}^3/_4, {}^3/_4; \text{ plus face centering}$$

Since the diffraction is due primarily to the lead atoms, the intensities of the powder diffraction lines are directly proportional to the multiplicities of the planes. Table I shows the calculated and observed intensities.

The interatomic distances in Å. are

$$
\begin{aligned}
Pb-8Li &= 2.90 \\
-6Li &= 3.34 \\
Li(I)-8Li &= 2.90 \\
-6Pb &= 3.34 \\
Li(II)-4Li &= 2.90 \\
-4Pb &= 2.90 \\
-6Li &= 3.34
\end{aligned}
$$

Each atom has eight nearest neighbors at 2.90 Å. There are no lead-to-lead contacts. This structure is similar to the lithium metal (body-centered cubic) structure where every other lithium in every other layer is replaced by a lead atom.

Li₇Pb₂.—A hexagonal cell was indexed for the material taken from the melt corresponding to Li_7Pb_2. The observed cell constants are: $a =$

(1) G. Grube and H. Klaiber, *Z. Elektrochem.*, **40**, 745 (1934).

(2) J. Czochralski and E. Rassow, *Z. Metallkunde*, **19**, 111 (1927).

(3) T. C. Wilson, *J. Chem. Phys.*, **8**, 13 (1940).

(4) H. Nowotny, *Z. Metallkunde*, **33**, 388 (1941).

(5) U. Dehlinger and H. Nowotny, *ibid.*, **34**, 200 (1942).

(6) J. Gundermann, *ibid.*, 120 (1942).

(7) F. Weibke and O. Kubaschewski, "Thermochemie der Legierungen," Springer Verlag, Berlin, 1943, p. 263.

(8) M. A. Rollier and E. Arreghini, *Z. Krist.*, **101**, 470 (1939).

(9) G. Brauer and E. Zintl, *Z. physik. Chem.*, **37B**, 323 (1937).

(10) Terminology from "International Tables for X-Ray Crystallography," pub. for International Union of Crystallography, Kynoch Press, Birmingham, England, 1952.

TABLE I

POWDER DIFFRACTION DATA FOR Li₃Pb[a]

d (Å.)	$I_{obsd.}$[b]	$I_{calcd.}$	hkl
3.85	m⁺	19	111
3.33	m	14	200
2.36	s	25	220
2.01	s	49	311
1.92	w⁺	16	222
1.67	w	12	400
1.53	m	45	331
1.49	m	43	420
1.36	m⁺	42	422
1.29	m⁺	55	{ 333 / 511 }
1.18	w	19	440
1.13	s⁻	76	531
1.11	m	47	{ 600 / 442 }
1.06	w⁺	36	620
1.02	m⁻	35	533
1.01	w⁺	34	622
0.96	vw	11	444
0.94	m	69	{ 711 / 551 }
0.93	w⁺	34	640
0.90	m⁺	67	642
0.87	s	100	{ 731 / 553 }
0.82	m⁻	40 { 8 / 32 }	{ 800 / 733 }
0.81	m⁺	64	{ 820 / 644 }
0.79	m	48	{ 822 / 660 }

[a] Obtained with Cu Kα radiation (λ = 1.5418 Å.); 35 kv., 15 ma. for 12 hours. [b] Visual estimates with no corrections for absorption or polarization.

4.751 ± 0.002 Å., c = 8.589 ± 0.004 Å., c/a = 1.808 ± 0.002 Å. The experimental density as determined with a helium displacement densitometer is 4.53 g./cc.; the X-ray density is 4.59 g./cc.

The diffraction line intensities from the powder pattern of Li₇Pb₂ compared well with those reported for the Na₃As type structures by Brauer and Zintl[9] on such compounds as: α-Li₃Sb, Na₃Bi and Na₃As. The possibility that Li₇Pb₂ was actually a beta form of Li₃Pb or a lead-deficient form of the same was ruled out on the basis of the analysis and the measured density. A calculated density for a lead-deficient compound of the proper composition is about 4.0 g./cc.

The apparent similarity between Li₇Pb₂ and the Na₃As type structure was used in the structure determination. The lead atoms in Li₇Pb₂ were placed in the same positions as the arsenic atoms in Na₃As. Since the heavy atoms in the Li₇Pb₂ do practically all of the diffracting, the positions of the lithiums are deduced from spatial and steric arguments. The structure of Na₃As as given by Brauer and Zintl[9] consists of rows of atoms in the c direction (see Fig. 1a). There are three rows per unit cell; two rows contain both light and heavy atoms, and one row contains only light atoms. By elaborating on this latter row, it is possible to intro-

duce an additional atom into this row and to maintain distances comparable to those in Li₃Pb (see Fig. 1b).
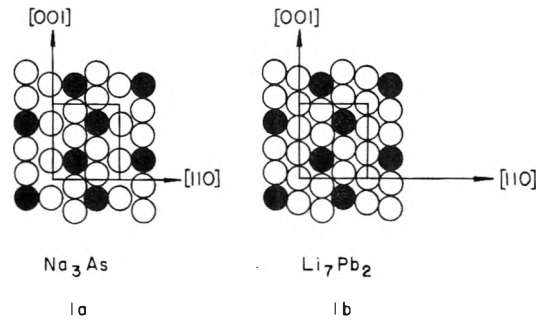
Fig. 1.—The Na₃As and the Li₇Pb₂ type packing as indicated in the (110) layer.

The space group for the arrangement in Fig. 1b is D_3^2 — P321; other acceptable space groups of lower symmetry are P3 and P3m1.

The positions suggested are[10]

2Pb   in 2(d) ⅓, ⅔, z; ⅔, ⅓, z̄; with z = +¼
4Li(I) in 2(c) ⅓, ⅔, z; ⅔, ⅓, z̄; with z = −½
        2(d) ⅓, ⅔, z; ⅔, ⅓, z̄; with z = −⁵/₁₂
2Li(II) in 2(c) 0, 0, z; 0, 0, z̄; with z = ⅓
1Li(III) in 1(a) 0, 0, 0
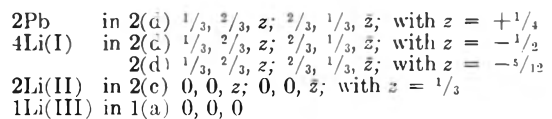
This arrangement of atoms was found to be similar to that found in Li₃Pb and Li metal; this is indicated in Fig. 2. The arrangements in Fig. 1b are slightly shifted from that shown in Fig. 2d. On the basis of the undistorted Li metal type arrangement, the lead z parameter in Li₇Pb₂ should be 2/9 as opposed to 1/4 mentioned above. Intensity calculations were made using both parameters (see Table II). These data indicated that z = 1/4 and that a slight shift of the atoms has occurred from the ideal stacking. This shift is also apparent in the c/a ratio. With a pure Li type arrangement, the ratio of c/a should be $3\sqrt{3}/2\sqrt{2}$ = 1.837, whereas in the actual structure it is 1.808 ± 0.002.
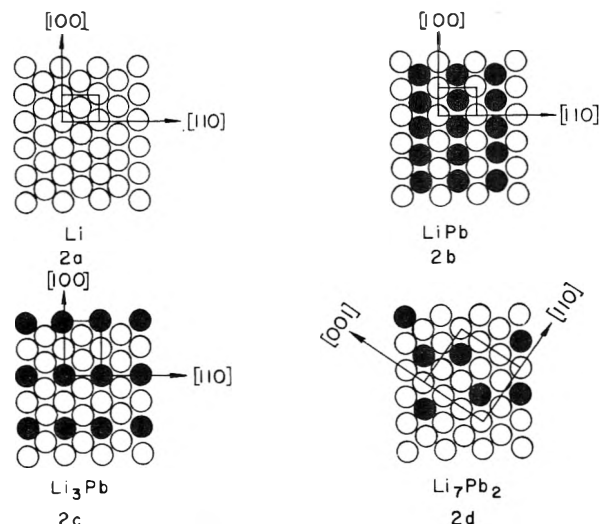
Fig. 2.—Schematic diagram showing the related stacking arrangements in a layer corresponding to the (110) plane in lithium. The cell directions in each case are indicated.

TABLE II
OBSERVED AND CALCULATED POWDER DIFFRACTION DATA FOR $Li_7Pb_2{}^a$

			$I_{calcd.}{}^c$	
hkl	d (Å.)	$I_{obsd.}{}^b$	$z = 1/4$	$z = 2/9$
001			0	1
002	4.25	w$^+$	15	13
100	4.06	w	10	12
101	3.67	m	65	65
102	2.95	w$^+$	21	26
003			0	3
110	2.36	m$^-$	39	40
103	2.33	m	59	49
111			0	2
004	2.13	w	12	7
112	2.07	m	75	67
200	2.05	vw	9	9
201	1.99	m$^-$	55	55
104	1.90	w$^+$	18	33
202	1.85	w$^+$	18	23
113			0	18
005			0	6
203	1.67	m$^+$	52	44
114	1.59	m$^+$	68	41
105	1.58	m	51	32
210	1.55	w	17	17
211	1.53	s	100	100
204	1.48	w	17	31
212	1.46	m$^-$	33	41
006	1.42	w$^+$	11	3
115	1.39	vw	0	40
300		m$^-$	32	33
213	1.36	s	97	82
301			0	2
106	1.35	m	16	40
205	1.31	m$^+$	47	29
302	1.30	s$^-$	63	56
214	1.26	m$^+$	30	57
303			0	16
007 } 116 }	1.22	s	61 { 0 / 61	21 { 6 / 15
220	1.19	s$^-$	30	31
221			0	2
107 } 206 }	1.17	s$^+$	60 { 45 / 15	56 { 19 / 37
304	1.16	s	58	35
215	1.15	s$^+$	88	54

^{a} Chromium Kα (λ = 2.2909 Å.); measured visually, 25 kv., 15 ma. for 30 hours. ^{b} Visual estimates uncorrected for absorption or polarization. ^{c} Calculated intensities do not include lithium contributions.

The interatomic distances in Å. are

$$
\begin{array}{rl}
Pb{-}5Li & = 2.82{-}2.86 \\
{-}6Li & = 3.08 \\
Li(I){-}1Pb & = 2.86 \\
{-}3Pb & = 3.08 \\
{-}4Li & = 2.82{-}2.86 \\
{-}3Li & = 3.08 \\
Li(II){-}3Pb & = 2.82{-}2.86 \\
{-}5Li & = 2.82{-}2.86 \\
Li(III){-}8Li & = 2.82{-}2.86
\end{array}
$$

Compound where Li/Pb $\approx$ 2.5.—The patterns of several samples of this material showed it alone or mixed with Li_3Pb. The powder patterns are moderately complex and were not indexed.

Subsequent single-crystal analysis has shown this material to have a monoclinic cell with a probable formula Li_8Pb_3. This work will be published separately.

Compound where Li/Pb $\approx$ 4.0.—This compound was observed in the lithium-rich melts where the Li to Pb ratio was greater than 7/2. A chip of the material was mounted on a single-crystal Weissenberg camera, and it gave patterns which were interpreted as due to a face-centered cubic cell with $a = 20.0$ Å. The details of the structure are to be worked out.

Some of the X-ray powder diffraction data are shown in Table III.

TABLE III
POWDER DIFFRACTION DATA FOR $Li_4Pb{}^a$

d	I	d	I
vw	6.01	m$^+$	2.78
vw	5.01	w$^+$	2.65
s$^-$	4.55	m$^-$	2.59
s	4.04	m	2.42
s$^+$	3.79	s	2.34
m$^-$	3.51	m	2.29
w	3.35	vw	2.18
vw	3.15	m	2.08
m	3.03	m$^-$	2.02
m$^-$	2.85	m$^+$	2.00

^{a} Cu Kα X-rays used (λ = 1.5418 Å.); 35 kv., 15 ma. for 12 hours.

Discussion

A comparison of four structures is made in Fig. 2; they are Li,[11] LiPb,[12] Li_3Pb and Li_7Pb_2. The similarity in the arrangement is indicated. Li_7Pb_2 is in reality shifted slightly from that shown in Fig. 2; this has been discussed previously. This figure illustrates that the basic arrangement of the atoms in metallic lithium is carried on into the lithium–lead compounds. There are indications that this is also true with the remaining two other lithium–lead structures.

The nearest neighbor situation is summarized in Table IV.

TABLE IV
INTERATOMIC DISTANCES IN Li–Pb SYSTEM

	Nearest Li–Li distances, Å.	Nearest Li–Pb distances, Å.	No. of lithium nearest neighbors to each Pb
Li	3.04	..	..
LiPb	3.53	3.06	8
Li_3Pb	2.90	2.90	8
Li_7Pb_2	2.82–2.86	2.82–2.86	5 } 11
	3.08	3.08	6 }

$Li_{10}Pb_3$ as described by Rollier and Arreghini[8] was not observed in any of the diffraction patterns obtained.

(11) H. Perlitz and E. Aruja, *Phil. Mag.*, **30**, 55 (1940); Li has a body-centered cell, a = 3.508 Å.

(12) H. Nowotny, *Z. Metallkunde*, **33**, 388 (1941); CsCl type, a = 3.529 Å.

SELF-DIFFUSION OF SODIUM ION IN A CATION-EXCHANGE RESIN[1]

By David Richman and Henry C. Thomas[2]

Contribution from Sterling Chemistry Laboratory, Yale University, New Haven, Conn.

Received July 25, 1955

By means of a procedure based on diffusion from a well-stirred bath into a long rod, the coefficient of self-diffusion of sodium in a cation-exchange resin at chemical equilibrium has been measured. Evidence is presented for the absence of a liquid film effect. The results at two temperatures indicate at least two mechanisms for the transport through the resin: in the absence of Donnan electrolyte an exchange between sites with activation energy about 10 kcal./mole, and a diffusion involving free anion with activation energy about 2 kcal./mole.

The diffusion of ions within the matrix of a solid cross-linked polyelectrolyte must be a very complicated process. In the study of such a process it is of course advantageous to simplify the situation as much as is consistent with retaining its essential features. Much simplification is obtained by limiting the study to self-diffusion and this in a material at chemical equilibrium. We have carried out such a study with the cation exchanger Nepton CR-51,[3] a phenolsulfonic acid–formaldehyde copolymer. The resin was obtained in the form of nearly cylindrical rods about 5 mm. in diameter. This simple and well-defined shape made possible an especially simple diffusion experiment: the measurement of diffusion from a limited bath into the end of an infinite uniform rod.

The solution of the equation for isotopic diffusion, with no gradient of excess chemical potential, *i.e.*, no gradient of activity coefficient, for the case of a well-stirred limited bath into an infinite rod with no boundary liquid film and with isotopic equilibrium at the interface is

$$\theta/\theta_0 = \exp\left(\alpha^2 A^2 Dt/V^2\right) \operatorname{erfc}\left(\alpha A \sqrt{Dt}/V\right)$$

Here θ/θ_0 is the relative isotopic content (relative radioactivity in our case) of the bath at time t, the rods being initially free of marked isotope; $\alpha = q/c$ is the distribution coefficient of the diffusing isotopic species, being merely the ratio of the equilibrium values of the volume concentrations (exchanger)/(solution); A, the total area of the ends of the rods exposed to the solution; V, the volume of the solution; and D, the coefficient of self-diffusion in the solid. It will be shown that a significant liquid film was absent under the conditions of our experiments.

Rods of length about 20 cm. were used. That these rods are effectively of infinite length is easily shown. The fraction of the activity initially in the bath which has diffused by time t beyond the point $x = \xi$ measured from the input end (of an infinite rod) is

$$\operatorname{erfc}\left(\xi/2\sqrt{Dt}\right) - \exp\left(\kappa^2 Dt + \kappa\xi\right)$$
$$\times \operatorname{erfc}\left\{(\xi/2\sqrt{Dt}) + \kappa\sqrt{Dt}\right\}$$

in which κ has been written for $\alpha A/V$. With moderately pessimistic estimates for the various quantities, in particular if we put $D = 10^{-5}$ (more than

twice our largest measured value) and $t = 10^5$ sec. (the average duration of a run), and $\xi = 10$ cm., this fraction turns out to be of the order 10^{-12}; *i.e.*, radiosodium never reached the ends of our rods.

Experimental

The procedure consisted in pumping continuously the radioactive bath solution through a jacketed Geiger–Mueller counter. A small glass centrifugal pump served to move the solution, and very vigorous stirring resulted. The solution, on entering the reaction chamber, was caused to impinge directly against the ends of the rods to eliminate as far as possible a static liquid film.

The counter ran continuously and was followed by a conventional scale-of-4096 circuit. The cumulative count and time were recorded at intervals of 100 × 4096 counts. Background and resolving time corrections were applied. If the cumulative count divided by the initial counting rate be called R, then because of the simple nature of the diffusion problem we have the following relation between R and its time derivative $dR/dt = \theta/\theta_0$

$$k^2 R - 2k\sqrt{t/\pi} - dR/dt + 1 = 0$$

in which $k = \alpha A \sqrt{D}/V$. Thus the determination of D results directly from the solution of a quadratic equation involving the experimental record and its time derivative. For each run some fifteen to twenty values of k were computed, the slope dR/dt being taken as $409600/\Delta t$ at $t + \Delta t/2$.

To obtain sufficiently large effects a group of three rods was used in each experiment. One end of each rod was flattened with a fine jeweler's file, and the surface area exposed to the solution was determined by several measurements of the diameter. Two groups of three rods were used, with satisfactory agreement between the groups (*vide infra*). The rods were soaked in concentrated NaCl solution to remove activity from previous experiments and then for several hours in distilled water. The equilibration with the desired solution was accomplished by slowly passing over the rods 2–4 liters of the solution during a period of 24–40 hours.

The ends of the rods to be exposed to the solution were defined by forcing the rod through a pin-hole in a piece of dental dam, the sides of the rods being protected by taping the rubber sheet into place.

Thermostat water (at 30 or 50°) was circulated around the chamber containing the radioactive solution and rods.

The exchange capacities of the polymer were determined by an isotopic dilution in the following manner. Small pieces of about 2-ml. volume were equilibrated with the desired solution (many hours rotation in the thermostat). The resin volume was then determined by weighing in a pycnometer filled with the appropriate solution, and, after wiping dry, quickly weighing the resin itself. The density of the solution and the volume of the pycnometer being known, the necessary information was available. The bits of resin were then placed in aliquots of a solution, carrying sodium-22 tracer, of the same gross concentration as the solution with which the rods were equilibrated. The rods were agitated in this solution for 10–20 hours in the thermostat. The initial activity of the solution and the activity after isotopic equilibrium was reached give immediately the total capacity of the resin under the conditions of the experiment. Typical results at 30° are as follows: three pieces of resin in 0.01 N NaCl gave 0.873, 0.897, 0.891 meq./ml.; three pieces in 0.05 N NaCl gave 0.914, 0.953, 0.954

meq./ml. The capacity of the exchanger in its dependence on the concentration of the external solution is sufficiently well reproduced by the linear relation

$$q = 0.865 + 1.73c$$

This relation is, of course, not consistent with the usual formulation of the Donnan effect, $q(+)q(-)/c^2 = 1$, which requires that in the limit of low concentration q be linearly related to c^2. Only below 0.03 N do our results show approximately this proportionality. Within the precision of our experiments no effect of temperature is discernible. This point, however, needs more careful study.

A preliminary experiment was designed to show any effect due to diffusion through a static liquid film at the end of the rods. A metal baffle was placed in the reaction chamber so that on changing its position (by means of a glass rod extending to the outside) the agitation of the solution in the neighborhood of the resin was materially reduced. No change in the course of the R vs. t curve was detected when the position of the baffle was changed. This fact coupled with a consideration of the values of D obtained show that liquid film diffusion was negligible.

Values of $k = \alpha A \sqrt{D}/V$ should, of course, be constant throughout a run. Typical results are shown in Table I. It is difficult to estimate how much scatter to expect in these results depending as they do in such a complicated manner on the results of radioactivity counting. After the initial stages of a run no trends are observable in the values of k. In the first two runs k failed to reach a steady value until after 25,000 sec. This effect appears to have been due to a partial drying at the ends of the rods. In subsequent experiments the ends of the rods were kept moist at all times during the handling, and k assumed essentially constant values after 5,000–10,000 sec.

TABLE I

Course of Self-diffusion of Na^+ from 0.03 N NaCl into Nepton CR-51

t, sec.	$k \times 10^{-4}$	t, sec.	$k \times 10^{-4}$	t, sec.	$k \times 10^{-4}$
12300	4.80	60700	4.98	88000	4.74
29600	5.38	65900	4.90	92700	4.94
47400	5.09	70800	4.74	129500	4.74
51600	5.02	76700	4.54	132700	4.81
56300	5.03	83500	4.67	140100	4.82

Independent experiments at 30° with 0.01 N solutions using different groups of rods, differing by a factor of two in total exposed area, gave 1.34×10^{-6} and 1.23×10^{-6} cm.^{2}/sec. for D. Perhaps the largest sources of error are in the capacity determinations and in the definition of the exposed surface. Errors due to lack of definition (smoothness) of the ends of the rods are impossible to estimate. The capacity determinations depend on differences in counting rates and are subject to errors of 2 to 5%. A 5 to 10% uncertainty in D seems reasonably pessimistic under the circumstances.

The experiments at 50° were beset with difficulties not met near room temperature. Among other things we found that warm neutral sodium chloride solutions will etch pinholes through the walls of thin stainless steel Geiger counters. Our results on the temperature effect are by no means as complete as could be desired.

The results of this work are summarized in Table II.

TABLE II

Capacity and Coefficient of Self-diffusion for Na^+ in Nepton CR-51 at Chemical Equilibrium

Bath N NaCl	Capacity, meq. Na/ml. resin 30°	50°	$D \times 10^6$, cm.^{2}/sec. 30°	50°
0.0025	...	0.860	...	...
.01	0.891	.964	1.32	3.79
.02	.912	...	2.43	...
.03	.930	...	4.69	...
.05	.954	...	4.88	...
.07	...	.974	...	6.01
.10	1.036	...	4.77	...

Discussion

When the diffusion coefficient is plotted against the concentration of the external solution, the curve obtained rises sharply up to 0.03 M after which it is nearly horizontal. The nature of this curve suggests immediately that at least two mechanisms are responsible for the transfer of the cation through the resin matrix. This effect was apparently first found and discussed by R. Schlögl.[4] In the leached state in which no free anions are present, the transfer must be an exchange between relatively widely separated sulfonic acid groups. This mechanism is characterized by a low diffusion coefficient, about 1×10^{-6} cm.^{2}/sec. As the free anion content of the resin increases an easier path for the transfer becomes available through the presence of the negative carrier. This mechanism is characterized by the considerably larger coefficient, 4.8×10^{-6} cm.^{2}/sec. The runs at 50° bear out these ideas both as to the relative magnitude of the constants and as to the temperature coefficients. Calculating activation energies from the formula $D = A \exp (E/RT)$, we obtain at 0.01 N, $E = 10.3$ kcal. and at 0.07 N, $E = 2.2$ kcal. Thus the formation of the activated state for the exchange between neighboring sulfonic groups requires much more energy than that for the exchange taking place through the medium of the free anion, as would certainly be expected.

According to the calculations of Wang[5] the activation energy for self-diffusion of Na^+ in NaCl solution (at infinite dilution) is 4.4 kcal. Our value of 10.3 kcal. (at 0.01 N) implies again that the process is not one of diffusion through a film of solution at the end of the rod.

There is little in the literature with which to compare these results. Spiegler and Coryell[6] find 1.95×10^{-6} cm. for the D of Na^+ in a sample of Nepton. Their experiment was carried out in an entirely different manner and on a different batch of resin; it is possible to state only that our results are not inconsistent with theirs. The extensive work of Boyd and Soldano,[7] where it is comparable with ours, produced results of the same order of magnitude. Their experiments are complicated by the fact that in most cases the exchanger was not initially at chemical equilibrium with the bath. Furthermore, in order to avoid effects of film diffusion Boyd and Soldano worked at higher concentrations and found no effect due to change in external concentration.

If one considers two mechanisms for transfer of ions through the resin which interact only to produce local isotopic equilibrium of the diffusing species, and are characterized simply by two coefficients, D_0 for interchange between fixed sites and D_1 for diffusion in the Donnan electrolyte, the relation between these coefficients and the observed value of D is[8]

$$D = D_0(q_0/q) + D_1(1 - q_0/q)$$

(4) R. Schlögl, Z. Elektrochem., **57**, 195 (1952).

(5) J. H. Wang, J. Am. Chem. Soc., **74**, 1612 (1952).

(6) K. S. Spiegler and C. D. Coryell, This Journal, **57**, 687 (1953).

(7) G. E. Boyd and B. A. Soldano, J. Am. Chem. Soc., **75**, 6091 (1953).

(8) This relation results immediately from the condition of conservation of the diffusing ion at local isotopic equilibrium.

in which q_0 is the concentration of fixed charges in the resin and q is the total concentration of gegenion. This formulation cannot account quantitatively for the observed dependence of D on the concentration of the external electrolyte; it gives much too gentle an increase in D. The picture, however, is evidently oversimplified. A rapid exchange between free and bound ions within the resin would certainly not be unaccompanied by a marked alteration of the field between bound ions. The presence of free ion pairs will act to decrease the activation energy for an exchange between sites. This ef-

fect will cause an exponential increase in the value of D_0 itself, leading to a rapid increase in the observed value of D. An exact formulation of this idea would be a very involved problem for the concentrated systems with which we are concerned; we do not attempt it.

It should be remarked that these considerations do not appear to apply to the results of the work of Schlögl,[4] who finds a rather slow increase in D with increase in concentration of the Donnan electrolyte. Evidently more work with a variety of well-characterized exchangers is much to be desired.

THE EQUILIBRIA BETWEEN TRI-*n*-OCTYLAMINE AND SULFURIC ACID

By Kenneth A. Allen

Oak Ridge National Laboratory, Oak Ridge, Tennessee

Received August 1, 1955

Benzene solutions of tri-*n*-octylamine have been equilibrated with aqueous sulfuric acid at 25°. The amine sulfate and bisulfate species remain in the organic phase, and the data are interpreted on the basis of polymerization of these salts. Equilibrium constants for the formation of the normal sulfate and for sulfate–bisulfate exchange within the colloid are evaluated, and a hypothesized distribution of free amine between solvent and colloid is shown to lead to a relation of the form of a solubility product for the reaction between free amine and sulfuric acid.

I. Introduction

The long chain amines have been shown to be efficient extractants of mineral acids. Smith and Page[1] used tertiaries such as methyldi-*n*-octylamine in chloroform or nitrobenzene to effect the quantitative separation of strong acids from water-soluble organics such as glycine and glutamic acid. There are other examples of similar applications of these amines; very little has been done, however, toward the elucidation of the fundamental processes which occur. It has been shown that the latter are by no means simple,[2] and considerable unpublished information on the reactions between benzene solutions of di-*n*-decylamine and aqueous sulfuric acid indicates polymerization of the amine salts in the organic phase.[3] The present investigation with a tertiary amine generally corroborates the qualitative conclusions obtained from the earlier work and has provided a quantitative theoretical treatment for the case of tri-*n*-octylamine.

II. Experimental

Materials.—The tri-*n*-octylamine (hereinafter this amine will be referred to as TOA) used in this work was from a special preparation supplied by Carbide and Carbon Chemicals Company. Its neutralization equivalent was 354 ± 1 (theor., 353.7) and its tertiary amine content was $100 \pm 1\%$.[4] A sample subjected to fractional distillation boiled at constant temperature with the exception of a trace of lower boiling forerun, and the neutralization equivalents of the first, middle and tail fractions were in excellent agreement with the theoretical value given above. Fischer titrations showed the water content of this amine to be less than one-half gram per mole, and a weighed sample exposed to the laboratory atmosphere for three days showed only a 0.1%

loss in weight, precluding any possibility of extensive take-up of water or carbon dioxide.

Standard solutions of TOA in benzene were prepared on a weight basis, diluted to the mark at $25.00 \pm 0.05°$ and stored in the 25° thermostat throughout their period of use. All other reagents used were of the standard C.P. reagent grade furnished by the large chemical supply houses. The distilled water was subjected to de-ionization[5] immediately before use and usually showed a *p*H of around 6.

Apparatus.—The only equipment of a specialized nature used in this work was a shaking apparatus. This assembly accommodated six separatory funnels in a thermostat regulated at $25.0 \pm 0.1°$ and the degree of agitation could be changed by means of a variable drive motor. A standard speed of agitation was determined from a few preliminary experiments and adhered to throughout the investigation. A series of rate studies with 0.5 and 0.05 *M* TOA equilibrated with widely varying sulfuric acid concentrations for shaking times of one-half, one and two hours showed that equilibrium was attained in all cases in a half hour. The data reported below are based on shaking times of one hour or more.

Procedure and Analyses.—A series of six 60-ml. separatory funnels were used for the equilibrations. In a typical run 20 ml. of water, varying amounts of standard sulfuric acid and 10 ml. of the appropriate amine solution were pipetted into each funnel. After agitation at 25° the funnels were usually allowed to stand in the bath overnight to allow complete phase separation. Each aqueous layer was then drained into a clean, dry beaker from which aliquot portions were pipetted for titration with standard base. In the low acid range 0.01 *N* NaOH was used, the samples being titrated to *p*H 7 on a meter. The higher acidities were measured with tenth normal base using phenolphthalein. The technique for the determination of H_2SO_4 adsorbed into the organic phases was as follows: 3–5 ml. of the benzene solution was pipetted directly from the funnel into a 150-ml. beaker, 20–25 ml. of acetone added, and one drop of the usual phenolphthalein indicator solution. The magnetically stirred solution was then titrated with standard aqueous base to a faint permanent pink. The solutions usually became quite cloudy during the titration; rapid stirring and strong illumination were necessary for good results. Checks run on 5-ml. portions of amine solutions to which known amounts of H_2SO_4 had been added were in excellent agreement with the calculated values.

(1) E. L. Smith and J. E. Page, *J. Soc. Chem. Ind. (London)*, **67**, 48 (1948).

(2) K. B. Brown, C. F. Coleman, D. J. Crouse, J. O. Denis and J. G. Moore, Classified Report ORNL-1734.

(3) K. A. Allen, C. F. Baes, Jr., and W. J. McDowell, unpublished report.

(4) These analyses were performed by J. G. Moore, of this Laboratory, using standard techniques.

(5) An "Illco-Way" research model de-ionizer made by the Illinois Water Treatment Co., Rockford, Illinois, was used according to the manufacturer's directions.

III. Results and Discussion

In all calculations involving aqueous sulfuric acid concentrations the appropriate activity was used.[6] The activity coefficients of all monomeric species in the organic phase were assumed to be unity. For brevity and convenience in the following discussion reacting sulfuric acid is written in the undissociated form and the symbol R is used for the amine molecule $(C_8H_{17})_3N$.

From the equilibration data obtained with a 0.1 M TOA solution a titration curve was constructed by plotting $a^{1/3}_{H_2SO_4}$ vs. the quantity $[H_2SO_4]_{org}/[\Sigma R]$. For comparison, a similar curve is shown for 0.1 M di-n-decylamine in Fig. 1. These plots show a striking comparative similarity to the titration curves for weak and strong base anion exchange resins given by Kunin and Myers.[8]
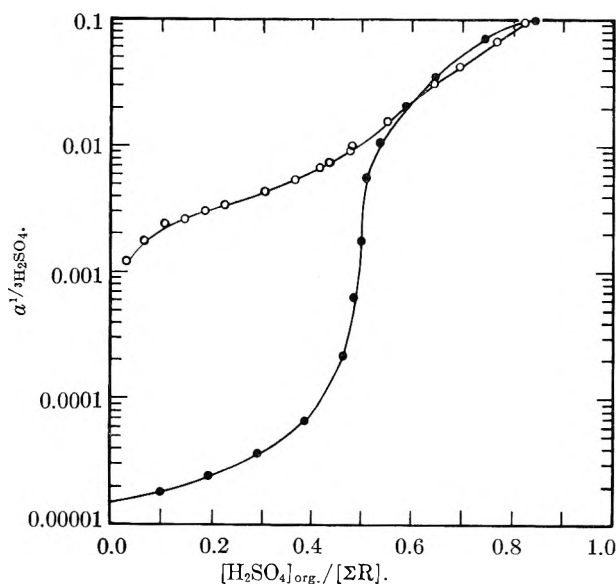
Fig. 1.—Titration curves: ◯, 0.1 M TOA; ●, 0.1 M di-n-decylamine.

The reaction between TOA and H_2SO_4 to form the normal sulfate is

$$H_2SO_4 + 2R = R_2H_2SO_4 \qquad (2)$$
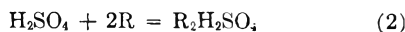
and the corresponding equilibrium constant K_1 should be given by the expression

$$K_1 = \frac{[R_2H_2SO_4]}{a_{H_2SO_4}\,[R]^2} \qquad (3)$$

In Table I are listed a large number of analytical results and in Fig. 2 the corresponding values of $a_{H_2SO_4}$ are plotted against the quantity $[R_2H_2SO_4]/$

(6) Values of the mean molal activity coefficient $\gamma\pm$ are listed in Harned and Owen[7] for varying sulfuric acid molalities. In the notation employed by these authors the mean molar activity coefficient $y\pm$ can be calculated from $\gamma\pm$ and the corresponding values of the molality m, the molarity c and the solvent density. The molar activity of sulfuric acid is then obtained from equation 1

$$a_{H_2SO_4} = y\pm^3c\pm^3 = 4y\pm^3c^3 \qquad (1)$$

where $c\pm$ is the mean ionic molarity. For convenience the quantity $\sqrt[3]{4}\,y\pm\,c$ was plotted vs. c on log-log paper over the range of concentrations encountered. Values of $a^{1/3}$ were then read from this plot as needed.

(7) H. S. Harned and B. B. Owen, "The Physical Chemistry of Electrolytic Solutions," 2nd Ed., Reinhold Publ. Corp., New York, N. Y., 1950.

(8) Robert Kunin and R. J. Myers, "Ion Exchange Resins," John Wiley and Sons, Inc., New York, N. Y., 1950, p. 40.

[R]² for 0.05, 0.1, 0.25 and 0.5 M TOA. The straight line was drawn with unit slope, and it is to be noted that while the points for the first three concentrations are in fair coincidence with the line at low activities, systematic departures are soon evidenced by the tenth and quarter molar data. The four points obtained with half molar TOA diverge widely.

TABLE I

[H₂SO₄]aq	[H₂SO₄]org	[H₂SO₄]aq	[H₂SO₄]org
A. TOA = 0.0500 M		C. TOA = 0.2474 M	
0.00156	0.0027	0.00073	0.00845
.00246	.0059	.00101	.0176
.00329	.0093	.00145	.03605
.00417	.0115	.00156	.04685
.00505	.0143	.00204	.0642
B. TOA = 0.100 M		.00256	.07915
0.00090	0.00324	.00267	.0845
.00138	.00675	.00328	.0925
.00223	.01515[a]	.00335	.0930
.00260	.01915	.00392	.101
.00303	.0229	.00468	.1055
.00415	.0312	.00497	.1085
.00477	.0341	.00605	.113
.00545	.0369	.00663	.1155
.00625	.0393	.00782	.119
.00728	.0419	.00863	.1205
.00820	.0440	.00883	.1225
.00909	.04545	D. TOA = 0.500 M	
.0100	.04675	0.00117	0.0985
.0110	.04795	.00154	.146
.0120	.0487	.00353	.2155
		.00515	.2345

[a] H₂SO₄ concentrations were originally calculated as normalities; in dividing by two to obtain molarities all significant figures were retained.

There is considerable evidence that the sulfate forms of the heavy amines are polymerized in organic solvents,[2,3] and it was expected that TOA would behave similarly. If it is reasonable to assume aggregation of the salt to be responsible for the deviations noted in Fig. 2, it is of interest to compare the values of the respective concentrations of $R_2H_2SO_4$ at which these departures commence. Calculated from the points at which $a = 4 \times 10^{-8}$ for the 0.1 M data and 3×10^{-9} for the 0.25 M data, the value 0.02 M is obtained in both cases on rounding off to one figure. A quantitative interpretation of the data above these points will be developed below after the introduction of the necessary auxiliary material. Below these points the straight line shown leads to a value for K_1 of 1.90×10^8 $(moles/liter)^{-4}$.

In Table II are shown data at sulfuric acid activities sufficient for the formation of appreciable amounts of amine bisulfate. The reaction can be written

$$H_2SO_4 + R_2H_2SO_4 = 2RH_2SO_4 \qquad (4)$$
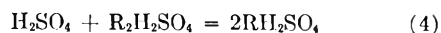
for which the appropriate equilibrium constant, if all species are in true solution, would be

$$K^*_2 = \frac{[RH_2SO_4]^2}{a_{H_2SO_4}\,[R_2H_2SO_4]} \qquad (5)$$

Log-log plots of $a_{H_2SO_4}$ vs. $[RH_2SO_4]^2/[R_2H_2SO_4]$
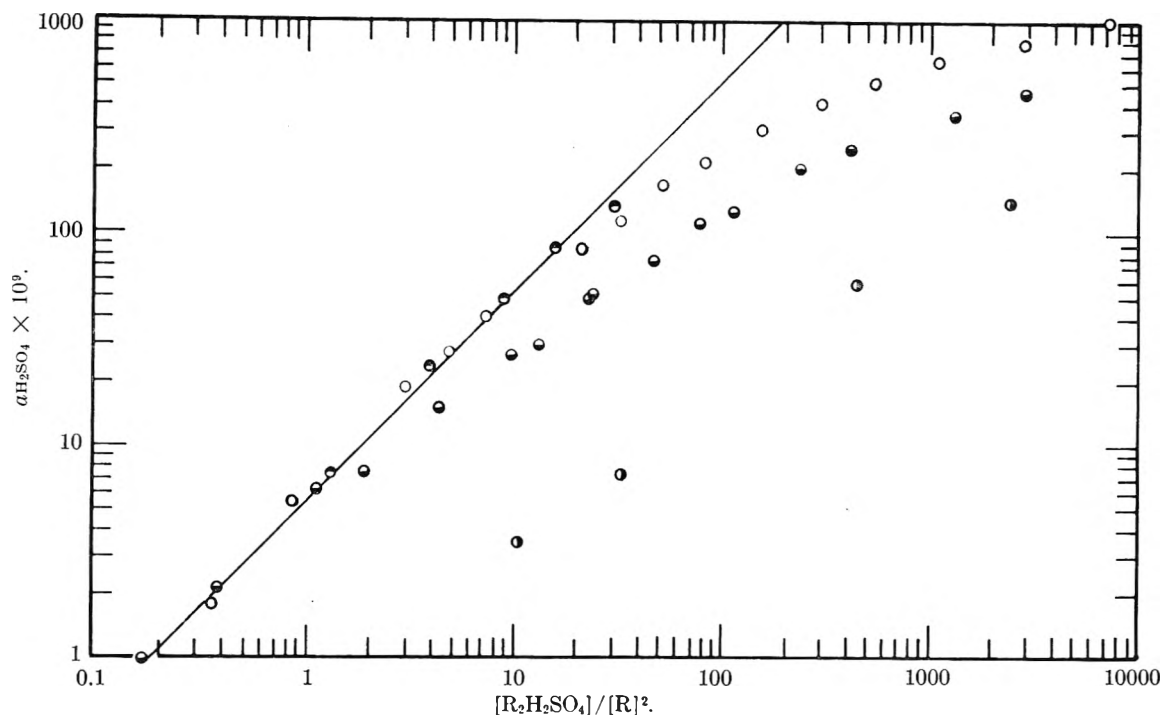
Fig. 2.—Equilibria for the reaction $H_2SO_4 + 2R = R_2H_2SO_4$: ◑, 0.05 M TOA; ○, 0.1; ◐, 0.25; ◑, 0.5.

exhibited straight lines of equal slope, but they were not superimposed for the two solutions. Accepting tentatively the assumption of colloidal aggregation of both salt forms, it becomes necessary to correlate the data on a different basis.

TABLE II

[H₂SO₄]aq	[H₂SO₄]org	[H₂SO₄]aq	[H₂SO₄]org
A. TOA = 0.100 M		B. TOA = 0.2474 M	
0.0626	0.0650	0.0608	0.161
.1017	.0698	.129	.179
.138	.0724	.270	.198
.173	.0745	.380	.206
.205	.0774	.449	.213
.234	.0779	.515	.217
.261	.0791		
.286	.0802		
.310	.0819		
.353	.0830		
.410	.0844		

It has been suggested that the extraction behavior of the heavy amines in organic diluents is analogous to that of weak base ion-exchange resins.[2] In many cases, ion exchange data can be at least empirically treated using an approach put forward by Vanselow.[9] It is assumed that the components of the solid phase form a series of completely miscible ideal solid solutions, and for the case

$$A + B_{Resin} = A_{Resin} + B \qquad (6)$$

activities in the resin are taken to be

$$a_{AR} = X_{AR}, \quad a_{BR} = X_{BR} \qquad (7)$$

where the X's are mole fractions. For the case of interest here, consider the reaction

$$2HSO_4^- + R_2H_2SO_4 = 2RH_2SO_4 + SO_4^=, \qquad (8)$$
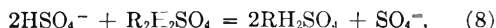
which is thermodynamically indistinguishable from reaction (4) above, as can be seen by introducing the

(9) A. P. Vanselow, *Soil Sci.*, **33**, 95 (1932).

second ionization equation for sulfuric acid into (8). From (7) and (8)

$$K_2' = \frac{X^2_{RH_2SO_4}}{a_{H_2SO_4} \, X_{R_2H_2SO_4}} \qquad (9)$$

For the dibasic acid the fractions were calculated on the basis of equivalents

$$X = X_{RH_2SO_4} = \frac{[RH_2SO_4]}{[RH_2SO_4] + 2[R_2H_2SO_4]} \qquad (10)$$

and

$$X_{R_2H_2SO_4} = 1 - X$$

where it was assumed that in this range of acid activities the amounts of unreacted amine were negligibly small. A plot of $\log a^{1/3} vs. \log X^2/(1 - X)$ is shown in Fig. 3, and it is apparent that within experimental error the points for the two solutions are now superimposed. The slope of the line shown is not $1/3$, however, as would be expected from (9); it was actually drawn with slope $1/2$, which would correspond to a constant

$$K_2'' = \frac{X^2}{a^{2/3}_{H_2SO_4} (1 - X)} \qquad (11)$$

or

$$K_2 = \frac{X^3_{RH_2SO_4}}{a_{H_2SO_4} \, X^{3/2}_{R_2H_2SO_4}} \qquad (12)$$

neither of which can be represented by a suitable reaction equilibrium.[10] The empiricism apparent here is quite reasonable from the point of view of ion exchange equilibria in general, however. Modified mass action expressions of the Rothmund-

(10) Other approaches to this problem were attempted. The calculation of colloid phase activity coefficients from the Duhem–Margules relationships as given by Boyd, *et al.*,[11] failed to provide even an empirical constant. A treatment found by Baes to be applicable to the acid extraction behavior of di-decylamine[12] met with only partial success; a reasonably good constant was obtained, but the resulting bisulfate corrections were of little value in interpreting the data in the range of high free amine concentrations (see below).

(11) G. E. Boyd, J. Schubert and A. W. Adamson, *J. Am. Chem. Soc.*, **69**, 2818 (1947).

(12) C. F. Baes, Jr., unpublished report.

Fig. 3.—Bisulfate equilibria: $\bigcirc$, 0.1 M TOA; $\ominus$, 0.25 M TOA.
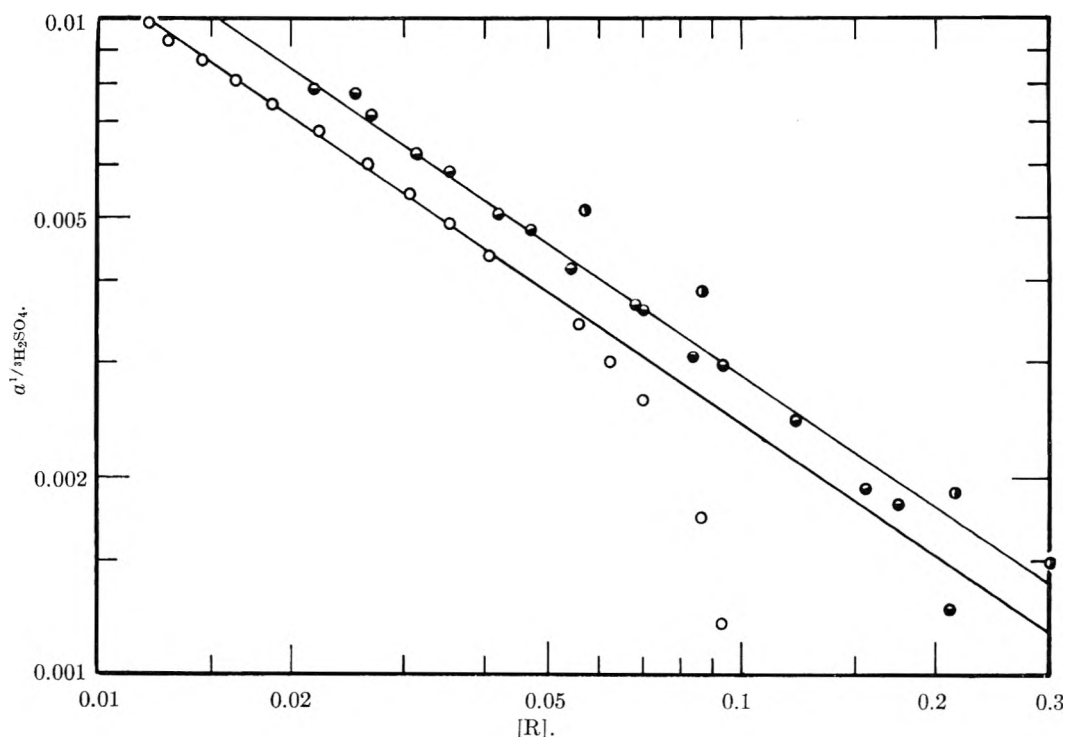
Fig. 4.—Plot of $a^{1/3}_{H_2SO_4}$ vs. free amine: $\bigcirc$ = 0.1 M TOA; $\ominus$, 0.25; $\oplus$, 0.5.

Kornfeld type (of which (12) is a good example, as can be shown from the equivalence of reactions (4) and (8)) are seldom found to exhibit the stoichiometric exponential relationships implicit in actual exchange systems.[13,14]

(13) V. Rothmund and G. Kornfeld, $Z.$ $anorg.$ $Chem.,$ **103**, 129 (1918); **108**, 215 (1919).

(14) H. F. Walton, "Ion Exchange Equilibria," in F. C. Nachod, "Ion Exchange Theory and Application," Academic Press, Inc., New York, N. Y., 1949, p. 6.

Evaluation of K_2 from the line in Fig. 3 gives $K_2 = 1.49 \times 10^3$ (moles/liter)$^{-3}$. Actually, for calculating the relative amounts of sulfate and bisulfate in the colloid, equation 11 is more convenient, and for this purpose

$$K_2'' = \frac{X^2}{a^{3/2}(1 - X)} = 131$$

where $X = X_{RH_2SO_4} = 1 - X_{R_2H_2SO_4}$, as before.

Returning now to the data which showed systematic deviations from the line in Fig. 2, it is to be pointed out first of all that the free [R] values used in calculating the quantity $[R_2H_2SO_4]/[R]^2$ were obtained from the material balance relation

$$[R] = [\Sigma R] - 2[\Sigma S] \tag{13}$$

in which $[\Sigma R]$ and $[\Sigma S]$ denote total amine and total organic sulfate, respectively. Bisulfate was assumed to be absent. Using K_2'' it is now possible to test this assumption; we obtain

$$X = 5.71a^{1/3}(\sqrt{4 + 131a^{2/3}} - 11.4a^{1/3}) \tag{14}$$

which, since in this range of acidities $131a^{2/3} \ll 4$, reduces to

$$X = 11.4a^{1/3}(1 - 5.71a^{1/3}) \tag{15}$$

Since $X = [RH_2SO_4]/[RH_2SO_4] + 2[R_2H_3SO_4])$, it follows that the free [R] as given in (13) must be corrected according to the equation

$$[R] = [\Sigma R] - 2[\Sigma S] + 2[\Sigma S]\frac{X}{1+X} \tag{16}$$

In Table III the values of X and [R] calculated for the 0.1, 0.25 and 0.5 M TOA data are listed together with the previous values of [R] obtained from (13). It is apparent that the corrections are appreciable, especially in the range of low free [R].

It should be emphasized here that this treatment assumes implicitly that in the range of acidities shown in Table II only a small fraction of the amine salt species remains in true solution, that the major part is in the form of a colloid and that within this colloid the relative quantities of sulfate and bisulfate are given by K_2'' over the entire range of acid activities under consideration.

The corrected values of [R] in Table III are plotted vs. $a^{1/3}_{H_2SO_4}$ in Fig. 4. If it is true that above a certain critical concentration of amine sulfate (already estimated to be $\sim 0.02\ M$) polymerization occurs and that the formation of more salt results only in increased amounts of colloid of constant activity, then equation 3 must still hold, and we have, rearranging

$$a_{H_2SO_4}[R]^2 = \frac{[R_2H_2SO_4]_c}{K_1} \tag{17}$$

where the subscript c indicates the true solution concentration of amine sulfate in equilibrium with the polymer. This quantity should be a constant, and we write

$$K_3 = a_{H_2SO_4}[R]^2 \tag{18}$$

which predicts a straight line of slope $-2/3$ for the plot of Fig. 4. The lines shown were drawn with the predicted slope and, although the fit in the case of each set of data is good, it is apparent that the lines are by no means superimposed. It is therefore postulated that part of the free amine is associated with the colloid, and that its activity in the resulting larger polymer is proportional to the first power of its equivalent fraction there. It follows that there exists a distribution D of free amine between solvent and colloid, independent of total amine concentration and the relative amounts of all other species present. We write

$$D = \frac{(1-\alpha)[R]}{[\Sigma R] - \alpha[R]}\frac{1}{\alpha[R]} \tag{19}$$

where α is that fraction of the free amine which is

TABLE III

$a^{1/3}_{H_2SO_4}$	$X_{I.H_2SO_4}$	$\dfrac{2[\Sigma S]}{1+X}X$	[R] Uncor.	[R] cor.	α^a
A. TOA = 0.100 M					
0.00120	0.0136	0.0001	0.0935	0.0936	0.981
.00174	.0196	.0003	.0865	.0868	.960
.00263	.0296	.0009	.0697	.0706	.920
.00300	.0336	.0012	.0617	.0629	.903
.00341	.0382	.0017	.0542	.0559	.890
.00436	.0485	.0029	.0376	.0405	.859
.00487	.0535	.0035	.0318	.0353	.850
.00540	.0596	.0041	.0262	.0303	.845
.00600	.0660	.0049	.0214	.0263	.836
.00675	.0740	.0058	.0162	.0220	.831
.00740	.0808	.0066	.0120	.0186	.828
.00803	.0872	.0073	.0091	.0164	.823
.00864	.0936	.0080	.0065	.0145	.820
.00927	.1004	.0088	.0041	.0129	.820
.00989	.1066	.0094	.0026	.0120	.816
B. TOA = 0.2474 M					
0.00127	0.0150	0.0005	0.2122	0.2127	0.861
.00182	.0200	.0014	.1753	.1767	.784
.00194	.0220	.0020	.1537	.1557	.755
.00245	.0276	.0034	.1190	.1224	.716
.00296	.0331	.0051	.0891	.0942	.688
.00307	.0344	.0056	.0784	.0840	.679
.00363	.0405	.0072	.0624	.0696	.667
.00368	.0411	.0073	.0614	.0687	.665
.00417	.0463	.0089	.0454	.0543	.654
.00479	.0531	.0106	.0364	.0470	.649
.00503	.0556	.0114	.0304	.0418	.646
.00586	.0646	.0137	.0214	.0351	.641
.00628	.0690	.0149	.0164	.0313	.639
.00714	.0780	.0172	.0094	.0266	.635
.00771	.0841	.0187	.0064	.0251	.637
.00785	.0855	.0193	.0024	.0217	.631
C. TOA = 0.500 M					
0.00150	0.0169	0.0033	0.303	0.306	0.549
.00192	.0216	.0063	.208	.214	.509
.00384	.0428	.0184	.069	.087	.471
.00517	.0573	.0254	.031	.056	.464

NOTE.—The data for 0.05 M TOA exhibited true solution behavior in Fig. 2 and at no point was the total organic sulfate as high as 0.02 M. Bisulfate corrections based on intra-polymeric exchange were not expected to be of value in further correlation of these data and calculations showed that such was the case. ^{a} The α-values are described later in this paper.

distributed to the solvent. The first term on the right is the equivalent fraction of amine in the colloid; the denominator in the second term is the molarity of the free amine remaining in the solvent. For vanishingly small free amine (19) becomes

$$D = \frac{1}{[\Sigma R]}\left(\frac{1}{\alpha_0} - 1\right) \tag{20}$$

and for two total amine concentrations $[\Sigma R]'$ and $[\Sigma R]''$, since D is a constant

$$\frac{1}{[\Sigma R]'}\left(\frac{1}{\alpha_0'} - 1\right) = \frac{1}{[\Sigma R]''}\left(\frac{1}{\alpha_0''} - 1\right) \tag{21}$$

The limiting ratio between the free amine concentrations predicted by the straight lines of Fig. 4 is 1.29, and since the desired result of this calculation is that $\alpha'[R]'$ shall be equal to $\alpha''[R]''$, we ensure this for infinitely dilute free amine by putting
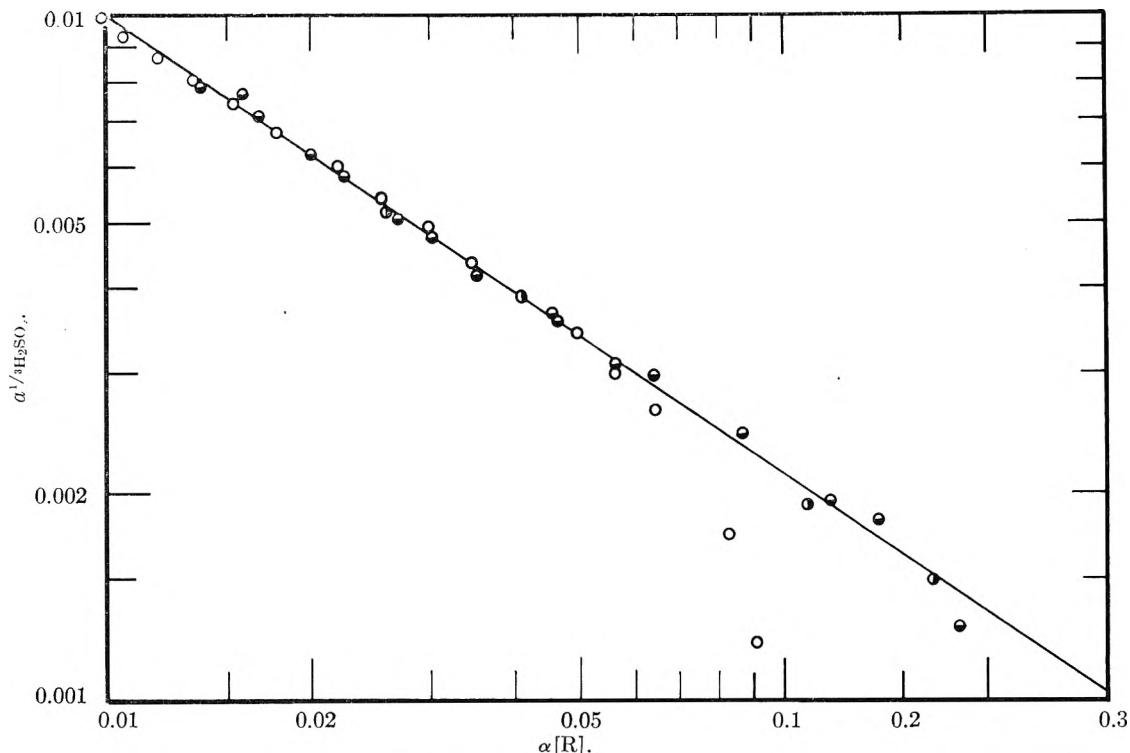
Fig. 5.—Plot of $a^{1/3}{}_{H_2SO_4}$ vs. $\alpha[R]$: $\bigcirc$ = 0.1 M TOA; $\ominus$, 0.25; $\oplus$, 0.5.
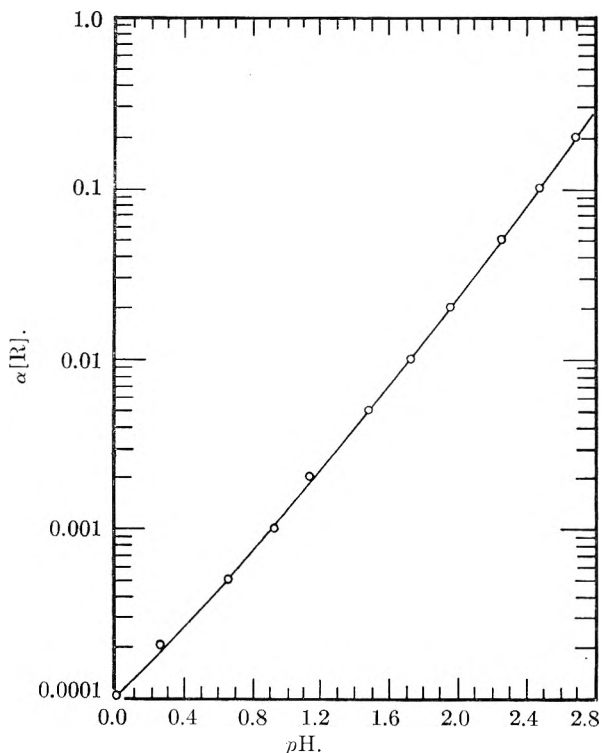
Fig. 6.—Free amine vs. pH of aqueous sulfuric acid.

Fig. 7.—Colloid composition vs. pH of aqueous sulfuric acid.

$\alpha_0{}'' = \alpha_0{}'/1.29$. With $[\Sigma R]' = 0.100$ and $[\Sigma R]'' = 0.2474$, (21) gives $\alpha_0{}' = 0.80$, which, substituted into (20) with $[\Sigma R] = 0.100$, results in a value for D of 2.50 (moles/liter)$^{-1}$. Solving (19) for α, we obtain

$$\alpha = \frac{1}{5[R]}\left(\frac{5[\Sigma R] + 2}{2} - \sqrt{\left(\frac{5[\Sigma R] + 2}{2}\right)^2 - 10[R]}\right)$$

(22)

The α-values listed in the right hand columns of Table III were obtained from (22). Log $a^{1/3}{}_{H_2SO_4}$ is plotted vs. log $[\alpha R]$ in Fig. 5, where it is apparent that the 0.1, 0.25 and 0.5 M TOA data are superimposed on one line of the predicted slope. From this line, $K_3 = 1.01 \times 10^{-10}$ (moles/liter)^5. The product K_1K_3 results in a value of 0.0192 M for the concentration of amine sulfate in equilibrium with the polymer, in good agreement with that esti-

mated from the departures from the line of Fig. 2. K_3 also confirms the assumption of negligibly small free amine concentrations made in treating the bisulfate equilibria (where $X_{RH_2SO_4}$ was taken equal to $1 - X_{R_2H_2SO_4}$). Graphs of free amine vs. pH and colloid composition vs. pH are to be found in Figures 6 and 7.

It is contemplated that physico-chemical measurements (e.g., freezing point lowering, osmotic pressure, etc.) may provide more evidence as to the nature of the heavy amine species. Calculations based on energetics, possibly from the point of view of Debye's treatment,[15] may also be of value. These will be presented in later publications.

IV. Summary

The distribution of sulfuric acid between water and benzene solutions of tri-*n*-octylamine ranging from 0.05 to 0.5 M has been shown to be consistent with a theoretical treatment based on partial polymerization of the amine salt species in the organic phase. Four constants describe the observed equilibria

$$K_1 = \frac{[R_2H_2SO_4]}{a_{H_2SO_4}[R]^2} = 1.90 \times 10^8 \text{ (moles/l.)}^{-4},$$

$$[R = (C_8H_{17})_3N]$$

$$K_2 = \frac{X_{RH_2SO_4}}{a_{H_2SO_4} X^{3/2}_{R_2H_2SO_4}} = 1.49 \times 10^3 \text{ (moles/l.)}^{-3}$$

$$K_3 = a_{H_2SO_4}[\alpha R]^2 = 1.01 \times 10^{-10} \text{ (moles/l.)}^5$$

(15) P. Debye, Ann. N. Y. Acad. Sci., 51, 575 (149).

and

$$D = \frac{X_{[(1 - \alpha)R]}}{[\alpha R]} = 2.50 \text{ (moles/l.)}^{-1}$$

K_1 is calculated in the usual way from the formal concentrations of the benzene soluble species and the aqueous acid activities, and it describes the formation of the normal sulfate for $[R_2H_2SO_4] < 0.02\ M$. Above this concentration the amine salt is assumed to polymerize and the remaining three constants describe, respectively, sulfate–bisulfate exchange in the polymer (expressed in equivalent fractions), the formation of colloidally dispersed amine sulfate of constant activity from the reaction between free amine and sulfuric acid and the distribution of free amine between benzene and the colloid, where α is the fraction of free amine remaining in the solvent and $X_{[(1 - \alpha)R]}$ is the equivalent fraction of the free amine distributed to the colloid.

The plots shown in Figs. 6 and 7 are included as a means of presenting the significant results of this investigation in an easily interpreted form. The points were calculated from the equilibrium constants given above. Acid activities were converted to molarity and then to pH graphically, using an experimentally determined calibration curve for the latter conversion. In the case of both graphs the tri-*n*-octylamine sulfate concentration must exceed 0.02 M and it is to be emphasized that the pH values are based on the activity of pure sulfuric acid in water. With these provisions the graphs do have the virtue that the relationships depicted are independent of total amine concentration.

LIQUID–VAPOR EQUILIBRIA IN THE SYSTEM AMMONIA–HYDRAZINE AT ELEVATED TEMPERATURES

By Russell S. Drago and Harry H. Sisler

Contribution from the McPherson Chemical Laboratories of The Ohio State University, Columbus, Ohio

The liquid–vapor equilibria in the binary system ammonia–hydrazine have been measured at various compositions and at 88.5, 100.3, 114.1 and 124.9°. Activities and activity coefficients for ammonia in the liquid phase were calculated. Partial fugacities calculated for hydrazine for solutions containing low concentrations of hydrazine are not in accord with Henry's Law even though the partial fugacities of ammonia for these solutions are in accord with Raoult's Law. This was interpreted as an indication of molecular association of hydrazine in liquid ammonia solutions.

The synthesis of hydrazine by the chloramine–ammonia reaction in liquid ammonia solution[1,2] has led us to investigate the vapor pressures and vapor compositions in equilibrium with liquid solutions of hydrazine and ammonia at elevated temperatures. Data are reported herein for measurements at 88.5, 100.3, 114.1 and 124.9°. Since both hydrazine and ammonia are capable of association through hydrogen bonding these measurements are of considerable theoretical interest.

Experimental

The autoclave, super-pressure valves and lines used in this study were fabricated of Type 347 stainless steel. The inner surfaces of the various parts of the apparatus were coated with "Teflon One-Coat Enamel" to inhibit surface

catalyzed decomposition of hydrazine. The solutions of ammonia and hydrazine were contained in a Pyrex autoclave liner which was fitted with a Teflon lid. Thin Teflon sheet was placed on the bottom of the autoclave and around the walls to prevent chipping of the Teflon enamel coating by the Pyrex liner. Teflon dip tubes extended into the autoclave for the purpose of withdrawing samples of liquid and vapor at equilibrium. The inside diameter of these tubes was minimized in order to reduce the quantity of material isolated in these lines.

The temperature of the two super pressure needle valves was controlled by wrapping them with flexible, electrical heating tape through which a variable electrical current was passed. The temperature of the liquid valve and liquid line was kept slightly below the autoclave temperature, whereas the temperature of the vapor valve and lines was kept at 5 to 10° above the autoclave temperature. The temperatures of the valves and lines were registered on a Leeds–Northrup Micromax self-recording potentiometer from a series of properly located copper–constantan thermocouples.

The autoclave was immersed in a well-stirred, thermostated oil-bath. The bath was heated by a primary, 500-

(1) R. Mattair and H. H. Sisler, J. Am. Chem. Soc., 73, 1619 (1951).

(2) H. H. Sisler, et al., ibid., 76, 3909 (1954).

watt heater which operated constantly and a secondary, 300-watt heater which operated intermittently. By this means the temperature was kept constant to within ±0.05°, using a Thyratron-controlled circuit[3] and a "Merc to Merc" thermoregulator. The temperature of the bath was measured by means of a calibrated ASTM thermometer.

The autoclave was loaded with solutions of hydrazine and liquid ammonia. Anhydrous hydrazine (95%) was redistilled *in vacuo* over sodium hydroxide to completely dehydrate it for use in this study. The purity of the hydrazine was checked by freezing point determination and was found to be better than 99%. Precautions were taken to eliminate absorption of water by the system during the loading procedure. After the autoclave was loaded, the system was allowed to warm up and a large vapor sample was withdrawn to remove any trace of foreign vapors that might have been introduced into the autoclave during the loading procedure.

TABLE I

DATA FOR THE SYSTEM AMMONIA-HYDRAZINE AT CONSTANT TEMPERATURE

Liquid compn. (mole % hydrazine)	Total vapor pressure abs., atm.	Total vapor fugacity exptl., atm.	Raoult's Law fugacity, atm.	Vapor compn. (mole % hydrazine)
		Temp. = 88.5°		
0.00	49.0	37.9	37.9	0.00
4.29	46.6	36.5	36.3	.195
18.93	38.4	31.4	30.8	.631
19.89	38.0	31.1	30.4	.673
29.37	33.7	28.2	26.9	.823
29.57	33.7	28.2	26.8	.842
35.80	31.6	26.7	24.5	.984
35.93	31.6	26.8	24.4	.991
36.12	31.5	26.7	24.4	.987
47.82	26.2	22.9	20.0	...
48.29	25.9	22.6	19.8	1.33
58.77	22.0	19.7	15.9	1.67
65.65	18.6	16.9	13.3	2.01
65.81	18.6	16.9	13.2	2.03
66.40	18.5	16.8	13.0	2.03
75.30	14.6	13.5	9.65	2.36
77.58	13.5	12.6	9.59	2.49
		Temp. = 100.3°		
0.00	62.2	46.4	46.4	0.00
4.86	58.1	44.2	44.1	.315
9.69	54.0	41.9	42.0	.501
9.76	54.1	42.0	41.9	...
10.00	53.8	41.8	41.8	0.538
10.10	53.9	41.9	41.8	...
10.24	54.1	42.0	41.7	...
10.54	53.6	41.7	41.6	0.537
13.35	52.1	40.8	40.3	...
13.93	51.6	40.5	40.0	...
19.65	48.0	38.3	37.4	0.901
20.47	47.8	38.2	37.0	0.928
25.47	...	...	...	1.06
26.57	...	...	...	1.11
31.91	40.8	33.7	31.8	...
31.77	40.9	33.7	31.8	...
36.79	38.4	32.1	29.5	1.42
48.88	31.8	27.4	24.0	1.76
60.21	26.5	23.4	18.8	2.20
67.64	22.4	20.1	15.4	2.74
68.20	22.2	20.0	15.2	2.77
75.80	17.6	16.2	11.7	3.20
79.51	15.2	14.2	10.0	3.66
		Temp. = 114.1°		
0.00	80.7	58.0	58.0	0.00
5.18	74.6	54.9	55.1	0.564
5.36	74.1	54.8	55.0	.565
5.76	...	...	...	.567
6.04	...	...	...	.603
6.95	...	...	...	.676
10.16	...	...	...	.913
10.62	...	...	...	.940
10.70	...	...	...	.939
10.97	67.8	51.4	51.8	...
11.87	67.6	51.3	51.2	...
11.96	...	...	...	1.01
12.08	67.2	51.1	51.2	...
12.40	67.0	51.0	51.0	0.993
12.69	...	...	...	1.05
14.75	65.0	49.9	49.6	...
15.71	64.4	49.5	49.0	1.13
20.88	60.1	47.0	46.1	1.41
22.76	...	...	...	1.48
23.82	...	...	...	1.46
34.82	50.4	41.0	38.2	1.82
35.33	49.6	40.5	37.9	1.79
37.86	48.2	39.6	36.5	1.91
50.28	39.1	33.3	29.3	2.30
51.83	38.0	32.5	28.5	2.41
61.43	32.0	28.1	23.0	2.94
69.54	27.2	24.4	18.4	3.50
70.00	26.9	24.1	18.1	3.55
76.52	21.2	19.4	14.4	4.11
77.66	21.0	19.3	13.7	...
81.85	17.6	16.5	11.4	4.95
		Temp. = 124.9°		
0.00	97.9	68.2	68.2	0.00
7.42	86.1	62.7	63.2	1.03
7.65	85.2	62.2	63.1	0.965
14.22	77.6	58.3	58.7	...
15.17	77.1	58.0	58.0	...
22.83	70.3	54.3	52.9	1.84
23.39	70.2	54.2	52.6	1.88
37.65	56.4	45.9	43.1	...
39.34	55.8	45.4	41.9	...
40.01	54.3	44.4	41.5	2.47
54.17	43.9	37.3	32.0	3.04
62.18	36.4	31.8	26.7	3.30
62.50	36.3	31.7	26.5	3.49
72.11	30.1	26.9	20.1	4.63
72.40	30.0	26.9	19.9	...
74.99	27.1	24.6	18.2	4.90
81.80	21.4	19.8	13.6	5.92
83.31	19.9	18.5	12.6	6.02

The loaded autoclave was left in the constant temperature bath for three days to allow equilibrium to be attained. The vapor pressure, liquid composition and vapor composition were then measured in that order.

The vapor pressures were measured with Bourdon type pressure gages which had been calibrated with an MIT type dead weight gage. The Bourdon gages were connected to high pressure fittings in such a manner that the pressure gage could be attached to the vapor valve on the autoclave and nitrogen could be introduced into the gage until the pressure was slightly below the estimated pressure in the autoclave. The vapor pressure of the system could then be obtained by opening the vapor line valve leading to the gage. By this technique a pressure determination could be made without removing a large gas sample from the autoclave and consequently disturbing the equilibrium in the system. The accuracy of this procedure was checked by

(3) A. Garrett, *Ind. Eng. Chem.*, **10**, 324 (1938).

reproducing measurements for the vapor pressures of pure, liquid ammonia[4] with an accuracy of ±0.4%.

The liquid composition was obtained from the analysis of a liquid sample which was removed from the autoclave immediately after a waste sample had been taken to eliminate material which had been isolated in the liquid lines. The liquid sample was condensed by a liquid nitrogen trap and then distilled into standard acid. The vapor sample was directly absorbed in standard acid after a waste sample had been removed. Analyses for total base and for hydrazine were performed on both liquid and vapor samples. The hydrazine was determined by the acid–iodate method and ammonia was determined from the difference in the analyses for total base and hydrazine.[5]

Results and Conclusions

The data actually obtained from measurements made in this study are listed in Table I.

Data could not be obtained for solutions with liquid compositions greater than 80% hydrazine because of the considerable amount of decomposition of hydrazine which occurs in this range.

The values reported for the Raoult's Law fugacities were calculated by using the following values for the vapor fugacities of pure ammonia and pure hydrazine (Table II).

TABLE II
VAPOR FUGACITIES OF PURE AMMONIA AND PURE HYDRAZINE

Temp., °C.	Fugacity of ammonia, atm.	Fugacity of hydrazine, atm.
88.5	37.9	0.407
100.3	46.4	0.627
114.1	58.0	1.00
124.9	68.2	1.46

The vapor fugacities of ammonia were obtained from thermodynamically derived relationships of pressure and fugacity. These relationships were calculated from the equation of state[6,7] for ammonia by the method of Lewis and Randall.[8]

The vapor fugacities of pure hydrazine were assumed to be equal to the values that have been reported for the vapor pressures of hydrazine.[9,10]

The values reported for the total experimental vapor fugacity were calculated from the measured total vapor pressure by assuming that the pressure–fugacity relationships for ammonia apply to the gas mixtures obtained in these studies. This assumption was made on the basis of an empirical relationship[11] from which the virial coefficient B_{mix} and therefore the fugacity of a binary mixture can be calculated from a knowledge of the virial coefficients of the components B_1 and B_2.

$$B_{mix} = N_1^2 B_1 + 2N_1 N_2 B_{12} + N_2^2 B_2 \qquad (1)$$

where $B_{12} = (B_1 + B_2)/2$ and N_1 and N_2 are the mole fractions of the two compounds. The virial coefficients for ammonia have been reported[6,7] but those for hydrazine have not. Limited P–V–T relationships have been obtained from experiments

(4) C. Cragoe, C. Meyers and L. Taylor, *J. Am. Chem. Soc.*, **42**, 206 (1920).

(5) R. Penneman and L. Audrieth, *Anal. Chem.*, **20**, 1058 (1948).

(6) F. Keyes, *J. Am. Chem. Soc.*, **60**, 1761 (1938).

(7) W. Stockmeyer, *J. Chem. Phys.*, **9**, 863 (1941).

(8) G. Lewis and M. Randall, "Thermodynamics," McGraw-Hill Book Co., Inc., New York, N. Y., 1923, p. 195.

(9) L. de Bruyn, *Rec. trav. chim.*, **15**, 174 (1896).

(10) W. Hieber and A. Woerner, *Z. Elektrochem.*, **40**, 252 (1934).

(11) R. Fowler and E. Guggenheim, "Statistical Thermodynamics," Cambridge University Press, Cambridge, England, 1952, p. 296.

on the gas density of hydrazine.[12] From this data approximate values for the virial coefficients of hydrazine were calculated using the equation

$$PV = nRT + Bp \qquad (2)$$

The virial coefficients thus calculated are listed in Table III.

TABLE III
VIRIAL COEFFICIENT FOR HYDRAZINE

Temp., °C.	Virial coefficient B(l./mole)
90	2.14
95	3.49
100	3.58
110	4.32
120	4.20

Substitution of these values for the virial coefficients of hydrazine and the reported values for the virial coefficients of ammonia into equations 1 and 2 showed that the virial coefficients for the gas mixtures encountered in this study could be represented within the precision of these experimental measurements by the virial coefficients for ammonia. It was, therefore, assumed that the pressure–fugacity relationships for ammonia could be applied to the gas mixtures encountered in this study. This treatment is possible because of the relatively small concentrations of hydrazine in the gas phase.

The total experimental vapor fugacity was divided into partial fugacities for ammonia and hydrazine by assuming that the partial fugacity of compound i is equal to the product of the mole fraction of component i in the vapor and the total fugacity. Activities and activity coefficients were calculated from the fugacities by choosing ammonia as the solvent. The data used in these calculations were obtained from curves obtained by plotting the values reported in Table I. The values for the activities, activity coefficients and partial fugacities thus obtained are presented in Table IV.

Activities and activity coefficients were not calculated for hydrazine because experimental difficulties made it impossible to obtain accurate data for the vapor composition of dilute hydrazine solutions in liquid ammonia. The lack of this information made it impossible to obtain the accurate extrapolations necessary for the determination of the fugacity corresponding to the standard state of hydrazine in infinitely dilute liquid ammonia solutions. The rational activity coefficients obtained from the above method give an indication of the deviations from Henry's Law. Activities based on the pure solute as the standard state do not give information concerning these deviations and, therefore, were not calculated.

The activity coefficients for ammonia indicate that ammonia is behaving in accordance with Raoult's Law over a considerable concentration range (up to approximately 15 mole % hydrazine). It is therefore theoretically necessary that the solute obey Henry's Law in the same region that ammonia obeys Raoult's Law. The calculated values for the Henry's Law ratios for hydrazine in the concen-

(12) P. Giguere and R. Rundle, *J. Am. Chem. Soc.*, **63**, 1135 (1941).

TABLE IV

ACTIVITIES, ACTIVITY COEFFICIENTS AND PARTIAL FUGACITIES

Liquid compn. (mole fraction ammonia)	Total vapor fugacity, atm.	Vapor compn., mole % NH₃	Vapor compn., mole % N₂H₄	Partial fugacity of ammonia, atm.	Activity of ammonia	Activity coefficient of ammonia	Partial fugacity of hydrazine, atm.
				Temp. = 88.5°			
0.950	36.1	99.76	0.235	36.01	0.950	1.001	0.0823
.900	34.3	99.60	.400	34.16	.901	1.001	.137
.850	32.6	99.46	.540	32.41	.855	1.006	.176
.800	31.1	99.34	.660	30.88	.815	1.019	.205
.750	29.6	99.24	.764	29.37	.775	1.033	.224
.700	28.2	99.14	.863	27.99	.739	1.056	.243
.650	26.9	99.02	.980	26.67	.704	1.083	.264
.600	25.4	98.90	1.10	25.16	.664	1.107	.279
.550	23.9	98.76	1.24	23.58	.622	1.131	.296
.500	22.3	98.61	1.39	22.00	.581	1.162	.311
.450	20.7	98.44	1.56	20.42	.539	1.198	.323
.400	19.3	98.25	1.75	18.91	.499	1.248	.336
.350	17.4	98.05	1.95	17.07	.451	1.289	.339
.300	15.4	97.85	2.15	15.04	.397	1.323	.333
				Temp. = 100.3°			
0.950	44.1	99.69	0.31	44.00	0.949	0.999	0.137
.900	41.8	99.46	.54	41.61	.896	0.996	.226
.850	40.0	99.27	.73	39.77	.857	1.008	.293
.800	38.2	99.10	.90	37.82	.815	1.019	.344
.750	36.3	98.94	1.06	35.94	.775	1.033	.385
.700	34.4	98.79	1.21	34.01	.733	1.047	.416
.650	32.7	98.64	1.36	32.28	.696	1.071	.445
.600	30.9	98.51	1.49	30.42	.656	1.093	.460
.550	28.9	98.35	1.65	28.44	.613	1.115	.479
.500	27.07	98.18	1.82	26.59	.573	1.146	.493
.450	25.37	98.00	2.00	24.86	.536	1.191	.508
.400	23.40	97.79	2.21	22.88	.493	1.233	.519
.350	21.29	97.50	2.50	20.76	.448	1.280	.533
.300	19.05	97.17	2.83	18.50	.399	1.330	.540
				Temp. = 114.1°			
0.950	54.97	99.46	0.54	54.67	0.942	0.992	0.297
.900	52.18	99.12	0.88	51.72	.891	.990	.460
.850	49.72	98.86	1.14	49.16	.847	.996	.566
.800	47.41	98.66	1.34	46.78	.806	1.007	.635
.750	45.17	98.49	1.51	44.49	.767	1.023	.680
.700	42.93	98.33	1.67	42.27	.728	1.040	.721
.650	40.75	98.17	1.83	40.00	.689	1.060	.748
.600	38.44	98.02	1.98	37.67	.649	1.082	.762
.550	36.05	97.86	2.14	35.29	.608	1.105	.771
.500	33.47	97.68	2.32	32.69	.563	1.126	.777
.450	31.09	97.45	2.55	30.29	.522	1.160	.796
.400	28.71	97.15	2.85	27.89	.481	1.203	.818
.350	26.46	96.81	3.19	25.62	.442	1.263	.844
.300	24.01	96.42	3.52	23.16	.399	1.330	.857
				Temp. = 124.9°			
0.950	64.35	99.24	0.76	63.86	0.937	0.986	0.496
.900	61.02	98.84	1.16	60.31	.885	.983	.707
.850	58.16	98.54	1.46	57.31	.841	.989	.850
.800	55.58	98.28	1.72	54.62	.801	1.001	.959
.750	52.93	98.06	1.94	51.90	.761	1.015	1.03
.700	50.34	97.87	2.13	49.30	.723	1.033	1.07
.650	47.48	97.70	2.30	46.39	.681	1.048	1.10
.600	44.83	97.54	2.46	43.73	.642	1.070	1.10
.550	42.11	97.35	2.65	40.99	.601	1.092	1.12
.500	39.32	97.14	2.86	38.20	.560	1.120	1.12
.450	36.46	96.91	3.09	35.33	.518	1.151	1.13
.400	33.47	96.60	3.40	32.33	.474	1.185	1.14
.350	30.68	96.19	3.81	29.51	.433	1.237	1.17
.300	28.03	95.69	4.31	26.82	.393	1.310	1.21

tration ranges where ammonia is behaving ideally are listed in Table V.

TABLE V

HENRY'S LAW RATIOS

Liquid compn. (molality of hydrazine)	Henry's Law ratios $\times 10^2$ at the temp.			
	88.5°	100.3°	114.1°	124.9°
3.096	2.66	4.43	9.59	15.8
4.420	2.49	3.91	8.44	13.4
5.115	2.33	3.77	7.92	12.4
6.535	2.10	3.46	7.04	10.8
8.021	1.93	3.18	6.38	9.55
8.784	1.86	3.06	6.06	9.04
10.38	1.70	2.82	5.15	8.18
12.03	1.57	2.61	4.90	7.45
14.71	1.39	2.34	4.32	6.49
16.56	1.29	2.17	3.96	5.97
19.57	1.14	1.97	3.50	5.31
21.72	1.07	1.84	3.22	4.83
25.17	0.965	1.65	2.86	4.29
27.63	0.912	1.55	2.65	3.92
31.62	0.835	1.41	2.36	3.46

The calculated values for the Henry's Law ratios are seen to decrease with increase in hydrazine concentration at the four temperatures that were studied. This trend can be explained reasonably by assuming the association of hydrazine molecules in solution, with the amount of association increasing with increase in hydrazine concentration. It is assumed that the concentration of associated molecules becomes negligible as the amount of hydrazine present in solution becomes small and as a result the true Henry's Law constant for monomer is approached in dilute solutions. It has been shown that hydrazine is monomeric in the vapor state at the temperatures employed in this study.[13] Therefore, the concentration of monomer is directly proportional to the fugacity of hydrazine. Theoretically, the concentration of hydrazine monomer can

be calculated in the solutions where ammonia obeys Raoult's Law from a knowledge of the fugacity of hydrazine and the extrapolated value of the Henry's Law constant, and the amount of associated material present can be obtained by difference of the total amount of material and the amount of monomer. Further, the amount of associated material can be converted to concentrations corresponding to the various degrees of association, and the equilibrium constants between monomer and the different polymers can be evaluated. Accurate values for the equilibrium constants between monomer and the various polymers could not be calculated in this study, however, because the lack of precise measurements in very dilute hydrazine solutions made it impossible to obtain sufficiently accurate extrapolations of the Henry's Law ratio to infinite dilution.

The lack of such measurements for dilute solutions likewise prevented the application of the mathematical expressions derived by Lassettre[14] for solutions of polymers.

Semi-quantitative calculations, however, strongly support the postulate that association of hydrazine presumably through hydrogen bonding, is a probable explanation for the observed trends. The approximate values calculated for the heats of association were of the order of magnitude corresponding to the weak forces of association that might be expected from hydrogen bonding between the hydrazine molecules.

Because of the complex nature of the solute in these solutions other thermodynamic data were not evaluated.

(13) W. Fresenius and J. Karweil, Z. physik. Chem., 44B, 1 (1939).

(14) E. N. Lassettre, J. Am. Chem. Soc., 59, 1383 (1937).

NOTES

KINETICS OF CHROMATOGRAPHY ON CLAYS[1]

By HENRY C. THOMAS AND C. NEALE MERRIAM, JR.

Contribution No. 1314 from the Sterling Chemistry Laboratory, Yale University, New Haven, Conn.

In our work on the ion-exchange equilibria of the clay minerals we have made much use of chromato-

graphic columns packed with clay dispersed on asbestos. While the principal results of our work have been made independent of the kinetic behavior of these columns, some interest is, nevertheless, attached to this behavior because of the possibility of obtaining from it at least an indirect measure of the diffusion of ions within the clay particles. Such measurements would evidently be of fundamental importance in the study of ionic binding in these interesting minerals. The experiment devised for this purpose has, somewhat unfortunately, shown quite conclusively that we cannot measure intraparticle diffusion by this means, but some features of the experiment warrant description because the

method can evidently be applied to exchangers of larger particle size where solid diffusion will be of importance.

Although it is certainly impossible to make absolute measurements of diffusion coefficients by any technique which uses a chromatographic column packed with particles of a variety of sizes and shapes, one can hope to get a measure of the change in self-diffusion coefficient of a given species with change in composition of the material within which the diffusion takes place. Any such study must certainly be limited to the case of isotopic diffusion; other cases lead to non-linear problems requiring too much computer time.

If we consider the extreme cases of column behavior in which the rates are determined (A) solely by diffusion in the moving fluid, and (B) solely by diffusion in the solid, the rate laws can be written

$$\frac{\partial \varphi}{\partial t} = \frac{D_l c}{S_l q} (\theta - \varphi) \quad \text{(A)}$$

$$\frac{\partial \varphi}{\partial t} = \frac{D_s}{S_s} (\theta - \varphi) \quad \text{(B)}$$

Here θ and φ are the fractions of tagged atoms in solution and in solid, respectively; c and q are the equilibrium concentrations of the ion of interest, in solution and in solid. These concentrations remain at fixed values throughout the column in an experiment involving only isotopic exchange, such as is considered in this note. D_l and D_s are the coefficients of self-diffusion in liquid and in solid at the fixed chemical compositions contemplated. S_l and S_s are constants summarizing the geometry of the diffusing systems in the two cases (A) and (B).
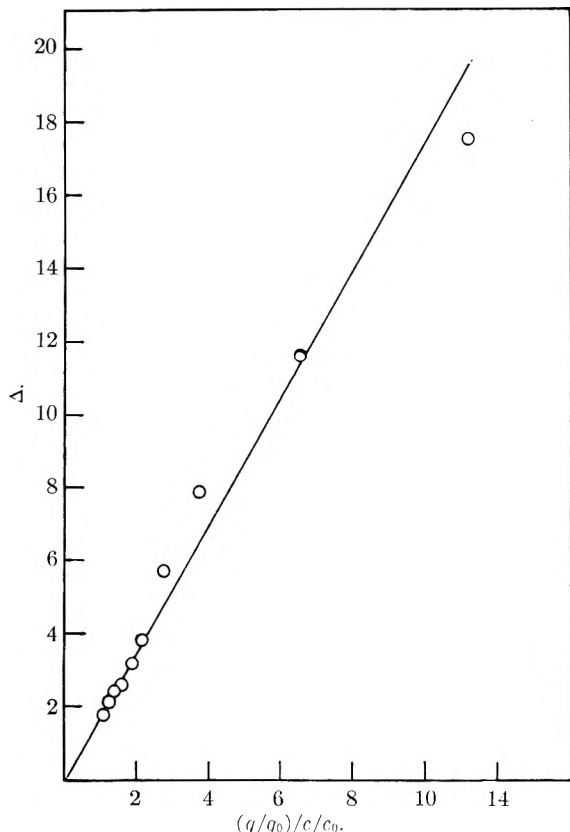
Fig. 1.—The column performance parameter for isotopic exchange.

These equations represent only useful first approximations to the complete mathematical problems for the two cases. It is not worthwhile to refine the mathematical treatment in view of the impossibility of taking into account all the other disturbances besetting the operation of chromatographic columns.

When the solid contents of a column are at chemical equilibrium with the solution passing through it, the rate equations can be combined with the equation for the conservation of marked isotopic species and the resulting expression solved for the concentration history of the effluent, giving, as is known[2]

$$\theta/\theta_0 = \exp\{-(y + qx/c)/\Delta\}\Phi(qx/c\Delta, y/\Delta) \quad (1)$$

where, for case (A)

$$\Delta = \dot{V}S_l q/D_l c$$

and, for (B)

$$\Delta = \dot{V}S_s/D_s$$

In these expressions $\dot{V}$ is the constant volume rate of flow of fluid in the column; and y, the total volume which has passed through the bottom of the column from the beginning of the experiment; x, the "length" of the column measured in grams of that substance chosen as the basis on which to express exchange capacity. (The total exchange capacity of the column is then xq.) If, instead of y, we introduce the quantity $r = y/(xq/c)$ (that is, the ratio of the effluent volume at a given stage of the experiment to the stoichiometric volume required for complete saturation), the equation for the ratio of effluent to initial concentration of tagged species may be written

$$\theta/\theta_0 = \exp\{-k(1 + r)\}\Phi(k, kr) \quad (2)$$

with $k = xq/c\Delta$. Thus if the results (θ/θ_0) of a series of experiments on a single column at different values of q/c be plotted against r and if the same curve is obtained in each case, then certainly k is not a function of q/c. If the flow rate has been maintained constant and if sufficient solution has previously been passed through the column so that no changes in S occur during the experiment, then either (A) is the true rate law, with $k = xD/\dot{V}S_l$, or (B) is the rate law and we have the extraordinary coincidence that D_s is just proportional to c/q within the range of the experiment.

The above ideas have been applied to the study of a clay-asbestos column in the following experiment. The column used contained $x = 2.446$ g. backbone[3] of attapulgite of exchange capacity 0.335 meq./g. backbone, having been prepared with 3.000 g. of attapulgite API No. 46 (one of the reference clay minerals of the American Petroleum Institute) dispersed on 3.0 g. of asbestos. This column was brought to equilibrium with CsCl—NaCl solutions of constant total concentration 0.0200 M containing 5, 10, 20, . . ., 90, 100% CsCl.

(2) See, for instance, J. A. Faucher, R. W. Southworth, and H. C. Thomas, J. Chem. Phys., **20**, 157 (1952).

(3) For convenience and to avoid uncertainties in the presentation of data, we define the "backbone" of a clay mineral as that mass of material left after ignition to constant weight at 1000–1100° and after the deduction of the total mass of exchangeable ions in the sample taken. In this manner we obtain a basis free from ambiguity as to water content and as to the nature of the exchangeable ions present.

The break-through curves at a constant flow rate of about 1 ml./min. were measured by radioactive tracer techniques using Cs^{137}. Previous experiments have indicated that the effects of downstream diffusion in these columns are minimized at the flow rate used. The reduced volumes r for the several runs fall nearly on the same curve, but the results of the experiment are better shown otherwise. In Table I are summarized the significant features

TABLE I

KINETICS OF CLAY-ASBESTOS COLUMN FOR CESIUM EXCHANGE

$q_0 x/c_0 = 0.335 \times 2.446/0.0200 = 41.0$

$c(Cs)/c_0$	$q(Cs)/q_0$	Δ
1.000	1.000	1.78
0.900	0.980	1.78
.800	.956	2.13
.700	.933	2.37
.600	.910	2.59
.500	.884	3.15
.400	.846	3.76
.300	.798	5.72
.200	.738	7.94
.100	.652	11.6
.050	.558	17.5

of the experiment together with the values of Δ obtained independently for each break-through curve by empirically fitting the curve with the aid of the table of $\exp\{-(u + v)\}\Phi(u,v)$ due to Brinkley.[4] This table is constructed in such a fashion that the curve fitting becomes quite simple. Since the ratio of the arguments of the function in equation 1 is independent of Δ and so is determined solely by experimental quantities, and since xq/c is fixed in a single experiment, one has only to try a few values to arrive at a selection for Δ which gives a nearly perfect fit, i.e., a series of values for y at the tabulated round values of θ/θ_0 which reproduces the experimental curve. When these values of Δ are plotted against $(q/q_0)/(c/c_0)$, the straight line of Fig. 1 is obtained. (The zero subscripts refer to the values for pure cesium solutions.) As is required by mechanism (A) this line passes through the origin. The discrepancies for large Δ probably represent only difficulties in curve fitting. Evidently the kinetics of the column are adequately described by the liquid diffusion mechanism.

(4) S. R. Brinkley, Jr., Report No. 3172, Feb. 2, 1951, Explosives and Physical Sciences Division, U. S. Department of the Interior, Bureau of Mines.

THE KINETICS OF DISPLACEMENT REACTIONS INVOLVING METAL COMPLEXES OF ETHYLENEDIAMINETETRAACETIC ACID. II

BY K. BRIL, S. BRIL AND P. KRUMHOLZ

Contribution from the Research Laboratory of Orquima S.A., São Paulo, Brazil

Received August 4, 1955

The initial velocity v_0 of the displacement reaction

$$Me_{(1)}^{2+} + Me_{(2)}Y^{2-} \longrightarrow Me_{(2)}^{2+} + Me_{(1)}Y^{2-} \quad (1)$$

where Y represents the ion of ethylenediaminetetraacetic acid (= Enta) and $Me_{(1)}$ and $Me_{(2)}$ stand for

the pairs: copper–cadmium[1] and lead–zinc,[2] respectively, was shown[1,2] to follow, in the pH range from 5 to 6, the rate expression

$$v_0 = -\left\{\frac{d(Me_{(1)})}{dt}\right\}_{t=0} =$$
$$(Me_{(1)})(Me_{(2)}Y)\left\{k_1^+ + k_2^+[H] + k_3^+\frac{[H]}{(Me_{(2)})}\right\} \quad (2)$$

if $(Me_{(1)}Y) = 0$ and $(Me_{(2)}) \gg (Me_{(1)})$.

The last term in equation 2 involving the rate constant k_3^+, can be interpreted[1,2] in terms of the reaction sequence

$$Me_{(2)}Y^{2-} + H^+ \rightleftarrows Me_{(2)}^{2+} + YH^{3-} \quad (3)$$
$$Me_{(1)}^{2+} + YH^{3-} \rightleftarrows Me_{(1)}Y^{2-} + H^+$$
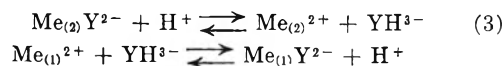
Using the steady-state approximation, the following rate expression was derived[2,3] for the reaction path (3)

$$v_0^{(3)} = -\left\{\frac{d(Me_{(1)})}{dt}\right\}_{t=0} =$$
$$\frac{k_a}{k_b(Me_{(2)}) + k_c(Me_{(1)})}(Me_{(2)}Y)(Me_{(1)})[H] \quad (4)$$

It can be shown that the rate expression (4) is valid for any reaction path[3] of the general form

$$Me_{(2)}Y^{2-} + H^+ \rightleftarrows \text{stationary intermediates} \rightleftarrows$$
$$Me_{(2)}^{2+} + YH^{3-} \quad (5)$$

$$Me_{(1)}^{2+} + YH^{3-} \rightleftarrows \text{stationary intermediates} \rightleftarrows$$
$$Me_{(1)}Y^{2-} + H^+$$
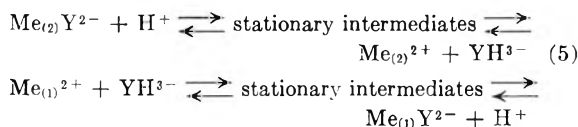
Thus the meaning of the constants k_a, k_b and k_c in (4) is complex and depends upon the detail of the reaction sequence assumed.[2] The mathematical form of equation 4 allows the determination of two independent parameters only, as for example k_a/k_c and k_b/k_c.

Under the condition $k_b(Me_{(2)}) \gg k_c(Me_{(1)})$ expression (4) takes the form of the third term in (2). This condition was fulfilled in the previous investigations.[1,2] It will be shown in the following that equation 4 is valid without any restriction regarding the concentrations of the competing metal ions.

Experimental

Material, apparatus, technique of calibrations and measurements were described in our previous communication.[2]

The rate of the exchange reaction between lead nitrate and the zinc–Enta complex, as well as that between copper nitrate and the cadmium–Enta complex, was measured in acetate buffered solutions $((AcONa) = 0.1\ M)$ of ionic strength of one (made up with potassium nitrate) at a temperature of $25 \pm 0.1°$, using the streaming mercury electrode as an indicator electrode of the reaction progress.

The initial velocity v_0 was determined in two different ways. The best curve was drawn (on a large scale) through the experimental points, $(Me) = f(t)$, and v_0 calculated from the tangent slope at $t = 0$. Alternatively the best straight line was drawn through the experimental points over a period of time corresponding to an exchange of about 10%. The slope of this line gave an approximate value v'_0 of the initial velocity. From a set of v'_0 values an approximate rate law was established, which allowed the estimation of approximate values of the formal rate constants involved. Using this rate law, the variation of the

(1) H. Ackermann and G. Schwarzenbach, Helv. Chim. Acta, 35, 485 (1952).

(2) K. Bril, S. Bril and P. Krumholz, THIS JOURNAL, 59, 596 (1955).

(3) Equation 4 implies that the proton equilibria of YH^{3-} are maintained throughout the exchange process. It is also assumed that any intermediate particle participating simultaneously in (3) or (5) and in some other reaction path, is in equilibrium with the analytical reaction partners.

reaction velocity over the first 10% exchange was evaluated in every experiment, taking into proper account the influence of the back reaction (1) as previously described.[2] Accordingly, v'_0 was multiplied by a correction factor to give the "true value" of the initial velocity. Since the correction factor was in general small (1.05 to 1.15) it was not necessary to apply further corrections. Both evaluation methods gave consistent values for v_0 within about 5%.

Experimental Results

In Fig. 1 the initial velocity v_0 of the reaction between lead nitrate and the zinc–Enta complex, divided by the initial zinc–Enta concentration, is plotted against the reciprocal zinc concentration, at [H] = 2.48×10^{-6} M and $(Me_{(1)}) = (Pb) = 1.21 \times 10^{-4}$ M. The line drawn in Fig. 1 was calculated according to equation 2, expression (4) being substituted for the last term of this equation. Following values[4] of the constants were used: $k_1^+ = 0.34$, $k_2^+ = 2 \times 10^4$ (see ref. 2), $k_a/k_b = 1.15 \times 10^3$ and $k_c/k_b = 3.7$. The values given above should be correct within at least 20%. Comparison of equation 4 with the third term in (2) (valid for $k_b(Zn) \gg k_c(Pb)$) shows that k_a/k_b is identical with k_3^+; indeed the value of 1.15×10^3 is in good agreement with the value previously reported for $k_3^+ = 1.1 \times 10^3$.
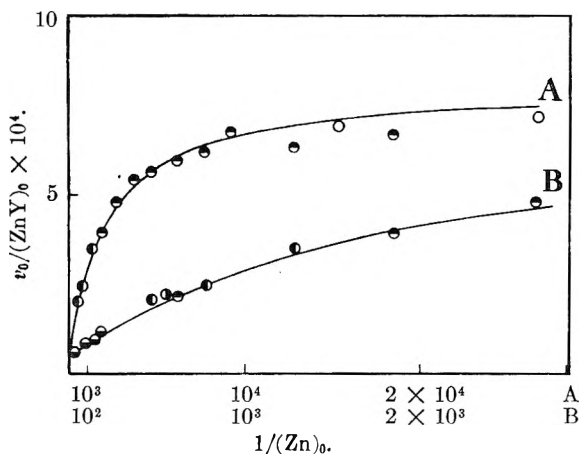
Fig. 1.—$v_0/(ZnY)_0$ as a function of the reciprocal zinc nitrate initial concentration; ionic strength = 1.00; nitrate solutions; acetate buffer; $t = 25°$; [H]$_0$ = 2.48×10^{-6} M; (Pb)$_0$ = 1.23×10^{-4} M; (ZnY)$_0$ concentrations in mM per liter are: ○, 0.134; ◕, 0.268; ◑, 0.671; ◐, 1.34; ◒, 4.69.

Additional experiments show that at low zinc concentrations the linear dependence of $v_0/(ZnY)$ upon the hydrogen ion activity previously reported[2] is still valid. The extrapolation to [H] = 0 at (Zn) = 5×10^{-5} M leads to $k_1^+ = 0.34$, in full agreement with the value previously reported.[2]

Equation 4 was tested further by studying v_0 at (Zn) = 0. According to this equation, the initial velocity of the exchange through path (3) should be independent of the lead concentration. Actually at [H] = 2.48×10^{-6} M and for (Pb) varying between 5×10^{-5} M and 2.5×10^{-4} M we found experimentally: $v_0^{(3)}/(ZnY) = (7.8 \pm 0.8) \times 10^{-4}$, whereas the value calculated according to eq. 4 is 7.7×10^{-4}.

In Fig. 2 the initial velocity v_0 of the exchange reaction between copper nitrate and the cadmium–Enta complex, divided by the initial cadmium–Enta
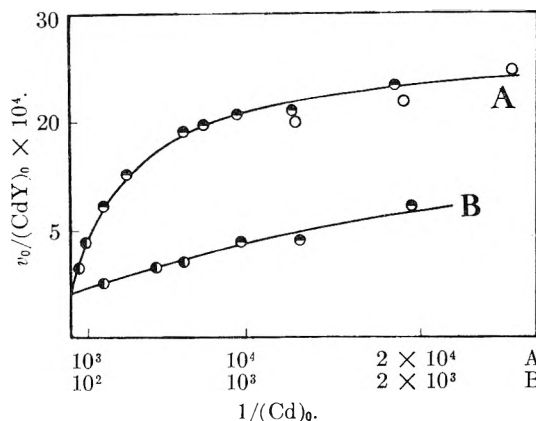
Fig. 2.—$v_0/(CdY)_0$ as a function of the reciprocal cadmium nitrate initial concentration; ionic strength = 1.00; nitrate solutions; acetate buffer; $t = 25°$; [H]$_0$ = 2.54×10^{-6} M; (Cu)$_0$ = 1.91×10^{-4} M; (CdY)$_0$ concentrations in mM per liter are: ○, 0.134; ◕, 0.268; ◑, 0.804.

complex concentration, is plotted against the reciprocal cadmium concentration, at [H] = 2.54×10^{-6} M and $(Me_{(1)}) = (Cu) = 1.91 \times 10^{-4}$ M. The line drawn in this figure was calculated according to equations 2 and 4. The following values of the constants were used: $k_1^+ + k_2^+[H] = 2.1$, $k_a/k_b = 1.25 \times 10^3$ and $k_c/k_b = 1.35$.

For (Cd) = 0 we found experimentally $v_0/(CdY) = (28 \pm 1) \times 10^{-4}$ in good agreement with the calculated value of 27.5×10^{-4}.

THE VAPOR PRESSURE OF ETHYL trans-β-(2-FURYL)-ACRYLATE

By F. Fromm and Sister M. Constance Loeffler, R.S.M.

Department of Chemistry, Mount Mercy College, Pittsburgh, Pa.

Information about the volatility of the ethyl ester of trans-β-(2-furan)-acrylic acid was needed in studies of its phytotoxicity,[1] but sufficient data could not be found in the literature. Accordingly, the vapor pressure of the compound was measured in a Ramsey–Young apparatus after preliminary experiments had shown that the Menzies–Smith apparatus was not suitable because the ester did not stand the prolonged heating needed to reach equilibrium. Doubly distilled ethyl trans-furylacrylate, prepared by Claisen synthesis,[2] was used. Table I gives the temperatures t in °C. and the corresponding vapor pressures p in mm.

TABLE I

t	155	168	168	177	194	205	215	220	222	227
p	62	98	99	133	234	341	437	502	546	603

The constants A and B in the equation

$$\log p = A/T + B$$

in which T is absolute temperature, were calculated by the method of the least squares. A was found to be -2.969×10^3, and B was equal to 8.727. The b.p. at 760 mm. was extrapolated as 235° in agree-

(1) F. Fromm, *Ciencia (Méx.)*, **9**, 40 (1948); *Acta cientif. venezol.*, in press.

(2) H. Posner, *J. prakt. Chem.*, [2] **82**, 425 (1910).

(4) Here and in the following the units used are: mole, liter, second.

ment with the observations of Claisen[3] of 233–235° and of Posner[2] of 232°; the value of 228–230°, reported by Marckwald[4] appears to be too low. Extrapolating over a somewhat wider range than usual, the b.p. at 15 mm. was calculated as 120° in agreement with 122–123° reported by Moureu, *et al.*[5]; the b.p. at 10 mm. would be 111° in fair agreement with the 115° given by Hinz, *et al.*[6] Shunsuke Murahashi's[7] report of b.p. 116–117° at 8 mm. seems to be too high. The latent heat of evaporation L was calculated from the constant A as 13.6 kcal./mole. Actual measurements of L in the Fisher-Engel heat of vaporization apparatus were attempted but could not be performed satisfactorily because of the thermolability of the ester.

(3) L. Claisen, *Ber.*, **24**, 144 (1891).
(4) W. Marckwald, *ibid.*, **21**, 1404 (1888).
(5) H. Moureu, P. Chevin and L. Petit, *Bull. soc. chim. France*, 203 (1951).
(6) A. Hinz, G. Meyer and G. Schücking, *Ber.*, **76B**, 676 (1943).
(7) Shunsuke Murahashi, *C. A.*, **42**, 1205h (1948).

INFLUENCE OF ELECTROLYTE ON EFFECTIVE DIELECTRIC CONSTANTS IN ENZYMES, PROTEINS AND OTHER MOLECULES

By Terrell L. Hill

Naval Medical Research Institute, National Naval Medical Center, Bethesda, Md.

The purpose of this note is to illustrate electrolyte effects on charge interactions in substrate–enzyme complexes, protein molecules, and in smaller molecules, as calculated from an approximate model.

It is instructive to represent the work W of bringing two point charges e_1 and e_2 to within a distance r of each other by an expression of the form

$$W = \frac{e_1 e_2}{D_E r} \tag{1}$$

regardless of the environment of the two charges. D_E is then by definition the *effective* dielectric constant. In a vacuum, $D_E = 1$. In pure solvent (water, 25°), $D_E = D = 78$. In a dilute electrolyte solution (point ions)

$$D_E = D e^{\kappa r} \tag{2}$$

where κ is the usual Debye–Hückel parameter.

Kirkwood has introduced an electrostatic model which we adopt in the examples included here. In fact, the equations we use follow directly from Kirkwood's paper.[1] The contribution of the present work is to write out explicit expressions for D_E (Kirkwood and Westheimer[2] did this for the special case $\kappa = 0$—no electrolyte present) and to present some numerical results[3] illustrating effects of electrolyte and charge configuration.

Enzyme–Substrate and Protein Model. — Kirkwood's model[1] consists of a sphere of low dielectric constant D_i ($\cong 2$) immersed in a solvent of dielectric constant D. Electrolyte (point) ions at low

(1) J. G. Kirkwood, *J. Chem. Phys.*, **2**, 351 (1934).
(2) J. G. Kirkwood and F. H. Westheimer, *ibid.*, **6**, 506 (1938).
(3) Calculated by the Computation Laboratory of the National Bureau of Standards.

concentration are present in the solvent and fixed (point) charges are imbedded at arbitrary locations in the sphere. For example, suppose substrate and enzyme possess charges as in Fig. 1a and the enzyme–substrate complex is approximately a sphere, as in Fig. 1b. Then Fig. 1c can be used as a model to calculate the electrostatic work of bringing enzyme and substrate together: Fig. 1a → Fig. 1b. Alternatively, Fig. 1c might represent a protein molecule (or a smaller molecule) with two of its charges located as shown. It is assumed throughout that electrolyte does not penetrate into the sphere.
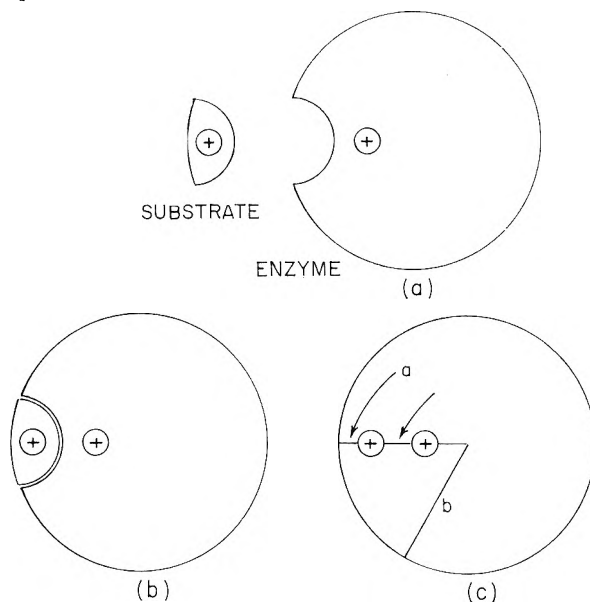
Fig. 1.

For the arbitrary geometry shown in Fig. 2, if Kirkwood's equations[1] are put in the form of eq. 1, we find

$$\frac{1}{D_E} = \frac{1}{D_i} + \frac{1}{D_i} \sum_{n=0}^{\infty} \frac{r}{b} y^n P_n (\cos \theta) \left\{ \frac{(n+1)(D_i - D)}{(n+1)D + nD_i} - \frac{(2n+1)DD_i x q_n(x)}{[(n+1)D + nD_i][(n+1)D + nD_i + Dx q_n(x)]} \right\} \tag{3}$$

where the $P_n(\cos \theta)$ are Legendre Polynomials and

$$y = r_1 r_2 / b^2 \tag{4}$$

$$x = \kappa b \tag{5}$$

$$q_n(x) = 1 - \frac{K_n'(x)}{K_n(x)} \tag{6}$$

$$K_n(x) = \sum_{s=0}^{n} \frac{2^s n! (2n - s)! x^s}{s! (2n)! (n - s)!} \tag{7}$$

This result is independent of the sign and magnitude of e_1 and e_2 and of the presence of other

Fig. 2.   Fig. 3.

TABLE I

EFFECTIVE DIELECTRIC CONSTANTS FROM EQ. 9

x \ $a/b =$	0	0.005	0.01	0.03	0.06	0.10	0.20	0.40	Eq. 1
				$r/b = 0.05$					
0	42.3	9.91	6.39	3.60	2.83	2.51	2.27	2.16	
0.5	43.0	9.94	6.41	3.60	2.83	2.52			
1	43.7	9.98	6.42	3.61	2.83	2.52			
2	45.2	10.05	6.45	3.61	2.84	2.52			
4	48.4	10.19	6.51	3.63	2.85	2.52			
6	51.7	10.32	6.56	3.64	2.85	2.53			
8	55.0	10.43	6.60	3.65	2.86	2.53			
10	58.2	10.53	6.63	3.66	2.86	2.53			
15	66.4	10.75	6.71	3.67	2.86	2.53			
				$r/b = 0.10$					
0	44.7	15.75	10.21	5.17	3.68	3.05	2.56	2.32	78.0
0.5	46.1	15.91	10.28	5.19	3.69	3.05			. . .
1	47.6	16.08	10.35	5.21	3.69	3.06			86.2
2	50.7	16.42	10.48	5.24	3.71	3.06			. . .
4	57.3	17.02	10.72	5.29	3.73	3.07			. . .
6	64.1	17.54	10.91	5.32	3.74	3.08			142
8	70.9	17.98	11.06	5.35	3.75	3.09			. . .
10	77.7	18.36	11.20	5.38	3.76	3.09			. . .
15	95.3	19.11	11.45	5.42	3.77	3.10			350
				$r/b = 0.25$					
0	50.7		19.7	9.87	6.36	4.78	3.52	2.89	78
0.5	54.8		20.3	10.01	6.41	4.81			. . .
1	59.1		20.8	10.14	6.46	4.83			100
2	68.0		21.8	10.35	6.53	4.87			. . .
4	86.6		23.3	10.64	6.63	4.91			. . .
6	106		24.4	10.83	6.69	4.94			350
8	125		25.3	10.97	6.74	4.96			. . .
10	146		25.9	11.07	6.77	4.97			. . .
15	197		27.0	11.23	6.81	4.99			3,320
				$r/b = 0.50$					
0	59.7		32.7	18.01	11.46	8.23	5.54	4.15	78
0.5	70.6		35.7	18.87	11.80	8.40			. . .
1	81.6		38.2	19.54	12.04	8.52			129
2	104		42.4	20.5	12.38	8.67			. . .
4	151		48.3	21.7	12.75	8.83			. . .
6	199		52.1	22.4	12.95	8.91			1,570
8	248		54.8	22.8	13.07	8.96			. . .
10	298		56.8	23.1	13.16	8.99			. . .
15	425		60.0	23.6	13.28	9.03			141,000

TABLE II

EFFECTIVE DIELECTRIC CONSTANTS FROM EQ. 10

x \ $y^{1/2} =$	0.1	0.2	0.3	0.4	0.5	0.6	0.7	0.8		0.9		1.0	
								Eq. 10	Eq. 1	Eq. 10	Eq. 1	Eq. 10	Eq. 1
0.0	2.48	3.20	4.32	6.12	9.17	14.64	25.2	46.8	78.0	88.0	78.0	127	78.0
0.5	2.48	3.22	4.37	6.25	9.51	15.69	28.9	63.5	174	187	192	652	212
1.0	2.49	3.23	4.39	6.30	9.66	16.12	30.4	70.8	386	257	472	3,320	576
2.0	2.49	3.23	4.41	6.35	9.79	16.46	31.5	75.7	1,914	306	2,850	46,200	4,260
4.0	2.49	3.24	4.43	6.39	9.88	16.69	32.2	78.4	46,900	329	104,500	. . .	. . .

charges in the sphere. That is, each pair of charges possesses its own D_E.

In the special case $x = 0$ (no electrolyte), D_i/D << 1 and $r_1 = r_2$, eq. 3 reduces to the Kirkwood-Westheimer formula[2] for D_E.

In the special case D_i/D << 1, eq. 3 becomes

$$\frac{1}{D_E} = \frac{1}{D_i}\left[1 - \frac{r}{b}\frac{1}{(1+y^2-2y\cos\theta)^{1/2}}\right] + \frac{1}{D}\frac{r}{b}\left\{\frac{2}{(1+y^2-2y\cos\theta)^{1/2}} + \frac{1}{y}\ln\frac{1-\cos\theta}{y-\cos\theta+(1+y^2-2y\cos\theta)^{1/2}} - \sum_{n=0}^{\infty}\frac{(2n+1)rq_n(x)y^nP_n(\cos\theta)}{(n+1)[n+1+xq_n(x)]}\right\} \quad (8)$$

To illustrate eq. 8, we make numerical calcula-

tions for the geometry of Fig. 1c. That is, we put $\theta = 0$, $r_1 = b - a$ and $r_2 = b - a - r$. Then eq. 8 simplifies to

$$\frac{1}{D_E} = \frac{1}{D_i}\left(1 - \frac{r}{b}\frac{1}{1-y}\right) + \frac{1}{D}\frac{r}{b}\left\{\frac{2}{1-y} + \frac{1}{y}\ln(1-y) - \sum_{n=0}^{\infty}\frac{(2n+1)xq_n(x)y^n}{(n+1)[n+1+xq_n(x)]}\right\} \quad (9)$$

D_E is a function of x, a/b and r/b. A typical choice of parameters (Figs. 1bc) might be $b = 32$ Å., $1/\kappa = 8$ Å. (about 0.15 M NaCl), $c = r = 3.2$ Å. Thus $x = 4$, $a/b = r/b = 0.1$. Table I gives the results, taking $D_i = 2$ and $D = 78$. A wide range of values of D_E is seen to be possible. D_E is larger for small values of a/b, large values of r/b and large values of x. D_E is rather insensitive to x except when a/b is quite small. For comparative purposes, a few values of D_E calculated from eq. 1

$$D_E = De^{\kappa r} = De^{x(r/b)}$$

are included in Table I.

Small Molecule Model.—The object here is to illustrate the extent to which electrolyte affects the Kirkwood–Westheimer results.[2] We consider the symmetrical arrangement in Fig. 3. In eq. 8 we put $\theta = \pi$, $r_1 = r_2 = r/2$, and $y = r^2/4b^2$. We find

$$\frac{1}{D_E} = \frac{1}{D_i}\left(1 - \frac{2y^{1/2}}{1+y}\right) + \frac{2y^{1/2}}{D}\left\{\frac{2}{1+y} - \frac{1}{y}\ln(1+y) - \sum_{n=0}^{\infty}\frac{(2n+1)xq_n(x)(-y)^n}{(n+1)[n+1+xq_n(x)]}\right\} \quad (10)$$

D_E is a function of x and $r/2b$. A typical choice of parameters might be $b = 4$ Å., $1/\kappa = 8$ Å., $r = 4$ Å. Thus $x = 0.5$ and $r/2b = y^{1/2} = 0.5$. Table II shows calculated values of D_E, with $D_i = 2$ and $D = 78$. The results for $x = 0$ agree with those of Kirkwood and Westheimer.[2] D_E increases with increasing x and y, but is quite insensitive to x unless $y^{1/2} \geqslant 0.7$. Very large values of D_E are obtained for $y^{1/2} = 1.0$ and $x > 1$. For comparison, some values of D_E from eq. 1

$$D_E = De^{\kappa r} = De^{2xy^{1/2}}$$

are included in Table II.

THE BASICITY OF THE SILVER BROMIDE COMPLEX ION

BY RICHARD C. DEGEISO AND DAVID N. HUME

Department of Chemistry and Laboratory for Nuclear Science, Massachusetts Institute of Technology, Cambridge, Mass.

Mitra, Gupta and Jain[1] recently reported polarograms and potentiometric titrations of hydrobromic acid solutions saturated with silver bromide which they interpreted as demonstrating the existence of the weak acid $HAgBr_2$. Several aspects of this work as reported were, however, puzzling: notably the failure of potassium bromide solutions saturated with silver bromide to show any buffering action, and the much greater solubility of silver bromide in hydrobromic acid than would be expected

from the observations of previous workers. Accordingly, we have repeated and extended the experiments and have found that the observations may be explained better in other ways.

When 0.5 M solutions of hydrobromic acid were saturated with silver bromide and titrated potentiometrically with sodium hydroxide, no evidence was at first obtained for the presence of a weak acid in the mixture. Repetition of the experiments with 3 M hydrobromic acid gave titration curves showing the presence of a weak acid, but the same effect was observed with the hydrobromic acid blank containing no silver bromide. This phenomenon was traced to the presence of carbonate in the sodium hydroxide. The carbon dioxide, freed during the titration of the hydrobromic acid and remaining in the solution, was titrated as a weak acid when excess of sodium hydroxide was added. Use of carbonate-free hydroxide, or removal of carbon dioxide by boiling the solutions at pH 3 before continuing to the end-point, resulted in a typical strong acid–strong base titration curve, with or without silver bromide present. Addition of a few per cent. of carbonate to the base used in titrating the 0.5 M hydrobromic acid solutions gave the same titration curves as observed by the Indian workers.

An attempt to measure the solubility of silver bromide in 0.5 M hydrobromic acid indicated that the solubility must be orders of magnitude less than the 2.4 mM value which had been reported. In 3 M hydrobromic acid and in 3 M potassium bromide, we obtained values in agreement with those of Erber[2] and Hellwig,[3] whose solubility data would lead one to predict by extrapolation that only extremely small amounts of silver bromide would dissolve in 0.5 M hydrobromic acid.

Examination of the polarograms published by Mitra, *et al.*, revealed that their technique for measuring diffusion current was erroneous and that much higher values for the silver concentration were being deduced than was actually justified. The instrument which they used was one which, in our experience, is capable of giving entirely misleading results unless one knows and takes into consideration its peculiar electrical characteristics. They had the misfortune to use it under circumstances where the extreme time-lag of the recorder caused it to draw a wave which was not there. This, together with the fact that they did not realize that the mercury pool potential varies with supporting electrolyte composition, or that excess potassium nitrate does not eliminate the effects of variable amounts of bromide, suggests that their conclusions should be disregarded. We have examined the polarographic behavior of silver in bromide–nitrate mixtures and found it to be exactly as would be predicted. The solubility of silver is negligible under the conditions used by Mitra and his coworkers, and the only wave observed is that of the anodic dissolution of mercury.

Finally, we have found that the pH of the 3 M potassium bromide solutions is unchanged by saturating with silver bromide (which is here soluble to the extent of about 0.015 M) and that the titration

(1) R. P. Mitra, A. R. Gupta and D. V. S. Jain, *J. Indian Chem. Soc.*, **31**, 346 (1954).

(2) W. Erber, *Z. anorg. Chem.*, **248**, 32 (1941).

(3) K. Hellwig, *ibid.*, **25**, 157 (1900).

of the saturated solution with hydrobromic acid gives a potentiometric curve indistinguishable from that of the titration of the potassium bromide alone, there being no buffer action. From all our observations we can only conclude that no evidence exists to show the substance $HAgBr_2$ is other than a strong acid.

Acknowledgment.—This work was supported in part by the United States Atomic Energy Commission.

COMMUNICATION TO THE EDITOR

THE THERMAL DECOMPOSITION OF NaNO₃

Sir:

There has been considerable recent interest in the kinetics and mechanism of the thermal decomposition of metal nitrates and other materials which are good oxidizing agents. Recently, data were presented for the kinetics of the thermal decomposition of $NaNO_3$ and N_2, O_2, and small amounts of NO_2 were assumed to be the main decomposition products.[1] In this laboratory some preliminary work has been done on this decomposition which sheds new light on the species probably involved in the actual decomposition process.

$NaNO_3$ was heated in gold boats at temperatures up to 865°. The gaseous decomposition products formed were studied by (1) obtaining absorption spectra of the products and (2) analyzing the gases mass spectrographically after they were swept into a sample bulb with helium or argon as inert sweep gases. A small Hilger quartz spectrograph for visible and ultraviolet work was used with a xenon high-pressure arc light source.

Ultraviolet absorption spectra showed that the 0,0 and 0,1 absorption bands of the γ-system of the

(1) E. S. Freeman, Abstracts of Papers Presented at the 127th Meeting of the American Chemical Society, Cincinnati, Ohio, 1955, p. 28-Q.

$NO(g)$ molecule began to appear at 700° very faintly and that they appeared with increased intensity at 775, 825 and 865°. Mass spectrographic analyses of the gases from the decomposing $NaNO_3$ at 800° showed that NO, N_2 and O_2 were present in large amounts while NO_2 and possibly N_2O were also detectable. The O_2 peak height was about twice that of N_2 while the NO peak height was about the same as that for N_2. At 400–600° there appeared to be only O_2 and N_2 formed by decomposition with NO first being detected both optically and mass spectrographically at about 700°C.

It is uncertain, of course, whether the NO detected is really a primary product of the decomposition or whether NO_2 is formed first and then decomposed thermally. The absorption spectra showed no traces of the known visible or ultraviolet NO_2 bands; the NO_2 detected mass spectrographically could have resulted from combination of the NO and O_2 in the sample bulbs.

DEPARTMENT OF CHEMISTRY
UNIVERSITY OF WISCONSIN   HENRY R. BARTOS
MADISON, WISCONSIN   JOHN L. MARGRAVE

AZEOTROPIC DATA

Table I. Binary Systems

Formula	B-Component Name	B.P., °C.	B.P., °C.	Azeotropic Data Wt. % A	Ref.
A	Argon Nitrogen, 500-1500 mm.	−186 −195	Nonazeotrope, V-l.		164 255
1 N₂	Silver Chloride Lead chloride	15?0 954	Nonazeotrope		263
AgCl			Nonazeotrope		263 262
2 Cl₂Pb	Boron Chloride	11.5 −92.5		77.2	262 590
BCl₃	boron hydride	−100 −92	−106	62 60	590 590
3 B₃H		100	46 180 43	65 80 42 52 62	590 590 262 262 590

CONTENTS

329 pages, cloth bound, $4